Investigations on the early biosynthetic steps of griseorhodin A

Dissertation

Zur Erlangung des Doktorgrades (Dr. rer. nat.)

der

Mathematischen-Naturwissenschatflichen Fakultät

der

Rheinischen Friedrich-Wilhelms-Universität Bonn

vorgelegt von

Minna Leena Eklund

aus

Kauniainen, Finnland

Bonn 2011

Angefertigt mit Genehmigung der Mathematisch-Naturwissenschaftlichen
Fakultät der Rheinischen Friedrich-Wilhelms-Universität Bonn

Gutachter: 1. Prof. Dr. Jörn Piel

2. Prof. Dr. Hans-Georg Sahl

Tag der Promotion: 16.12.2011

Erscheinungsjahr: 2012

For my parents

Acknowledgements

The present study was carried out in the Kekulé Institute for Organic Chemistry and Biochemistry at the University of Bonn under the supervision of Prof. Dr. Jörn Piel.

First of all I thank Prof. Dr. Jörn Piel for providing me with this interesting research topic and giving me the opportunity to work in his research group. I appreciate his valuable guidance, support and encouragement during my study. It has been a great opportunity to learn from his knowledge and experience.

I thank Prof. Dr. Hans-Georg Sahl his critical reading and helpful contributions.

I would like to thank the committee members, Prof. Dr. Albert Haas and Prof. Dr. Gabriele König for their refereeing and evaluation of my research.

Mass department at the Kekulé Institute is greatly appreciated for mass measurements. Special thanks go to Karin Peters-Pflaumenbaum.

Furthermore, I thank Research Training Group GRK 804 for the financial support, especially Dr. Sven Freundenthal.

Prof. Dr. Hertweck is thanked for providing the vector pKJ55.

Prof. Dr. Alfonso Mangoni and Dr. Roberta Teta at the University of Naples are deeply thanked for their efforts for recording cryogenic NMR spectra.

During my stay at the University of Canterbury in Christchurch, New Zealand, I was supported by Prof. Dr. Murray Munro, Prof. Dr. John Blunt, Dr. Marie Squire and Gill Ellis. I deeply appreciate this opportunity and I am

very thankful for the great experience. I thank my lab mate Richard James Johori for a wonderful team work during these months.

In these years I have benefited from a wonderful lab team providing deep knowledge and experience. The working environment was always enjoyable and supportive in every situation. My colleagues´ help in many situations is gratefully acknowledged. My thanks go to every old and present lab member, especially to Dr. Christian Gurgui, Max Crüsemann, Dr. Michael Freeman, Martina Heycke, Thomas Hochmuth, Katja Jensen, Christoph Kohlhaas, Stefan Künne, Dr. Jana Moldenhauer, Christine Beus, Dr. Kathrin Reinhardt, Dr. Sonia van der Sar, Zeynep Yunt and Dr. Katrin Zimmermann. Furthermore, I thank my students who helped me to carry out research in many respects.

Max Crüsemann, Dr. Michael Freeman, and Dr. Jana Moldenhauer are thanked for critical proofreading of the thesis.

I thank Mark, my soul mate, for his support and patience.

Finally, and most importantly, I would like to thank my family for their constant support throughout the years at the university.

Table of contents

List of figures

List of tables

1 Abstract

Presented here are the results concerning the early biosynthesis of the telomerase inhibitor griseorhodin A.

The griseorhodin biosynthetic gene cluster encodes components of a type II polyketide synthase (PKS). The cluster consists of 33 genes, many of which encode oxidoreductases. The *grh* biosynthetic cluster was isolated from *Streptomyces* sp. JP95, a bacterium isolated from the marine tunicate *Aplidium lenticulum* collected in the Great Barrier Reef, Australia. The complete *grh* cluster is available for expression on the cosmid pMP31, which can be heterologously expressed in *S. albus* J1074.

To investigate the early biosynthetic steps in *grh* biosynthesis, the genes *grhA*, *grhB*, *grhC*, *grhE*, *grhT* and *grhQ* were cloned for heterologous expression in the host organism *S. albus*. *S. albus* strains expressing the *grh* minimal PKS with and without the *grh* cyclases did not result in detectable amounts of polyketides or shunt products. This is in high contrast to other type II PKS systems. In an alternative approach, all cyclase genes were individually deleted withinin the *grh* cluster. Based on these results, the enzyme GrhE does not seem to play a significant role in the *grh* biosynthesis since griseorhodin A was still produced. The deletion of the other cyclases, GrhT and GrhQ, abolished the biosynthesis and no polyketides were detected. This suggests that a multienzyme complex is required for early polyketide assembly. To further investigate early griseorhodin A biosynthesis, two other griseorhodin A gene deletion mutants, *ΔgrhH-P* (deletion of all post-PKS genes) and *ΔgrhH-Q* (deletion of all post-PKS genes and a cyclase gene), were generated during the present study. The *ΔgrhH-P* mutant contained only the proposed early griseorhodin genes. Heterologous expression of this construct led to the production of a complex mixture of compounds. It produced identical intermediates to the Δ*grhM* mutant, which was generated and expressed during a previous study[1] and for which an early oxygenation role is proposed during

griseorhodin A biosynthesis. Four compounds from the Δ*grhH-P* mutant expression were isolated and analysed indicating potentially new early intermediates. However, insufficient material was isolated for structure elucidation by 2D NMR.

To further investigate whether a functional protein complex is relevant at the early stage of griseorhodin A biosynthesis, in the second mutant *ΔgrhH-Q*, the cyclase GrhQ was additionally deleted, and the expression led to abolishment of griseorhodin A biosynthesis. This was in agreement with the GrhQ inactivation study. These results indicate and further support the presence of a multienzyme complex during the course of griseorhodin A biosynthesis. To date, griseorhodin A is one of the longest aromatic polyketides and therefore, could require the synergistic actions of cyclases (GrhQ) and other stabilising enzymes such as GrhS for correct polyketide assembly.

In order to gain deeper insights into the enzymatic activities responsible for griseorhodin A biosynthesis, two constructs with single gene deletions within the cluster, constructed in a previous study were further investigated. The two deleted genes, *grhU* and *grhV* encode proteins with unknown function. In the present study, these modified clusters were subsequently heterologously expressed in *S. albus* and analysed by high performance liquid chromatography (HPLC), high resolution mass spectroscopy (HRMS) and cryogenic or capillary NMR for the production of secondary metabolites. Heterologous expression of both mutants resulted in complex mixtures of compounds, and 21 pure compounds were isolated by various chromatographic methods. The structure of one of the compounds originating from the *ΔgrhV* gene deletion mutant was elucidated from 500 µg of sample and the structure revealed the decarboxylated 13,13´- fused tridecaketide dimer. The structure suggests that GrhV is responsible for an oxidative modification in the griseorhodin A molecule. To our knowledge, the present study gives first insights into the oxygenase function of GrhV and its homologues found in other pentangular biosynthetic pathways.

2 Introduction

2.1 Polyketides

Polyketides are a notable class of natural products that represent a group of structurally and functionally highly diverse substances found in bacteria, fungi and plants.[2] They have different biological functions in organisms, such as pigments, defence or communication molecules. However, in most cases their ecological role is not yet known.[3] Many of these compounds are very interesting to humans due to their pharmacological properties ranging from antibiotics (erythromycin A, **1**), anticancer drugs (doxorubicin, **2**) and cholesterol-lowering agents (lovastatin, **3**), to antiparasitics (avermectin B1b, **4**) and immunosuppressants (rapamycin, **5**).[4] Representative examples of polyketides and their natural producers are shown in Figure 1.

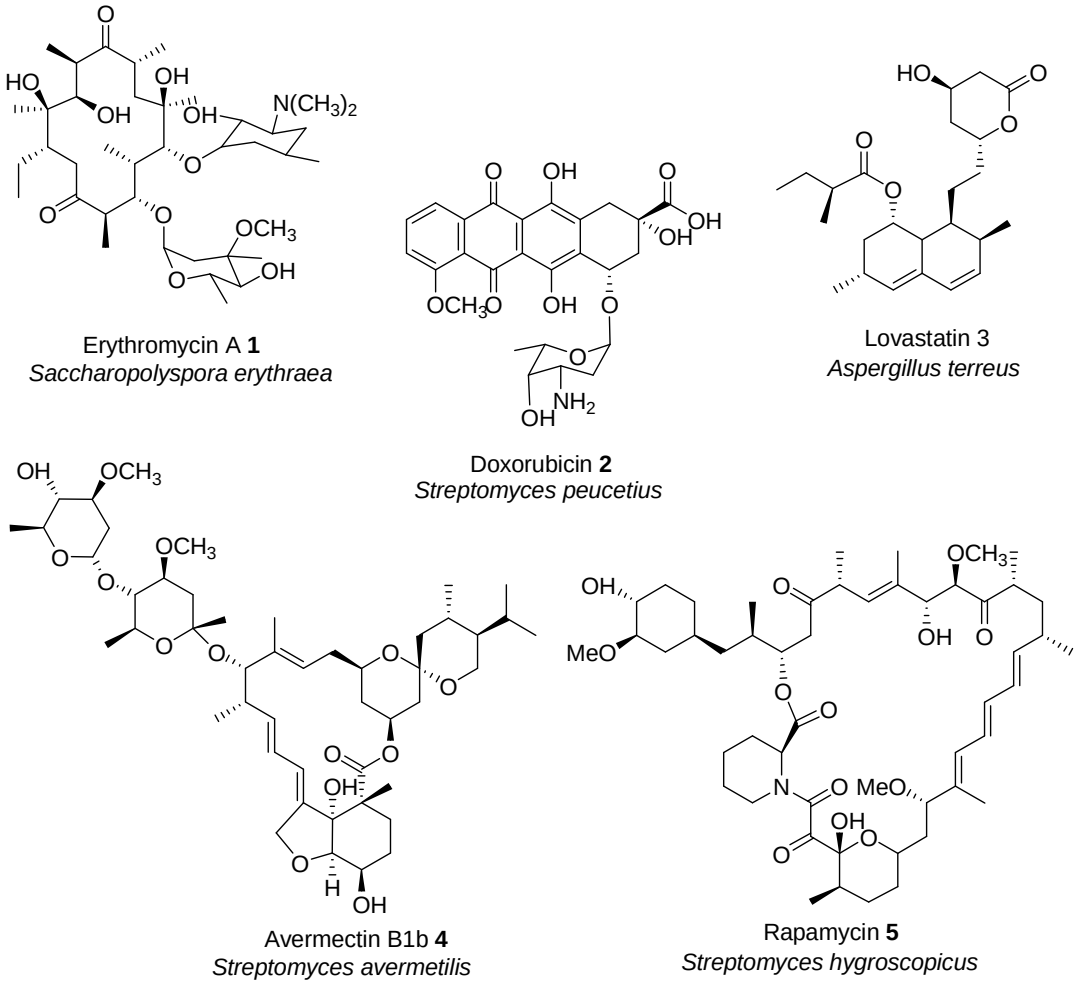

Fig. 1: Representative examples of polyketides and their natural producers.[4]

Erythromycin A is an antibiotic that inhibits protein biosynthesis in Gram-positive bacteria.[5] Doxorubicin is used in chemotherapy against different cancer types such as breast cancer, childhood solid tumours and soft tissue sarcomas.[6] Avermectin plays a role in parasitic diseases, while rapamycin is an immunosuppressant that inhibits T-cell distribution by specifically binding to intracellular receptors.[4, 7]

First investigations on polyketides were carried out in 1883 by James Collie, who discovered the aromatic substance orcinol.[8] Since then, the research interest in polyketides has been enormous. Collie assumed that orcinol-like natural products were derived from two-carbon "CH_2-CO" building blocks by cyclisation of poly-β-keto intermediates which led to the definition "polyketon".[9] Later, this name changed to polyketide.[10]

2.1.1 Polyketide biosynthesis

Despite their structural and functional diversity, polyketides possess the similar biosynthetic pathways. Polyketides are synthesised by multifunctional enzymes called polyketide synthases (PKSs) by repeated rounds of carbon chain extensions and further tailoring modifications.[11, 12] PKSs are related to fatty acid synthases (FASs), but PKSs usually produce metabolites with more complex structural architectures.[8] The variability of the structure is influenced by how the PKSs are programmed: choice of starter unit, the nature and number of the chain extender units, control of the β-keto group on oxidation level of the growing carbon chain, stereochemistry of hydroxyls and alkyl side groups and pattern of cyclisation of the nascent carbon chain.[11]

Figure 2 displays the different functionalities of PKS and FAS mechanisms.[11, 13] Polyketides consist of a long carbon chain constructed from small organic molecules; for example (e.g.) acetic acid **6** and malonic acid **7** that are first activated as coenzyme A (CoA) esters. FASs use acetyl-CoA **8** as a starter unit and malonyl-CoA **9** as extender units whereas PKSs can use different acyl-CoA substrates.[14] The starter unit is attached to the active site of the ketosynthase (KS), while the chain

extender unit is loaded onto an acyl carrier protein (ACP). Both units are Claisen condensed by the KS resulting in a loss of carbon dioxide and production of a carbon chain attached to the ACP. This is then transferred back to the KS and further rounds of condensations take place with malonyl-CoA (FAS, PKS) or other extender unit (PKS), where the chain is extended by two carbons at each step.

Depending on the PKS system, the extended carbon chain is either partially, fully, or not reduced. Enzymes or domains labelled ketoreductase (KR), dehydratase (DH) and/or enoylreductase (ER) are responsible for these modifications. In fatty acid (FA) synthesis, all possible reduction steps take place to produce a fully saturated chain.[11]

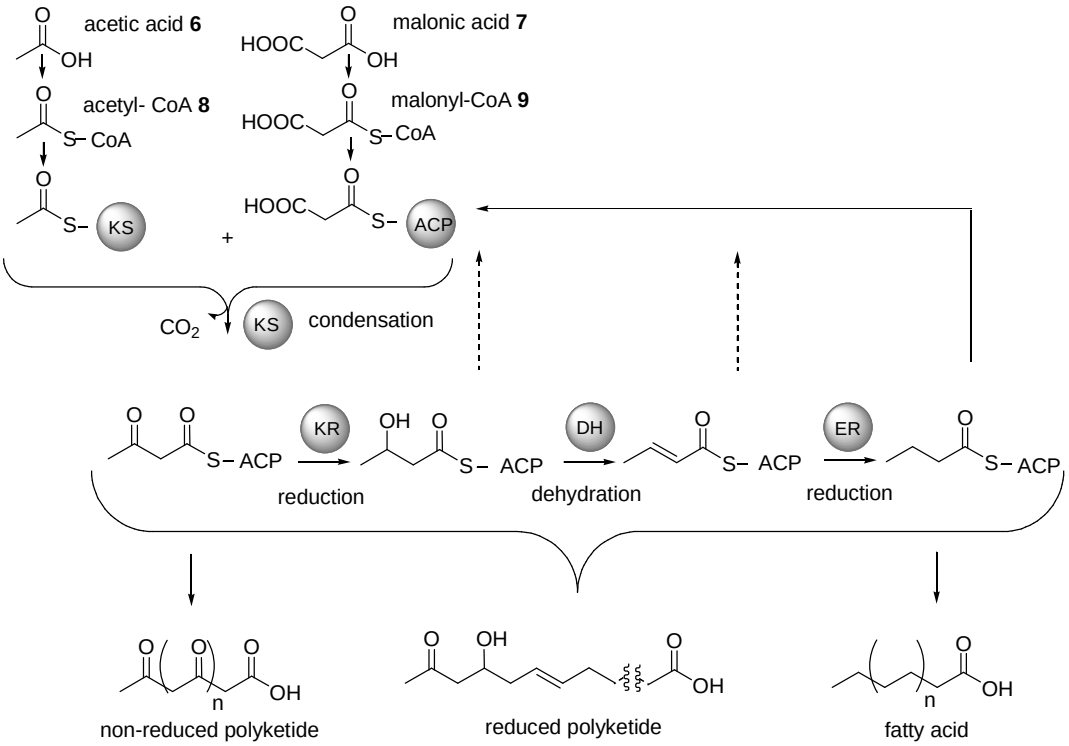

Fig. 2: General reaction scheme for FASs and PKSs.[11, 13]

2.1.2 Classification of PKS types

PKSs are categorised into three different classes: type I, type II and type III. Each type possesses different types of functions; modular and iterative, which lead to the structural differences in polyketides.[2] Type I PKSs are present in bacteria and fungi, type II PKSs are found only in bacteria and type III PKSs can be found in plants, bacteria and fungi.[15] Type I and type II PKSs use ACPs to activate acyl-CoA substrates and to transfer the growing polyketide intermediates, whereas type III PKSs lack this enzymatic relay mechanism.[2]

Modular type I PKSs are multifunctional enzymes that are organised into modules and to date, these are among the largest proteins encountered in nature.[16] Every module possesses non-iteratively acting domains responsible for polyketide chain elongation.[2]

The antibiotic erythromycin A **1** PKS (6-deoxyerythronolide B synthase - DEBS) is the most thoroughly investigated example of modular type I PKSs. An illustration of this system is shown in Figure 3.[4] The DEBS uses one propionyl-CoA as a starter unit and six (*2S*)-methylmalonyl-CoA as extender units for erythromycin A biosynthesis and comprises of one loading module, six chain-extension modules and a chain-terminating thioesterase (TE). The system is distributed on three gigantic proteins which are named DEBS 1, 2 and 3. The loading module contains an acyl transferase (AT) and an ACP domain and each chain-elongation module contains an AT, a KS and an ACP domain along with additional reductive elements such as KR, ER and DH domains. The TE catalyses the release of the aglycon from the PKS and tailoring enzymes form the fully active erythromycin A **1**.[17] The linear organisation of modules and their domains as seen in Figure 3, determine the structure of the polyketide, a feature known as the collinearity rule.[18]

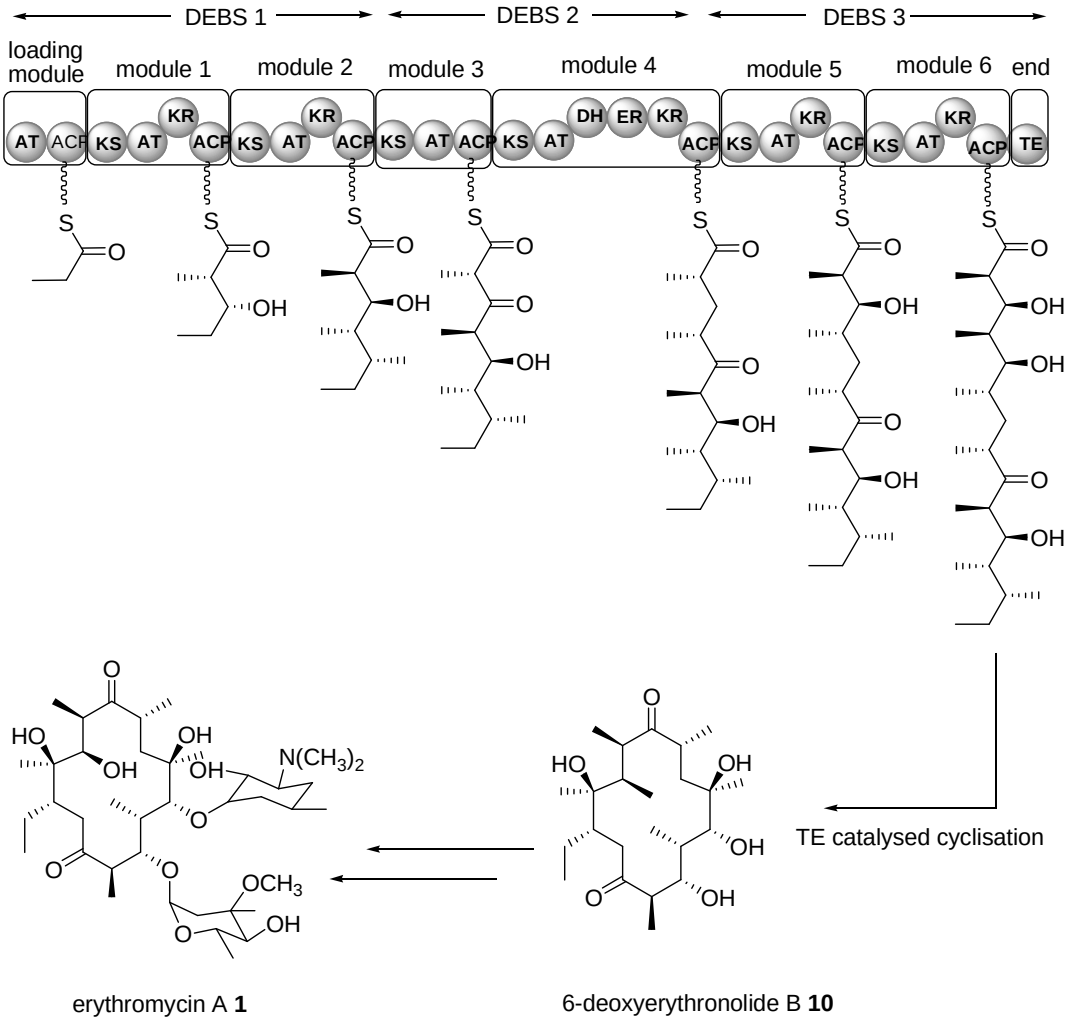

Fig. 3: The modular PKS paradigm.[4]

In this figure, erythromycin A (1) biosynthesis is used to illustrate the modular PKS reaction scheme. DEBS, 6-deoxyerythronolide B synthase; AT, acyl transferase; ACP, acyl carrier protein; KR, ketoreductase; DH, dehydratase; ER, enoylreductase; TE, thioesterase.

Iterative type I PKSs are mainly found in fungi.[19] These PKS systems exist as iterative-acting modules and each module is used in every elongation cycle.[20] In fungi, type I PKSs are responsible for the biosynthesis of the aromatic polyketide 6-methylsalicylic acid from *Penicillum patulum*[21, 22] and of lovastatin, the cholesterol lowering agent from *Aspergillus terreus*.[8, 23] More rare examples from bacteria include avilamycin from *Streptomyces viridochromogenes* Tu57.[24]

Type II PKSs comprise of multienzyme complexes that act iteratively in carbon chain elongation. The aromatic polyketide compound griseorhodin A that is investigated in the present study is synthesised by a type II PKS,[25] and therefore this type of PKS is highlighted in section 2.1.3.

Type III PKSs, also known as chalcone/stilbene-synthase-like PKSs are homodimeric enzymes that function iteratively and catalyse decarboxylation, condensation, cyclisation and aromatisation.[26] These PKSs act directly on the acyl-CoA due to the lack of an ACP.[2] Flavolin, an aromatic polyketide is synthesised by a type III PKS.[27]

2.1.3 Type II PKSs

Type II PKSs are structurally analogous to bacterial FASs consisting of several individual enzymes.[28] The investigation of polyketide assembly by type II PKSs has proven to be more difficult than other PKS types due to its multienzymatic characteristics.[6] In addition to that, the poly-β-keto intermediates are highly unstable and tend to cyclise spontaneously.[6] In the 1980s, Hopwood and co-workers pioneered genetic studies aimed at understanding the biosynthesis of polyketides using the polyketide actinorhodin as a suitable test system due to its characteristic blue color.[29] To date, the antibiotic actinorhodin PKS (*act* PKS) is the most heavily investigated example of an iterative type II PKS. The poly-β-keto chain of aromatic polyketides is synthesised by a minimal set of iteratively used enzymes, the so-called minimal PKS, each expressed from a distinct gene.[6] The minimal PKS is comprised of two KS units, KS_{α} and KS_{β}, and an ACP that serves as an anchor for the growing polyketide chain.[30] The genes encoding these proteins are usually grouped together in type II PKS biosynthetic gene clusters. However, in the biosynthetic gene cluster of griseorhodin A, the investigated gene cluster in this study, the ACP gene *grhC* is located 26 kb upstream of the ketosynthase genes *grhA* and *grhB*.[25] The structure of the nascent poly-β-keto intermediates is further processed by a KR, cyclases (CYC) and aromatases (ARO).[31] The final modifications

are carried out by post-PKS enzymes such as oxidoreductases, glycosyl transferases and methyl transferases.[8]

2.1.3.1 Minimal PKS

The minimal PKS catalyses iteratively the Claisen condensation of a starter acyl and a defined number of extension units; different starter units can be used but the extension unit is always derived from malonyl-CoA (Figure 4).[6] This is a remarkable difference to modular PKSs.[32] However, there is some speculation regarding the transfer of the malonyl extension unit and the presence of a potential malonyl-CoA:APC transferase (MCAT) in the minimal PKS. Currently, it is assumed that endogenous MCATs are recruited from FA biosynthesis due to the absence of these genes in most type II PKS gene clusters.[6, 33] More information is known concerning the roles of KSs encoded within the minimal PKS. The subunit KS_α catalyses decarboxylative condensation, while the KS_β subunit is largely responsible for the determination of the polyketide chain length and was thus termed chain length factor (CFL).[34]

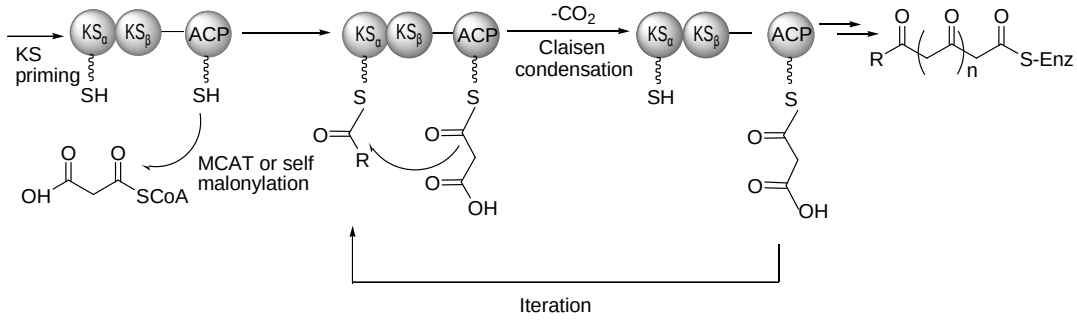

Fig. 4: Basic mechanisms of aromatic polyketide biosynthesis by type II PKS.[6]

KS_α, ketosynthase α; KS_β, ketosynthase β; ACP, acyl carrier protein; MCAT, malonyl-CoA:APC transferase.

2.1.3.2 Polyketide chain length

Investigations of the actinorhodin KS_α-KS_β crystal structure revealed an alternating α-helix and β-fold heterodimeric structure.[35] The polyketides are elongated inside an amphipathic tunnel at the heterodimer interface (Figure 5). Here, the nascent polyketide chain is protected from spontaneous

intramolecular reactions due to the steric separation of reactive keto groups.[36] A study by Tang *et al.* confirmed that the length of the chain is controlled by the interface of the KS_α-KS_β heterodimer.[35] In this study they performed structure-based mutagenesis to confirm that a small set of amino acid residues serve as gatekeepers of the tunnel. By reducing the size of these residues, two more elongation cycles were allowed in the tunnel. Therefore, filling the heterodimer tunnel is crucial for chain length elongation and by engineering the polyketide tunnel gates, novel chain lengths can be generated.[6, 35] In addition to that, a study by Xu *et al.* indicated that the size of the starter unit acts a part in the determination of the polyketide chain length.[37] The bigger or smaller the starter units are, the less or the more chain elongations are accomplished respectively. Other studies have shown that cyclases also play a role in determination of polyketide chain length and these are discussed in detail in section 2.2.1.

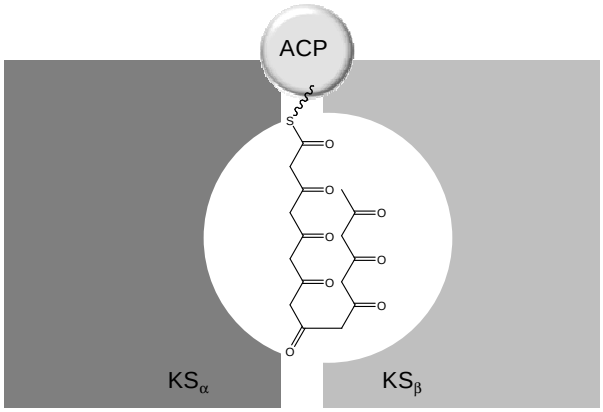

Fig. 5: Model for minimal PKS complex with chain elongation.[6]

2.1.3.3 PKS priming

Most type II PKSs utilise an acetyl as a starter unit. The biosynthesis and attachment of other starter units, such as propionate, (iso)butyrate, malonamate and benzoate have been reviewed by Moore and Hertweck.[38] Two biosynthetic pathways to starters other than of acetyl were proposed. Candidates responsible for alternative starter units are the FabH-like KSIII and an additional ACP, which have homology to proteins responsible for the biosynthesis and priming of short-chain fatty acids.[6]

FabH is an enzyme carrying out the condensation of acetyl and malonyl units in bacterial fatty acid synthesis.[39] FabH homologs are found in the biosynthetic pathways of daunorubicin (DpsC),[40] frenolicin **12** (FrnI),[41] R1128 **13-16** (ZhuH),[42] and benastatin A **17** (BenQ)[43] and are responsible for the biosynthesis and attachment of short-chain fatty acids (Figure 6). Another KSIII (HedS) was identified in hedamycin biosynthesis, which belongs to the group of pluramycin antibiotics.[44] Here, an iterative type I PKS (HedT and HedU) is used for the biosynthesis of a short-chain unit. The second hypothesis for alternative starter unit incorporation describes insertion of the malonamate and benzoate starter units by activation and transfer through an acyl-CoA ligase followed by AT-mediated transfer onto the PKS in the biosynthetic pathways of tetracycline and enterocin.[38]

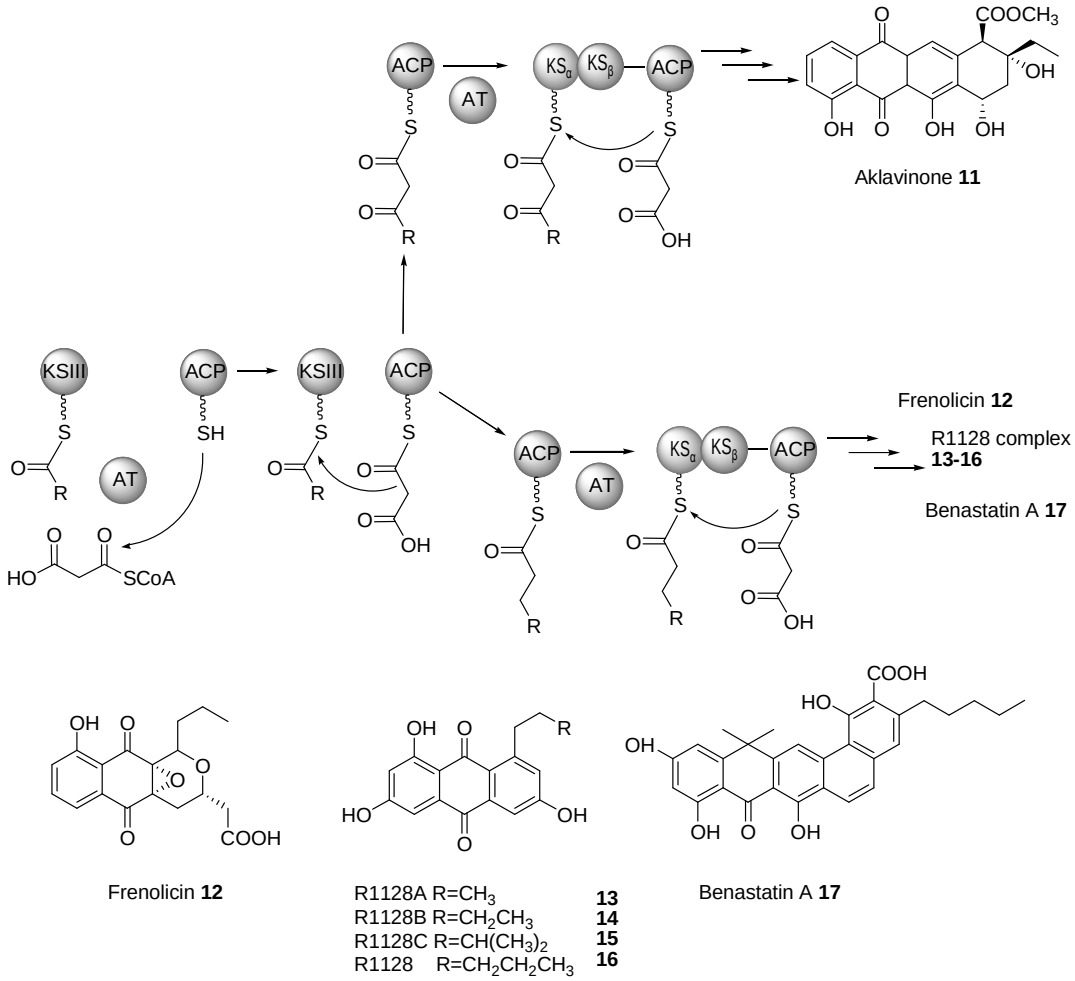

Fig. 6: PKS priming involving KSIII components.[6]

2.2 Early PKS genes

2.2.1 Type II PKS cyclases

For the production of any polyketide, the minimal PKS is always required (section 2.1.3.1). The expression of the minimal PKS results in highly reactive poly-β-keto intermediates that can undergo spontaneous cyclisation reactions.[6] Cyclases (CYC) are enzymes suppressing these spontaneous aldol reactions and hence, promote cyclisation specificity of polyketide intermediates.[31] The cyclisation process is often supported by aromatases and they dehydrate cyclic alcohols to yield aromatic rings.[6]

The regioselectivity of the first intramolecular aldol condensation must be fixed by aromatic PKS immediately upon/following completion of the polyketide chain.[31] This action also dictates the structure of the final aglycon in that it determines where the carbon backbone "turns the corner" as described by Rawlings.[32] The first cyclisation step and the corresponding cyclases are well studied, among which C7-C12 and C9-C14 cyclisations are the most common cyclisation patterns.[32] These patterns lead to the formation of the most important bacterial aromatic polyketide scaffolds, including tetracyclines, anthracyclines, tetracenomycins, angucyclines, pentangular polyketides and benzoisochromanequinones.[31] Other first ring cyclisation patterns have been observed in the presence of nonacetate starter units or longer polyketides.[45]

Analyses of deduced gene products from different type II PKSs revealed that cyclases may occur as didomain enzymes with internally duplicated motifs, such as ActVII in actinorhodin biosynthesis[41, 46] and that expression of the *N*- or *C*-termini alone resulted in loss of function. Alternatively, CYCs may also exist as bifunctional enzymes, e.g. TcmN containing both, a cyclase and an aromatase (ARO) function.[47] In various cases, these CYC domains are fused with other functionalities, e.g. CYC/MT or CYC/KR.[6] Despite the large number of cloned CYC genes, the only biochemically characterised cyclases are the TcmI cyclase[48] and TcmN cyclase/aromatase[49, 50] from the tetracenomycin pathway, and the ester

cyclases SnoaL and AknH involved in nogalamycin and aclacinomycin biosynthesis.[51]

2.2.1.1 C7-C12 first-ring cyclisation

It has been shown that the minimal PKS synthesises C7-C12 first-ring cyclisation of polyketides such as SEK4 **18** (*act* minimal PKS),[52] SEK12 **19** (*tcm* minimal PKS),[52] and a set of compounds such as TW93c **20** (*whiE* minimal PKS) (Figure 7).[45] These compounds are all derived from regioselective C7-C12 aldol condensations followed by spontaneous cyclisation of the remaining polyketide chain. The formations of SEK4 **18**, SEK12 **19** and TW93c **20** in the absence of any cyclases suggest various KS_α-KS_β have influence on product folding and promote C7-C12 cyclisation. Investigations of the act KS_α-KS_β crystal structure revealed that the tunnel (section 2.1.3.2) not only determines polyketide chain length but also directs where the linear intermediate folds in order to fit fully into the tunnel.[36] Furthermore, in the act KS_α-KS_β heterodimer, a water molecule is present in the middle of the tunnel and is proposed to act as a proton donor and to facilitate the C7-C12 aldol condensation.[31]

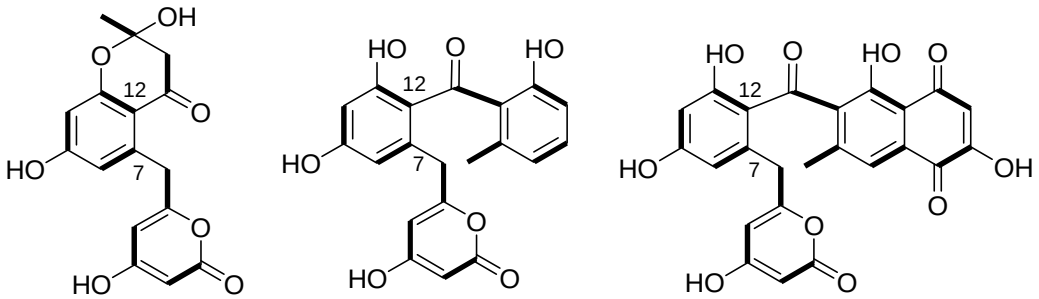

Fig. 7: Representative C7-C12 first-ring cyclisation products.[31]

Additionally, several cyclases such as ZhuI (R1128),[42] StfQ (steffimycin),[53] and MtmQ (mithramycin) have been identified that catalyse the C7-C12 first-ring cyclisation in unreduced polyketides.[54] The crystal structure of ZhuI resembles TcmN (C9-C14 first-ring cyclase from tetracenomycin biosynthesis). However, ZhuI shows a smaller substrate binding pocket and,[50] therefore, favors cyclisation of the polyketide intermediate between C7 and C12 instead of at C9 and C14.[55]

2.2.1.2 C9-C14 first-ring cyclisation

For unreduced aromatic decaketides or larger polyketides, the C9-C14 cyclisation pattern is observed.[31] TcmN is a well-studied example for a cyclase catalysing this type of cyclisation and is known to suppress the C7-C12 cyclisation of the minimal PKSs. Co-expression of *tcmN* with the *act*, *fre*, *tcm* or *whiE* minimal PKSs led to C9-C14 cyclisation products RM77 **21**,[56] PK8 **22**,[47] RM80 **23**,[56] and TW95a **24**, respectively (Figure 8).[45]

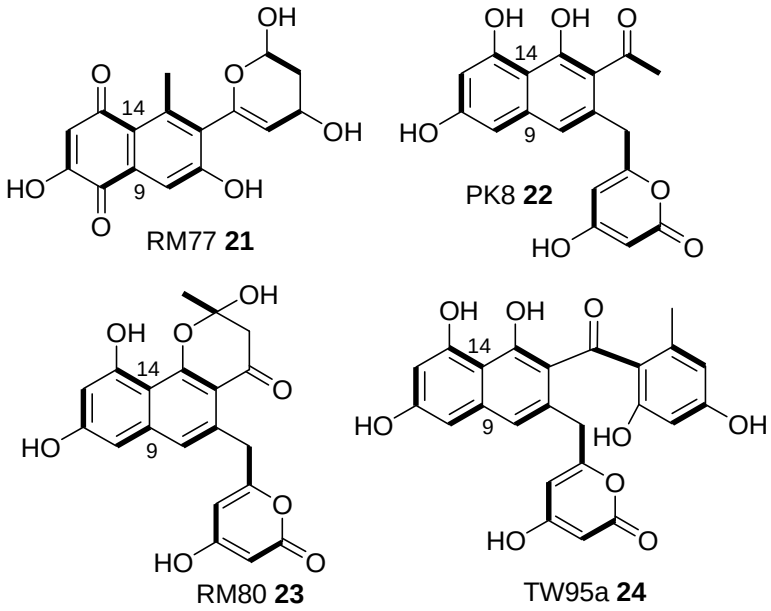

Fig. 8: Representative C9-C14 first-ring cyclisation products.[31]

In tetracenomycin biosynthesis, the *tcm* minimal PKS produces a linear decaketide intermediate that is folded, cyclised and aromatised by TcmN via aldol condensation and dehydration reactions to form the first two aromatic rings (C9-C14 and C7-C14) (Figure 9).[49] Hence, this enzyme seems to play a role in the second-ring cyclisation in longer polyketides. The *N*-terminus of the TcmN crystal structure revealed that the substrate binding pocket favors C9-C14 regioselectivity in the polyketide intermediates.[50] Docking simulation studies confirmed this result; however, docking simulations with C7-C12 regioselectivity predicted a much weaker interaction with the pocket and the polyketide intermediate. Mutagenesis

studies of TcmN residues R69 and Y35, which are essential for the C9-C14 regioselectivity, resulted in the loss of the C9-C14 regioselectivity and led to the synthesis of C7-C12 cyclised products. In comparison to the *N*-TcmN structure, the crystal structure of WhiE-OrfVI, which directs C9–C14 cyclization of dodecaketides, indicates a larger cyclization chamber that is needed to harbour a longer polyketide backbone.[50]

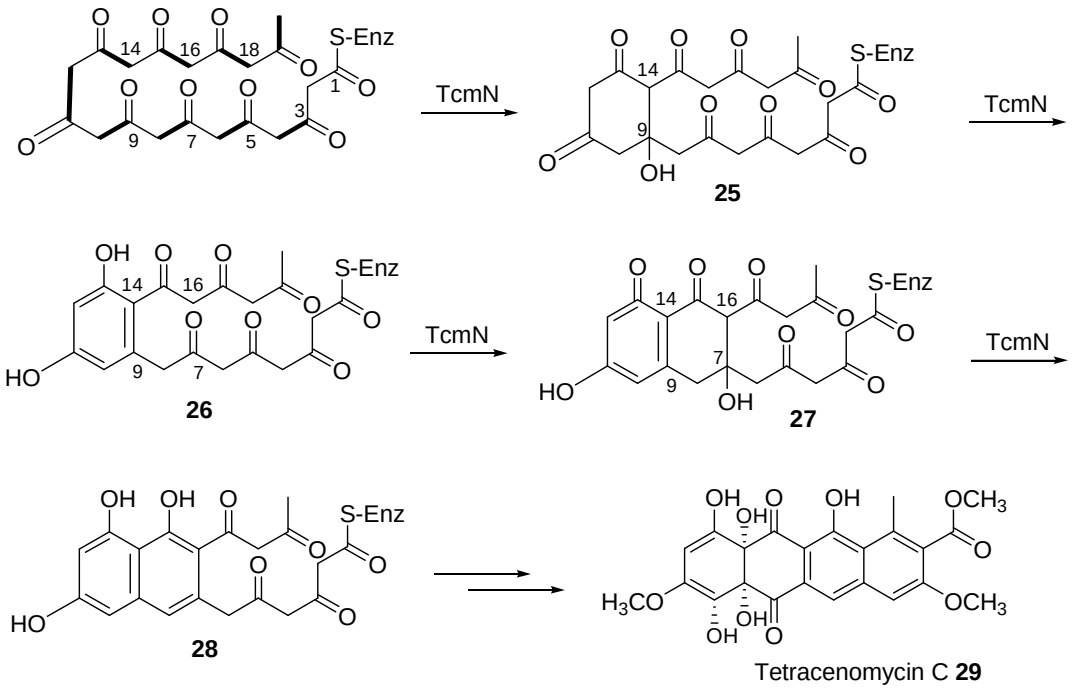

Fig. 9: C9-C14 and C7-C14 cyclisations in tetracenomycin C biosynthesis.[50]

2.2.1.3 Additional cyclisation steps

Following the initial first-ring cyclisations, the subsequent regioselective cyclisations lead to the folding of the polyketide intermediates either in a linearly fused fashion resulting in tetracyclines, anthracyclines or tetracenomycins or in an angularly fused fashion, producing angucyclines and pentangular polyketides. Both polyketide structural types possess the first-ring C7-C12 and C9-C14 cyclisation steps.

In the biosynthesis of the linear fused oxytetracycline, OxyN directs the second-ring C5-C14 cyclisation. The third ring is probably cyclised spontaneously, and so far no enzyme has been identified for the fourth-ring

cyclisation.[31] Another example for the linearly cyclised polyketides are the tetracenomycins. In the biosynthesis of tetracenomycin C **29** (Figure 10), the first- and the second-ring cyclisations are mediated by the well investigated TcmN, followed by the third-ring cyclisation C5-C18 to form Tcm F2 **30**,[57] which is either enzyme-mediated or form spontaneously. The cyclase TcmI catalyses the fourth-ring formation at C2-C19, resulting in Tcm F1 **31**.[58]

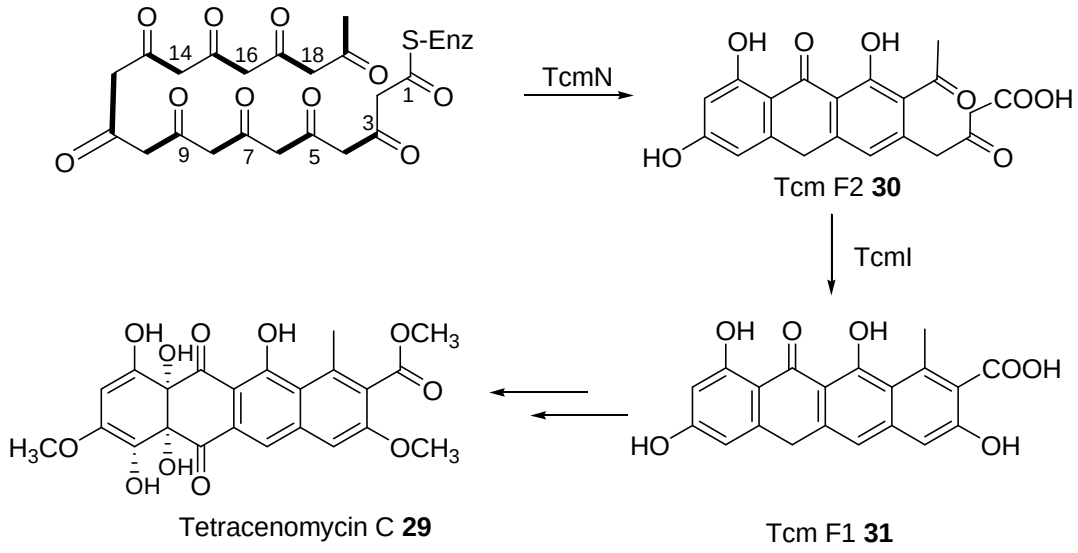

Fig.10: Linearly cyclised polyketide scheme.[31]

Tetracenomycin C biosynthesis scheme. TcmN directs the first- and the second cyclisation leading to Tcm F2 30; TcmI is responsible for the fourth-ring cyclisation resulting in Tcm F1 31.

The angularly cyclised polyketides are usually derived from backbones that are dodecaketides or longer. The third ring closure at C4-C17 in angucyclines is a critical step in differentiating the tailoring steps of anthracyclines and angucyclines. In the biosynthesis of jadomycin B **32** (Figure 11), the most well studied angucycline, the cyclase JadI (jadomycin B from *Streptomyces venezuelae*)[59] was identified and proposed to direct the angular cyclisation steps of C4-C17 and C2-C19 to form UWM6 **33**, a common angucycline intermediate leading to jadomycin B **32**.

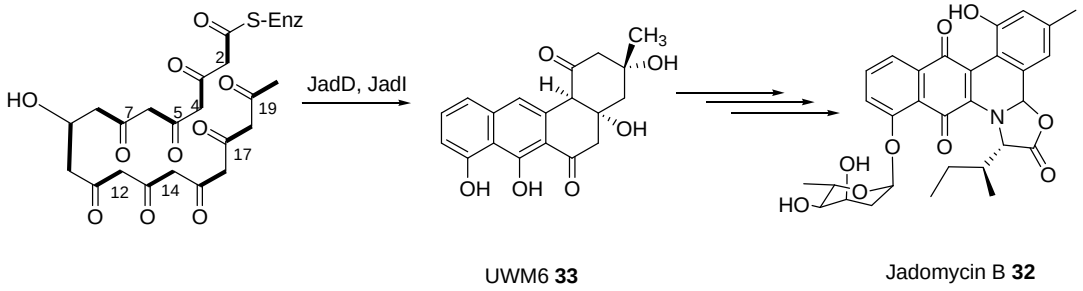

Fig. 11: Angularly cyclised polyketide scheme.[31]

Jadomycin B biosynthesis scheme. JadD directs the first- and the second ring cyclisation; JadI is proposed to dictate the angular cyclisation steps of C4-C17 and C2-C19 leading to UWM6 29 and eventually to jadomycin B 28.

The fourth-ring closure between C4 and C21 in polyketide backbones with more than 24 carbon atoms induces bending of the structure and, thereby promoting additional cyclisation such as C2-C23. This leads to the benzonaphthacene quinone skeleton common to many compounds in this family.[31] Pentangular compounds such as benastatin J **34**, pradimicin A **35**, griseorhodin A **36** and fredericamycin A **37** are examples of this cyclisation pattern (Figure 12).[31]

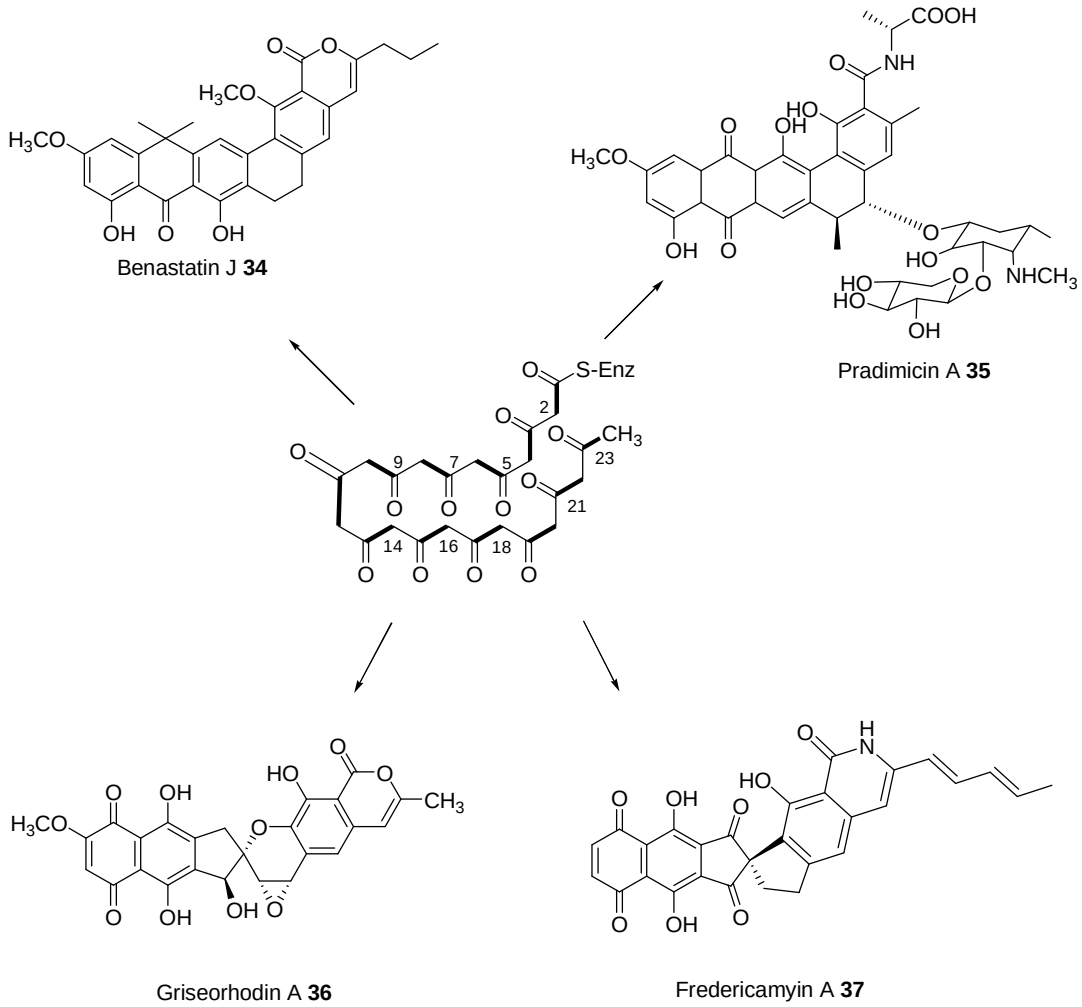

Fig. 12: Representative pentangularly cyclised polyketides with more than 24 carbon atoms.[31]

2.3 Post-PKS enzymes

The polyketide poly-β-keto chain is usually further modified by post-PKS enzymes such as oxidoreductases, reductases, glycosyl transferases and methyl transferases, resulting in highly structural diversity.

2.3.1 Oxidoreductases

Oxidoreductases are enzymes comprising of oxygenases, oxidases, peroxidases, reductases and dehydrogenases. Among these, oxygenases are the most important post-PKS tailoring enzymes, because they generate an enormous structural diversity within polyketides due to their various types of functions. In general, they carry out the incorporation of oxygen atoms into a substrate. These enzymes are divided into monooxygenases

and dioxygenases, differentiated by the number of oxygen atoms that are incorporated.[6, 60] Monooxygenases incorporate a single atom of molecular oxygen, whereas the other oxygen atom is reduced to water (Figure 13 A). Dioxygenases incorporate both atoms of molecular oxygen atoms to generate very reactive peroxides and dioxanes that further react to produce rearrangements and cleavages (Figure 13 B). The enzymes catalyse such reactions as hydroxylations, epoxidations, quinone formation and oxidative rearrangements of the Baeyer-Villiger or the Favorskii type.[6] Recently, bifunctional oxidoreductases have been identified, e.g. TcmG (monooxygenase /dioxygenase),[61] JadH (oxygenase/dehydratase),[62] and LndM2 (oxygenase/reductase).[63] In the following sections, oxygenases are described in more detail that act a part in the griseorhodin A biosynthesis.

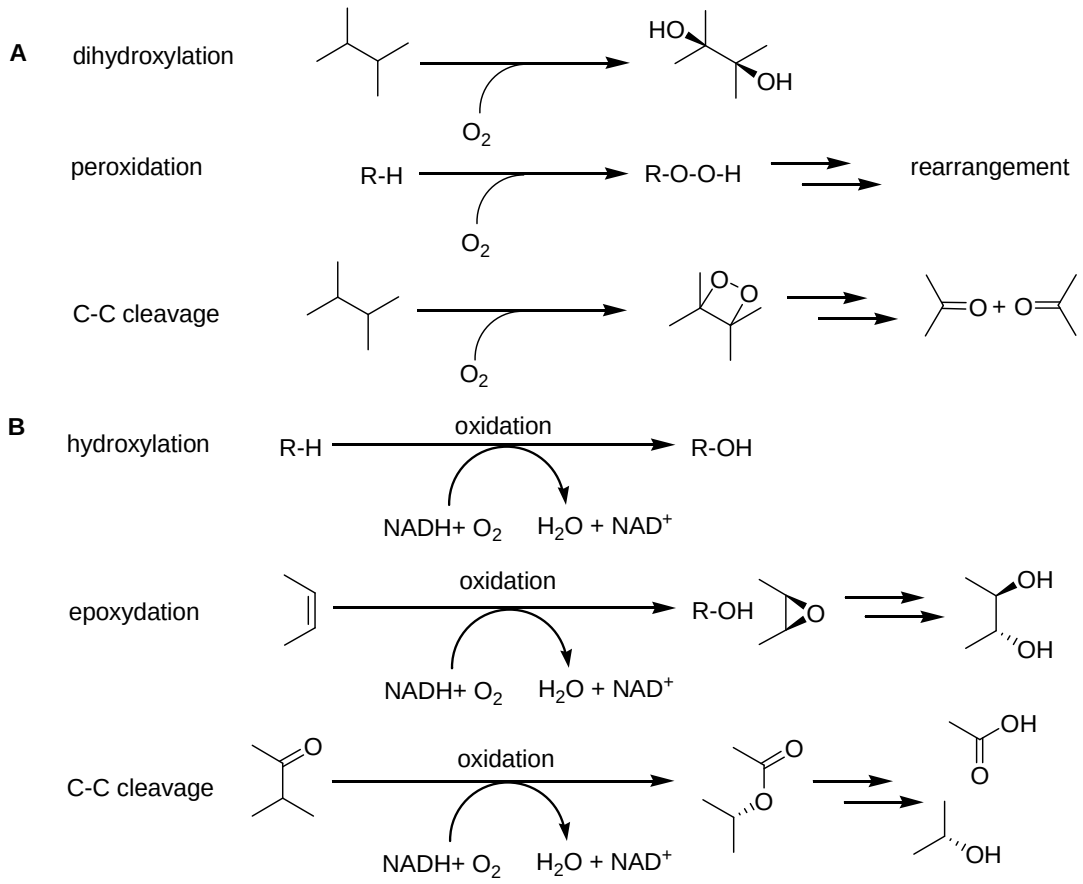

Fig. 13: Generation of structural diversity by oxygenases.[60]

Examples of immediate products of mono (A)- and dioxygenases (B), and possible follow-up reactions.

Cytochrome P-450 (CYP450) oxygenases are a diverse class of heme-containing enzymes found ubiquitous in mammals, bacteria and plants.[64] They are potent oxidants and catalyse hydroxylation of saturated carbon-hydrogen bonds, the epoxidation of double bonds, perform dealkylation reactions and oxidations of aromatics.[64] For the reconstitution of the oxygenase activity, CYP450 additionally require the presence of a NADPH-cytochrome-P-450 reductase and a ferredoxin-like iron-sulfur protein. However, these enzymes are not often clustered with the CYP450-encoding genes.[60]

CYP450 catalyses the following reaction:

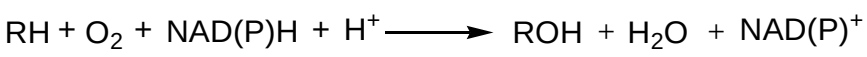

Fig. 14: CYP450 catalysed reaction.[65]

RH represents any substrate of the broad substrate specificity of CYP450. Many of the substrates are harmful lipophilic compounds such as polycyclic aromatic hydrocarbons, chlorinated diphenyls and steroids that are hydroxylated by CYP450 for better degradation or excretion.[65]

To date, only few CYP450 monooxygenases have been described in the context of bacterial aromatic polyketide biosynthesis. EncR, a CYP450 monooxygenase from enterocin biosynthesis, catalyses the hydroxylation step from desmethyl-5-deoxyenterocin **47** to the final product enterocin **48**, assisted by the translationally coupled ferredoxin-like EncQ (Figure 17).[66] Another example is a CYP450 monooxygenase DoxA from daunorubicin and doxorubicin biosynthetic pathways that catalyses hydroxylations on C-13 and C-14 positions of anthracyclines.[67]

Flavin-dependent oxygenases catalyse oxidations and hydroxylation reactions and are involved in dehydrogenation reactions and are also involved in light emissions and in one- and two-electron transfers.[68-70] They are highly regio- and/or enantioselective and employ a purely organic

cofactor flavin adenine dinucleotide (FAD) **41**.[71] For reactivity with molecular oxygen the co-factor has to be in the reduced form **38**. The biocatalysis begins with the reduction of the bound FAD **41** by NADPH to **38** which is then oxygenated using molecular oxygen to form peroxyflavin **39** (Figure 15).[71] FAD-dependent monooxygenases are able to stabilise peroxyflavin to hydroperoxy species **40** and prevent peroxyflavin from decay as it is unstable and otherwise decays to form hydrogen peroxide and oxidised flavin **42**. Depending on the protonation state of the peroxyflavin **39**, either a nucleophilic **39** or electrophilic attack **40** on the substrate occurs. Finally, a single atom of molecular oxygen is incorporated into the substrate, while the other oxygen atom is reduced to water. The cycle ends with the dissociation of the product and the co-factor from the enzyme.[71, 72]

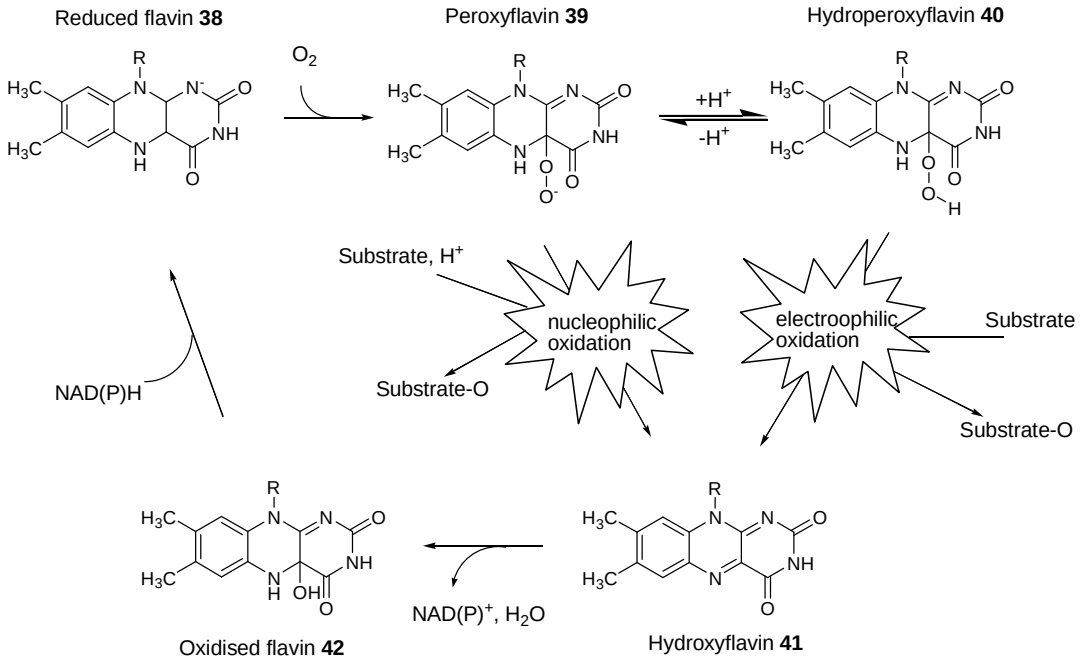

Fig. 15: General mechanism of oxygenation reactions by external flavoprotein monooxygenases.[71]

R = Ribitol adenosine diphosphate.

In the flavin-dependent oxygenases, the FAD cofactor is usually non-covalently bound, but there are also oxygenases where it is covalently bound. For example, the vanillyl-alcohol oxidase contains FAD linked to a

histidine.[73] It was shown that the covalent linkage enhances the oxidative power of the flavin cofactor. Another example for covalently bound oxidases is EncM in enterocin biosynthesis as shown in Figure 17. In polyketide biosynthesis, additional reactions that increase structural diversity include hydroxylations, epoxidations and Baeyer-Villiger oxidations and Favorskii rearrangements.[38, 74-76] TcmG, a monooxygenase/dioxygenase from tetracenomycin biosynthesis, carries out a triple hydroxylation of tetracenomycin Tcm A2 to form tetracenomycin C **29**.[61] The Baeyer-Villiger monoxygenases (BVMOs) catalyse molecular oxygen reactions as described above. The best studied BVMO, a cyclahexanase monooxygenase isolated from an *Acinetobacter*, catalyses the reaction of cyclohexanone and a "Criegee" intermediate leading to a formation of a lactone **45** (Figure 16).[72, 76]

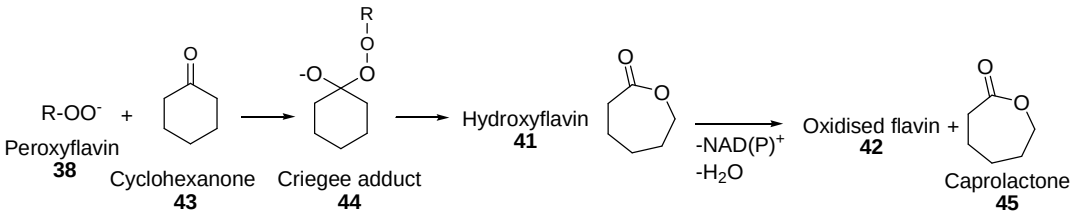

Fig. 16: Mechanism of the BVMO cyclohexanose monooxygenase.[72]

BVMOs are the most common FAD-dependent oxygenases in type II PKSs. In mithramycin biosynthesis, the tetracyclic intermediate premithramycin B is formed and further processed to a tricyclic mithramycin precursor by the BVMO MtmOIV, which finally results in the active mithramycin after a decarboxylation.[77] Other BVMOs have been characterised in biosynthesis of urdamycin A (UrdM)[78, 79] as well as JadF, JadH and JadG from jadomycin A biosynthesis.[80]

To date, only one example of a Favorskii-type oxidative rearrangement is described, namely EncM that is involved in enterocin **52** biosynthesis (Figure 17).[75] EncM uses **47** as a substrate to form the 11,12,13-trione intermediate **49**. In addition, EncM acts as a dioxygenase and oxidatively

cleaves **48** to **49**. EncM also catalyses the Favorskii-like rearrangement and facilitates aldol condensations and two heterocycle-forming reactions in the formation of desmethyl-5-deoxyenterocin **51**.

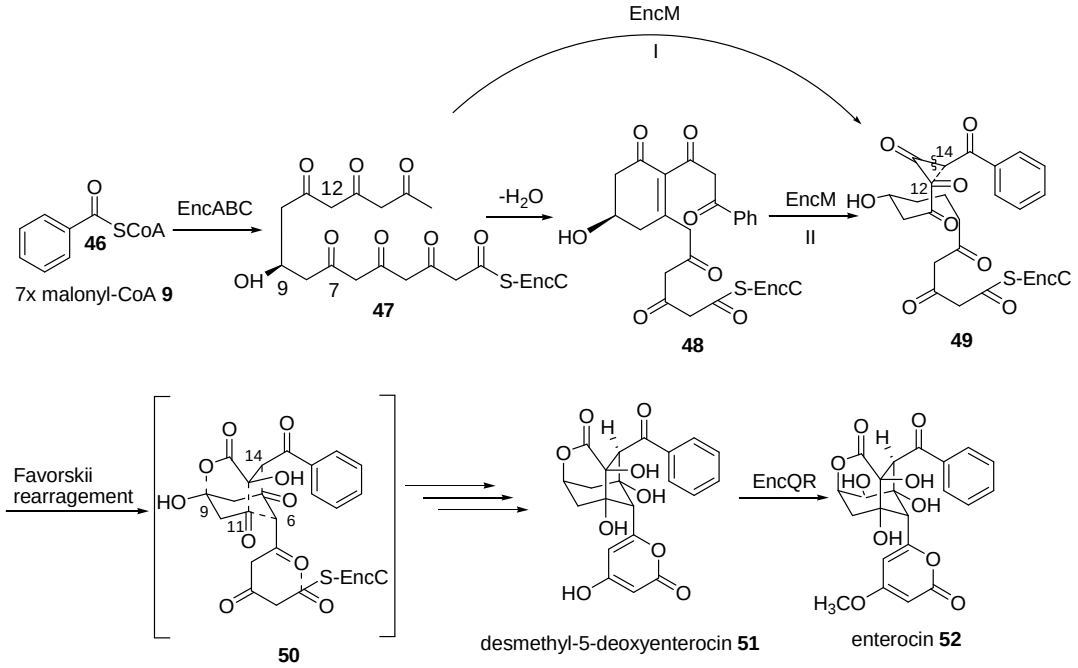

Fig. 17: Proposed biosynthetic pathway of enterocin.[75]

In compounds 47-50, the carbon numbering is based on linear 47 in which priority is given to the carboxyl carbon; the numbering of 51 and 52 is defined for enterocin and its derivatives. Dashed lines in structures 49 and 50 represent newly created bonds.

Ketoreductases catalyse the stereospecific hydrogen transfer from NAD(P)H onto a keto group, leading to a formation of an alcohol. Most of the aromatic polyketides are reduced by a KR during the polyketide backbone assembly.[32] The growing acyl chain is folded due to a transition from sp^2 to sp^3 hybridisation and reduced, respectively, at the keto group nine carbons (C9) from the final position of thioester carbonyl.[6] This strict regiochemistry is independent from the polyketide chain length as well as from the nature of the starter unit. The extensively studied *act* KR reduces polyketide backbones of nearly all lengths.[32] Another type of KR was observed during enterocin biosynthesis, where ketoreduction by EncD takes place during polyketide assembly.[81] Ketoreduction can lead to the formation of a chiral carbon centre as was observed in doxorubicin from *S.*

peucetius. Its C-17 keto group is stereospecifically reduced by the aklaviketone reductase DnrH.[82]

2.3.2 Transferases

Transferases catalyse transfer reactions and are comprised of methyl transferases (MT), alkyl transferases, acyl transferases, amino transferases, glycosyl transferases (GT) and kinases.[60] They introduce novel functional groups such as methyl, acetyl, sugar and phosphate moieties and hence, the characteristics of a molecule and even the biological activity are modified in this manner (Figure 18).[60, 83] In the following, GTs and MTs, the most important transferases in the context of polyketide synthesis,[60] are described.

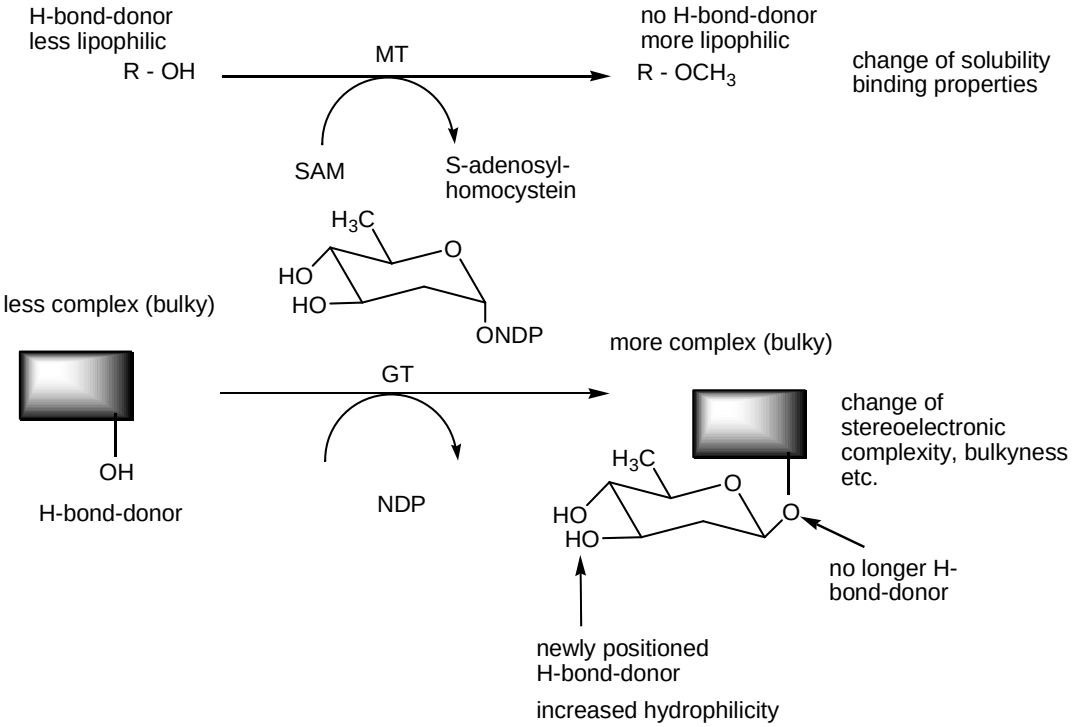

Fig. 18: Possible effects of group transferases on the biological activities.[60]

Effects of manipulation of methyl- and glycosyltransferases, MT = methyltransferase, GT = glycosyltransferases, SAM = *S*-adenosyl-L-methionine, NDP = nucleoside diphosphate. In arrow-direction: recombination with a gene encoding additional enzyme; against arrow direction: gene inactivation experiment.

GTs attach sugar moieties to the polyketide aglycons by catalysing the sugar transfer from an NDP-activated sugar donor to an acceptor molecule.[84] Most of the sugars belong to the 6-deoxyhexane (6-DOH) family and are linked to the aglycone as saccharides of variable sugar

lengths.[85] Through sugar attachment, the structural diversity of polyketides is increased and often modulates the biological activity of natural products.[85, 86]

MTs use SAM as a cofactor to methylate nitrogen, carbon, sulfur and oxygen atoms.[6] The methyl transfer occurs via an S_N2 mechanism that has a steric impact on methylations, especially on the *C*-methylation in generating a chiral centre.[6] In addition, *O*- (DnrK from *S. peuceticus*) and *N*-methylations increase the lipophilicity of a molecule and remove hydrogen-bond sites.[60] The methylation reactions take place at the polyketide-derived-aglycon moiety or on sugar residues, either prior to or after the glycosyl transferase step.[60]

2.4 Ongoing search for novel bioactive metabolites

To date, most bioactive metabolites are found from soil microorganisms and about half of all of these compounds are produced by the actinomycetes, mainly by the genus *Streptomyces*.[87, 88] Furthermore, bioactive metabolites have been isolated from marine actinomycetes as well, suggesting such marine bacteria organisms as a second potential niche for discovering novel drugs.[89-91] Due to the emergence of multi-drug resistant microbes, it is significant to discover novel drugs for the treatment of microbial, fungal and parasitic infections.[92] Furthermore, anti-cancer therapies require novel anti-tumour compounds with fewer side effects and improved therapeutic properties.[93] In the following, several approaches in the discovery of novel drugs are discussed.

Novel natural products can be discovered e.g. by intensive screening.[94] An example for this is the antibiotic platensimycin, produced by *S. platensis*. The compound was identified through a systematic screening of natural product extracts and belongs to a previously unknown class of antibiotics.[95, 96]

More recent methods in novel bioactive natural product discovery involve genome mining and metagenomic approaches. Genome mining uses bioinformatics to predict the presence of potential natural product biosynthesis genes in microbial genomes.[97] In metagenomics, genetic

material is directly recovered from environmental samples and enables so access to organisms that are not (easily) cultured in laboratory.[98] These techniques allow accession to yet, undiscovered cryptic, inactive and/or intractable biosynthetic gene clusters in their native hosts.[99] These gene clusters subsequently can be identified, cloned and heterologously expressed efficiently in more suitable host organisms. [100]

A very useful method that is widely applied in drug discovery is genetic engineering. It can be applied to manipulate biosynthetic pathways to increase the chemical diversity and bioactivity of natural products.[12] Inactivation of specific biosynthetic genes lead to mutants that accumulate different compounds with possible improved pharmacological properties, e.g. increased biological activity.[101] Isolation and structure elucidation of such compounds then allow the functional analysis of the involved enzymes. Oviedomycin from *S. antibioticus* ATCC 11891[102] exhibits *in vitro* anti-tumour activity and induces apoptosis in cancer cell lines.[103, 104] During the inactivation of oxygenase genes, two new metabolites were produced with improved anti-tumour activity compared to oviedomycin.[104]

In combinatorial biosynthesis, biosynthetic pathway genes are combined and/or replaced to produce “unnatural” natural products in a mix-and-match fashion.[32, 105] This method results in novel molecules never encountered in nature and therefore represents an important new source of chemicals for use in drug discovery.[106, 107] David Hopwood and co-workers combined different antibiotic gene clusters, medermycin or granaticin, with actinorhodin to produce the first hybrid aromatic polyketide mederrhodin.[108] Since then, many type II PKS systems have been found and characterised, leading to the production of hybrid metabolites.[28, 32] Combinatorial biosynthesis has been successfully applied in post-PKS steps such as oxidation, *O*-methylation or glycosylation.[60] For example, through co-expression of the doxorubicin genes with a sugar gene *eryBIV* from the erythromycin cluster in *S. peucetius* ATCC 29050, the anti-cancer agent derivative epirubicin, previously generated by semisynthesis, was produced for the first time using fermentation.[109]

While combinatorial biosynthesis has been widely used for post-PKS genes, there are studies revealing the potential of combinatorial biosynthesis for exploiting the early biosynthetic type II PKS genes such as minimal PKSs and cyclases. Through exchange of cyclases, the cyclisation patterns of polyketides can be influenced.[110] Furthermore, spontaneous cyclisations take place through expression of only the minimal PKS in the absence of cyclases, as was shown by study of Shen and co-workers.[111] The expression of *whiE* minimal PKS in *S. coelicolor* resulted in a diverse substance library comprising more than 30 polyketides differing in chain lengths and cyclisation patterns (Figure 19).[111] To date, this is the largest and the most complex substance library produced by combinatorial biosynthesis. However, these kinds of systems are rare and have not yet been investigated in this respect.

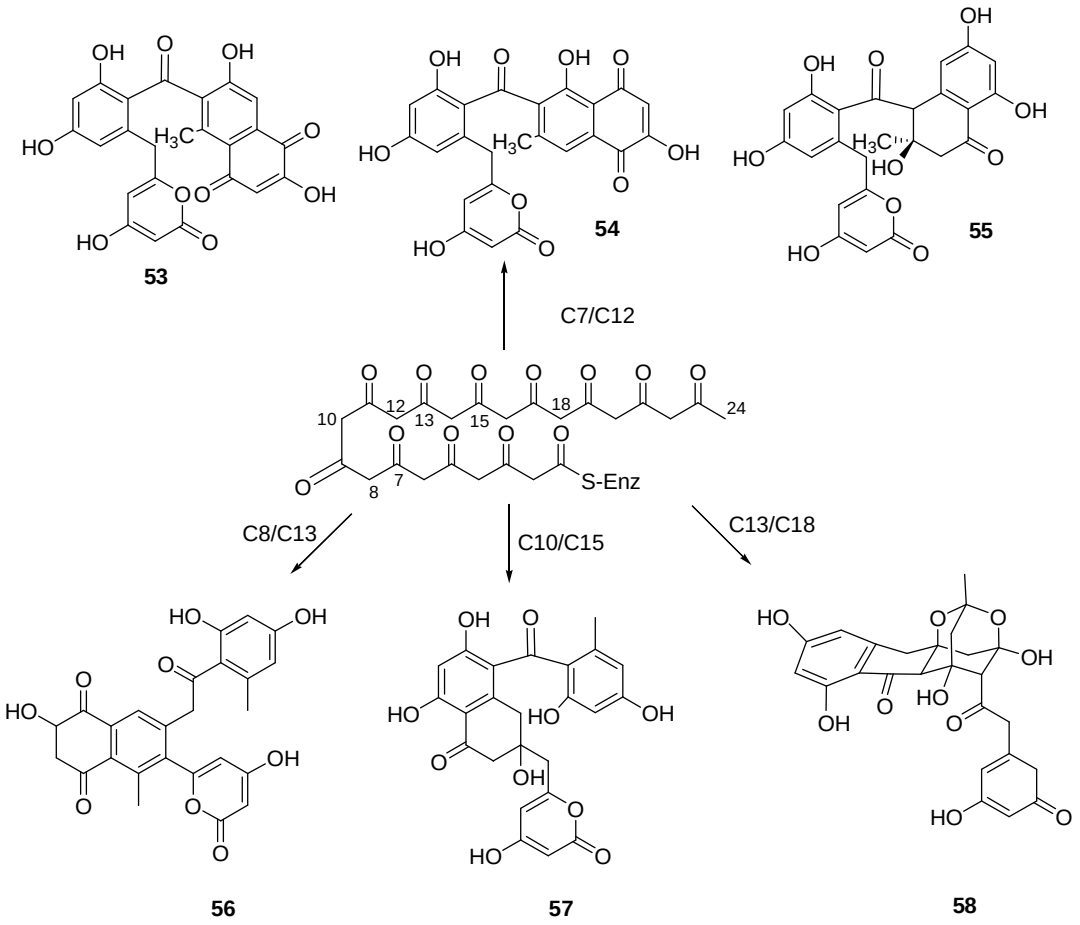

Fig. 19: Representative polyketide structures through the expression of the *whiE* minimal PKS.[45]

The numbers represent the cyclisation topologies of the first rings.

Furthermore, the primer unit of a polyketide backbone is an attractive site for introducing unnatural building blocks resulting in novel structures. Genes encoding for KSIII-like enzymes are found in frenolicin, R1128 and hedamycin (section 2.1.3.3). In the biosynthesis of R1128, the *zhu* PKS uses butyryl, valeryl and 4-methyl starter units; its loading complex comprises of a KS (ZhuH), an AT (ZhuC), and an additional ACP (ZhuG).[42] Khosla and co-workers engineered modified aromatic polyketides by recombination of the R1128 loading complex with the *act* and *tcm* minimal PKSs (Figure 20).[112] The expression of the *act* minimal PKS alone leads to the octaketide DMAC **59**. Co-expression of the *act* minimal PKS and the *act* KR with the R1128 initation module resulted in two novel hexaketide structures YT46 **60** and YT46b **61**. The *tcm* minimal PKS produces octa- and decaketides when expressed alone. Co-expression with the R1128 iniation module and the *act* KR, ARO and CYC genes leads mainly to octaketide-DMAC derivatives YT127 **62** and YT127b **63**. Incorporation of bigger building blocks resulted in fewer chain length elongations, whereas the chain length stays the same. Similar results were produced by the deletion of BenQ in the benastatin A gene cluster.[43] The starter units were recruited from FA biosynthesis and incorporation of the butyryl starter unit led to an additional chain elongation step.

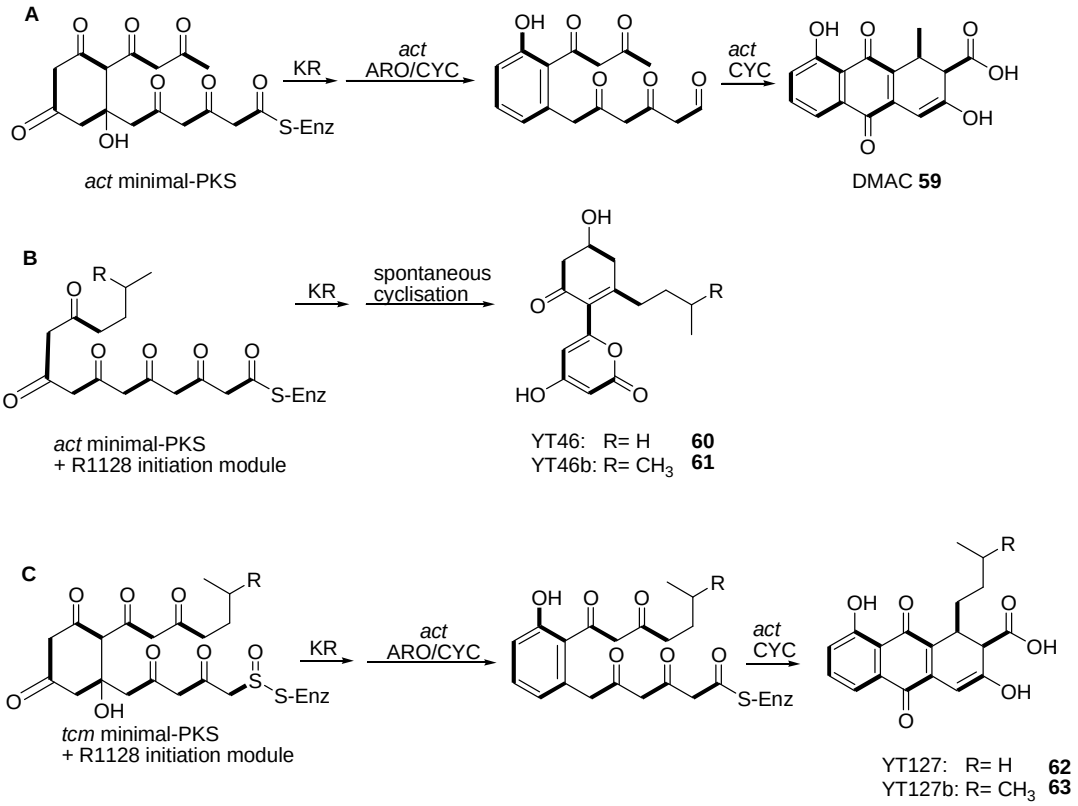

Fig. 20: Engineered biosynthesis of aromatic polyketides.[112]

(A) Actinorhodin (*act*) minimal PKS

(B) *act* minimal PKS and R1128 initation module

(C) Tetracenomycin (*tcm*) minimal PKS and R1128 iniation module

ARO, aromatase; DMAC, dihydroxymethylanthraquinone; bold bindings represent acetate units.

In the biosynthesis of griseorhodin A, a successful combinatorial biosynthetic approach was carried out by complementing the griseorhodin A minimal PKS by co-expressing the benastatin A minimal PKS; BenA (KS_α), BenB (KS_β), BenC (ACP) and BenQ (KSIII homolog). BenQ is responsible for selection of the hexanoyl starter unit in benastatin A biosynthesis (section 2.1.3.3). The expression resulted in the successful production of the novel polyketide hybrid benarhodin A **65** (Figure 21).[1]

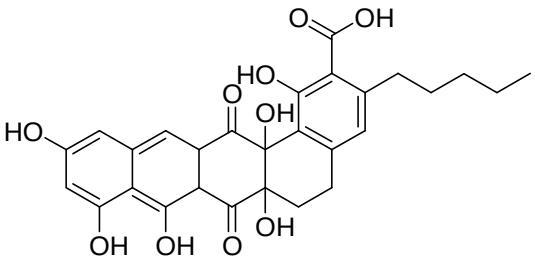

Benarhodin A **65**

Fig. 21: Benarhodin A.[1]

So far, combinatorial biosynthesis has been demonstrated as a powerful method for generating versatile natural products.[113] However, several technical bottlenecks in this approach still exist.[114] In addition, often narrow substrate specificities play significant roles affecting optimal biosynthesis of compounds. A general lack of suitable heterologous expression systems limits genetic engineering of interesting metabolic pathways. Therefore, further investigations are necessary to overcome these challenges.

2.5 Griseorhodin A

Griseorhodin A was first isolated from *S. griseus* JA2640 extracts and its biological activity was described by Treibs and Eckardt in 1961.[115] The structure was elucidated in late 1970s,[116, 117] and the absolute configuration of griseorhodin A was determined in 2008.[118]

Griseorhodin A is a tridecaketide and belongs to the rubromycin family (Figure 22).[119] Most rubromycins are strong inhibitors of human telomerase and retroviral reverse transcriptase.[120, 121] They possess an aplanar, axially chiral structure due to the presence of a highly unusual spiroketal moiety.[122] This pharmacophore is responsible for its inhibition, as an open spiroketal decreases the activity by two orders of magnitude as seen in α-rubromycin.[120]

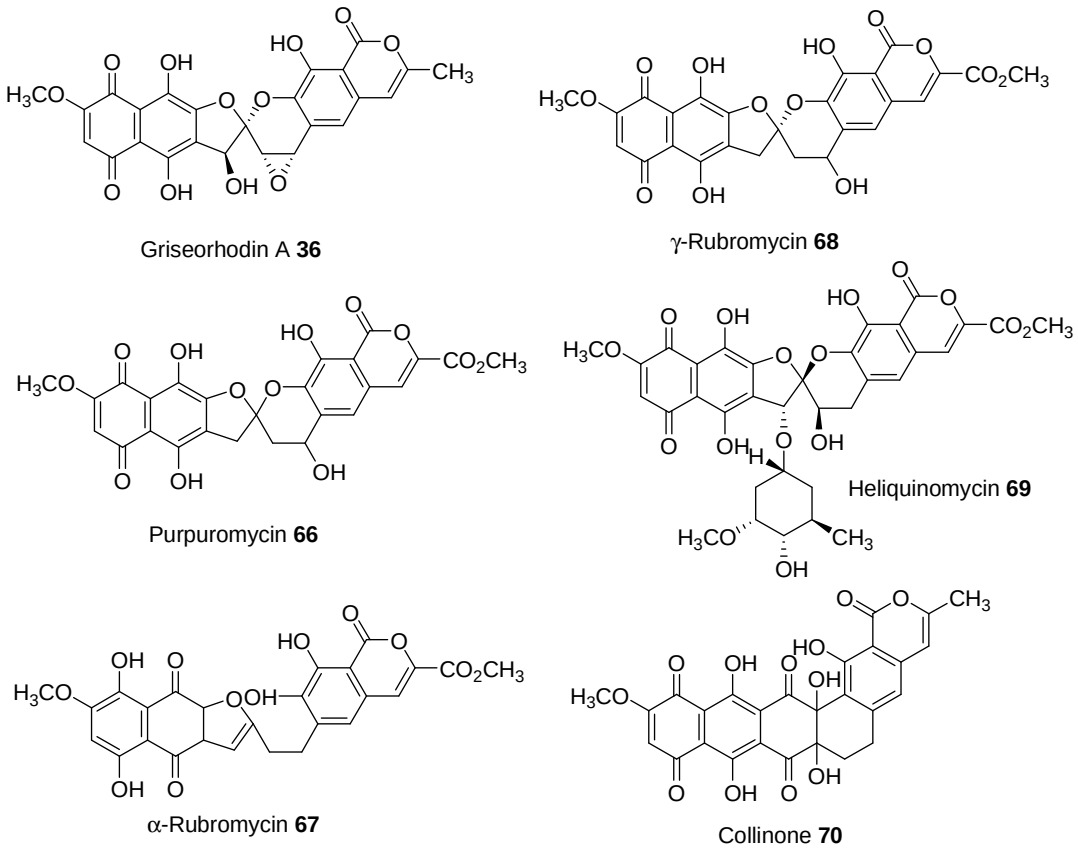

Fig. 22: Representative members of the rubromycin family.[119]

During a study on bacterial symbionts of marine invertebrates, a bacterial strain, Streptomyces sp. JP95, was isolated from the marine tunicate *Aplidium lenticulum* and was found to produce a number of rubromycin-type compounds with griseorhodin A as the major compound.[25] A DNA cosmid library was constructed, resulting in the isolation of the griseorhodin A gene cluster. For heterologous expression, the gene cluster was cloned into an *E. coli-Streptomyces* shuttle cosmid pMP31 and successfully expressed in *S. lividans* and *S. albus*.[25]

The griseorhodin A biosynthetic cluster is 34.2 kilobases (kb) in length (Figure 23). The gene cluster is comprised of 33 open reading frames (ORF) encoding a type II minimal PKS (ACP and KS_α-KS_β), cyclases (GrhE, GrhQ and GrhT), and enzymes involved in regulation, resistance and post-PKS tailoring activities (11 redox-tailoring enzymes, several FAD-

dependent monooxygenases, one NADPH:chinone oxidoreductase, one CYP-450 oxygenase and two KRs).[25]

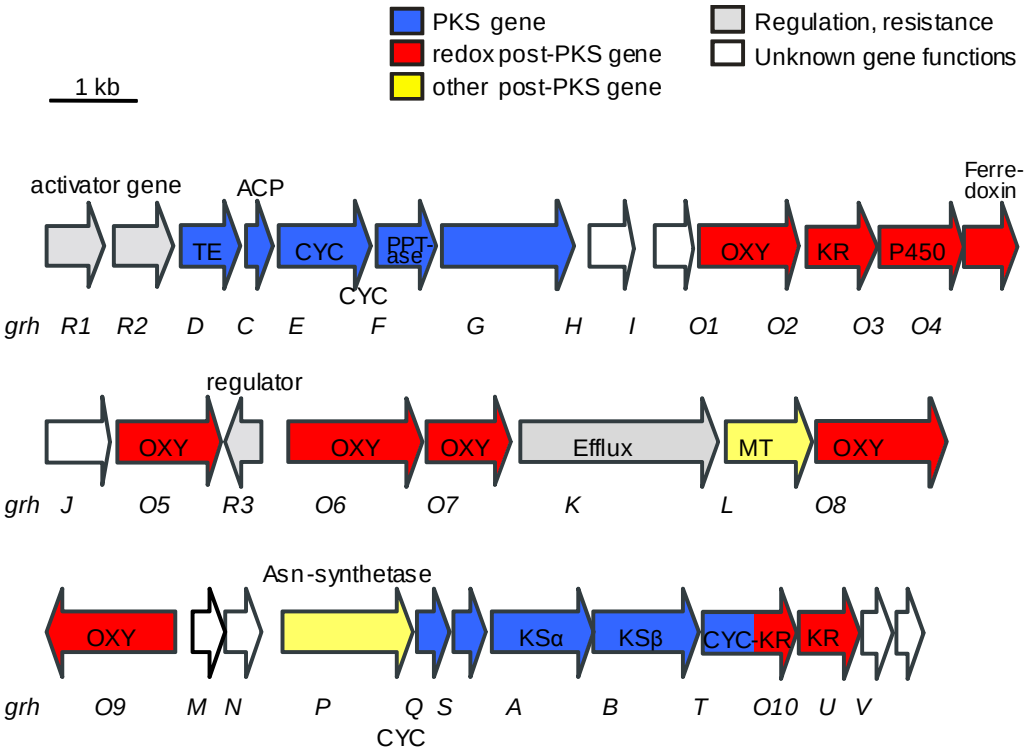

Fig. 23: Organisation of the *grh* biosynthetic pathway gene cluster.[25]

Every arrow represents the direction of the transcription of an open reading frame (ORF)

In year 2009, griseorhodin A biosynthesis was postulated by gene knock-outs and analysis of the corresponding intermediates (Figure 24).[1] After formation of the poly-β-keto chain, early oxidation/cyclisation/methylation steps take place at the same time and/or in parallel routes on a multi-enzyme complex. At this stage, collinone **70**, is formed and three carbon-carbon bonds are cleaved by GrhO5 in cooperation probably with GrhO1 leading to the spiro compound lenticulone **71**. A further carbon-carbon bond is cleaved to reduce a six-membered ring by one carbon unit by GrhO6 and GrhJ, respectively, generating 7,8-dideoxy-6-oxogriseorhodin C **72**. The reduction of the keto functionality of 7,8-dideoxy-6-oxogriseorhodin C takes place, and the enzymes GrhO3 and GrhO7 catalyse the epoxidation of dideoxygriseorhodin C **73** leading to the polyketide griseorhodin A **36**. Herewith, many of the Grh enzyme functions have now been elucidated but the enzymes catalysing the early steps remain uncharacterised.

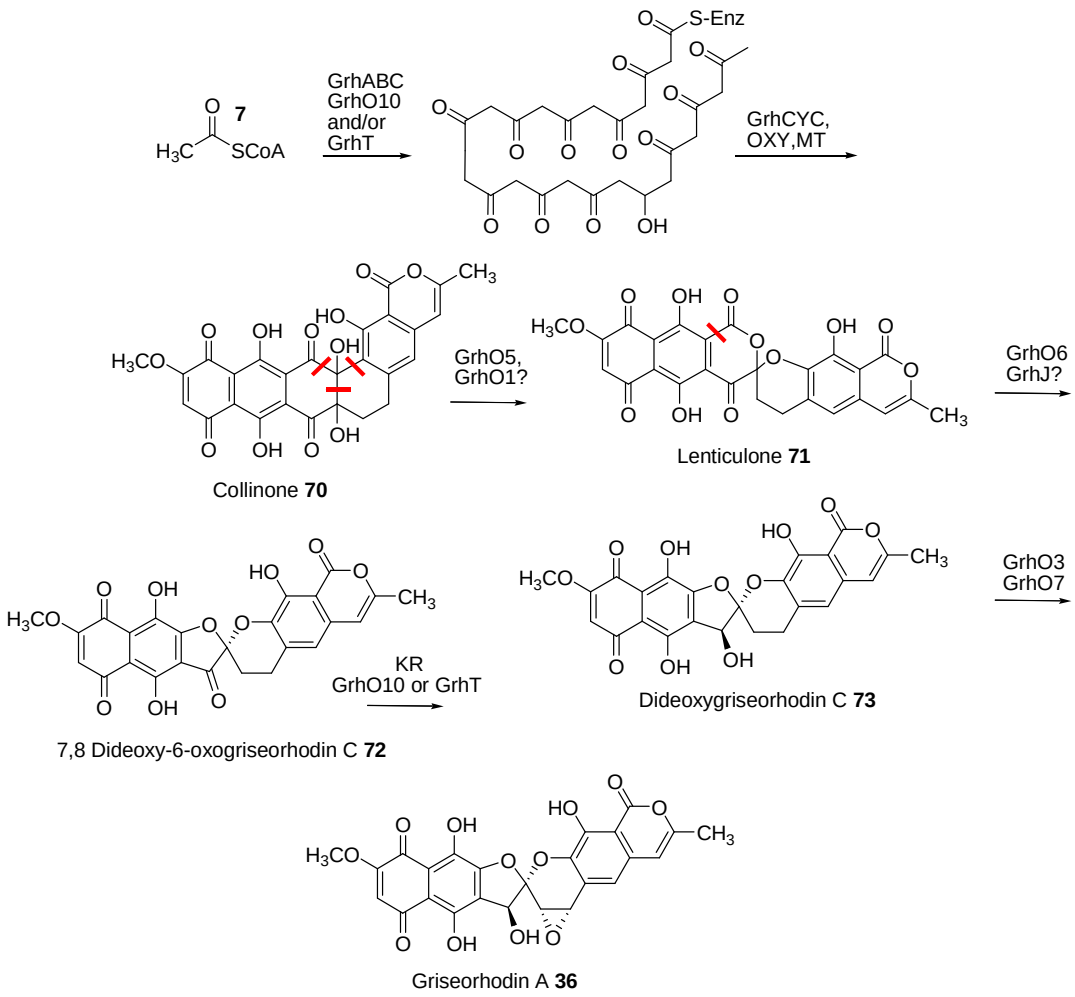

Fig. 24: In year 2009 postulated *grh* biosynthetic pathway (red lines indicate the carbon-carbon bonds cleaved during the biosynthesis).[1]

3 Aims of the study

Previous studies by Dr. Kathrin Reinhardt and Zeynep Yunt characterised the griseorhodin A post-PKS enzymes and gave insights concerning the interesting post-PKS steps, especially how the spiroketal moiety is formed;[1, 123] this functionality is responsible for the telomerase inhibiting activity of griseorhodin A.[1, 120]

However, some enzymes still remained uncharacterised in griseorhodin A biosynthesis. Two of them, GrhU and GrhV, are further investigated in the present study by gene knock-outs and investigations of the accumulated compounds by high pressure liquid chromatography (HPLC), LH20 chromatography, mass spectrometry (MS) and nuclear magnetic resonance (NMR)

A further goal was to gain deeper insights into the early biosynthetic steps of griseorhodin A biosynthesis. The early steps in griseorhodin A biosynthesis are encoded by minimal PKS genes, *grhC*, *grhA*, *grhB* and the three cyclase genes *grhE*, *grhQ* and *grhT*[25]. In the present study, the generated mutants of the early griseorhodin A genes are investigated by conjugation and heterologous expression in the host organism *S. albus* and analysed for the production of secondary metabolites by HPLC, HRMS and NMR.

Thus, the main aims of the study were:

- To analyse secondary metabolite production of the *ΔgrhU* and *ΔgrhV* mutants
- To isolate and analyse the secondary metabolites produced by the *ΔgrhU* and *ΔgrhV* mutants to characterise their functions in griseorhodin A biosynthesis
- To subclone the suspected early griseorhodin A biosynthetic genes into a suitable vector for the heterologous expression in the host organism *S. albus*

- To generate gene knock-outs by deleting cyclases and all tailoring genes on the cosmid pMP31 using homologous recombination technique for heterologous expression in the host organism *S. albus*
- To propose a biosynthetic model from the obtained genetic and chemical data

4 Results and discussion

4.1 Characterisation of the early griseorhodin A genes

In the present study, heterologous expression was applied to investigate the early griseorhodin A biosynthetic steps by combining the *grh* minimal PKS and *grh* cyclase genes from the griseorhodin A biosynthetic gene cluster. Several previous studies have revealed that minimal PKSs expressed alone are able to generate metabolite shunt products.[45, 52] To date, the most impressive minimal PKS compound library was obtained by expressing the *whiE* minimal PKS, resulting in a diverse library comprising more than 30 polyketides differing in chain lengths and cyclisation patterns.[45] The addition of cyclase genes to the minimal PKS genes could lead to more advanced polyketides and give insights into the formation of specific polyketide ring structures, as was the case in the expression of the *whiE* minimal PKS with *whiE* cyclase genes.[45]

4.1.1 Sequence analysis of the early-stage griseorhodin A biosynthetic proteins

Table 1 lists the comparative results for GrhC, GrhE, GrhQ, GrhA, GrhB and GrhT with known sequences in the NCBI database using BLAST analysis (search with blastp).

Table 1: Proposed functions of the ORFs shown in Figure 23.

Protein	AS	Proposed function	Protein/organism/ accession number	Similarity/ Identity [%]
GrhC	86	ACP	ORF3, *S. rochei*[124]/ BAA87909	63/58
GrhE	323	CYC	SimA5, *S. antibioticus*[125]/ AF324838	51/35

GrhQ	123	CYC	RubE, *S. collinus* (unpublished)/ AGG03065	89/78
GrhA	426	KS_{α}	RubA , *S. collinus* (unpublished)/ AGG03067	91/85
GrhB	420	KS_{β}	RubB, *S. collinus* (unpublished)/ AGG03068	83/77
GrhT	402	Bifunctional CYC-3-oxoacyl-ACP reductase	RubF, *S. collinus* (unpublished)/ AGG03070	77/69

All of the homologues encode for known proteins that were subsequently cloned for heterologous expression.

4.1.2 Clone constructions for the minimal PKS and cyclase expressions

In order to investigate the role of genes *grhC*, *grhA*, *grhB*, *grhT*, *grhE* and *grhQ*, each gene was individually PCR amplified from the cosmid pMP31 containing the complete *grh* gene cluster (Appendix 8.1). They were cloned with their native ribosomal binding sites (RBSs) and with integrated restriction sites *Mfe*I and *Eco*RI into the *E. coli* cloning vector pBluescript SK+ (pSK+) and subsequently into the integrative *E. coli-Streptomyces* shuttle vector pKJ55. PCR conditions were optimised for each step, and the products were confirmed by gel electrophoresis (Figure 25).

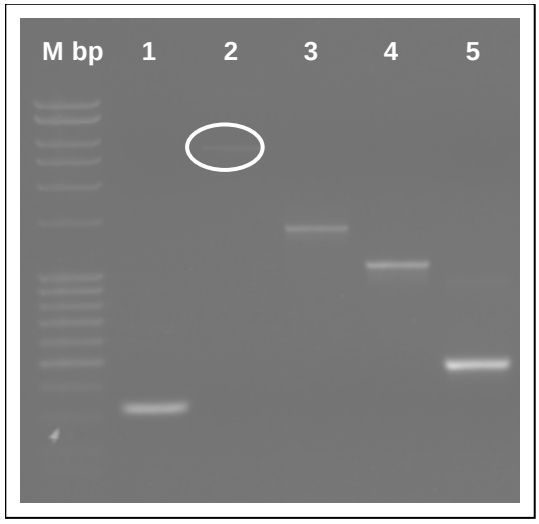

Fig. 25: Agarose gel of PCR-amplified early *grh* genes from the cosmid pMP31.

Appropriately sized DNA fragments were identified using the 100 bp DNA Ladder extended (Roth, Karlsruhe, Germany) that is denoted as Mbp. Lanes 1: *grhC*, 2: *grhAB* 3: *grhT*, 4: *grhE* and 5: *grhQ*.

In each case a PCR product of the correct size was obtained. They were first cloned into the *E. coli* vector pSK+ for sequence analysis. Positive inserts were further cloned into the *Eco*RI restriction site of the *E. coli-Streptomyces* shuttle vector pKJ55 using the compatible restriction enzymes *Eco*RI and *Mfe*I. This resulted in a successive cloning strategy of the *grh* minimal PKS and the *grh* cyclases into pKJ55 (Figures 26 and 27).

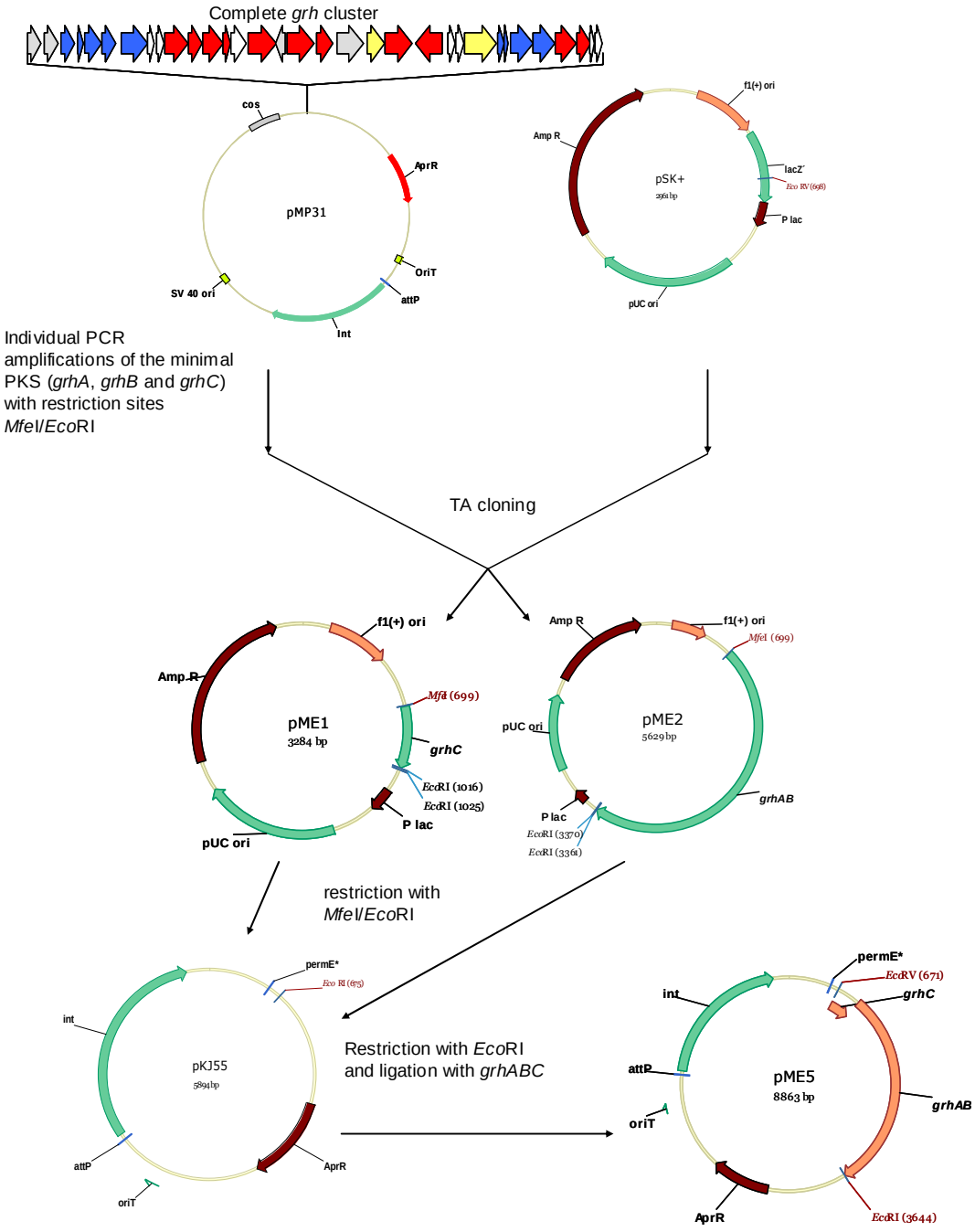

Fig. 26: Cloning strategy of the *grh* minimal PKS.

The *grh* minimal PKS genes were individually PCR-amplified from the cosmid pMP31 containing the complete *grh* gene cluster and TA-cloned[126] (insertiom of 3' T overhangs into the pSK+ vector for subsequently cloning of the PCR-amplified insert) for sequencing. Finally, the inserts were subcloned into the *E. coli-Streptomyces* shuttle vector pKJ55.

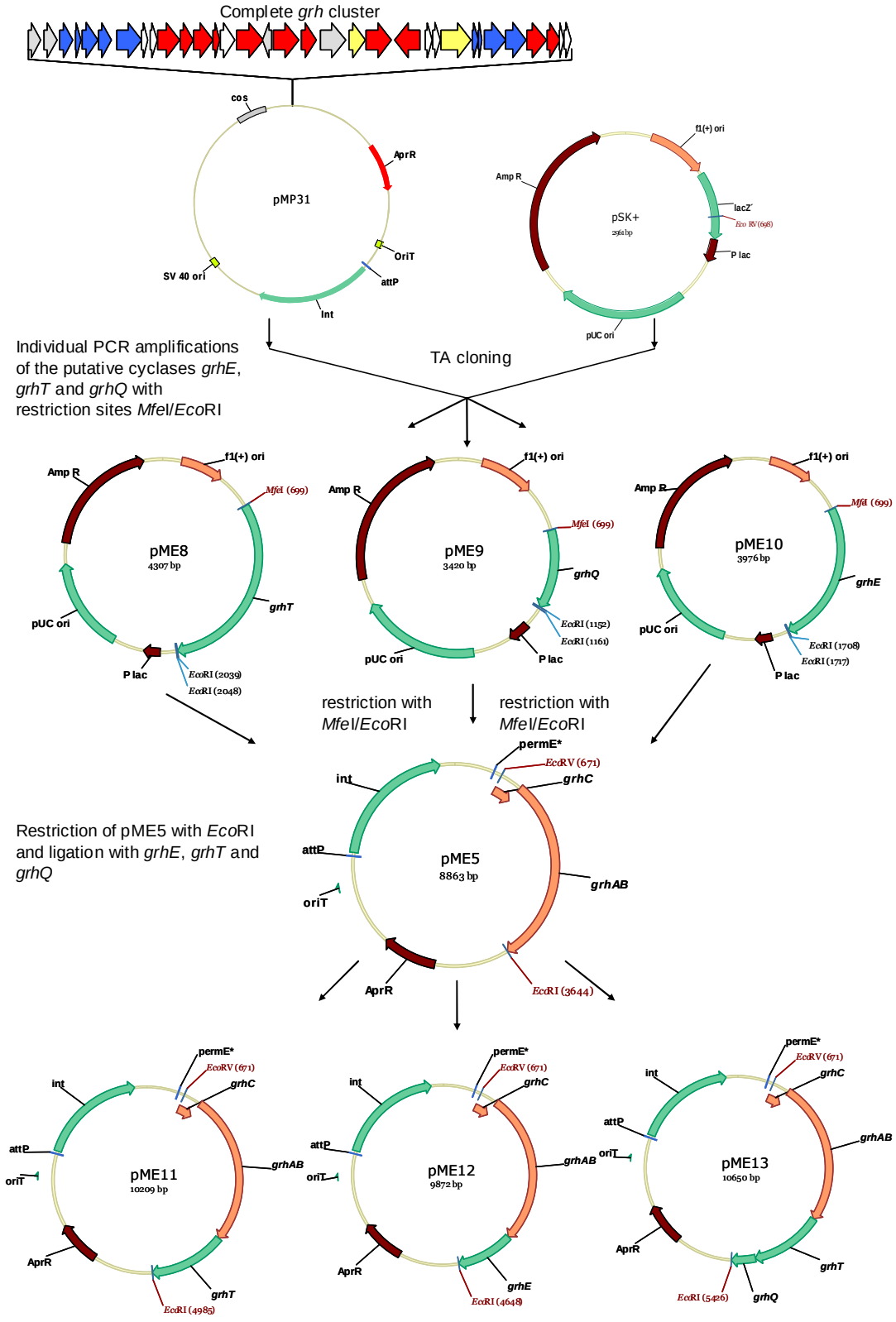

Fig. 27: Cloning strategy of the *grh* cyclases into the *grh* minimal PKS vector pME5.

The *grh* cyclase genes were individually PCR-amplified from the cosmid pMP31 containing the complete *grh* gene cluster and TA-cloned for sequencing. Finally, the inserts were subcloned into the *grh* minimal PKS vector pME5.

The determination of positive clones was carried out by restriction analysis. The resultant constructs are listed in Table 11. The constructs were subsequently conjugated into the host organism *S. albus* (section 5.7.3) for further investigation in heterologous expression.

4.1.3 Expressions of early griseorhodin A genes

Heterologous expression of the minimal PKS genes *grhC*, *grhA* and *grhB* and the coexpression of the cyclase genes *grhT*, *grhE* and *grhQ* with the minimal PKS in the host organism *S. albus* were investigated. The production of secondary metabolites was monitored by HPLC.

4.1.3.1 *grh* minimal PKS expression

The *grh* minimal PKS is highly similar to other type II minimal PKSs. However, a unique feature of the *grh* minimal PKS is its disconnectivity of genes within the cluster; the ACP gene *grhC* is located 26 kb upstream from the KS_α and KS_β genes *grhA* and *grhB*. Two similar examples are found in the daunorubicin and R1128 biosynthetic gene clusters.[40, 42] The HPLC trace from heterologous expression of the *grh* minimal PKS using solid 2CM media in the host organism *S. albus* is shown in Figure 28.

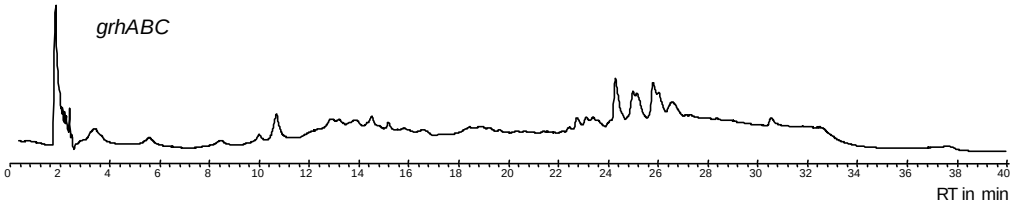

Fig. 28: HPLC trace from the heterologous expression of the *grh* minimal PKS in *S. albus* using solid 2CM media at 254 nm.

The expression of the *grh* minimal PKS did not result in the production of detectable amounts of polyketides as judged by HPLC (section 5.15.4.1, method 1). To further investigate the potential for *grh* minimal PKS expression, different media such as MS, TSB, LB and R5 in liquid and solid forms were tested. The use of different nutrient media did not have any

effect on the production of the secondary metabolites by the *grh* minimal PKS (data not shown).

One reason for the extremely low production of polyketides could be the metabolic conditions of the host organism *S. albus*. Through the integration of foreign DNA into the *S. albus* genome, over-producing strains and strains with little or no production of polyketides can result.[127] This has been observed in a previous study where different clones of the same mutants produced different levels of polyketides.[1] To overcome this challenge, several conjugations were performed with many screenings for arising exconjugants to identify a clone that had increased production of secondary metabolites. Despite many attempts, the expression of pME5 did not produce detectable polyketides or shunt products. The failure of *grh* minimal PKS expression is in high contrast to other type II PKS systems investigated to date (section 2.2).

Another reason for this unsual observation could be that the *grh* minimal PKS only functions properly or is sufficiently stabilised in the presence of additional pathway enzymes. Similar results were observed in the case of enterocin biosynthesis.[66, 81] It was shown that the *enc* minimal PKS does not yield polyketides unless the functional endogenous ketoreductase EncD is co-expressed. The *enc* minimal PKS expression alone did not lead to polyketide production. Co-expression with the homologous actinorhodin KS or with the *encD* gene harbouring active site mutations did not improve expression. This indicates that the *enc* minimal PKS requires EncD to serve a catalytic role to produce a functional enterocin PKS complex. To further investigate if the performance of the *grh* minimal PKS is context dependent, coexpressions with *grh* putative cyclase genes *grhE*, *grhT* and *grhQ* were carried out, which likely form a complex with the minimal PKS at the early biosynthetic stage.

4.1.3.2 Co-expressions of *grh* cyclases with the *grh* minimal PKS

In aromatic polyketide synthesis, at least two cyclases are required for cyclisation of the poly-β-keto chain.[31] For griseorhodin A biosynthesis, the putative cyclase genes *grhT*, *grhE* and *grhQ* were identified using BLAST (blastp) (Table 7).[25]

The *grhE* gene was found to encode a protein highly homologous to bidomain CYCs. These are known to perform C7-C12 first-ring cyclisations as seen with ActVII.[32] The second cyclase gene *grhQ* from the griseorhodin A gene cluster possesses similarity to the rubromycin cyclase gene *rubE*, tetracenomycin gene *tcmI*, and to the jadomycin gene *jadI*, indicating a putative cyclase for third- and fourth-ring cyclisations. The gene *grhT* encodes a protein comprised of two halves homologous to CYCs and oxidoreductases, respectively, and was found to be highly similar to RubG encoded by the rubromycin gene cluster. Furthermore, the cyclase domain possesses the strongest similarity to the C9-C14 first- and second-ring cyclase protein, TcmN from tetracenomycin biosynthesis (section 2.3.1). The HPLC traces from heterologous expressions of the *grh* minimal PKS with *grhE*, *grhT* and *grhTQ* using solid 2CM media in the host organism *S. albus* are shown in Figure 29.

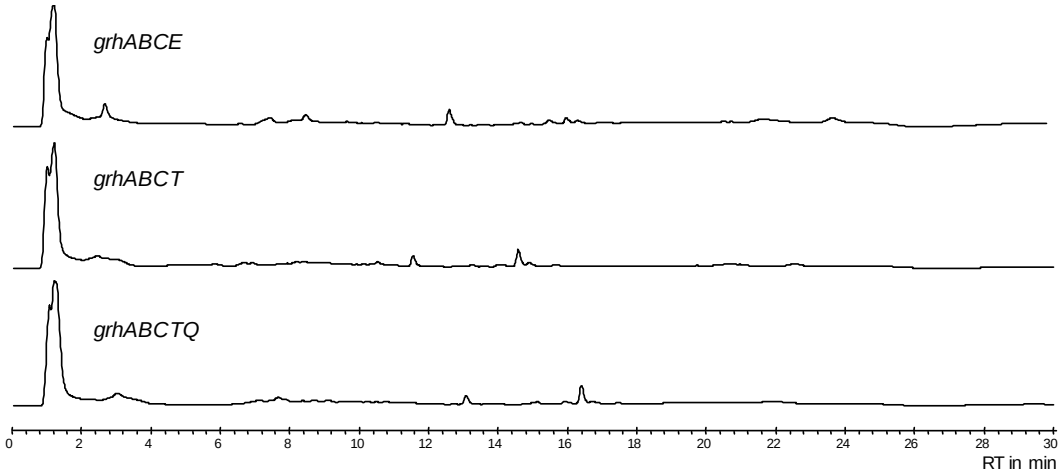

Fig. 29: HPLC traces from the heterologous expressions of *grh* minimal PKS with *grhE*, *grhT* and *grhTQ* in *S. albus* using solid 2CM media at 254 nm.

The co-expression of the *grh* minimal PKS genes with *grhE*, *grhT* and *grhTQ* did not result in the production of detectable amounts of polyketides by HPLC (section 5.15.4.1, method 2). To further investigate the potential for co-expression of the cyclases with the minimal PKS, the same media were tested as described in section 4.4.3.1. No secondary metabolite production was observed in any of these nutrient media for the mutants (data not shown). As described in section 4.1.3.1, several conjugations were performed with many screenings for exconjugants to identify a clone that had increased production of secondary metabolites. Despite many attempts, coexpressions of the cyclases with the *grh* minimal PKS did not result in the detectable production of polyketides or shunt products.

The encoding of both GrhE and GrhT in the griseorhodin A biosynthetic cluster is unsual as both enzyme types perform the first ring cyclisation of open polyketide precursors. The ActVII type, corresponding to GrhE, promotes C7-C12 cyclisation while the TcmN type, corresponding to GrhT, is responsible for C9-C12 cyclisation. Compounding this fact, the presence of both types should theoretically result in a mixture of differently cyclised products.[25] Furthermore, no ActVII homologue is known from other clusters with similar sets of CYCs. This suggests that either GrhE carries out either chemistry different to ActVII or is inactive[25]. It was therefore hoped that an inactivation study of *grhE* could assist the functional elucidation of GrhE during the early biosynthetic steps of griseorhodin A (section 4.6.3.1).

Surprisingly, the *grh* minimal PKS with *grhT* did not produce expected shunt product such as RM80 **23**.[52, 56] Similar results were obtained in the examination of resistomycin biosynthesis.[128] Resistomycin shares early biosynthetic steps with linear decaketide tetracenomycin and the first ring closure is identical in both pathways. The *rem* minimal PKS expression with RemI (possessing high sequence similarity to TcmN like GrhT) did not lead to production of the expected shunt product RM80 **23**. The results indicated that at least one additional cyclase is required for efficient polyketide formation and/or release of the polyketide intermediate. This supports the hypothesis that the multienzyme complex forms a pocket in which the

polyketide is then fully cyclised. This is in contrast to a sequential cyclisation of the polyketide chain by individual enzymes. Concluding this, an inactivation study of the gene *grhT* is necessary to further investigate its function in the early biosynthesis of griseorhodin A (section 4.5.3.2).

The expression of the *grh* minimal PKS with *grhT* and additionally the cyclase gene *grhQ* did not yield detectable products. This could suggest that the presence of a multienzyme complex for griseorhodin A biosynthesis is also required as discussed above, where an additional stabilising enzyme might be required. One such potential candidate in the *grh* gene cluster could be GrhS, which possesses strong homology to WhiE-ORFII and TcmJ.[45, 129] These types of enzymes seem to stabilise the minimal PKS protein assembly.[25] The synergistic actions of cyclases and other stabilising/tailoring enzymes may be a general mechanism for longer polyketides as was shown in pradimicin biosynthesis.[130] The study showed that an alternative modification step before the cyclisation of the C-, D- and E-rings of the pradimicin takes place (Figure 30). The *pdm* minimal PKS and the cyclase PdmD form **74** followed by the monooxygenase PdmH and the two cyclases PdmK and PdmL that oxidise the B-ring and cyclase the C- and D-rings in **75**. Deletion of any of these enzymes abolished all ring formations, confirming that the enzymes cannot act independently without their associated partners. This was the first example of multiple cyclases and a monooxygenase working in concert for the regioselective tailoring of a polyketide backbone. In the study, it was speculated that the sequential binding and tailoring of the long poly-β-ketones by individual enzymes may not be fast enough to prevent spontaneous cyclisations of the reactive backbone. A multienzyme complex can effectively act on the entire length of the uncyclised polyketide to lock the reactive backbone and suppress aberrant cyclisations. Griseorhodin A is one of the longest aromatic polyketides with 25 carbon atoms, and therefore it could require additional enzymes for stabilisation of its polyketide chain. An inactivation study may provide more insights into cyclisation mechanism of the gene *grhQ* in early griseorhodin A biosynthesis (section 4.4.3.2).

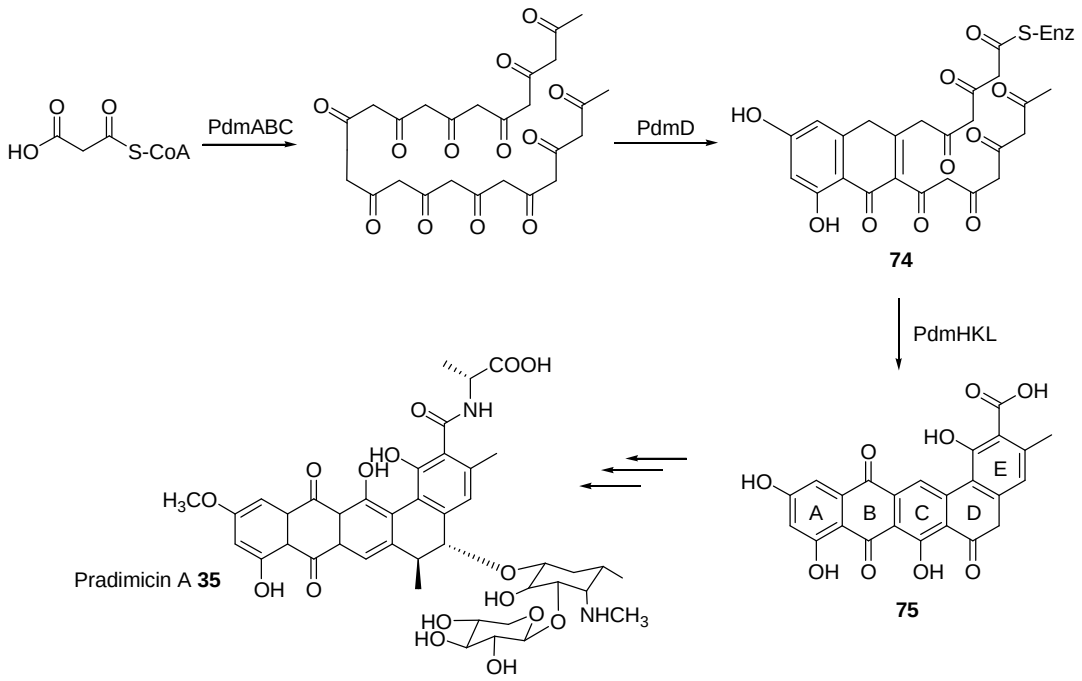

Fig. 30: Early steps in pradimicin A biosynthesis.[130]

A further possible reason for the previous unsual results could be that the early griseorhodin A genes are not transcribed. To test this, transcriptional analysis of *grh* minimal PKS was carried out.

4.2 Transcriptional analysis of the *grh* minimal PKS

Due to the unexpected results in sections 4.3.3.1 and 4.3.3.2, the functionality of the *grh* minimal PKS required testing whether the mRNA from the *grh* minimal PKS is transcribed. Therefore, *grh* minimal PKS RNA was isolated and the cDNA synthesised using reverse transcriptase-PCR (RT-PCR).

4.2.1 Isolation of RNA from MP31 and ME5

RNA was isolated from MP31 fermented in MS liquid nutrient media as well as from ME5 fermented in liquid MS, TSB and LB nutrient media. The RNA isolations were confirmed by gel electrophoresis (Figure 31).

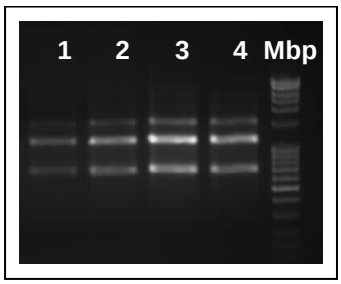

Fig. 31: Agarose gel of RNA isolation.

RNA was isolated from the cosmid pMP31 and from the minimal PKS grown in the media MS, TSB and LB. Appropriately sized RNA fragments were identified using the 100 bp DNA Ladder Extended (Roth, Karlsruhe, Germany) that is denoted as Mbp. Lanes 1: MP31 in MS; 2: ME5 in MS; 3: ME5 in TSB and 4: ME5 from LB.

In each case RNA was successful isolated. The RNA was then further used for RT-PCR.

4.2.2 RT-PCR

RT-PCR was used to amplify *grhC* and a portion of *grhAB* from MP31 and ME5, and as a positive control, DNA from the cosmid pMP31 and the plasmid pME5 were used (Figure 32).

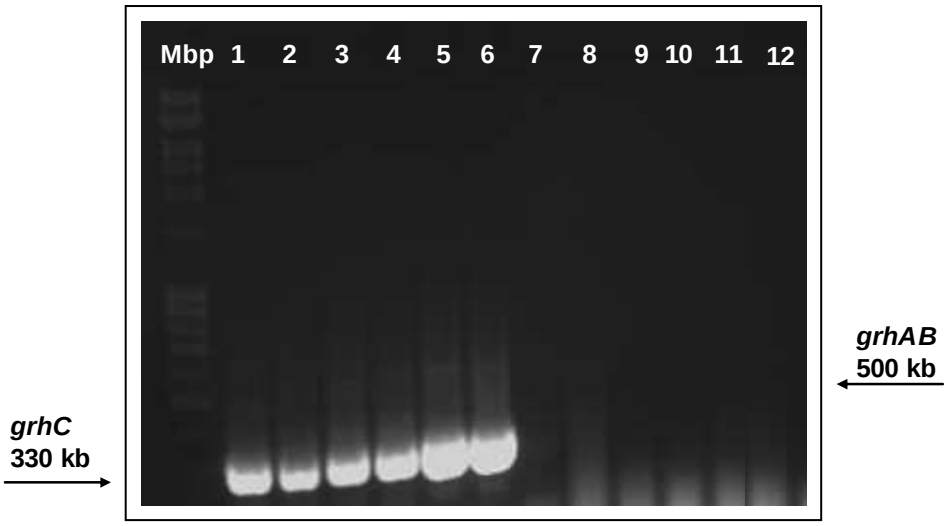

Fig. 32: Agarose gel of the RT-PCR.

The appropriately sized DNA fragments were identified using the 100 bp DNA Ladder Extended (Roth, Karlsruhe, Germany) that is denoted as Mbp. Lanes 1: *grhC* from MP31 ; 2: *grhC* from ME5 in MS; 3: *grhC* from ME5 in TSB; 4: *grhC* from ME5 in LB; and the positive controls for *grhC* 5: cosmid pMP31 and 6: plasmid pME5; 7: portion of *grhAB* from MP31; 8: portion of *grhAB* from ME5 in MS; 9: portion of *grhAB* from ME5 in TSB;10: portion of *grhAB* from ME5 in LB and the positive controls for *grhAB* 11: cosmid pMP31 and 12: plasmid pME5.

For the minimal PKS, the RT-PCR resulted in successful amplification with *grhC*-specific primers. Concluding this, the gene *grhC* is transcribed using the ermE* promoter in the vector pKJ55. However, the amplification of the genes *grhA* and *grhB* and their positive controls failed. Therefore, RT-PCR conditions were varied for optimisation of *grhA* and *grhB* gene amplification (section 4.2.3).

4.2.3 Optimisation of the RT-PCR

The conditions used for RT-PCR were varied to optimise the resulting products. This was accomplished through varying the times and temperatures for PCR amplification at various stages. First of all, new RT primers for *grhA* and *grhB* were designed, targeting different areas of the genes and possessing different annealing temperatures. By changing the

annealing temperatures the specificity of primer binding can be influenced. Here, the annealing temperature was decreased in order to decrease the binding specificity of the primers on the DNA template. Furthermore, the temperature for cDNA synthesis was varied between 45° C and 55° C to improve the cDNA synthesis. However, these alterations did not have any influence on the amplification and no bands for *grhA* and *grhB* were obtained. At this point, no conclusion can be drawn whether the genes *grhA* and *grhB* are functional in the construct pME5, as the positive controls failed during the optimisation. Thus, to gain more insights into the early steps of griseorhodin A biosynthesis, inactivation studies of the putative *grh* cyclase genes were performed.

4.3 Early griseorhodin A biosynthetic studies by in-frame gene deletions

4.3.1 Construction of early griseorhodin A gene knock-outs

In order to further investigate early griseorhodin A biosynthesis, the cyclase genes *grhE*, *grhT* and *grhQ*, as well as post-PKS genes from *grhH* to *grhP* and from *grhH* to *grhQ*, respectively, had to be deleted on the cosmid pMP31. Therefore, λ-Red recombineering was applied to generate in-frame gene deletions. In this technique, a gene knock-out is performed in a one-step directed insertion via a double crossover of linear DNA fragments into the target DNA (Figure 33).[131]

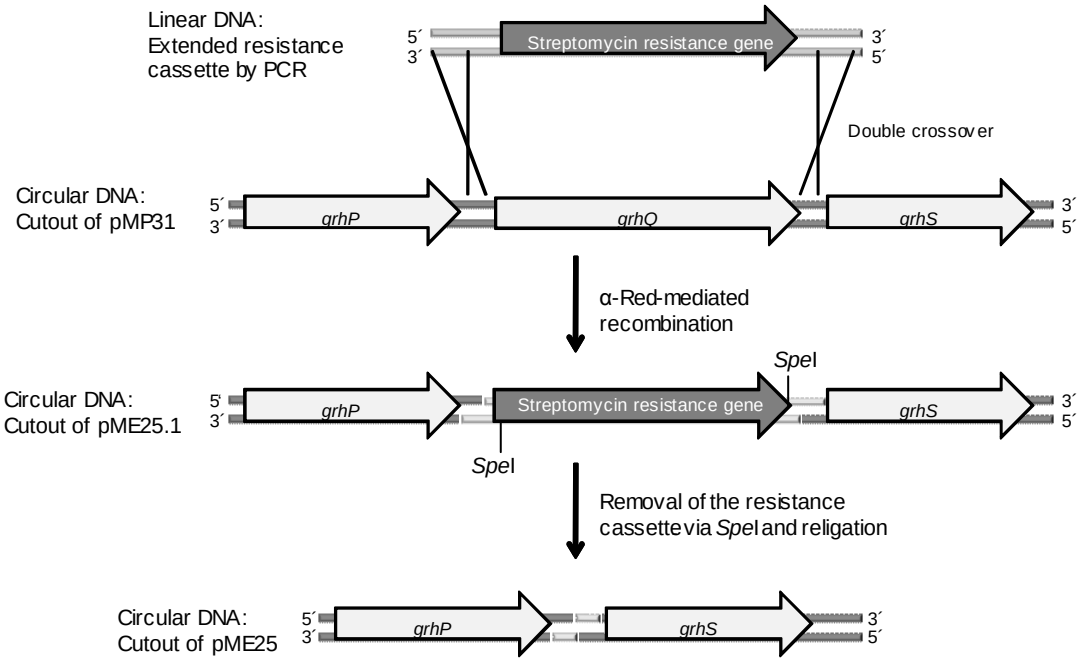

Fig. 33: Schematic overview of the λ-Red-mediated recombination technique for deleting the gene *grhQ* in the *grh* gene cluster.

Therefore, the streptomycin resistance cassette containing homologous areas to the target DNA and the restriction sites for *Spe*I was amplified individually for each gene knock-out. The size of the product was confirmed by gel electrophoresis (Figure 34). Figure 34 shows only one cassette as the size of each cassette was the same for each gene knock-out.

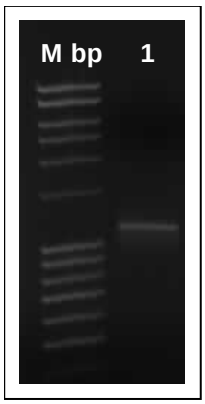

Fig. 34: Agarose gel of the PCR amplified streptomycin resistance cassette from the vector pIJ778.

The appropriately sized DNA fragment was identified using the 100 bp DNA Ladder Extended (Roth, Karlsruhe, Germany) that is denoted as Mbp. Lane 1: streptomycin resistance cassette.

In each case the correct size of the resistance cassette was obtained. For λ-Red recombineering, the resistance cassettes were inserted into the cosmid pMP31 using electroporation (section 5.7.2). The determination of the positive clones carrying the streptomycin resistance cassette was confirmed by colony PCR and restriction analysis. The cassette was then removed to avoid polar effects on the transcription of the downstream genes[131] using the restriction enzyme *Spe*I and the determination of positive clones was again carried out by colony PCR and restriction analysis.

The deletion constructs resulted in cyclase Δ*grhT* (pME23), Δ*grhE* (pME24), Δ*grhQ*, (pME25) mutants (Table 11), as well as in post-PKS Δ*grhH-P* (pME26) and Δ*grhH-Q* mutants (Table 11), whereas in this clone the cyclase gene *grhQ* was additionally deleted to the post-PKS genes *grhH-P*.

4.3.2 Expression of the cyclase gene knock-outs and the post-PKS gene knock-outs

Heterologous expression of the cyclase gene Δ*grhT*, Δ*grhE* and Δ*grhQ* mutants and the post-PKS Δ*grhH-P* and Δ*grhH-Q* mutants in the host organism *S. albus* were investigated and the production of the secondary metabolites was monitored by HPLC.

4.3.3 Cyclase gene knock-outs expression in *S. albus* and the analysis of the secondary metabolic production

4.3.3.1 Analysis of *ΔgrhE* (predicted C7-C12 cyclase)

The HPLC traces and UV profiles from heterologous expressions of the Δ*grhE* mutant and the cosmid pMP31 using solid 2CM media in the host organism *S. albus* are shown in Figure 35.

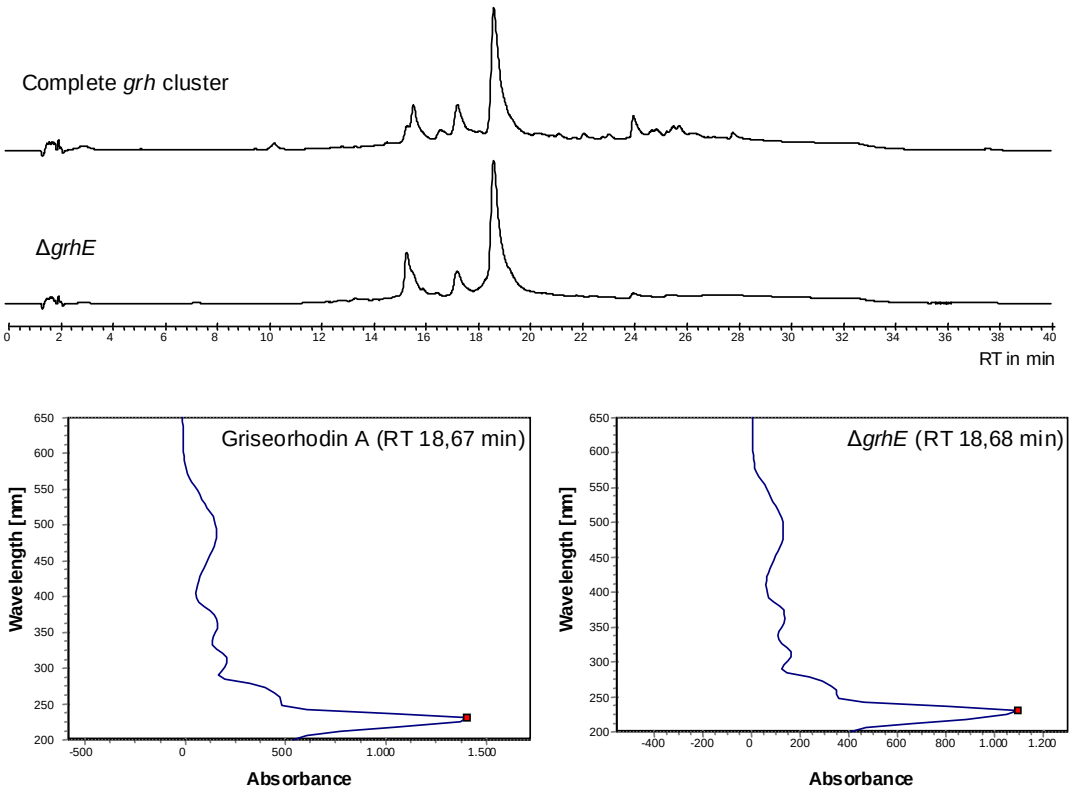

Fig. 35: HPLC traces and UV profiles from the heterologous expression of the complete *grh* gene cluster and *ΔgrhE* in *S. albus* using solid 2CM media at 254 nm.

Deletion of *grhE* in the griseorhodin A gene cluster did not affect griseorhodin biosynthesis; the polyketide was still produced by the Δ*grhE* mutant. Concluding this, GrhE does not play any significant role in griseorhodin A biosynthesis and confirms the prediction that the enzyme is not needed for griseorhodin A biosynthesis (section 4.3.3.2). Furthermore, this result confirmed the functionality of the gene knock-out technique applied in the present study.

4.3.3.2 Analysis of *ΔgrhT* (C9-C14 cyclase) and *ΔgrhQ*

The similarity of *grhQ* to the genes *rubE*, *tcmI* and *jadI* indicates that *grhQ* is a putative cyclase for bent third- (such as angucyclines, Fig. 10)[31] and fourth-ring (such as tetracenomycins, Fig. 9)[31] cyclisations and could therefore generate a structurally related cyclised moiety. To investigate the functions and the order of the cyclisation steps, individual inactivations of

the two other putative cyclase genes *grhT* and *grhQ* in *grh* gene cluster were performed and the heterologous expressions were investigated by HPLC.

The HPLC traces from heterologous expressions of the Δ*grhT* and Δ*grhQ* mutants using solid 2CM media in the host organism *S. albus* are shown in Figure 36.

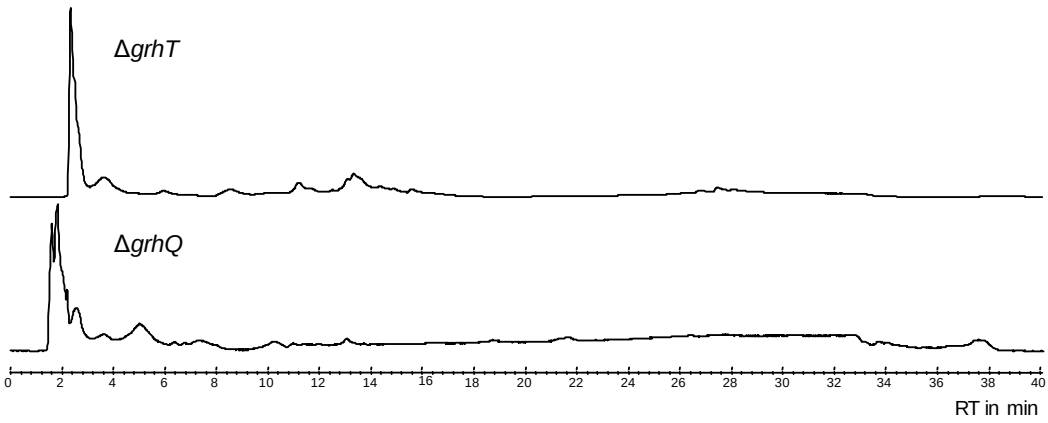

Fig. 36: HPLC traces from the heterologous expressions of Δ*grhT* and Δ*grhQ* in *S. albus* using solid 2CM media at 254 nm.

Remarkably, the expression of the Δ*grhT* and Δ*grhQ* mutants did not result in the production of detectable amounts of polyketides by HPLC. To further investigate the potential of the mutant expressions, different media such as MS, TSB, LB and R5 in liquid and solid forms were tested. The use of different nutrient media did not have any effect on the production of secondary metabolites (data not shown). As in the earlier experiments, several conjugations for the clones were carried out and many screenings for exconjugants were performed to identify appropriate clones that could result in improved production of secondary metabolites. Despite many attempts, the expression of the *ΔgrhT* and *ΔgrhQ* mutants did not result in detectable production of polyketides or shunt products.

Deletion of *grhT* in the griseorhodin A gene cluster abolished griseorhodin A biosynthesis; the polyketide or some shunt products were not detected and is therefre in agreement with the result from the earlier characterisation

approach (section 4.3.3.2). Similar results were generated by a study by Ostash and co-workers in the investigation of landomycin cyclases and their effect on landomycin biosynthesis.[132] The inactivation of the putative landomycin cyclase LndL led to the abolishment of biosynthesis, where neither intermediates nor novel metabolites were detected. The *lnd* minimal PKS lndABC which is essential for the polyketide biosynthesis, could be not affected by the inactivation of LndL as it located downstream. This applies for the *grh* minimal PKS as well as it is located upstream of the cyclase gene *grhT*. Compounding these results, this nonproducing phenotype could not arise from an interrupted polyketide pathway. Furthermore, it was previously speculated that each enzyme would have a single function, but many genetic experiments have shown that many components have more than one role and that these depend on other components present in PKSs.[8, 32] Current results support the speculation that components having several roles could exist and explain the absence of detectable amounts of polyketides or shunt products for the *ΔlndD* and *ΔgrhT* mutants.

The inactivation of the other putative cyclase, GrhQ, led to the abolishment of griseorhodin A production. This is also in agreement with the result from the earlier characterisation approach (section 4.3.3.2). This result could be due to the presence of an operon within the griseorhodin A gene cluster where *grhQ* is located. In the study by Sandmann *et al.*, aurachin (*aur*) biosynthesis was investigated and inactivation of gene(s) in a putative *aur* operon resulted in abolishment of the biosynthesis.[133] Another example for a presence of an operon within polyketide core genes is in the lysolipin (*llp*) biosynthesis gene cluster.[134] It contains three putative cyclases whose start and stop codons overlap with the *llp* minimal PKS and indicates a core *llp* operon. However, there are no investigations thus far concerning this operon and its genes. In the *grh* gene cluster, GrhQ, GrhS, GrhA and GrhB seem to be translationally coupled due to the overlapping of their start and stop codons by 4 nt.[25] This could indicate that the grh core cluster forms an operon that directs tight co-expression of the enzymes. Under this hypothesis, the genes are either expressed together or not at all when one gene is missing, e.g. through inactivation of GrhQ. To further investigate

early griseorhodin A biosynthesis, two new mutants, Δ*grhH-P* and Δ*grhH-Q*, were generated, where in the first mutant all tailoring genes from *grhH* to *grhP* were deleted and in the second mutant the mutation was extended through *grhQ*.

4.3.4 Expressions of tailoring gene knock-outs in *S. albus* and the analysis of the secondary metabolite production

4.3.4.1 Analysis of Δ*grhH-P*

The Δ*grhH-P* mutant produced a complex compound mixture of secondary metabolites in solid 2CM media. The HPLC traces and UV profiles from the Δ*grhH-P* mutant were compared with the Δ*grhM* mutant using solid 2CM media in the host organism *S. albus* as shown in Figure 37.

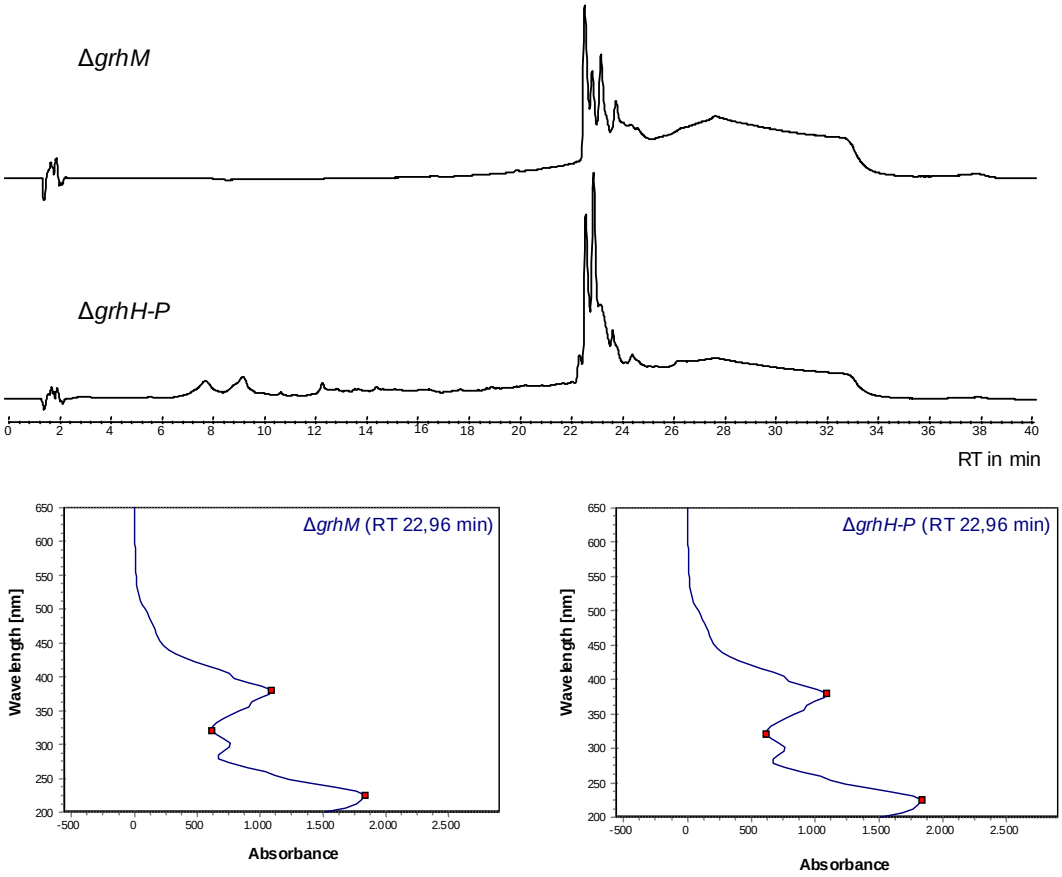

Fig. 37: HPLC traces and UV profiles from heterologous expressions of Δ*grhM* and Δ*grhH-P* in *S. albus* using solid 2CM media at 254 nm.

In the present study, the *grhM* and all post-PKS genes from *grhH* to *grhP* were deleted in the Δ*gr*H-P mutant, while the Δ*grhM* mutant contained all *grh* genes except *grhM*. The Δ*grhM* mutant was constructed in a previous study by Dr. Kathrin Reinhard using the λ-Red recombineering technique.[1, 131] Comparison with the retention times and the UV profiles of both mutants provided evidence that identical compounds were detected in both mutants.

4.3.4.2 Analysis of secondary metabolite production from the *ΔgrhM* and *ΔgrhH-P* mutants

Secondary metabolite production of the *ΔgrhM* mutant was investigated by Zeynep Yunt.[123] For **76** in Figure 38, HRESIMS indicated a mass of $C_{26}H_{20}O_8$, however a complete structure elucidation by NMR was not possible due to the instability of the intermediate and therefore, **76** represents a speculative structure. Another compound that was isolated and fully characterised using HRESIMS and NMR by Zeynep Yunt, was structurally identical to KS-691-1 **77** (Figure 38). This compound has been isolated earlier from the culture broth of *S. californicus* and is an inhibitor of Ca^{2+} and calmodulin-dependent cyclic nucleotide phosphodiesterase.[135] Comparison of the proposed structures of both compounds, suggests that KS-691-1 **77** could be derived from **76** by spontaneous oxidation. Due to the data obtained by Zeynep Yunt, GrhM was tentatively placed into an early biosynthetic enzyme group according to the number of carbon and oxygen atom of the intermediate. The rationale was that the level of oxygenation should increase while the number of the carbon atoms should decrease to 25 en route to **36**. Identification of compounds that contain a much smaller number of oxygen atoms (7-10) than **36** (12 oxygen atoms), consistent with an upstream biosynthetic position, assists in allocation of corresponding enzymes during polyketide assembly. Furthermore, GrhM homologues are found in other pentangular biosynthetic pathways. E. g., FdmM, a GrhM homologue from the fredericamycin A biosynthesis, was investigated by in-frame gene deletion and the study suggested that the enzyme is responsible for the hydroxylation of C6 in the pentangular core

during the fredericamycin A biosynthesis.[136] Concluding this, the proposed compound structures **76** and **77** represent very likely very early intermediates in the griseorhodin A biosynthesis and indicates an early oxygenase role for GrhM during griseorhodin A biosynthesis.

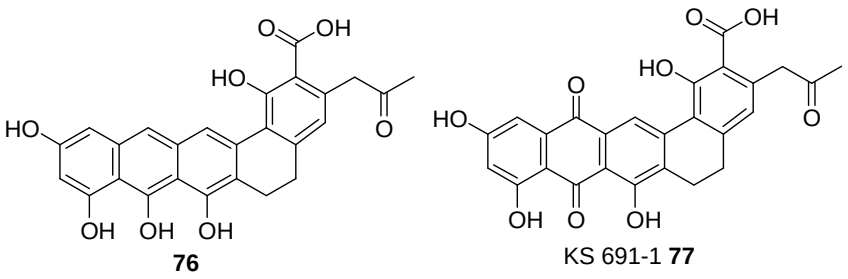

Fig. 38: Speculative structure 76 and KS691-1 77 isolated from the *ΔgrhM* mutant.[123, 137]

For the secondary metabolite analysis of *ΔgrhH-P*, 10 L of liquid TSB media was fermented and the cells and the media extracted with 100% EtOAc with an acidifying step (sections 6.15.1.2 and 6.15.1.2.1) In the first purification step, a semi-praparative HPLC was used (section 5.15.4.3) and two fractions were obtained, ME13 and HP, which required further purifications. Fraction HP was purified using LH20 (section 5.15.3.2) resulting in an HPLC profile shown in Figure 39. The final purification step was carried out using HPLC (section 5.15.4.2) resulting in compound HP1 (Table 7).

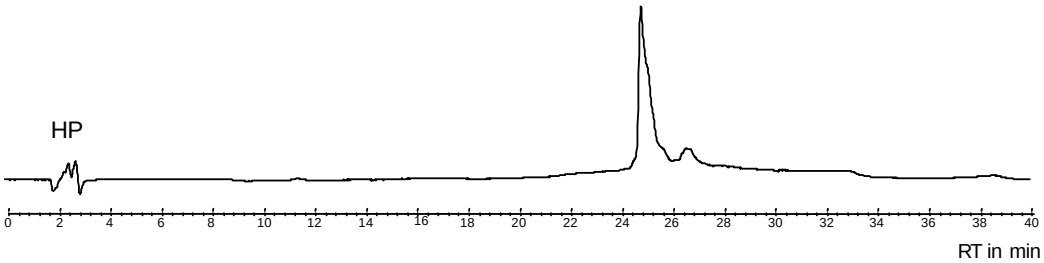

Fig. 39: HPLC traces of the fraction HP after LH20 separation at 254 nm.

The fraction ME13 was directly separated by semi-preparative HPLC using a gradient system (section 5.15.4.3) at the Kekulé-Institute HPLC pool, resulting in seven new fractions ME13_1 to ME13_7 (Figure 40).

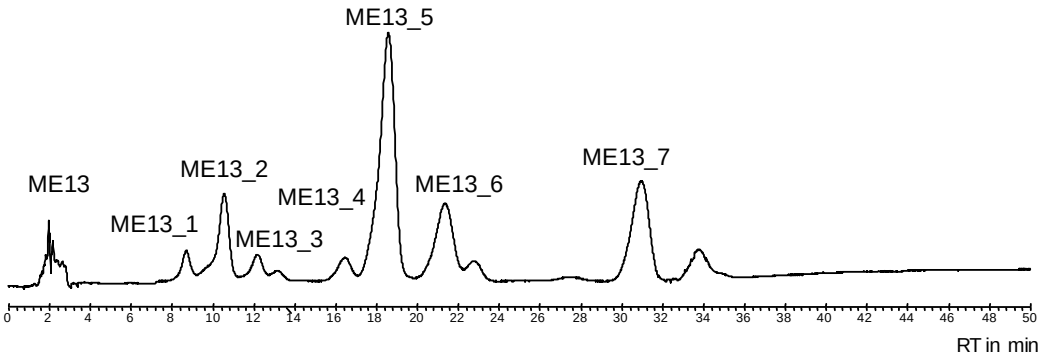

Fig. 40: HPLC trace of the fraction ME13 from semi-preparative HPLC at 254 nm.

These fractions were analysed by HPLC (section 5.15.4.2). The fraction ME13_2 was chosen for further purification as the compounds in the other fractions possessed too similar retention times for a further separation. Work on fraction ME13_2 led to a separation of three pure compounds ME13_2_1, ME13_2_2 and ME13_2_3 (Figure 41, Table 2).

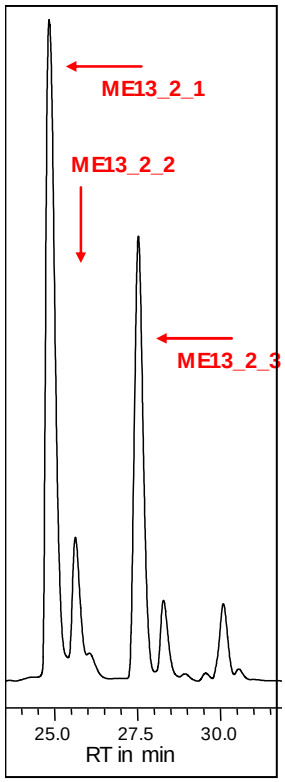

Fig. 41: Cutout of the HPLC trace of fraction ME13_2 at 254 nm.

The arrows indicate the separated compounds as indicated in Table 2.

In the present study, HPLC and LH20 were used to separate fractions from the crude cellular extract of the *ΔgrhH-P* mutant. It resulted in four pure compounds followed by a HRESIMS analysis (Table 2).

Table 2: Compounds isolated from the mutant Δ*ghrH-P* using LH20 and HPLC with retention times, yields, masses determined by HRESIMS in the positive (+) or negative (-) mode and proposed molecular formulas.

Compound	Retention time (t_R) [min]	Yield[µg]	Mass *m/z* $(M+H)^+$ *m/z* $(M-H)^-$	Proposed molecular formula
Griseorhodin A	19.0	-	509.0720	$C_{25}H_{16}O_{12}$
HP1	24.9	200	520.0714(+)	$C_{19}H_{20}O_{17}$
ME13_2_1	25.0	400	460.1109(-)	$C_{26}H_{20}O_8$
ME13_2_2	25.8	300	n.d.[a]	n.d.[a]
ME13_2_3	27.4	400	459.1034(-)	$C_{26}H_{20}O_8$

UV and HRESIMS spectra are presented in Appendix 8.3 and 8.4. [a] No determination for the mass.

The molecular formula of $C_{19}H_{20}O_{17}$ for HP1 proposes an early intermediate in the griseorhodin A biosynthesis due to lower amount of carbon atoms than in griseorhodin A. Therefore, HP1 was characterised by cryo NMR and promising ^{1}H- and COSY spectra were recorded. However, to obtain 2D NMR data using HSQC and HMBC spectroscopy techniques for a complete structure elucidation, the yield of 200 µg was insufficient and the molecule could not be further investigated during the present study. The masses of the compounds ME13_2_1 and ME13_2_3 possess the same proposed molecular formula than the proposed molecular formula ($C_{26}H_{20}O_8$) of the speculative intermediate **76** isolated in a previous study (Figure 38).[1] They predict the same or similar structure for ME13_2_1 and ME13_2_3. However, for both, ME13_2_1 and ME13_2_3, a preliminary ^{1}H NMR showed no representative $-CH_2$ groups around 2 ppm and no protons bound on the double bonds were observed between 6 and 7 ppm. One reason for this could be the relatively small amount of the isolated compounds.

Taken together, the previous HRESIMS and NMR data for the Δ*grhM* mutant, the present HRESIMS data for the Δ*grhH-P* mutant and the comparison of presence of the genes in both mutants propose an early oxygenase role of GrhM in the griseorhodin A biosynthetic pathway.

In order to get more insights into the early biosynthetic steps of griseorhodin A, many attempts to individually delete more genes (*grhT*, *grhU* and *grhV*) in the Δ*grhH-P* mutant were carried out, but all of them failed. The conditions during λ-Red recombineering were varied as much as possible; however, there was no success. As the putative *grh* cyclase gene *grhQ* is adjacent to *grhP* (section 2.5, Figure 23), it could be additionally deleted by extending the gene mutant *ΔgrhH-P* to *grhQ*.

4.3.4.3 Analysis of *ΔgrhH-Q*

The HPLC trace from heterologous expression of the *ΔgrhH-Q* mutant in the host organism *S. albus* in 2CM media is shown in Figure 42.

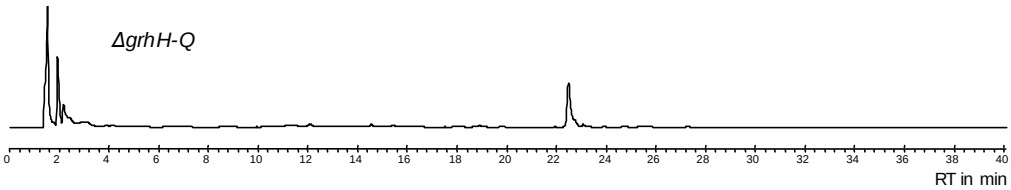

Fig. 42: HPLC trace from heterologous expression of Δ*grhH-Q* in *S. albus* using solid 2CM media at 254 nm.

The peak between 22 and 24 minutes in the trace originates from the extraction with 95:5:1 EtOAC:MeOH:AcOH and is not relevant to secondary metabolite analysis.

The expression of the Δ*grhH-Q* mutant did not result in the production of detectable amounts of polyketides by HPLC (section 6.15.4.1). To further investigate the potential of the mutant expression, the same media were tested as described in section 4.5.1. No effect was observed on the production of secondary metabolites in any of these nutrient media for Δ*grhH-Q* (data not shown). As in earlier experiments, several conjugations for the clones were carried out and many screenings for exconjugants were

performed to identify appropriate clones that could result in improved production of secondary metabolites. Despite many attempts, the expression of *ΔgrhH-Q* did not produce detectable polyketides or shunt products.

The extension of inactivation to the putative cyclase gene *grhQ* in *ΔgrhH-P* led to the abolishment of griseorhodin A production and no detectable amounts of polyketide or shunt products were detected. This result is in agreement with the experiment in section 4.3.3.2, where the cyclase gene *grhQ* was independently inactivated, leading to an abolishment of griseorhodin A biosynthesis. Furthermore, the co-expression with the *grh* minimal PKS in section 4.4.3.1 did not result in detectable amounts of polyketide shunt products. In contrast to these results, the heterologous expression of *ΔgrhH-P* produced a complex mixture of secondary metabolites. This mutant harbours all potential early *grh* genes, including the *grh* minimal PKS, *grhQ* and as well as the potential stabilising gene *grhS*. Therefore it is highly likely that a functional protein complex is relevant at the early stage of griseorhodin A biosynthesis. Furthermore, the results indicate that GrhQ is necessary but still insufficient for a functional PKS, since GrhABCQ does not produce secondary metabolites. To date, griseorhodin A is one of the longest aromatic polyketides and, therefore, it could likely require synergistic actions of cyclases and other stabilising enzymes such as GrhQ and GrhS for its polyketide. The additional proteins could form a pocket with the *grh* minimal PKS in which the multienzyme complex can act and stabilise the entire polyketide assembly simultaneously.

4.4 Griseorhodin A biosynthetic studies by in-frame gene deletions

4.4.1 Sequence analysis of the griseorhodin A proteins GrhU and GrhV

Table 3 lists the comparative results for GrhU and GrhV with known sequences in the NCBI database using “Basic Local Aligment Search Tool” (BLAST) analysis (search with blastp).

Table 3: Proposed functions of the *grh* ORFs shown in Figure 23.

Protein	AA	Proposed function	Protein/organism/compound produced	Similarity/ Identity [%]
GrhU	107	Unknown	RubH/*S.collinus* (unpublished)/rubromycin	83/72
			LlpOIII/*S. tendae*/lysolipin,[134]	80/67
			PdmH/*Actinomadura hibisca*/pradimicin[138]	
GrhV	102	Unknown	RubT/*S. collinus* (unpublished)	
			FdmQ/*S. griseus*/fredericamycin[139]	78/70
			LlpOII/*S. tendae*[134]	66/45
			BenJ/*Streptomyces* sp.	66/47
			A2991200/benastatin A[43]	65/47
			ORF9/*Actinomadura hibisca*/pradimicin[138]	54/38

At the beginning of the present study, none of the homologues encode characterised proteins and therefore they represented interesting targets for functional elucidations.

For the uncharacterised genes, *grhU* and *grhV*, in the griseorhodin A gene cluster, the *ΔgrhV* (KR58) and *ΔgrhU* (KR61) mutants were constructed by Dr. Kathrin Reinhardt using the λ-Red recombineering technique.[1] In this technique, a gene knock-out is performed in a one-step directed insertion

via a double crossover of linear DNA fragments into the target DNA (Figure 43).[131]

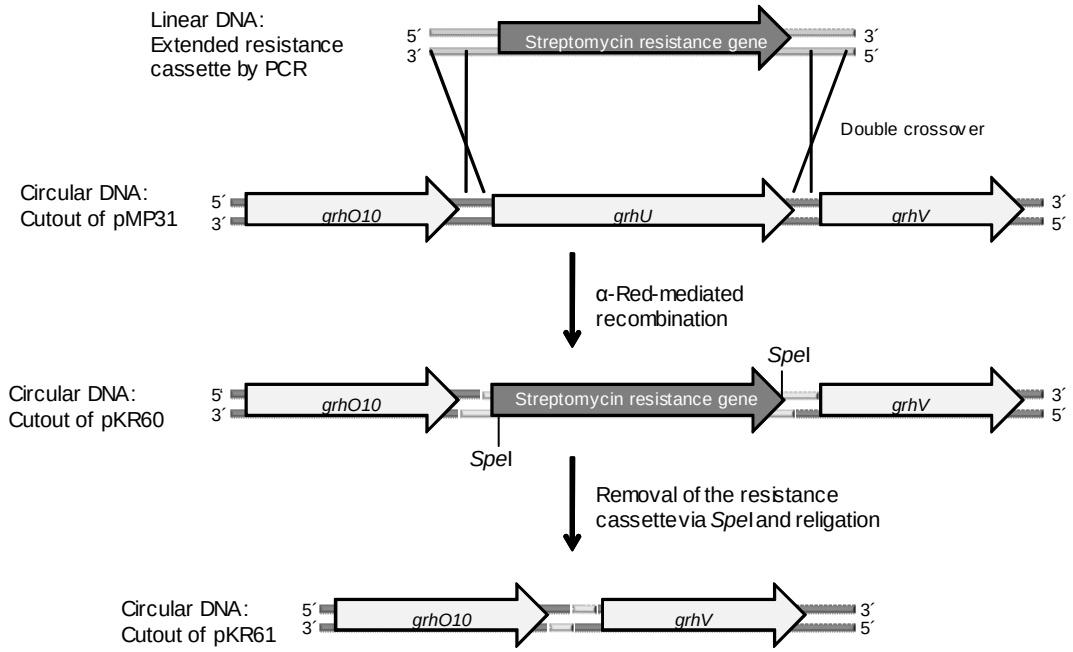

Fig. 43: Schematic overview of the λ-Red-mediated recombination technique for deleting the gene *grhU* in the *grh* gene cluster.

In the present study, secondary metabolites resulting from the heterologous expressions of *ΔgrhU* and *ΔgrhV* mutants in *S. albus* were to be isolated and analysed to elucidate the functions of these genes in griseorhodin A biosynthesis.

4.4.2 Secondary metabolite analysis of the *ΔgrhV* mutant by LH20 chromatography, HPLC and HRMS

A portion of freeze-dried *ΔgrhV* mutant cells were extracted as decribed in section 5.15.1.2.2. The extraction resulted in 250 mg of the crude cell extract and it was analysed by HPLC (section 5.15.4.2, Figure 44).

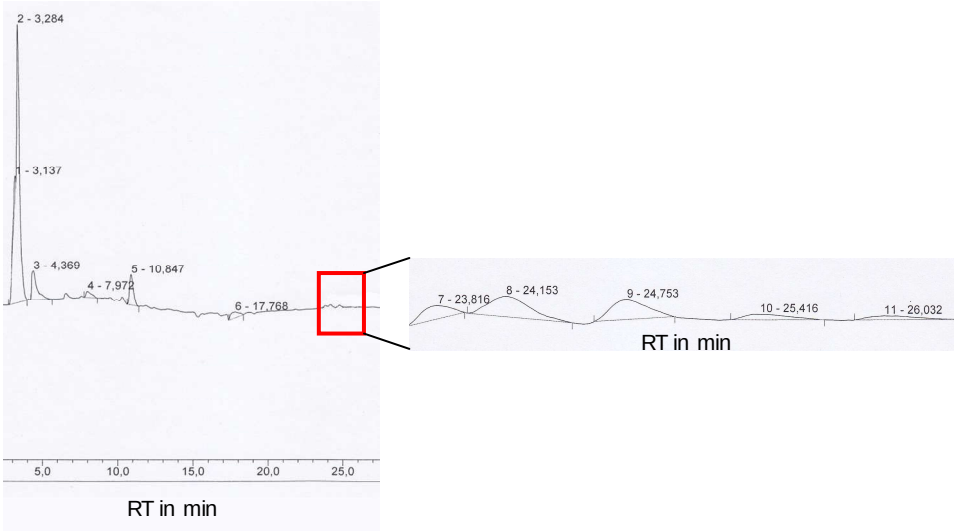

Fig. 44: Cutout of the HPLC chromatogram of the Δ*grhV* crude extract cell at 254 nm.

The box on the right side magnifies the area from 23 minutes to 26 minutes that contain potential interesting compounds from griseorhodin A biosynthesis.

The analytical HPLC analysis of the cellular crude extract indicated a complex compound mixture where compounds with higher amounts have retention times below 10 minutes. Potential interesting compounds from griseorhodin A biosynthesis come between 23 minutes and 26 minutes. This area is magnified in the box on the right side of the HPLC chromatogram in Figure 44. The crude cell extract was then subjected to a LH20 chromatography column (section 5.15.3.2), resulting in fractions 1 to 121, where every fifth fraction was analysed by HPLC (section 5.15.4.2). HPLC analysis indicated these fractions contained both pure compounds as well fractions requiring more purification steps. However, only fractions 103 to 120 contained potential interesting compounds for the griseorhodin A biosynthesis and only these were further investigated. The fractions 103 and 104 contained the same pure compound by comparing the retention times (24.9 min) and the UV profiles (Appendix 8.3). These fractions were combined (labelled as 103 in Table 4), dried and stored at 4℃. The fractions from 106 to 109 were combined and further purified by HPLC (section 5.15.4.2). These fractions contained one main compound at the

retention time of 24.0 min which was isolated (labelled as 106 in Figure 45 and Table 4).

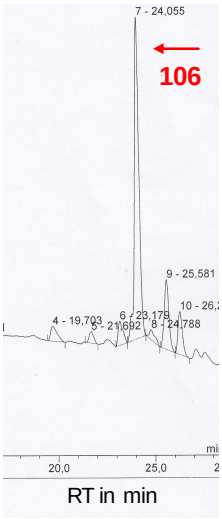

Fig. 45: Cutout of the HPLC chromatogram from combined fractions 106-109 at 254 nm.

The arrow with the number indicates the isolated compound 106 (Table 4)

Fractions 105 and 110 to 120 were combined for further purification by HPLC (section 5.15.4.2). These samples contained five main fractions with retention times of 23.8 min, 24.2 min, 24.7 min, 25.4 min and 26.0 min, all of which which were isolated (110_1 to 110_5, Table 4). However, these fractions were not checked for purity due to very small amounts of compound (less than 50 µg). The rest of the fractions from the column and HPLC were not further analysed due to the complexity of the mixtures and the time scope of the project.

In the present study, the LH20 chromatography in conjuction with HPLC resulted in two pure compounds from the *ΔgrhV* mutant. 106 and other compounds were not further investigated by HRESIMS due to the time scope of the project (Table 4).

Table 4: Compounds isolated from the Δ*grhV* mutant via LH20 chromatography and HPLC with retention times, yields, masses and proposed molecular formulas.

Compound	Retention time (t_R) [min]	Yield[µg]	Mass *m/z* $(M+H)^+$	Proposed molecular formula
Griseorhodin A	19.0	-	509.0720	$C_{25}H_{16}O_{12}$
103	24.8	700 µg	475.0982	$C_{26}H_{18}O_9$
106	24.0	50 µg	n. d.[a]	n.d.[a]
110_1	n. d.[a]	Less than 50 µg [b]	n. d.[a]	n. d.[a]
110_2	n. d.[a]	Less than 50 µg*	n. d.[a]	n. d.[a]
110_3	n. d.[a]	Less than 50 µg*	n. d.[a]	n. d.[a]
110_4	n. d.[a]	Less than 50 µg*	n. d.[a]	n. d.[a]

UV and HRESIMS spectra are represented in Appendix 8.3.1. [a] These compounds were not further investigated by HRESIMS due to the time scope of the project.

No structure was elucidated for 103 due to the time scope of the project and therefore, no conclusion can be drawn. However, the proposed molecular formula of $C_{26}H_{18}O_9$ could indicate a carboxylated quinone compound of **83**, **84** or **85** (Figure 58) due to the higher amount of carbon and the lower amount of oxygen atoms.

4.4.3 Secondary metabolite analysis of the *ΔgrhU* mutant by LH20 chromatography, HPLC and HRMS

A portion of freeze-dried *ΔgrhU* mutant cells were extracted as decribed in section 5.15.1.2.2. The extraction resulted in 350 mg of the crude extract that was analysed by HPLC (Figure 46).

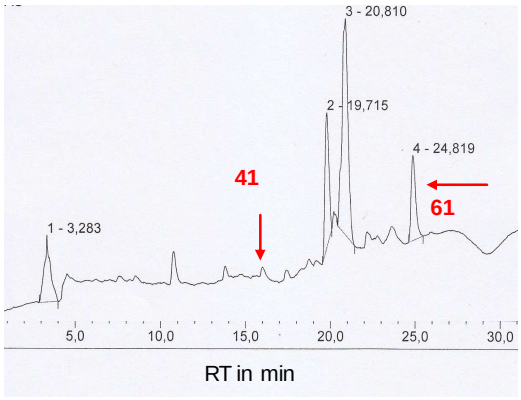

Fig. 46: Cutout of the HPLC chromatogram of the cell crude extract isolated from Δ*grhU* at 254 nm.

The numbered arrows indicate pure peaks in the cellular crude extract.

The analytical HPLC analysis indicated a complex compound mixture. The potentially interesting compounds for the griseorhodin A project come between 15 minutes and 25 minutes.

350 mg of the cellular crude extract were separated on a LH20 chromatography column (section 5.15.3.2). This column resulted in 63 collected fractions, of which every fifth fraction was analysed by HPLC (section 5.15.4.2). The HPLC analysis indicated fractions containing pure compounds as well fractions that required more purification steps.

Fraction 41, labelled with an arrow and the number 41 in the crude extract HPLC chromatogram (Figure 46), was isolated and contained a pure solid orange compound (labelled as 41 in Figure 46 and Table 5) with a retention time of 16.0 min. Fractions 61 and 62 contained the same compound, labelled with a red arrow and the number 61 in the crude extract HPLC chromatogram, (labelled as 61 in Figure 46 and Table 5) by comparing the retention times (24.9 min) and the UV profiles.

For the second LH20 chromatography, fractions 51 to 60 from the first column were combined and it resulted in fractions 64 to 94 from the second column. The fractions were then analysed by HPLC (section 5.15.4.2). The analysis indicated fractions again containing pure compounds as well as fractions that required more purification steps. The comparison of fractions 90-93 showed one main peak at 19.4 min. The fractions were combined and the main peak was isolated, labelled with a red arrow and the number 90 (labelled as 90 in Figure 47 A and Table 5). Fractions 82 to 86 and fraction 89 were combined and further purified by HPLC (section 5.15.4.2). These fractions contained two main compounds at the retention time of 19.7 min, labelled with a red arrow and the number 19.7 (labelled as 19.7 in Figure 47 B and Table 5) and at 24.8 min, labelled with a red arrow and labelled as 61_U (labelled as 61_U in Figure 47 B and Table 5) that were both isolated. Unfortunately, the first fraction at 19.7 min was lost due to instability. The second fraction, labelled as 61_U, was compared to compound 61 from the first column due to its same retention time at 24.9 min. Further comparison of the UV profile confirmed that 61_U is the same compound as 61 and therefore the fractions were combined.

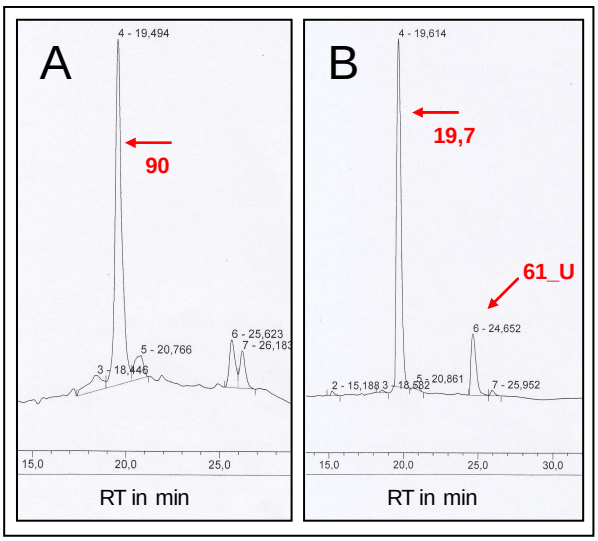

Fig. 47: Cutouts of the HPLC chromatograms for fractions 90-93 (A) and 82-86 and 89 (B) at 254 nm.

The peaks with the arrows and numbers 90, 19.7 and 61_U indicate the isolated compounds (Table 5).

Fractions 40 and 42-50 from the first LH20 column and fractions 39-44 from the second LH20 column contained several peaks and were combined for a separation on a third LH20 column. 37 fractions were collected and analysed by HPLC (section 5.15.4.2). Fractions 18-25 contained several peaks and three compounds were isolated, resulting in compounds 18_1, 18_2 and 18_3 (data not shown; Table 5). Fractions 31-37 contained two peaks at the retention times of 17.4 min and 20.8 min that were isolated by HPLC (section 5.15.4.2). This resulted in two solid pure compounds, U31_1 and U31_2; U31_2, however was lost due to instability (Table 5). The rest of the fractions from the columns and HPLC were not further analysed due to the complexity of the mixtures and the time scope of the project.

In the present study, the LH20 chromatography in conjuction with HPLC, resulted in seven pure compounds from the *ΔgrhU* mutant. 41, 61 (combined with 61_U) and 90 were further investigated by HRESIMS. The other compounds (U31_1, 18_1, 18_2, 18_3) were not further investigated by HRESIMS due to the time scope of the project and two compounds were lost due to instability (Table 5).

Table 5: Compound isolated from the Δ*ghrU* mutant via LH20 chromatography with retention times, yields, masses and proposed molecular formulas.

Compound	Retention time (t_R) [min]	Yield[µg]	Mass *m/z* $(M+H)^+$	Proposed molecular formula
MP31/*grh* A	19.0	-	509.0720	$C_{25}H_{16}O_{12}$
41	16.0	700 µg	No mass found[a]	-
61 combined with 61_U	24.9	600 µg	No mass found[a]	-
90	19.8	300 µg	No mass found[a]	-
U31_1	17.4	100 µg	n.d.[a]	n.d.[a]
18_1	15.8	50 µg	n.d.[a]	n.d.[a]
18_2	19.3	50 µg	n.d.[a]	n.d.[a]
18_3	20.9	50 µg	n.d.[a]	n.d.[a]
19.7/U31_2	-	Were lost due to instability	n.d.[a]	n.d.[a]

UV spectra are represented in Appendix 8.3. [a] These compounds were not further investigated by HRESIMS due to the time scope of the project.

The preliminary HRESIMS analyses did not indicate potential masses for the *ΔgrhU* mutant and due to the time scope of the project, no further investigations of the isolated compounds were carried out.

4.4.4 Secondary metabolite analysis of the Δ*grhV* mutant by HPLC and HRMS

For secondary metabolite analysis of the Δ*grhV* mutant, the MS, TSB and LB media were tested and the best production resulted in the liquid TSB media. For further investigation, 10 L of TSB media were fermented and the cells and the media extracted with 100% EtOAc (sections 6.15.1.2 and 6.15.1.2.1). The extraction resulted in complex compound mixtures (Figure 48).

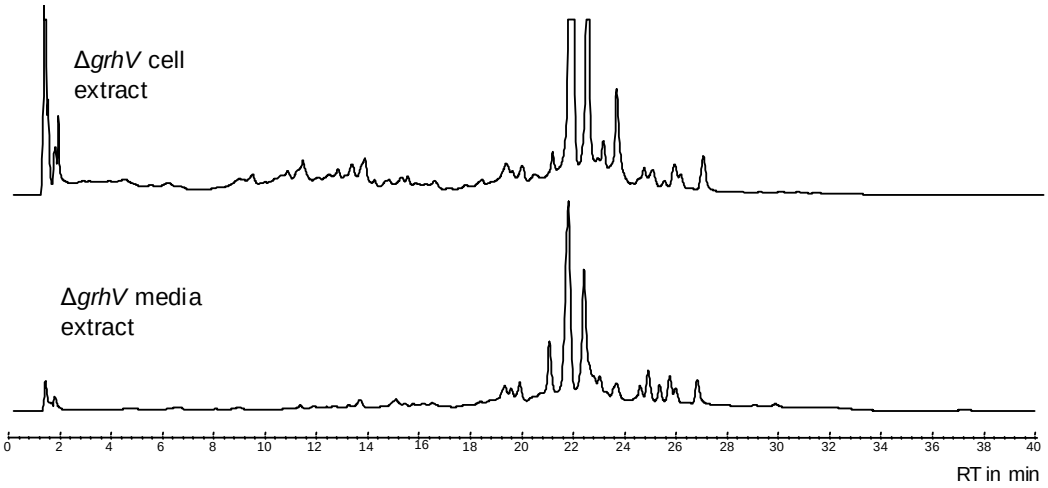

Fig. 48: Representative HPLC chromatograms of the Δ*grh*V cellular and TSB media crude extracts at 254 nm.

Retention time (RT) in minutes is denoted in minutes (min).

In the first purification step, the crude extracts were tested and run using silica gel flash chromatography (section 5.15.3.1) followed by preparative HPLC (section 5.15.4). The preparative HPLC separation resulted in four fractions from the cell extracts collected from 7.5 to 9 min (KR58Z1), from 10 min to 12 min (KR58Z2), from 14 min to 16 min (KR58Z3) and from 17

min to 20 min (A in Fig. 49) and four fraction from the media extracts collected from 7.5 to 9 min (KR58M1), from 10 min to 12 min (KR58M2), from 14 min to 16 min (KR58M3) and from 17 min to 20 min (KR58M4) (B in Figure 49).

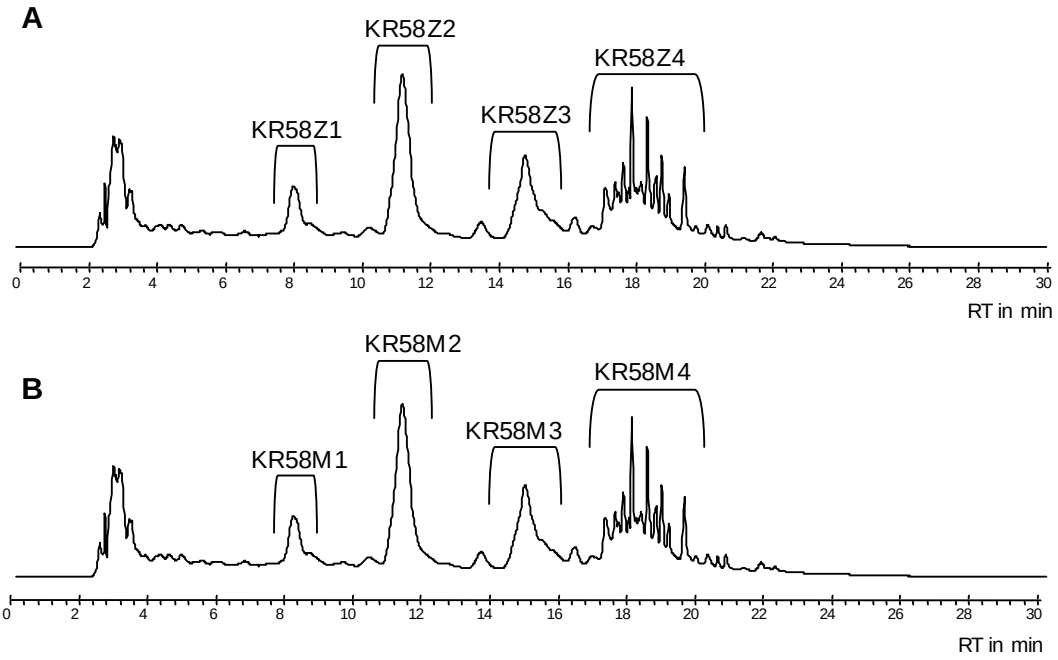

Fig. 49: Preparative HPLC traces of Δ*grh*V at 254 nm.

(A) cell crude extract from Δ*grh*V and (B) media crude extract from Δ*grh*V

The resulting preparative HPLC fractions KR58M1, KR58M1, KR58M3, KR58M4, KR58Z1, KR58Z2, KR58Z3 and KR58Z4 were monitored by HPLC (section 5.1.4.1) and it indicated two to four compounds being present in the fractions KR58M1, KR58M2, KR58Z2 and KR58Z4 as collected by preparative HPLC (Figure 50 and Figure 51). These fractions were then further separated by semi-preparative HPLC (section 5.15.4.3) at the Kekulé-Institute HPLC pool. Semi-preparative HPLC led to an improved separation of the compounds in the fractions and the following fractions were obtained from the media fractions KR58M1 and KR58M2: KR58M1_1, KR58M1_2, KR58M1_3 KR58M1_4, KR58M2_1, KR58M2_2, KR58M2_3, and KR58M2_4 (data not shown). The following fractions were obtained from the cellular fractions KR58Z2 and KR58Z4: KR58Z2_1, KR58Z2_2, KR58Z2_3 KR58Z2_4, KR58Z4_1, KR58Z4_2 and KR58Z4_3 (data not shown). The fractions from KR58M3, KR58M4, KR58Z1 and KR58Z3 were

separated by semi-preparative HPLC too, leading to new fractions (data not shown). However, these were not further investigated due to the time scope of the project.

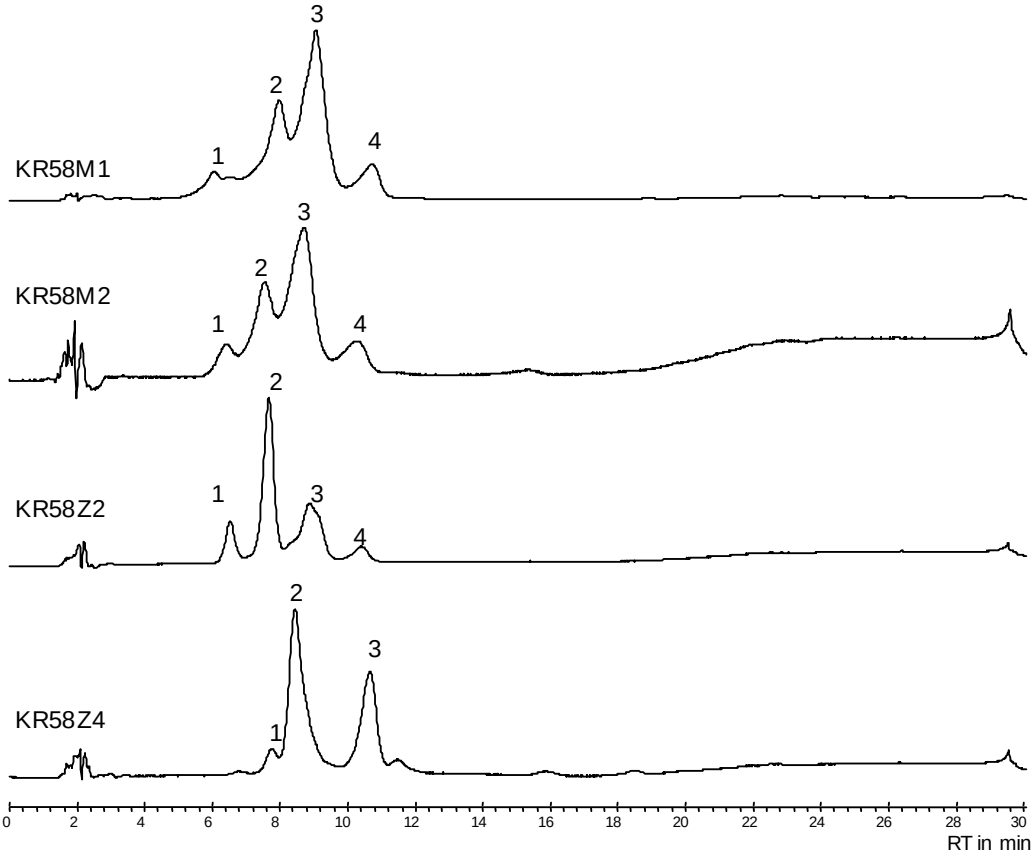

Fig. 50: Representative HPLC chromatograms of the fractions KR58M1, KR58M2, KR58Z2 and KR58Z4 containing several compounds in each fraction at 254 nm.

The numbers at the peaks indicate the new fractions within each fraction leading to the fractions KR58M1_1, KR58M1_2, KR58M1_3 KR58M1_4, KR58M2_1, KR58M2_2, KR58M2_3, KR58M2_4, KR58Z2_1, KR58Z2_2, KR58Z2_3 KR58Z2_4, KR58Z4_1, KR58Z4_2 and KR58Z4_3.

The new fractions KR58M1_1, KR58M1_2, KR58M1_3 KR58M1_4, KR58M2_1, KR58M2_2, KR58M2_3, and KR58M2_4, KR58Z2_3 KR58Z2_4, KR58Z4_1, KR58Z4_2 and KR58Z4_3 were monitored by HPLC (section 5.15.4.2), indicating impure compounds (data not shown). They required further separations using HPLC (section 5.15.4.2). Figure 50

illustrates the separation scheme of the media and cell fractions from Δ*grh*V.

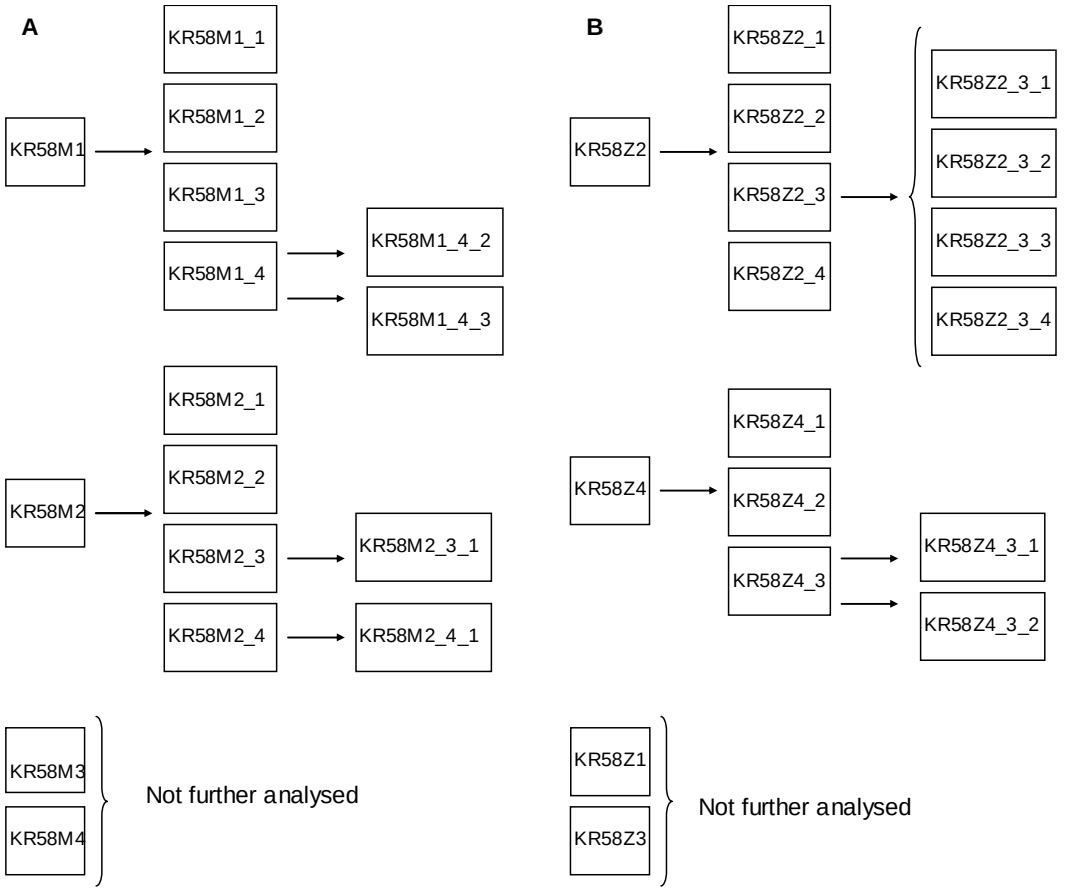

Fig. 50: Separation scheme of the media and cell fractions from Δ*grh*V.

(A) KR58M1 and KR58M2 and (B) KR58Z2 and KR58Z4.

Figure 52 shows representative the final separations of fractions of KR58Z4_3 and KR58M2_4, each resulting in two pure compounds KR58Z4_3_1 and KR58Z4_3_2 (Figure 52 A, Table 6) and KR58M2_4_1 and KR58M2_4_2 (Figure 52 B, Table 6), respectively

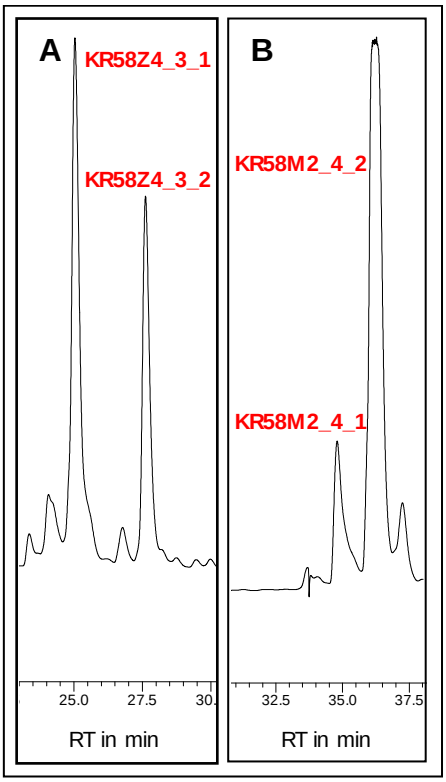

Fig. 52: Cutouts of the representative HPLC chromatograms from separations of fractions Z4_3 (A) and KR58M2_4 (B) at 254 nm.

The chromatograms represents the separation of fractions KR58Z4_3 and KR58M2_4 resulting in the pure compounds Z4_3_1, Z4_3_2, KR58M2_4_1 and KR58M2_4_2 (Table 6).

Finally, the sequential fractional separations led to 15 pure compounds from the Δ*ghrV* mutant via HPLC and these were further investigated by HRESIMS (Table 6).

Table 6: Compounds isolated from the Δ*grhV* mutant via HPLC with retention times, yields, masses and proposed molecular formulas.

Compound	Retention time (t_R) [min]	Yield[µg]	Mass *m/z* $(M+H)^+$	Proposed molecular formula
Griseorhodin A	19.0	-	509.0720	$C_{25}H_{16}O_{12}$
KR58M2_3_1	24.0	1200 µg	No mass found	-
KR58M2_4_2	25.0	500 µg	438.1128/ 853.2232	$C_{25}H_{19}O_6$/ $C_{50}H_{38}O_{12}$
KR58Z2_2	24.0	400 µg	453.0994	$C_{27}H_{16}O_7$

KR58M1_4_2	25.0	300 µg	415.1216	$C_{25}H_{19}O_6$
KR58M1_1	23.7	300 µg	448.1120	$C_{21}H_{20}O_{11}$
KR58Z2_3_3	24.3	300 µg	415.1244	$C_{18}H_{22}O_{11}$
KR58Z4_3_1	25.0	200 µg	415.1248	$C_{18}H_{22}O_{11}$
KR58Z2_3_2	24.3	200 µg	No mass found	-
KR58M2_4_1	24.0	200 µg	460.1110	$C_{26}H_{20}O_8$
KR58M2_2_1	23.4	200 µg	501.1130	$C_{28}H_{20}O_9$
KR58Z4_1	24.0	100 µg	453.0991	$C_{27}H_{16}O_7$
KR58M1_4_3	27.6	100 µg	No mass found	-
KR58Z4_3_2	27.6	100 µg	No mass found	-
KR58Z2_3_1	24.0	100 µg	453.0991	$C_{27}H_{16}O_7$
KR58Z2_3_4	25.0	50 µg	No mass found	-

UV and HRESIMS spectra are represented in Appendix 8.3 and 8.4. Griseorhodin A is used for the comparison with the other compounds.

The compound KR58M2_4_2, which originated from the major peak in the mixture (Figure 52), was analysed by the positive-ion ESI mass spectrometry, showing two main peaks at *m/z* = 438 and 853. Their presence indicated a sodiated radical cation[140] ($M^{+\cdot}$) and its sodiated dimeric form $[2M+Na]^+$. To determine the molecular formulas of these two ions, HRESIMS was performed and the following molecular formulas were proposed: $C_{25}H_{19}O_6Na$ (*m/z* 438.1061 calcd. 438.1074) and $C_{50}H_{38}O_{12}Na$ (*m/z* 853.2232, calcd. 853.2255) respectively (Figure 53 A). A further analysis by a MS/MS measurement was carried out using 853 as the parent mass that confirmed this hypothesis. The MS/MS spectrum showed the pseudomolecular ion peak $[M+Na]^+$ at *m/z* = 439.1146 corresponding to the monomer form (Figure 53 B). The compound was further characterised by cryo NMR (section 4.1.2.1.1).

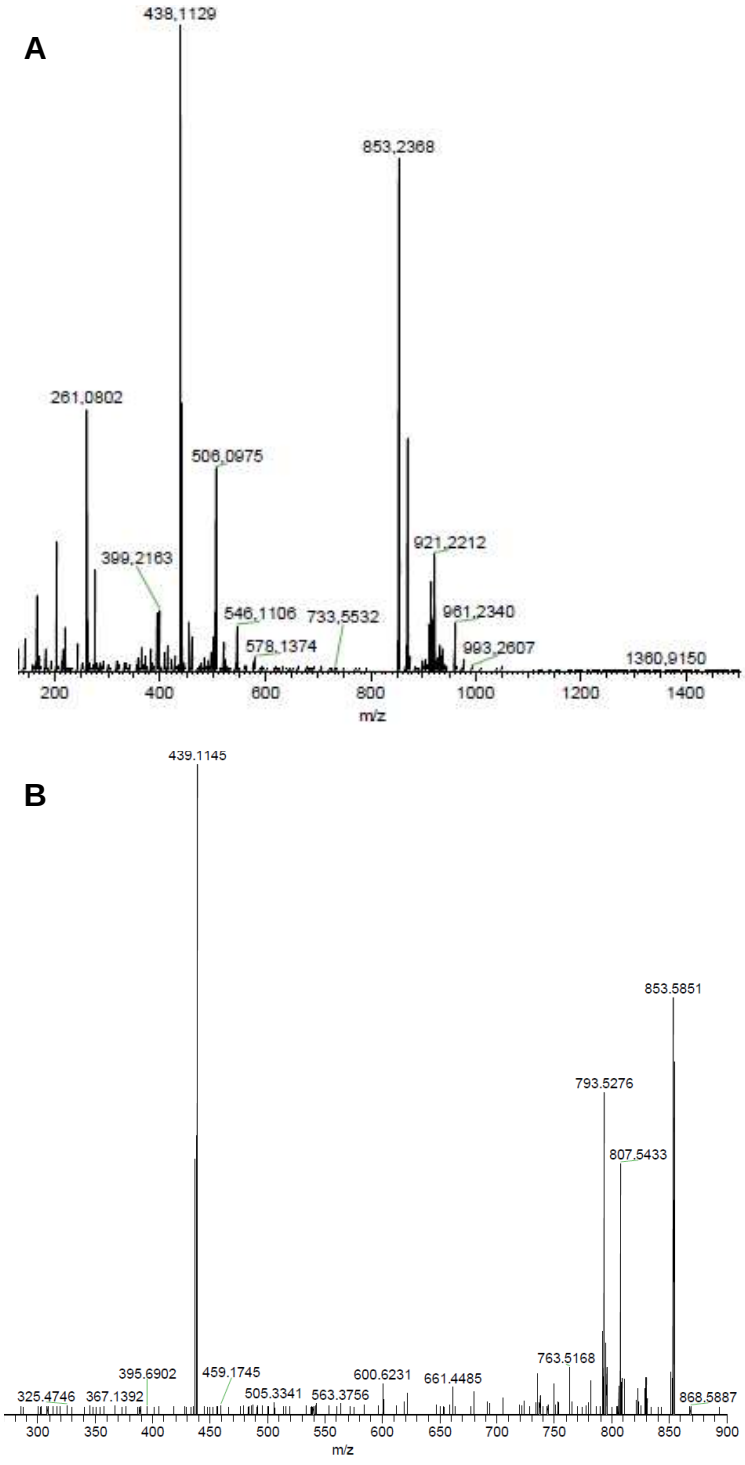

Fig. 53: Mass spectra of KR58M2-4-2.

(A) HRESIMS and (B) MS/MS spectra of KR58M2_4_2 in the ranges of *m/z* 0-1500 and 0-900 respectively.

For the compound KR58M2_4_1, *m/z* = 460.1110 was identified that corresponds to $C_{26}H_{20}O_8$ and therefore could be the carboxylated product

of KR58M2_4_2. The mass of the compound KR58M1_4_2 (*m/z* = 415.1216) indicates the proposed molecular formula of $C_{25}H_{19}O_6$ corresponding to $C_{50}H_{38}O_{12}$, possessing the same molecular formula and the retention time as KR58M2_4_2. However, the different UV profiles indicate configurational changes (Appendix 8.3). The rest of the identified masses and the corresponding molecular formulas have a higher number of carbon atoms and a lower number of oxygen atoms than griseorhodin A. Therefore, they could represent early intermediates of griseorhodin A biosynthesis. However, for final conclusions of the intermediates, characterisations by NMR are required. Due to time scope of the project, repetitions of HRESIMS analyses were not further carried out, for the compounds where a mass was not found.

4.5 Structure elucidation by NMR

Structure elucidation was carried out by NMR in the research group of Murray Munro and John Blunt at the University of Canterbury (Department of Chemistry) in Christchurch, New Zealand. Due to the small amount of the samples, capillary probe NMR (capNMR) was chosen as a method for the structure elucidation.

4.5.1 An introduction into capillary probe NMR

A capillary probe has a flow cell that typically possesses a flow rate in the NMR probe of 1-50 µL/min and a sample volume in the range of 1-10 µL.[141] Therefore, the capillary probe is sometimes known as a capillary microflow probe, although a capillary probe can also have a much larger volume capacity. CapNMR probes were designed to obtain NMR spectra on mass-limited samples. The probes allow the acquisition of quality spectra from low sample amounts such as 20 µg.[142] CapNMR can also be used for larger amount to achieve the same signal-to noise (s/n) ratio in a shorter period of time.[143] The first small volume NMR flow probes were constructed in the laboratories of Sweedler and Albert in the 1990s.[144-146] These were

designed for coupling to capillary electrophoresis (CE) and capillary HPLC (capLC) to handle the small volumes associated with these techniques.

4.5.2 Analysis of the mutants utilising capNMR

Several pure compounds obtained during isolations from the *ΔgrhV* and *ΔgrhU* mutants (Tables 2, 4 and 5) were subjected to capNMR (section 5.15.6.1) for structure elucidation. Many 1D and 2D spectra were recorded testing different deuterated solvents such as CD_3Cl, CD_3OD and DMSO-d_6. However, it was not possible acquire any sensible spectra; broad signals and low sensitivity were acquired (data not shown). Furthermore, the fact that samples were more or less irreversibly absorbed onto the silica of the interior of the probe made the analysis even more challenging.

Broadened signals come from two common sources: slow exchange (rotamers) near the Larmor frequency of the NMR signals and the presence of paramagnetic species including transition metal ions and organic radicals.[147] Slow exchange happens if compounds are reactive with MeOH. In order to avoid reversible Michael additions with CD_3OD, NMR spectra were recorded in DMSO-d_6, but the phenomena of broad signals still appeared. Furthermore, the broad signals could also indicate a paramagnetic contamination within the samples due to the presence of metal ions such as Fe(II) and Fe(III). These are likely candidates since the naphthoquinones are good chelators.[147] The way to eliminate this is to pass the samples through Chelex mixed bed ion exchange resin. Another possibility is the presence of free radicals generated from autoxidation; the highly coloured naphthoquinones could be O_2 sensitizers under normal laboratory lighting and thereby limit the ability to record high quality spectra.[147] To eliminate this and other possible exchange processes, the OH groups of the compounds can be converted into methyl esters.[147]

4.5.2.1 Diazomethane derivatisation

Due to the difficulties encountered during the NMR data acquisition using capNMR, the sample KR58Z4_1 was derivatised with diazomethane. Diazomethane converts naphthoquinones (the OH groups are capped as OMe groups) into methyl esters and the derivatised compounds become less polar, which are less sticky and easier to handle.[147]

Diazomethane was prepared by hydrolysis of an ethereal solution of an *N*-methyl nitrosamide with aqueous base (section 5.16). The precursor was *N*-methyl-*N*-nitroso-p-toluenesulfonamide (Diazald).[148]

The sample was derivatised with diazomethane and, as a positive control for this reaction, phenol was derivatised simultaneously. After the derivatisation, both compounds were analysed using HPLC (section 5.15.4.2; Figure 54 A-D). The analysis suggested successful derivatisation of the compounds, producing later eluting peaks, indicating the incorporation of methyl esters into the molecules (labelled with stars in Figure 54 C and D). The derivatised sample was then collected using HPLC (section 5.15.4.2) and subjected to capNMR for structure elucidation. However, this did not improve the measurement as broad signals were still present (data not shown) and structure elucidation by capNMR was not possible.

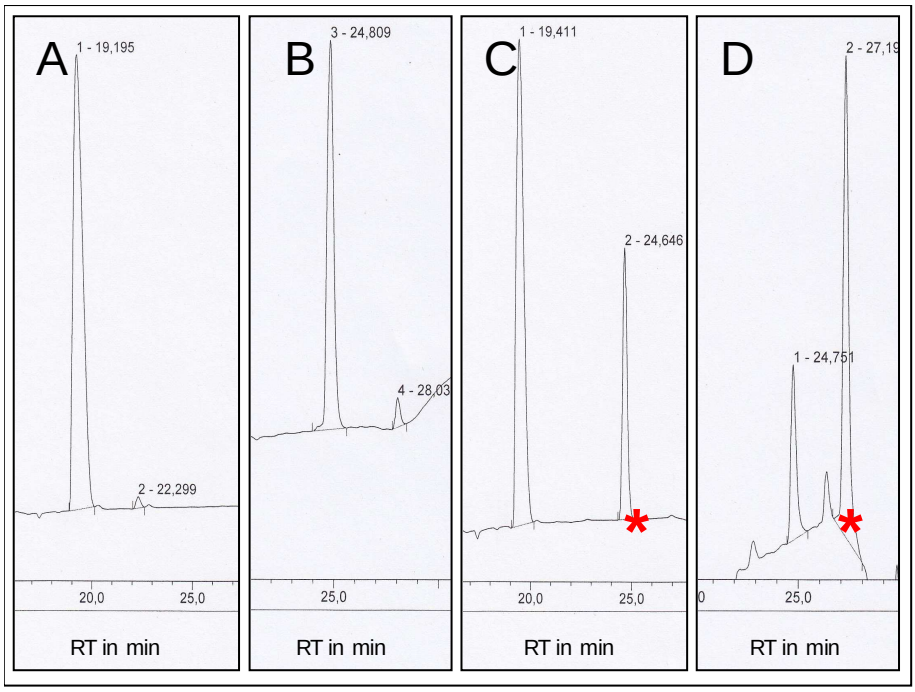

Fig. 54: HPLC chromatograms of phenol (A) and KR58Z4_1 (B) and the derivatised samples phenol (C) and KR58Z4_1 (D) at 254 nm.

The stars represent the derivatised compounds.

In the present study, cryogenic NMR was chosen as a second NMR type to carry out further structur elucidations of the compounds. It is suitable for low amounts of samples as well and acquires NMR data at a very cold temperature. This part of the project was carried out with our cooperation partner at the University of Naples in the group of Prof. Mangoni, using a 700 MHz cryogenic NMR.

4.5.2.2 Introduction into cryogenic NMR

Cryogenic NMR (cryo NMR) is a NMR technique that is suitable for low amounts of sample material. It typically uses a 3 or 5 mm diameter probe that is designed with cryogenically cooled coils at temperatures reaching -248℃ (25 K). [149] Thermal noise is reduced, thereby increasing sensitivity up to 3-4 times in s/n ratio compared to conventional NMR (warm probe). To hold the temperature, helium gas provides the probe and the electronic

circuitry housed in the probe body, such as the preamplifier, with cold helium gas (~10 K) that is then heated in the probe to 25 K.[150]

4.5.2.2.1 Structure elucidation by cryogenic NMR

To further characterise the compound KR58M2_4_2, cryogenic NMR was performed and analysed by Dr. Roberta Teta at the University of Naples. The NMR experiments were carried out in CD_3OD. Both 1D and 2D NMR spectra were acquired using a Varian cryo probe with 700 MHz and 175 MHz (section 5.15.6.2). The resulting data are summarised in Figure 55 and Table 7. The ^{13}C NMR spectrum displayed a signal at 209.2 ppm indicating the presence of a carbonyl group. The presence of an aldehyde function could be excluded as there was no correlation signal in the HSQC spectrum between the carbonyl carbon and the aldehydic proton. Therefore, this keto function was determined as a starting pojnt for the structure determination. The corresponding keto carbon (C-16) was coupled in the HMBC spectrum with the three methyl protons at 2.22 ppm ($H_{\alpha,\beta,\gamma}$-17) and the two equivalent methylene prontons at 3.68 ppm (H-15). These were coupled with a quarternary carbon atom at 137.3 (C-3) and showed two intense correlation peaks with carbons at 116.7 and 121 ppm. The HSQC spectrum showed corresponding aromatic protons at 6.64 (H-2) and 6.68 (H-4) ppm. The position of H-2 and H-4 in the first aromatic ring was determined as *meta*, as the *ortho* position could be excluded based on the multiplicity of the corresponding proton signals (singlets) and no COSY correlation was observed between those hydrogens. The *para* position was also excluded due to the presence of the HMBC ^3J correlation between C-2 and H-4. A long-range coupling was observed between H-2 and C-1 at 150.0 ppm and the downfield chemical shift of the aromatic carbon suggested it to be connected to an OH group. The observation of the couplings of both H-2 and H-4 with the carbon at 120.5 ppm and the coupling of H-4 with the carbon at 143.3 ppm allowed the assignment as C-14b and C-4a, respectively. C-4a coupled to two methylene protons at 2.75 ppm ($H_{\alpha,\beta}$-5) and one proton at 3.70 ppm (H_α-6). The protons $H_{\alpha,\beta}$-5 correlated with the same H_α-6 and with the proton at 2.74 ppm with H_β-6

and furthermore, a correlation peak between $H_{\alpha,\beta}$-5 and H_{α}-6 was visible in the COSY spectrum. H_{α}-6 was coupled with the carbon at 125.4 ppm and 140.9 ppm. $H_{\alpha,\beta}$-5 showed only a coupling with the carbon at 125.4 ppm. Thus, these carbons were defined as C-6a and C-14a. In addition to that, H_{α}-6 showed a ^{3}J correlation with the hydroxy carbon at 159.0 ppm. Essential information about the complete structure was obtained by the analysis of the HMBC couplings of the proton at 4.48 ppm, identified as H-13. This proton coupled with the carbon at C-13 (C-13´) at 58.3 ppm, thus supporting the dimeric characteristic of the molecule. Furthermore, H-13 was coupled with the carbon at 109.6 ppm (C-12) and 121.4 ppm (C-14). Their corresponding protons were defined by the HSQC spectrum as H-12 at 6.26 ppm and H-14 at 6.70 ppm. H-14 was strongly overlapped to H-4 and coupled in HMBC with C-14b. Concluding this data, the identified structure is unknown to date. This unsual molecule was assigned as 13,13´-fused bis-tridecaketide dimer **78** (Figure 55). The compound is structurally related to the benastatin A dimer **79** (Figure 56).[151] However, **78** is decarboxylated at H-2 which might have occured during the extraction process. Interestingly, HRESIMS analyses (Table 2) also indicated the mass of $C_{26}H_{20}O_8$ for KR58M2_4_1 that could be the carboxylated product of **78**. **79** (Figure 56) was isolated from the benastatin biosynthetic pathway in the absence of BenF. BenF encodes a novel *C*-methyltransferase that catalyses a geminal bismethylation in the benastatin A biosynthetic pathway at the position corresponding to C13 in **78**.[151]

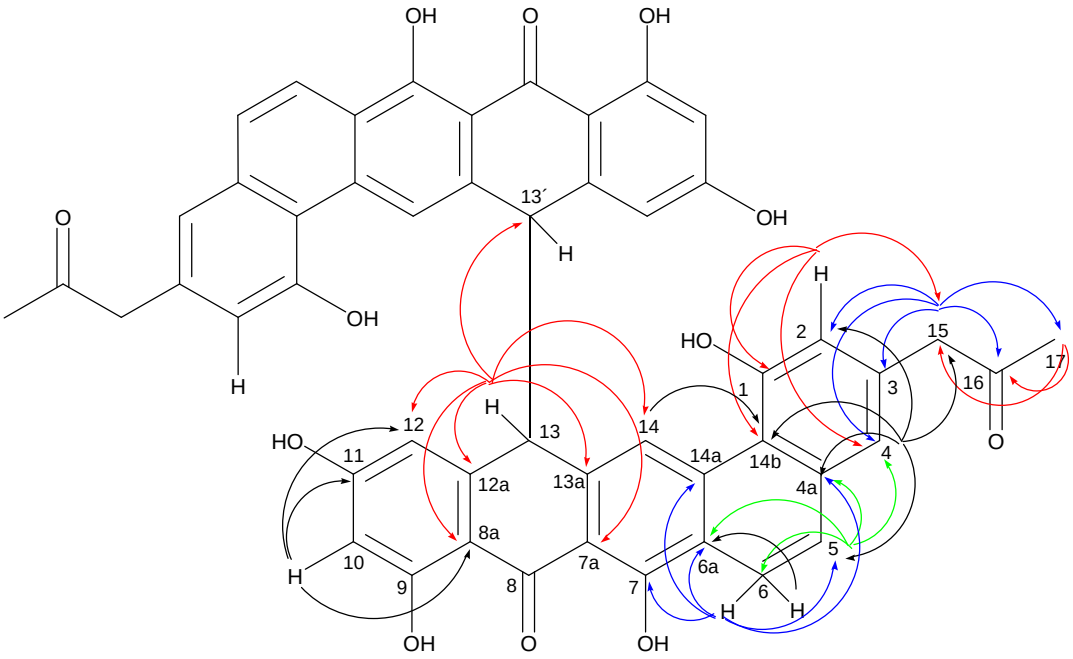

13,13´-fused bis tridecaketide dimer **78**

Fig. 55: 13,13´-fused bis-tridecaketide dimer 78.

All HMBC couplings are shown in arrows. Each colour represents couplings originating from the same proton.

Table 7: Summary of the NMR data for 13,13´-fused bis-tridecaketide dimer 78 **from *S. albus* KR58.**

Position	^{13}C	^{1}H (J[Hz])	COSY	HMBC
1	157.0			
2	116.7	6.64 (s)		1, 4, 14b, 15
3	137.3			
4	121.5	6.68 (s)	3,68	2, 4a, 5, 14b, 15
4a	143.3			
5	30.5	2.75 (dd, 11.6, 5.6)	6,68, 3,01	4, 4a, 6, 6a
6	21.2	3.07 (ddd, 14.8, 5.1, 5.1) 2.74[a]	2,75, 6,68	4a, 5, 6a, 5, 14a
6a	125.4			
7	159.0			
7a	115.1			
8	190.0			
8a	111.7			
9	173.7			
10	102.6	6.12 (s)		8a, 11, 12
11	165.8			
12	109.6	6.26[a]		
12a	146.3			
13	58.3	4.48 (br. S)		7a, 8a, 12, 12a, 13a, 13´, 14

13a	138.8			
14	121.4	6.70 (s)		14b
14a	140.9			
15	51.4	3.68 (s)	2,22, 6,64, 6,68	2, 3, 4, 16, 17
16	209.2			
17	29.1	2.22 (s)	3,68	16, 15

The data was acquired in CD^3OD. [a] Overlapping signal.

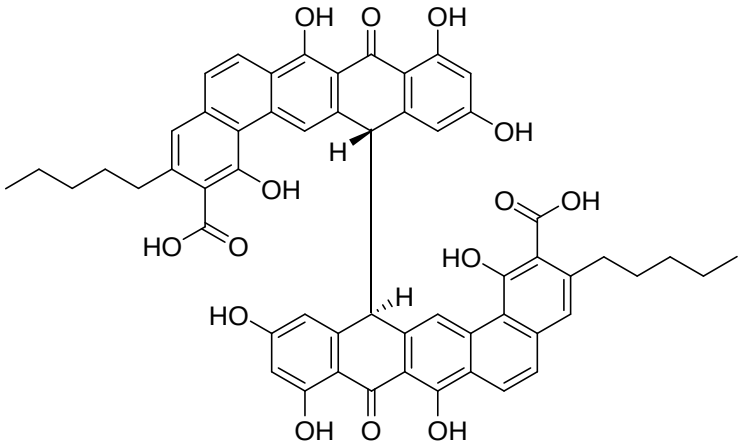

13,13´-fused bis-nor-benastatin A **79**

Fig. 56: 13,13´-fused bis-nor-benastatin A 79.

Both dimers (78 and 79) resemble various plant-derived bisanthrones.[152] An important example for this is emodin bianthrone **80**, the proposed key intermediate in hypericin **81** biosynthesis (Figure 57).[153] **81** is a naphthobianthrone compound produced in the dorsal leaf glands of *Hypericum perforatum* L., commonly known as St. John´s wort, and it has been tested positively in numerous studies for the treatment of mild and moderate depression.[153-155] Nonsubstituted anthrones are highly unstable and rapidly oxidise to quinones and dimeric products through benzyl radicals.[153, 156-158] In these reactions no biocatalysts are required in contrast to enzymatic aryl couplings.[159, 160]

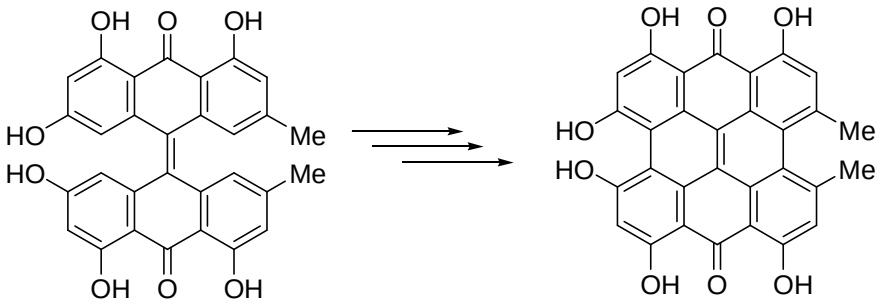

Fig. 57: Emodin bianthrone 80 and hypericin 81.[153, 154]

In the case of benastatin A, the absence of BenF led to alternative reaction channels such as quinone formation and dimerisation.[151] It was speculated that the geminal bismethylation of the benastatin anthrone precursor by BenF blocks quinone formation and oxidative dimerisation during the polyketide assembly.[151] GrhV homologues are found in other pentangular biosynthetic pathways such as pradimicin (PdmI), benastatin (BenJ), rubromycin (RubT), lysopilin (LlpOII) and fredericamycin (FdmQ), but none of them encode characterised proteins (Table 3). Given the structural and biosynthetic resemblance, the presence of these genes encoding unknown functions in the gene clusters and the fact that the molecules from pradimicin A, griseorhodin A, rubromycin and fredericamycin A biosynthetic pathways are considered to be among the most heavily oxidised aromatic polyketides known to date,[25] these findings support the hypothesis that such genes play roles in oxidative steps during polyketide assembly. However, very little is known about the oxygenation of aromatic polyketide natural products derived from polyketide chains longer than 18 carbons and to date, GrhV homologues have not been investigated by e.g inactivation studies. The intermediate of *ΔgrhV* mutant contains a low number of oxygen atoms and a higher number of carbon atoms than griseorhodin A, indicating a very early involvement of the enzyme in griseorhodin A biosynthesis. Therefore, the results of this study suggest that GrhV could catalyse the first quinone formation in ring A **83** in Figure 58, B **84** in Figure 58 or C **85** in Figure 58, followed by oxygenations of the other rings by griseorhodin oxygenases such as GrhO8 and GrhO9, as their HRESIMS

data indicated in a previous study.[1] In the absence of GrhV, the highly unstable anthrone-like precursor **82** is oxidised through a benzyl radical **86** to the carboxylated dimeric product **87** (Figure 58). Compound **87** could have converted into **78** during extraction process, suggesting that **78** is the decarboxylated product of **87**.

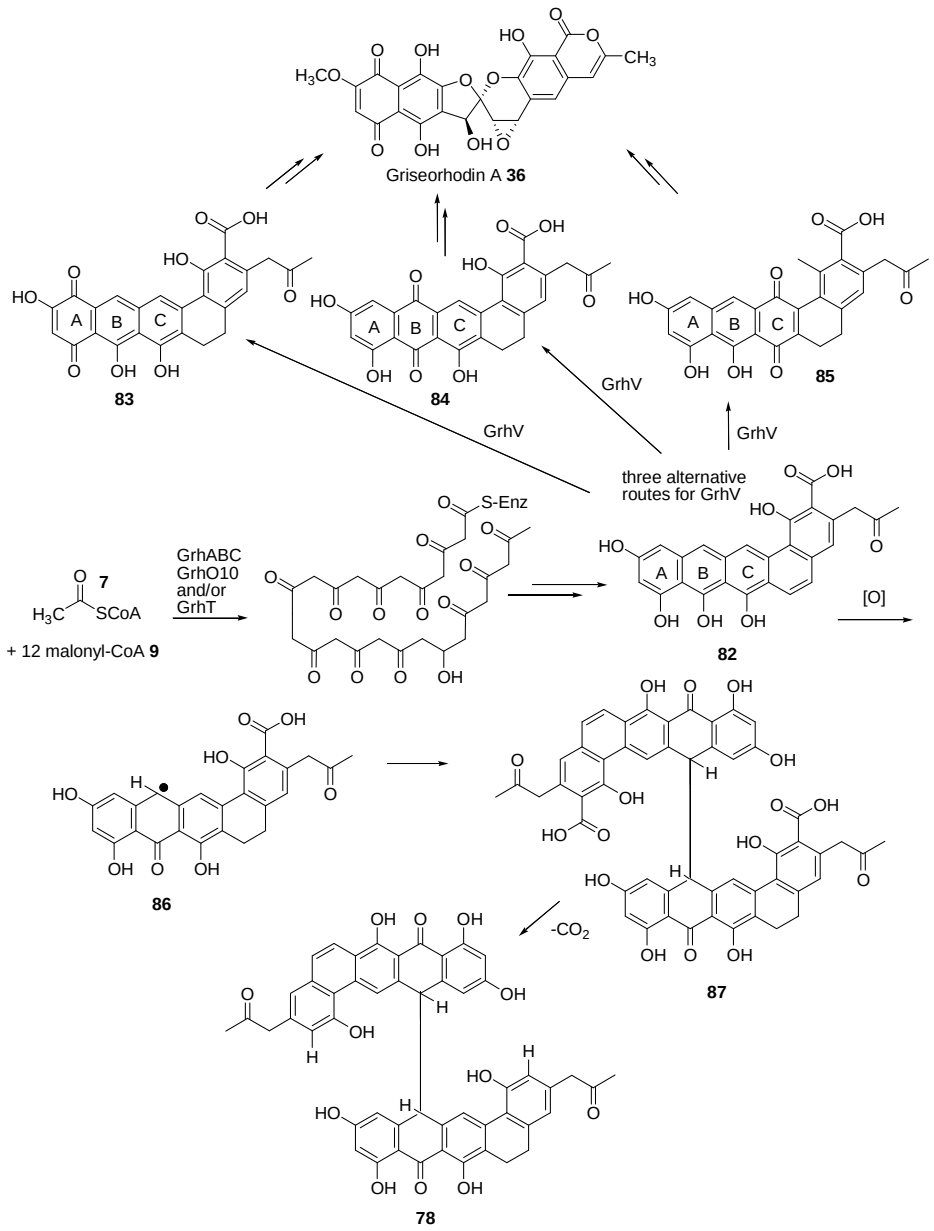

Fig. 58: The proposed reaction pathway for GrhV.

To our knowledge, the present study gives first insights into the function of GrhV as a novel oxygenase and its homologues found in other pentangular biosynthetic pathways.

4.6 Summary and outlook

In the present study, early biosynthetic steps of the telomerase inhibitor griseorhodin A **36** were investigated utilising heterologous expression and in-frame gene deletions by subsequently analysis of secondary metabolites generated as well as functions of the uncharacterised enzymes GrhV and GrhU.

The present study investigated the early biosynthesis of griseorhodin A by heterologous expression and gene inactivation studies using λ-Red-mediated recombineering. Generated constructs were conjugated into the host organism *S. albus* for heterologous expression. Secondary metabolite productions were investigated by HPLC, HRMS and cap and cryo NMR. The early griseorhodin A genes comprise of the *grh* minimal PKS genes *grhA* (KS_α), *grhB* (KS_β) and *grhC* (ACP) as well as the cyclase genes *grhE*, *grhQ* and *grhT*.

Heterologous expression was applied to express the *grh* minimal PKS independently and with *grh* cyclases. These genes were individually amplified from the griseorhodin A gene cluster by PCR and subcloned into the *E. coli-Streptomyces* shuttle vector pKJ55. The expression of the *grh* minimal PKS did not result in detectable amounts of polyketides or shunt products. This is in clear contrast to other type II minimal PKSs such as the *tcm*, *act* and *whiE* minimal PKSs that produce characteristic products such as **21**-**24** (Figure 8). Different media in liquid and solid forms were tested, and many screenings were performed to identify a clone that had increased production of secondary metabolites. However, no clone producing characteristic products was idenfied. Similar results were observed in the case of enterocin biosynthesis, namely that the *enc* minimal PKS requires an additional factor, in this case the ketoreductase EncD, to be fully functional.[81] Therefore, to test whether the performance of the *grh* minimal PKS is context-dependent, co-expressions with putative *grh* cyclases, GrhE, GrhT and GrhQ, were carried out. The expressions with cyclases did

not result in the production of detectable amounts of polyketides. This suggests that the presence of a multienzyme complex for the griseorhodin A biosynthesis is required, where not only *grh* cyclases are significant, but also an additional stabilising enzyme could be required. One such potential candidate could be GrhS, which possesses strong homology to enzymes stabilising the minimal PKS protein assembly.[25] In early biosynthesis of pradimicin A, a highly similar polyketide to griseorhodin A, *pdm* cyclases and a monooxygenase work in concert for the regioselectivity tailoring of a polyketide backbone and cannot act independently without their associated partners.[130] Griseorhodin A is one of the longest aromatic polyketides and could therefore require additional enzymes for stabilisation of its polyketide chain.

Furthermore, due to the unexpected results in the heterologous expression of the *grh* minimal PKS, the functionality of the *grh* minimal PKS in the *E. coli* - *Streptomyces* shuttle vector was tested using RT-PCR. In conclusion, the gene *grhC* is transcribed using the ermE* promoter, but no clear result could be obtained for *grhAB* as no bands were obtained for *grhAB* or its positive controls. Another technique to test the functionality of a construct could be accomplished by a subsequently cloning of an antibiotic resistance cassette into corresponding expression vector.

To gain more insights into the early biosynthetic steps of griseorhodin A, putative *grh* cyclases were individually deleted in the gene cluster and the modified clusters were heterologously expressed in *S. albus* J1074. Deletion of *grhE* did not affect griseorhodin A biosynthesis; the polyketide was still produced. Therefore GrhE does not play a significant role in the griseorhodin A biosynthesis. Inactivations of GrhT and GrhQ abolished griseorhodin A biosynthesis and did not result in the production of detectable amounts of polyketides. The current results are in agreement with earlier experiments from the heterologous expression approach and provide further evidence that GrhQ is needed for a functional protein complex.

To further investigate early griseorhodin A biosynthesis, two new mutants, Δ*grhH-P* and Δ*grhH-Q*, were generated. In the first mutant, all tailoring genes from *grhH* to *grhP* were deleted and in the second gene deletion mutant the mutation was extended to *grhQ*. Heterologous expression of the *ΔgrhH-P* mutant led to production of a complex compound mixture of secondary metabolites. It produced identical intermediates to the Δ*grhM* mutant from a previous study for which an early oxygenase role was proposed during grioserhodin A biosynthesis. For the Δ*grhH-P* mutant, four pure compounds were isolated. HRESIMS revealed the proposed molecular formula of $C_{19}H_{20}O_{17}$ for the compound HP1, indicating an early intermediate in griseorhodin A biosynthesis. Promising ^{1}H and COSY spectra were recorded by 700 MHz using cryo NMR. However, 2D NMR was not possible due to the small amount of compound (200 µg) and it was not further investigated during the present study. The other compounds also indicated intermediates in the early steps of griseorhodin A biosynthesis pathway. Compouding the results for the Δ*grhM* and Δ*grhH-P* mutants from the previous and the present study, the role of GrhM could be propose an early oxygenase role of GrhM in the griseorhodin A biosynthetic pathway. However, for final conclusion, structure elucidation of the corresponding intermediates by NMR is required.

In order to obtain more insights into the early biosynthetic steps of griseorhodin A, many attempts to individually delete further genes (grhT, grhU and grhV) in the *ΔgrhH-P* mutant were carried out, but all of them failed. However, putative *grh* cyclase gene *grhQ* is adjacent to *grhP* gene and it could be additionally deleted by extending the gene mutant *ΔgrhH-P* to *grhQ*. The heterologous expression of the mutant *ΔgrhH-Q* led to the abolishment of griseorhodin A biosynthesis. This is in agreement with the *grhQ* inactivation study. In contrast to these results, heterologous expression of *ΔgrhH-P* produced a complex mixture of secondary metabolites. This mutant harbours all potential early *grh* genes, including the *grh* minimal PKS, *grhQ* and as well as the potential stabilising gene *grhS*. Concluding these results, GrhQ is needed for a protein complex but it is still insufficient for a functional PKS, since for GrhABCQ no products

were detected. To date, griseorhodin A is one of the longest aromatic polyketides and therefore, it could likely require synergistic actions of cyclases (GrhQ) and other stabilising enzymes such as GrhS for its polyketide assembly. The additional proteins may form a pocket with the *grh* minimal PKS in which the multienzyme complex can act and stabilise the entire polyketide assembly simultaneously.

The uncharacterised genes in the griseorhodin A gene cluster, *grhU* and *grhV*, encode for unknown functions and therefore represent interesting targets for functional elucidations. The *ΔgrhV* (KR58) and *ΔgrhU* (KR61) mutants were constructed during a previous study using λ-Red recombineering and the modified *grh* clusters were subsequently conjugated into *S. albus* J1074 for heterologous expression.[1] Both mutants produced complex mixtures of secondary metabolites which were investigated by HPLC, LH20, HRESIMS, cap- and cryo NMR. 21 pure substances were isolated by different chromatography methods and finally, after several analysis approaches, a compound originating from the *ΔgrhV* mutant was structure elucidated in the present study. It revelead the decarboxylated 13,13´-fused bis-tridecaketide dimer **78** (Figure 59).

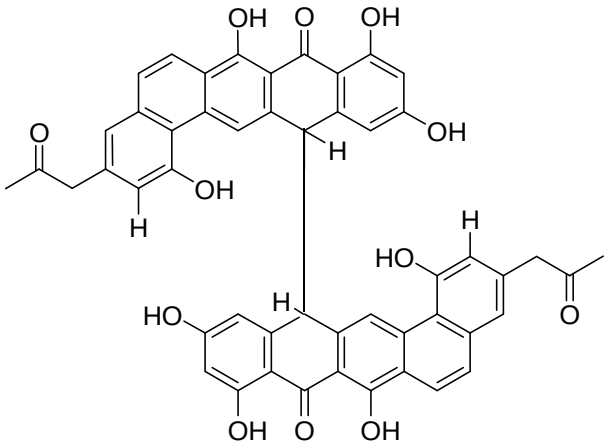

13,13´-fused bis-tridecaketide dimer **78**

Fig. 59: 13,13´-fused bis-tridecaketide dimer 78

The results of this study suggest that GrhV is responsible for an oxidative modification of the griseorhodin pharmacophore and could catalyse the first

quinone formation in the ring A, followed by oxygenations of the other rings.[1] In the absence of GrhV, the highly unstable griseorhodin anthrone precursor A **82** is oxidised through a benzyl radical **83** to the decarboxylated product 13,13´-fused bis-tridecaketide dimer **78** via **84.** To further investigate **78**, conformational and stereochemical studies are required to assign possible *meso* (*R*,*S*) and racemic configurations (*R*,*R*/*S*,*S*). For compounds originating from the *ΔgrhU* mutant, no structures could be elucidated and therefore, no conclusions can be drawn about the function of GrhU in the biosynthesis of griseorhodin A. However, the present study gives first insights into the function of GrhV and its homologues found in other pentangular biosynthetic pathways.

After the early steps in the biosynthetic pathway, collinone **70** is formed and three carbon-carbon bonds are cleaved by GrhO5 in cooperation probably with GrhO1 leading to the spiro compound lenticulone **71**. A further carbon-carbon bond is cleaved to reduce a six-membered ring by one carbon unit by GrhO6 and GrhJ, respectively, generating 7,8-dideoxy-6-oxogriseorhodin C **72**. The reduction of the keto functionality of 7,8-dideoxy-6-oxogriseorhodin C takes place, and the enzymes GrhO3 and GrhO7 catalyse the epoxidation of dideoxygriseorhodin C **73** leading to the polyketide griseorhodin A **36**.

The present study investigated the early griseorhodin A biosynthesis and figure 60 summarises the updated version of the griseorhodin A biosynthetic pathway based on the data obtained from a previous and the present study.[1, 123] The minimal PKS GrhABC assembles the poly-β-keto chain from one acetyl starter unit and from 12 malonyl extension units followed by the C19 keto reduction of the chain catalysed via GrhO10 or GrhT. In the present study, the heterologous expressions of the early grisoerhodin A genes experiments suggest that a multienzyme complex is needed for the early griseorhodin A biosynthesis comprised of GrhABCQST to generate the pentangular polyketide core structure. To date, griseorhodin A is one of the longest aromatic polyketides and therefore, it could likely require synergistic actions of cyclases (GrhQ) and other stabilising

enzymes such as GrhS for its polyketide assembly. The additional proteins may form a pocket with the *grh* minimal PKS in which the multienzyme complex can act and stabilise the entire polyketide assembly simultaneously.

The present study also included investigations of other uncharacterised griseorhodin A enzymes such as GrhM and GrhV. For GrhM, the previous HRESIMS and NMR data from the Δ*grhM* mutant,[1, 123] the present HRESIMS data from the Δ*grhH-P* mutant propose an early oxygenase role of GrhM in the griseorhodin A biosynthetic pathway. Another enzyme which was investigated during the present study was GrhV. For the *ΔghrV* mutant, a novel dimer structure was determined and it suggests that GrhV could catalyse the first quinone formation in ring A, B or C (Figure 60). The structure obtained from the *ΔghrV* mutant and the structures obtained from the *ΔghrM* mutant studies propose, that both enzymes are acting as first oxygenases on the pentangular polyketide core structure. However, it cannot be concluded which one of the enzymes, GrhV or GrhM, is acting first on the pentangular core structure. Compounding this fact, the early acting enzymes possess substrate flexibility depending on the intermediate present from the previous step.

Analysis of the mutants of the asparagine synthase GrhP, methyltransferase GrhL, oxidoreductases GrhO8 and GrhO9 by HRESIMS experiments in a previous study indicated variable structures with different oxygenations grades.[1] Based on HRESIMS data, GrhO8 could act as first of the enzymes mentioned[1], however for a final conclusion, a complete structure of the intermediate is required.

For GrhP, an amide transferase function has been proposed by comparing its homologues from other aromatic polyketide biosynthetic gene clusters. However, griseorhodin A does not contain an amide linkage and therefore a different function than an amide installation for GrhP has been proposed.[161]

Oxygenation by GrhO9 and *O*-methylation by GrhL takes place on lower or higher oxygenated intermediates depending on the intermediate present from the previous steps. These results confirm the substrate flexibility of the early enzymes acting after the pentangular polyketide core assembly through to the uncleaved tridecaketide collinone **70**. To date, the timing of ring 6 cyclisation remains unclear, but as the ring is still open in the griseorhodin A core structure, it can be assumed that the cyclisation takes place after oxygenations, but it cannot be concluded after which oxygenation step. After the early steps in the biosynthetic pathway, collinone **70**, is formed and three carbon-carbon bonds are cleaved by GrhO5 in cooperation with GrhO1 leading to the spiro compound lenticulone **71**. A further carbon-carbon bond is cleaved to reduce a six-membered ring by one carbon unit by GrhO6 and GrhJ, respectively, generating 7,8-dideoxy-6-oxogriseorhodin C **72**. The reduction of the keto functionality of **72** takes place, and the enzymes GrhO3 and GrhO7 catalyse the epoxidation of dideoxygriseorhodin C **73** leading to the polyketide griseorhodin A **36**.

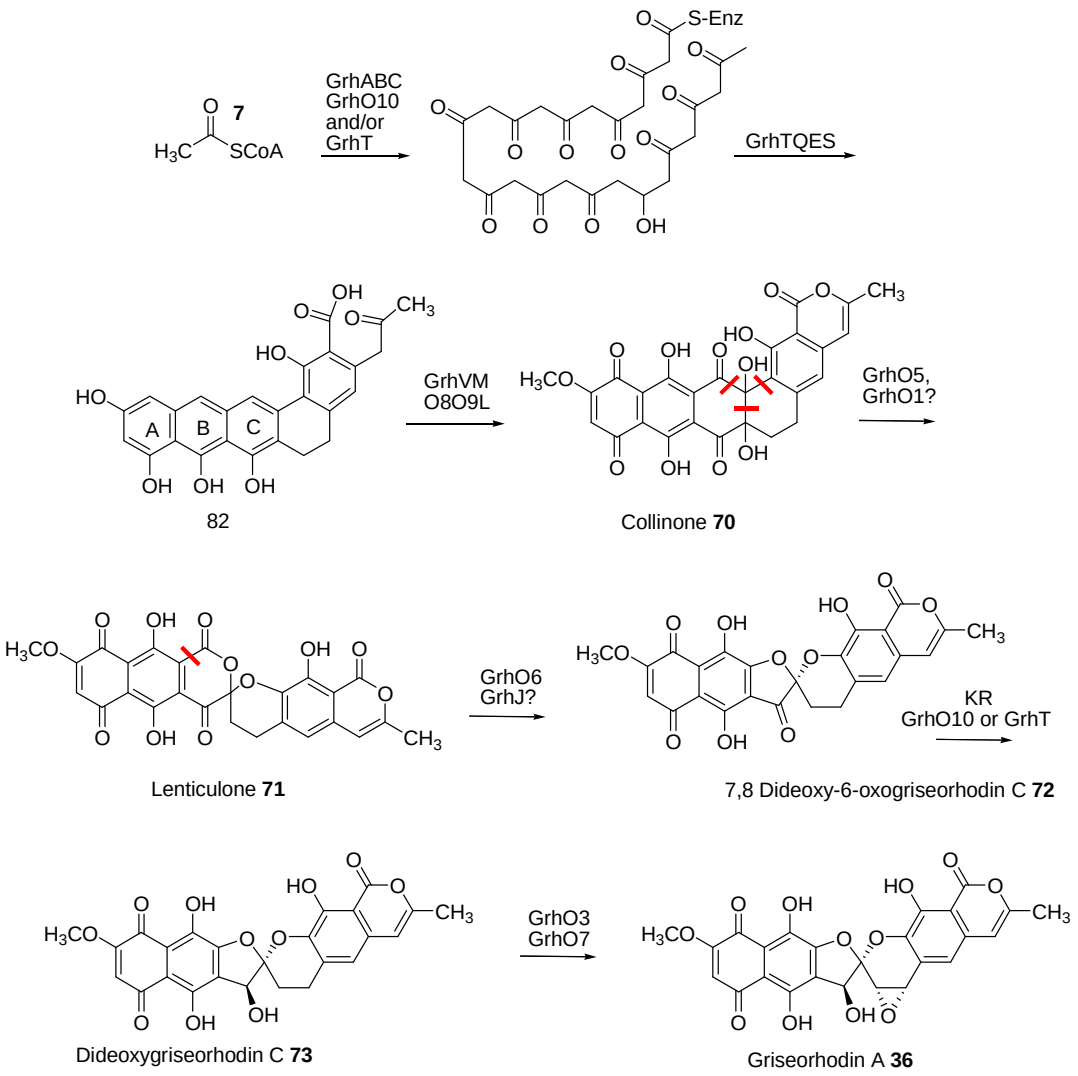

Fig. 60: The updated version of the biosynthetic pathway of griseorhodin A.

The red lines indicate C-C cleavages during the biosynthesis.

In summary, the present study gives further insights into the early steps of griseorhodin A biosynthesis. The results suggest that the presence of a multienzyme complex is significant for the assembly of the pentangular polyketide core. Furthermore, the allocation of GrhV as a novel oxygenase provides new information about how griseorhodin A and other related heavily oxidised pentangular polyketides could be formed.

5 Material and methods

5.1 Bacterial strains, vectors, primers and clones

The following bacterial strains, vectors, primers, clones and strains were used in this study (Tables 8-12).

Table 8: Bacterial strains used in the study.

Strains	Characteristics	Reference
E. coli XL1 blue	*rec*A-, *thi, hsd*R1, *sup*E44, *rel*A1, *lac*F, *pro*AB, *lac*lq, *lac*Z ΔM15, Tn10 (Tc), Tc^R	Stratagene, Amsterdam, Netherlands
E.coli BW25113/pIJ790	Δ(*araD-araB*)*567*, Δ*lacZ4787*(::*rrnB-4*), *lacIp-4000* ($lacI^+$), λ^-, *rpoS369*(Am), *rph-1*, Δ (*rhaD-rhaB*)568, *hsdR514* pIJ790: *[oriR101], [repA101*(ts)*]*, *araBp-gam-be-exo*	Datsenko and Wanner[162] Gust *et al*.[131]
E.coli ET12567/pUZ8002	*$Dam^-dcm^-hsdM^-$* pUZ8002: RK2 derivative with defective *oriT* (*aph*)	MacNeil *et al.* [163] Paget *et al.*[164]
Streptomyces albus J1074	Expression strain for grh cluster (ilv-1, sal-2)	José Salas[165]
S. albus MP31	Contains the complete *grh* gene cluster	Li and Piel[25]

Table 9: Vectors and cosmids used in the study.

Vector/Cosmids	Characteristics	Reference
pBluescriptSK+ (pSK+)	High copy vector, $ampicillin^R$	Fermentas
pIJ778	P1-FRT-*oriT-aadA*-FRT P2, $streptomycin^R$	Gust *et al.*[131]
pKJ55	Integrating *Streptomyces E. coli* shuttle vector for gene expression containing a constutive promoter ermE*, $apramycin^R$	Christian Hertweck[43]

pMP31	Integrative cosmid based on pSET152 and pWEB containing the *grh* gene cluster	Aiying Li[25]

The primers were designed using Vector NTI and were ordered at Invitrogen (Karlsruhe, Germany). Upon arrival, the primers were dissolved in TE buffer or in ddH_2O in order to prepare a 500 µM solution. This was then diluted 1:10 (50 µM) with ddH_2O for the PCR reaction mix.

Table 10: Primers used in this study.

Primer	Sequence (5´- 3´)	Tm [℃]
ACP_MfeI_for	AAA*CAATTG*CACACCTGTCACGACACGACACGAG	63.4
ACP_EcoRI_rev	AAA*GAATTC*TCAGGCGGTGGCCTGCGGAGACA	71.1
KSab_MfeI_for	*CAATTG*AGCTGGGCCACGTCGACA	65.8
KSab_EcoRI_rev	*GAATTC*TCAATGCGTTCGCTCATGTCGTGCTCTCT	66.9
permE*_for	TCCACACGTGGCACCGCGAT	63.9
E_CYC_MfeI_for	AAA*CAATTG*TCGCGTGTGCCGAAGAAAGGAAC	64.0
E_CYC_EcoRI_rev	AAA*GAATTC*GTTCAGGGCTTCGGCGTGATCACG	67.2
O2_KR_MfeI_for	AAA*CAATTG*GCGGACGACGCAACCAGGACGA	67.8
O2_KR_EcoRI_rev	AAA*GAATTC*TCACAGGCCGCCGGTGACGC	67.9
T_CYC-KR_MfeI_for	AAA*CAATTG*CGAACCGACCACACCGCCTGAG	65.3
T_CYC-R_EcoRI_rev	AAA*GAATTC*CGAGTTCCACGGGCCTGTCCTT	63.1
Q_CYC_MfeI_for	AAA*CAATTG*CCAGGCCGGTTCGAGACAGCT	62.2
Q_CYC_EcoRI_rev	AAA*GAATTC*GTCATCGGCCACCGCCCAGGTTCG	72.1
O10_KR_MfeI_for	AAA*CAATTG*AACATCCACGTCGACGGCTGCGTGT	68.8
O10_KR_EcoRI_rev	AAA*GAATTC*TCGCGTCGGACACGTCAGAT	58.7
J_MfeI_for_2	AAA*CAATTG*GACCCCGCCACGATCGATCT	67.8
J_EcoRI_rev_ME	AAA*GAATTC*TCACGCCTTGACGGCGTTCGT	68.1
T3	ATTAACCCTCACTAAAGGGA	56.4

T7	TAATACGACTCACTATAGGG	53.2
19bp_MfeI	AAA*CAATTG*TGTAGGCTGGAGCTGCTTC	64.9
20bp_PacI_EcoRI	AAA*TTAATTAA*AAAA*GAATTC*ATTCCGGGG ATCCGTCGACC	69.6
O1_MfeI_for	AAA*CAATTG*GTGACCCACCGAGGAGGC ACCA	64.8
O1_EcoRI_rev	AAA*GAATTC*TCCGGTCAGGAGCCGATG CT	62.2
P_MfeI_for	AAA*CAATTG*ACCGCATCCGTCACGAAC GAGA	63.3
P_EcoRI_rev	AAA*GAATTC*CCTCAGAGCCGCAGGTCG ACCC	65.8
P_EcoRI_rev	AAA*GAATTC*CCTCAGAGCCGCAGGTCG ACCC	65.8
ResCas_Rev	TCGCTCTCTCCAGGGGAA	52.4
P_test_FOR	ACTTCGTGCGCCAACGGTTC	59.6
G-test_FOR	ACATCCACGCCAGCGAGAAG	57.4
F_test_rev	ATGCCCCCGAGGGTTTTG	56.8
A_test_rev	GACCGGGTCGAAGTCGCATT	58.5
S_test_rev	GTGTCGACGTGGCCCAGCTC	60.1
KS_RT	GGAGGGCGGGGCCATGCTCC	68.2
KS_RT_2	CTCGGCATCGACCTGGTCGT	59.5
KS_RT_3	TGGACGTGGTCTTCGCCGA	59.6
KS_RT_rev	CGCTCATGTCGTGCTCTCTCCTC	60.0
E_ko_FOR	CGCGTGTGCCGAAGAAAGGAACGAACACC GATGCCCGAG *ACTAGT*AAAATGCCGGCCTTTGAATG	Section 5.11.1
E_ko_REV	AAGGGGCGCACGGGCGGCCGCCGTTCAG GGCTTCGGCGT *ACTAGT*AAATGTAGGCTGGAGCTGCTT C	Section 5.11.1
T_ko_FOR	CGACATGAGCGAACGCATTGAGGAGGCCC GATTCTGATG *ACTAGT*AAAATGCCGGCCTTTGAATG	Section 5.11.1
T_ko_REV	GGGGGTGCGCGCCGCGCGGGCGGCGGC CTCGATCCTGGA *ACTAGT*AAATGTAGGCTGGAGCTGCTTC	Section 5.11.1
Q_ko_FOR	TGGTTCCAGGACCGAAAGCGCAAGGAGGG CACCGTGCAC *ACT AGT*AAAATGCCGGCCTTTGAATG	Section 5.11.1
Q_ko_REV	CCAGGTTGACCTTGGCCGGGGTGGCCGC CGCGGTCGTCA *ACTAGT*AAATGTAGGCTGGAGCTGCTTC	Section 5.11.1
H-P_ko_FOR	GCAACCCCCCGGTGTGAGGGGGCGGCGG AGACGATGACA *ACTAGT*AAAATGCCGGCCTTTGAATG	Section 5.11.1
H-P_ko_REV	CTGGACCGGCCTCCGGCGGCCTCAGAGC CGCAGGTCGAC*ACT AGT*AAATGTAGGCTGGAGCTGCTTC	Section 5.11.1

The areas in italics and underlined indicate a digest enzyme site.

Table 11: Clones constructed in the study.

Construct	Characteristics	Reference
pME1	Contains the ACP gene *grhC* in the vector pSK+ from the construct pMP31, size 3.2 kb	This study
pME2	Contains the KS_{α} and KS_{β} genes *grhA* and *grhB* in the vector pSK+ from the construct pMP31, size 5.6 kb	This study
pME3	Contains the ACP gene *grhC* in the vector pKJ55 from the construct pME1, size 6.2 kb	This study
pME4	Contains the genes *aad*A/*oriT* in the vector pMP27, size 24.9 kb	This study
pME5	Contains the ACP, KS_{α} and KS_{β} genes *grhC*, *grhA* and *grhB* in the vector pKJ55 from the constructs pME1 and pME2, size 5.5 kb	This study
pME6	Contains the KR gene *grhO2* in the vector pSK+ from the construct pMP31 , size 3.7 kb	This study
pME7	Contains the KR gene *grhO10* in the vector pSK+ from the construct pMP31, size 3.7 kb	This study
pME8	Contains the CYC gene *grhT* in the vector pSK+ from the construct, size 4.3 kb	This study
pME9	Contains the CYC gene *grhQ* in the vector pSK+ from the construct pMP31, size 3.4 kb	This study
pME10	Contains the CYC *grhE* in the vector pSK+ from the construct, size 3.9 kb	This study
pME11	Contains the ACP, KS_{α}, KS_{β} and CYC genes *grhC*, *grhA*, *grhB* and *grhT* in the vector pKJ55 from the constructs pME5 and pME8, size 10.2 kb	This study
pME12	Contains the ACP, KS_{α}, KS_{β} and CYC genes *grhC*, *grhA*, *grhB* and *grhE* in the vector pKJ55 from the constructs pME5 and pME10, size 9.8 kb	This study
pME13	Contains the ACP, KS_{α}, KS_{β} and CYC genes *grhC*, *grhA*, *grhB*, *grhT* and *grhQ* in the vector pKJ55 from the constructs pME5, pME8 and pME9, size 10.6 kb	This study
pME14	Contains the J gene *grhJ* in the vector pSK+ from the construct pMP31, size 3.9 kb	This study

pME15	Contains the ACP, KS_{α}, KS_{β} and J genes *grhC*, *grhA*, *grhB* and *grhJ* in the vector pKJ55 from the constructs pME5 and pME14, size 9.8 kb	This study
pME16	Contains the ACP, KS_{α}, KS_{β}, J and CYC genes *grhC*, *grhA*, *grhB* and *grhJ* and *grhT* in the vector pKJ55 from the constructs pME1, pME2, pME8 and pME14, size 11.1 kb	This study
pME17	Contains the ACP, KS_{α}, KS_{β}, J and CYC genes *grhC*, *grhA*, *grhB* and *grhJ* and *grhE* in the vector pKJ55 from the constructs pME1, pME2, pME10 and pME14, size 10.8 kb	This study
pME19	Contains insert *aadA*/*oriT* in the vector pSK+, size 4.3 kb	This study
pME21	Contains the asparaginsynthase gene *grhP* in the vector pSK+ from the construct pMP31, size 4.8 kb	This study
pME22	Contains the oxygenase gene grhO1 in the vector pSK+ from the construct pMP31, size 4.4 kb	This study
pME23.1	Contains the construct pMP31; the CYC gene *grhT* is replaced by the str resistance cassette *aad*, size 48.7 kb	This study
pME23	Contains the construct pMP31; the CYC gene *grhT* is deleted and the str resistance cassette *aad* is removed, size 47.7 kb	This study
pME24.1	Contains the construct pMP31; the CYC gene *grhE* is replaced by the str resistance cassette *aad*, size 46.7 kb	This study
pME24	Contains the construct pMP31; the CYC gene *grhE* is deleted and the str resistance cassette *aad* is removed , size 45.7 kb	This study
pME25.1	Contains the construct pMP31; the CYC gene *grhQ* is replaced by the str resistance cassette *aad*, size 47.3 kb	This study
pME25	Contains the construct pMP31; the CYC gene *grhQ* is deleted and the str resistance cassette *aad* is removed, size 46.3 kb	This study
pME26.1	Contains the construct pMP31; the grh genes between *grhG* and *grhQ* are replaced by the str resistance cassette *aad*, size 26.9 kb	This study
pME26	Contains the construct pMP31; the grh genes between *grhG* and *grhQ* are deleted and the str resistance cassette *aad* is removed , size 25.9 kb	This study
pME27.1	Contains the construct pMP31; the grh genes between *grhG* and *grhP* are replaced by the str resistance cassette *aad*, size 26.9 kb	This study

pME27	Contains the construct pMP31; the grh genes between *grhG* and *grhP* are deleted and the str resistance cassette is removed aad, size 25.9 kb	This study
pKR58	Contains the construct pMP31; the V gene *grhV* is deleted, size 47.4 kb	Dr. Reinhardt.[1]
pKR63	Contains the construct pMP31; the U gene *grhU* is deleted, size 47.4 kb	Dr. Reinhardt.[1]

Table 12: Strains constructed in this study.

***S. albus* strain**	**Characteristics**	**Reference**
ME1-ME4	Contains pME5 integrated into the *S. albus* genome	This study
ME5	Contains pME11 integrated into the *S. albus* genome	This study
ME6	Contains pME12 integrated into the *S. albus* genome	This study
ME7	Contains pME13 integrated into the *S. albus* genome	This study
ME8	Contains pME13 integrated into the *S. albus* genome	This study
ME9	Contains pME15 integrated into the *S. albus* genome	This study
ME9	Contains pME16 integrated into the *S. albus* genome	This study
ME10	Contains pME17 integrated into the *S. albus* genome	This study
ME11-ME13	Contains pME26 integrated into the *S. albus* genome	This study
ME14	Contains pME25 integrated into the *S. albus* genome	This study
ME15	Contains pME24 integrated into the *S. albus* genome	This study
ME16	Contains pME23 integrated into the *S. albus* genome	This study

*S. albus*ME17	Contains pME27 integrated into the *S. albus* genome	This study
KR58	Contains pKR58 integrated into the *S. albus* genome	PhD thesis,Dr. K. Reinhardt 2009[1]
KR61	Contains pKR61 integrated into the *S. albus* genome	PhD thesis, Dr. K. Reinhardt 2009[1]

5.2 Media and supplements

All media were autoclaved at 121℃ before use. Anti biotics and supplements were added after the media was cooled down to 55-60℃.

5.2.1 *E. coli* cultivation media

5.2.1.1 LB media[126]

Sodium chloride	10.0 g
Tryptone	10.0 g
Yeast extract	5.0 g
Agarose (only for solid medium)	15.0 g
ad 1000 mL ddH_2O	

5.2.1.2 SOB media[166]

Difco Bacto tryptone	20.0 g
Difco Bacto yeast extract	5.0 g
NaCl	0.5 g
KCl	0.186 g
ad 1000 mL ddH_2O	

5.2.2 *S.albus* cultivation media

5.2.2.1 2CM media[167]

NaCl	1.0 g
K_2HPO_4	1.0 g
Soluble potato starch	0.5 g

Inorganic salt solution*	1.0 ml
$MgSO_4$ x $7H_2O$	2.0 g
Tryptone	2.0 g
$CaCO_3$	2.0 g
$(NH_4)_2SO_4$	2.0 g
Agar	22.0 g
ad 1000 mL ddH_2O	

* inorganic salt solution

$FeSO_4$ x $7H_2O$	1.0 g
$MgCl_2$ x $6H_2O$	1.0 g
$ZnSO_4$ x $7H_2O$	1.0 g
ad 1000 mL ddH_2O	

5.2.2.2 Double strength germination media[168]

Difco yeast extract	1.0 g
Difco casaminoacids	1.0 g
$CaCl_2$ (5 M)	200 µl
ad 1000 mL ddH_2O	

5.2.2.3 Soya flour mannitol media (MS media)[169]

Soya flour	20.0 g
Mannitol	20.0 g
Agar	20.0 g
ad 1000 mL ddH_2O	

5.2.2.4 TSB media[168]

Tryptic soy broth	30.0 g
ad 1000 mL ddH_2O	

5.2.2.5 R5 media[170]

Sucrose	103 g
K_2SO_4	0.25 g
$MgCl_2$ x $6H_2O$	10.12 g
Glucose	10 g
Casaminoacids	0.1 g
Trace element solution*	2 ml
Yeast extract	5 g
TES	5.73 g
ad 1000 mL ddH_2O	

Aliquots of 100 ml of the solution were added into 250 ml flasks with 2.2 g agar and autoclaved. For use, the media was re-melted and the following sterile solutions were added:

KH_2PO_4 (0.5%)	1.0 ml
$CaCl_2$ x $2H_2O$ (5 M)	0.4 ml
L-Prolin (20%)	1.5 ml
NaOH (1 M)	0.7 ml

* Trace element solution:		
	$ZnCl_2$	40 mg
	$FeCl_3$ x $6H_2O$	200 mg
	$CuCl_2$ x $2H_2O$	10 mg
	$MnCl_2$ x 4H2O	10 mg
	Na_2B_4O7 x $10H_2O$	10 mg
	$(NH_4)_6Mo_7O_{24}$ x $4H_2O$	10 mg
	ad 1000 mL ddH_2O	

5.2.3 TFB I and TFB II solutions

Table 13: TFB I solution.

TFB I	Stock	g/100 mL	Use for 50 mL	Result conc.
KOAc	5 M	49.125	0.3 mL	30 mM
$CaCl_2$	1 M	11.098	0.5 mL	10 mM
KCl	1 M	7.455	5 mL	100 mM
$MnCl_2$	1M	16.187	2.5 mL	50 mM
Glycerol	50%--40%	50 mL + 50 mL H_2O	15 mL--18.75 mL	15%
H_2O	-	-	26.7mL--22.95 mL	-

Table 14: TFB II solution.

TFB II	Stock	g/100 mL	Use for 50 mL	Result conc
MOPS	1 M	4.186 g/20 mL pH 7.0 with NaOH, 0.2 µm sterile filtration	0.25 mL	10 mM
$CaCl_2$	1 M	11.098	1.875 mL	75 mM
KCl	1 M	7.455	0.25 mL	10 mM
Glycerol	50%---40%	50 mL + 50 mL H_2O	7.5 mL---9.3 mL	15%
H_2O	-	-	15.1mL---13.2 mL	-

5.2.4 Antibiotics and supplements

Table 15: Antibiotics and supplements used in this study.

Antibiotic/supplement	Final concentrations in media [µg/mL]		Solvent
	E. coli	*S. albus*	
Apramycin	100	100	ddH_2O
Kanamycin	25	-	ddH_2O
Ampicillin	50	-	ddH_2O
Chloramphenicol	25	-	EtOH
Tetracycline	5	-	ddH_2O/EtOH
IPTG	100	-	ddH_2O
X-Gal	50	-	DMF

5.3 Bacterial cultivation

5.3.1 *E. coli* culture

E. coli was cultivated overnight in 5 mL LB media at 37℃ and 30℃, respectively, with the corresponding antibiotics at 200 rpm. For storage, a stock solution was prepared as glycerol cultures. Therefore, 750 µL of an *E. coli* overnight culture were mixed with 750 µl sterile 30% (v/v) glycerol solution in a 2-mL cryotube, flash-frozen with liquid nitrogen and stored at -80℃.

5.3.2 *S. albus* culture

S. albus was cultivated using an MS agar. A single colony was streaked out on the MS agar plate. After an incubation time of 7-10 days, the spores were scraped off the plate using a sterile cotton tip and resuspended in 2 mL with sterile 20% (v/v) glycerol solution. The suspension was then aliquoted into 2-mL cryotubes, flash-frozen with liquid nitrogen and stored at -80℃.

For larger fermentations, *S. albus* strains were incubated in liquid cultures using 500 mL – 2 L baffled Erlenmeyer flasks at 30°C and 200 rpm for 3-5 days. Different liquid cultures (LB, TSB and MS) were used to obtain optimal metabolite production. The liquid cultures were inculated with overnight preparatory cultures originating from spore stocks.

5.4 Determination of cell density in bacterial cultures

5.4.1 *E. coli* culture

The determination of cell density from liquid media was performed with the photometer using one-way cuvettes with path lengths of 1 cm (Sarstedt, Nürmbrecht, Germany). The optical density of a liquid culture was measured at the wavelength of 600 nm (OD_{600}) with a UV/visible spectral photometer (Eppendorf, Hamburg, Germany) and pure LB media was used as reference.

5.4.2 *S. albus* culture

The concentration of the spore suspension was calculated using colony forming units (cfu). Therefore, a dilution series was prepared (10^{-5}, 10^{-6} and 10^{-7}) and from each dilution 500 µL was streaked out on MS agar plates. After three days incubation at 30°C, single colonies were counted and the concentration of the spore suspension was calculated as follows:

$$c = \frac{\text{number of colonies}}{\text{dilution x 500 µL}}$$

5.5 Isolation of DNA

5.5.1 Plasmid isolation from *E.coli*[126]

One mL of an overnight culture in LB medium was centrifuged for two minutes at 13,000 rpm and the supernatant was removed. The pellet was resuspended in 200 µL buffer P1 and 200 µL of buffer P2 was added and inverted four times. After adding 200 µL buffer P3 it was inverted four times and centrifuged for 5 minutes at 13,000 rpm. The supernatant was transferred into an Eppendorf-tube containing 500 µL chloroform and shaken vigorously. After 3 minutes centrfugation, the upper layer was transferred into a new tube containing 350 µL isopropanol and was shaken. The tube was then placed for 1 h at -20℃ and centr ifuged at 4℃ for 20 minutes. The supernatant was removed and the pellet was washed with ice-cold 70% ethanol. The pellet was spun down shortly and the supernatant was removed. The pellet was then dried in a speed-vac (Speedvac 5301 Eppendorf, Hamburg, Germany) for 5 minutes and dissolved in 50 µL ddH_2O. The DNA sample was stored at -20℃.

The P1, P2 and P3 buffers[126] were prepared as follows:

P1 buffer (sterile-filtered):

EDTA	0.74 g
Tris-HCl	1.21 g
ad 200 mL ddH_2O	
pH 8.0	

P2 buffer (sterile-filtered):

NaOH	4.0 g
SDS	5.0 g
ad 500 mL ddH_2O	

P3 buffer (sterile-filtered):

Potassium acetate	62.73 g
ad 200mL ddH_2O	200 ml
pH 5.5 (with acetic acid)	

5.5.2 Genomic DNA isolation from *Streptomyces*

Bacterial colonies were dissolved in 20 ml LB and 500 µL 20% glycine that were then incubated for 24 hours at 30℃ and at 200 rpm. 1.5 mL of the culture was harvested by centrifugation at 14,000 rpm for 2 minutes. The supernatant was removed and the pellet was resuspended in 500 µL STE with 5 mg/mL lysozyme and incubated for 3 h at 37℃. 500 µL 10% SDS and 100 µL 3 M NaOAc (pH 5.3) was added and then vortexed. Next, the mixture was shaken at 200 rpm for 45 minutes at 37°C. 250 µL of phenol/choloroform/isoamylalcohol (P/Chl/I) was added and vortexed for 30 seconds. The tube was centrifuged for five minutes at 14,000 rpm. Subsequently, 800 µL from the upper layer was taken and mixed again with 250 µl P/Chl/I and vortexed for 30 seconds. These steps were repeated two times. In the last step, 750 µL from the overlay was taken and mixed with 750 µL isopropanol. After centrifuging for two minutes at 10,000 rpm, the supernatant was removed and the pellet was washed with 500 µl ice-cold 70% EtOH. The pellet was dried for one hour under a clean bench and dissolved in 50 µL ddH_2O overnight at 4℃.

STE buffer

EDTA (0.5 M, pH 8	400 µl
Tris-HCl (1M), pH8	2 ml
NaCl	1.17 g
ad 200 mL ddH_2O	

5.6 Photometric determination of DNA concentration

The concentration of the isolated plasmid and genomic DNA was determined by a Biomate 3 spectrophotometer (Thermo Electron, Cambridge, UK). The DNA sample was diluted in a ratio to 1:20 using ddH_2O. The measurement was carried out at wavelengths 260 nm and 280 nm which correspond to the absorption maxima of DNA and protein, respectively.

5.7 Transfer methods for DNA

5.7.1 Heat shock transformation

First, chemically competent *E. coli* cells were prepared. A preparatory culture of *E. coli* XL1 blue was incubated in 5 mL LB at 37℃ overnight at 200 rpm. 100 mL LB media was then inoculated with 1 mL of the preparatory culture at 37℃ and 200 rpm, until the optical density at 600 nm (OD_{600}) reached 0.4. The culture was then transferred into two cold sterile 50 mL Falcon tubes. The cells were harvested by centrifugation at 4℃ for five minutes at 5000 rpm. The supernatants were removed and the pellets were dissolved in 12.5 mL TFB I. After five minutes of centrifugation at 5000 rpm, the supernatants were removed, and the pellets were dissolved in 2 mL TFB II and added to one tube. The cells were aliquoted into 100 µL portions, flash-frozen in liquid nitrogen and stored at -80℃.

To carry out the heat shock transformation, chemically competent *E. coli* XL1 blue cells were thawed for 5 minutes on ice. After adding up to 10 µL DNA from the ligation to the cells, the mixture was incubated for 30 minutes on ice. The heat shock was performed for exactly 60 seconds at 42℃ and then the cells were immediately incubated for 2 minutes on ice. 900 µL liquid LB media was added and incubated for 1 hour at 37℃. The culture was then centrifuged at 10,000 rpm for 30 seconds. 700 µL was discarded and the pellet was resuspended in the remaining 300 µL and streaked out. The plates were incubated overnight at 37℃.

5.7.2 Electroporation

First, electrocompetent *E. coli* cells were prepared. A preparatory culture of *E. coli* XL1 blue was incubated in 5 mL LB at 37℃ overnight at 200 rpm. 200 ml LB media was then inoculated with 5 mL of the preparatory culture at 37℃ and 200 rpm until the optical density at OD_{600} reached 0.4. The culture was then transferred into cold sterile 50 mL Falcon tubes. The cells were harvested by centrifugation at 4℃ for five minutes at 5000 rpm. The supernatant was discarded and the pellet was carefully resuspended in 50 mL of sterile 10% glycerol. After six to seven times of washing the cells, the

pellet was resuspended in 1 mL 10% ice-cold glycerol. Aliquots of 50 µL portions were prepared and the cells were flash-frozen with liquid nitrogen and stored at -80℃.

Electroporation was carried out by using a Biorad electroporator with a shocking cuvette chamber (Munich, Germany) and by mixing 0.05-0.5 µg of plasmid with 50 µL electrocompetent *E.coli* XL1 blue cells and incubating that for 5-10 minutes on ice. The sample was transferred into a chilled electroporation cuvette (0.2 cm electrode cap) on ice and then electro-pulsed with the parameters:

Voltage	2500 V
Resistance	200 Ω
Condenser capacity	25 µF

After the electro-pulse, 1 mL of LB was immediately added into the cuvette and the sample was transferred into a sterile 1.5 mL tube. Next, the cells were incubated for 1 h at 37℃ shaking at 200 rpm and 75 µL of the mix was plated onto selective agar plates.

5.7.3 Conjugation into *S. albus* after Flett *et al*.[171]

The conjugation construct was transferred into the *E. coli* ET12567/pUZ8002 using electroporation (section 5.7.2). The plasmid pUZ8002 is a helper plasmid for *oriT*-containing plasmids, that is however not transferred due to a mutation in its *oriT*. Transformations were confirmed using colony PCR by picking single colonies from the plate. The positive clones were then incubated at 37℃ overnight in 5 mL LB media containing Kan^{25}, Cm^{25} and Apr^{50}.

The next day, 100 µL of the preparatory *E. coli* cultures were re-inoculated in 5 ml LB containing the corresponding antibiotics and grown until an OD_{600} of 0.4 was reached. Furthermore, approximately 2 x 10^8 of *S. albus* spores from the stock solution (5.3.2) were resuspended in 500 µL TES buffer (0.05 M TES, pH 8.0). The spores were then heat shocked at 50℃

for 10 minutes; subsequently 500 µL of the double strength germination media were added, and the spores were incubated for a further 1.5 h at 37℃ and at 200 rpm. 1 mL of the *E. coli* cells was then washed three times using LB media. Subsequently, the supernatant was discarded. For conjugation, the spore suspension was mixed with the *E. coli* cells and centrifuged for 30 seconds at 10,000 rpm. The supernatant was discarded, and the pellet was resuspended in the remaining media. The mixture was then streaked out on a 2CM agar plate until the plate surface was dry. After an incubation time of 16-18 h at 30℃, the plate was overlayed with an antibiotic solution of 1 mL nalidixic acid. Subsequently, the incubation was continued for 3-5 days at 30℃ until potential exconjugants appeared.

Potential exconjugants were re-inoculated on 2CM- and MS plates for 3-7 days at 30℃. Afterwards, the spores were inoculated in 20 mL LB liquid cultures for the isolation of genomic DNA (5.5.2). The DNA was then used as a template for the confirmation of DNA integration into the genome of *S. albus* using PCR (section 5.8.1).

5.8 Polymerase chain reaction (PCR)

PCR is a standard method used in molecular biology and it allows a rapid amplification of specific known DNA sequences for further analysis. There are three major steps in PCR: denaturation, annealing and elongation, which are repeated at varying temperatures and numbers of cycles depending on the experiment.

5.8.1 Preparative PCR

In the present study, a Biometra PCR Thermocycler T-Gradient (Göttingen, Germany) was used to amplify the *grh* minimal PKS (*grhA*, *grhB* and *grhC*), cyclases (*grhE*, *grhQ* and *grhT*) from the griseorhodin gene cluster. All PCR reactions were performed using a Expand High Fidelity^{PLUS} PCR System (Roche, Grenzach-Wyhlen, Germany). In case of control reactions, *Taq* polymerase (Jena Bioscience, Jena, Germany) was used.

Buffer (5 x for *Taq* and for Hifi 10x)	5.0 µL resp.10 µL buffer
dNTP (10 mM)	1.00 µL
DMSO (100%)	2.5 µL
DNA (µg/mL)	1.00 µL
Forward primer (50 µM)	0.50 µL
Reverse primer (50 µM)	0.50 µL
Expand Hifi polymerase/*Taq* polymerase	0.50 µL/0.25 µL
ad 50 µL ddH_2O	

The annealing temperature T_{anneal} in the PCR programme is calculated as follows:

$T_{anneal} = T_m - 5℃$ where the lower T_m value (Table 10) of the applied primers is used.

PCR programme:

Lid temperature	105℃		
Initial denaturation	94℃	2 min	
Denaturation	94℃	1 min	34 cycles
Annealing	x ℃	1 min	
Extension (1 kb/min)	72℃	x min	
Final extension	72℃	10 min	
Cooling	4℃		

5.8.2 Colony PCR

For colony PCR, a master mix was prepared as indicated. The master mix was then aliquoted into reaction mix tubes, colony material was taken directly from the plate and mixed with the reaction mix. The initial denaturation time was increased up to five minutes.

Master mix:

Buffer (5x)	5 µL buffer
dNTP (10 mM)	1.00 µL
DMSO (100%)	1.25 µL
DNA	small amount of colony material
Forward primer (50 µM)	0.25 µL
Reverse primer (50 µM)	0.25 µL
Taq polymerase (5 U/µl))	0.125 µL
ad 25 µL ddH_2O	

PCR programme:

Lid temperature	105℃		
Initial denaturation	94℃	5 min	
Denaturation	94℃	1 min	34 cycles
Annealing	x ℃	1 min	
Extension (1 kb/min)	72℃	x min	
Final extension	72℃	10 min	
Cooling	4℃		

5.9 Agarose gel electrophoresis

The products from PCR, enzyme digests, gel extractions and plasmid isolations were analysed by gel electrophoresis (Biometra agarose gel electrophoresis system with a power source Standard Power Pack P25, Göttingen, Germany) in 1.0% agarose using 1x TAE buffer diluted from 50x TAE buffer (2 M Tris-acetate, pH 8.0, 0.1 M EDTA) with 0.1 µg/mL ethidium bromide. Prior to electrophoresis, the products were mixed with 1µL of 6 x loading buffer (0.25% (w/v) bromophenol blue, 0.25% (w/v) xylene cyanol, 30% (w/w) glycerol). Electrophoresis was performed at 100 V for 10-35 minutes. Gels were viewed and photographed by ultraviolet (UV) transillumination (Syngene Gene Genius gel documentation system, Cambridge, United Kingdom).

5.10 Isolation of DNA from agarose gel

The gel extraction was performed with the QIAgen Gel Extraction Kit (Qiagen, Hilden, Germany). All buffers were supplied with the kit. The target DNA fragment was cut from the gel using a sharp scalpel and transferred to a 1.5 mL tube. To 1 volume of gel (100 mg ~ 100 µl) 3 volumes of QC buffer were added, and the sample was incubated for 10 minutes at 50℃ to completely dissolve the fragment in buffer. The solution was then transferred into a Qiaquick column and centrifuged at 13,000 rpm for 1 minute. After discarding the flow-through, 500 µl of QC buffer was added and the column was centrifuged at 13,000 rpm for 1 minute. The flow-through was discarded and 750 µL PE buffer added and was centrifuged again for 1 minute at 13,000 rpm. After discarding the flow-through it was centrifuged for 1 minute at 13,000 rpm to remove the residual PE buffer. The Qiaquick column was transferred into a new 1.5 ml E-tube and after adding 30 µL sterile ddH_2O the column was incubated for 1 minute at RT. To collect the DNA from the column it was centrifuged for 1 minute at 13,000 rpm. The DNA sample was conserved at -20℃.

5.11 TA cloning

5.11.1 Construction via TA cloning[126]

10 µl of the vector pKS+ was digested with 2.5 µl *Eco*RV and incubated for 2 hours at 37℃. The restriction enzyme was heat-in activated at 80℃ for 20 minutes. 3´ T overhangs were added using 0.5 µl of *Taq* polymerase and 10 µL of 10 mM dTTP. The reaction tube was then incubated at 70℃ for two hours. 100 µL of chloroform was added and the E-tube was shaken vigorously. After centrifugation at 13,000 rpm for five minutes, the supernatant was transferred into a new E-tube filled with 70 µL isopropanol and was shaken vigorously. The reaction tube was precipitated at -20℃ for one hour and centrifuged for 20 minutes at 13,000 rpm and 4℃. The supernatant was removed and 200 µL of ice-cold 70% ethanol was added. The tube was centrifuged shortly and the ethanol was removed. The pellet was dried in a speed vac at 45℃ for five minutes a nd dissolved with 30 µL ddH_2O. The vector portion was then stored at -20℃ for further use.

5.11.2 Ligation into TA vector

The following ligation reagents were used for TA cloning applying the NEB protocol using T4 ligase (NEB, Frankfurt am Main, Germany):

T4 ligase buffer (10x)	1 µL
Insert DNA (µg/mL)	7 µL
Vector DNA (µg/mL)	1 µL
T4 ligase (5 U/µl)	1 µL

The ligation portion was incubated overnight at 4°C and the next day, a heat-inactivation at 65°C was carried out prior to electroporation or heat shock transformation respectively. To screen for positive clones, a blue/white selection was used based on the disruption of the *lacZ* gene in the TA vector. The white clones were positive clones and were then inoculated overnight at 37°C with corresponding antibiotics for plasmid DNA isolation.

5.11.3 Sequencing of TA vector

Prior to further cloning, TA vectors containing the PCR inserts were sequenced at the sequencing company GATC (Constance, Germany). For this purpose, standard sequencing primers T7 and T3 (Table 5.3) were used. The obtained sequences were analysed using the software Vector NTI (Invitrogen, Karlsruhe).

5.12 Enzymatic modification of DNA

5.12.1 Enzyme digests

For enzyme digest reactions, various endonucleases (NEB, Frankfurt am Main, Germany) were applied. The following reagents were mixed together:

Restriction enzyme buffer (10x)	1.0 µL
DNA (µg/mL)	0.75 µL

Restriction enzyme (5 U/µl)	0.5 µL
ad 10 µL ddH_2O	

The digests were incubated at 37℃ for 1-3 hours. For control digests, a 10 µl portion was used; for larger cloning batches, 50 µL portions were prepared. A heat-inactivation step at 65℃ for 20 min was required if the material was further used for desphosphorylation.

5.12.2 Dephosphorylation of DNA

Dephosphorylation was required to avoid religation of the digested vector. The following reagents were mixed together applying the Fermentas shrimp alkaline phosphatase (SAP) (Fermentas, Frankfurt am Main, Germany):

Digestion enzyme buffer (10x)	5.0 µL
DNA (µg/mL)	40.0 µL
SAP (5 U/µl)	1.0 µL
ad 50 µL ddH_2O	

The dephosphorylation reaction was incubated at 37° C for 45 min. A heat inactivation step at 65℃ for 20 min was required to inactivate the enzyme.

5.12.3 Ligation

The ligation was performed by applying the NEB protocol using T4 ligase. The reagents were mixed together as follows. The ratio between insert and vector was 1:1 to 3:1 depending on the yield of the target DNA.

T4 ligase buffer (10x)	1 µL
Insert DNA (µg/µL)	x µL
Vector DNA (µg/µL	x µL
T4 ligase (5 U/µl)	1 µL
ad 10 µL ddH_2O	

The ligation was incubated at 4℃ overnight. A heat-inactivation step at 65℃ for 20 min was required to inactivate the enzyme.

5.13 λ-Red-mediated homologous recombination[131]

During this study, the λ-Red-mediated recombination technique was applied to create in-frame deletions in the griseorhodin biosynthetic gene cluster. Gene knock-out is performed in a one-step directed insertion of linear DNA fragments into the target DNA. The linear DNA fragment used in this study was a streptomycin resistance gene cassette *aadA* (Figure 61) amplified from the plasmid pIJ778 (Appendix 8.1).

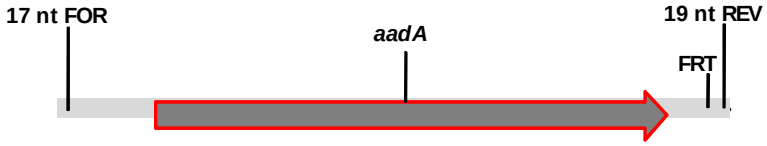

Fig. 61: The streptomycin resistance cassette used for generating gene knock-outs in the present study.

The resistance cassette contains short homologous areas that control the double crossover after electroporation of the cassette. In the present study, the cyclase genes *grhE*, *grhQ* and *grhT* as well as the genes from *grhH* to *grhP* and from *grhH* to *grhQ* in the griseorhodin gene cluster were deleted. For each gene knock-out, two long primers were designed (section 5.3) containing the 5´ end matching 39 nucleotides (nt) to the target gene to be deleted and the 3´ end with 19 or 17 nt matching to the right or the left side of the resistance cassette. Furthermore, a *Spe*I restriction site ACTAGT was integrated into the sequences of the homologous areas of the cluster and the resistance cassette sequences for a later restriction of the cassette.

5.13.1 PCR amplification of the resistance cassette for the homologous recombination

In the present study, this PCR was used to amplify the streptomycin resistance cassette *aadA* from the plasmid pIJ778. All PCR reactions were performed using a PCR Expand High Fidelity^{PLUS} PCR System and a Thermocycler. The following reagents were mixed together:

Hifi buffer (10x)	10 µL
dNTP (10 mM)	1.00 µL
DMSO (100%)	2.5 µL
DNA (µg/mL)	1.00 µL
Forward primer (50 µM)	0.50 µL
Reverse primer (50 µM)	0.50 µL
Expand Hifi polymerase	0.50 µL
Ad 50 µL ddH_2O	

PCR programme:

Lid temperature	105℃		
Initial denaturation	94℃	2 min	
Denaturation	94℃	1 min	10 cycles
Annealing	50℃	1 min	
Extension (1 kb/min)	72℃	1 min 30 sec	
Denaturation	94℃	1 min	15 cycles
Annealing	55℃	1 min	
Extension	72℃	1 min 30 sec	
Final extension	72℃	10 min	
Cooling	4℃		

5.13.2 Electroporation of pMP31 into *E. coli* BW25113/pIJ790

The cosmid pMP31 contains the complete griseorhodin A gene cluster. In order to perform gene knock-outs, it needs to be transformed into the *E. coli* strain BW25113/pIJ790 for subsequent homologous recombination. The vector pIJ790 contains the lambda phage genes *exo*, *bet* and *gam* which are controlled by the arabinose-induced promoter. Expression in *E. coli* BW25113/pIJ790 leads to dramatically enhanced recombination frequencies. Therefore, the *E. coli* strain BW25113/pIJ790 was grown overnight at 30°C in 5 mL LB with glucose containing Cm^{25}. 300 µL of the overnight culture were inoculated into 30 mL SOB and grown at 30°C shaking at 200 rpm until OD_{600} reached 0.4 The cells were then prepared for electroporation (section 5.6.2); the cosmid pMP31 was transformed and streaked out on selective LB agar plates with Cm^{25} and Apr^{50} and incubated overnight at 30°C.

5.13.3 Electroporation of the streptomycin resistance cassette into *E. coli* BW25113/pIJ790/pMP31

To perform gene knock-outs in the griseorhodin cluster, the *E. coli* strain BW25113/pIJ790/pMP31 was grown overnight at 30°C and 200 µL of the preparatory culture were reinoculated into a 50 mL SOB culture. To induce the lambda phage genes *exo*, *bet* and *gam* on the vector pIJ790, 500 µL of 1 M L-arabinose stock solution (final concentration 10 mM) were added. The culture was grown at 30°C and at 200 rpm to an OD_{600} of 0.4. The cells were then prepared for electroporation, and 2 µL of the amplified and purified streptomycin resistance cassette were transformed into the cells. These were then streaked out on LB agar plates with Apr^{50} and Str^{50} and incubated at 37°C.

5.13.4 Removal of the resistance cassette

5.13.4.1 Digest of the streptomycin cassette

To ensure a successful expression of the gene cluster after the gene inactivation, the streptomycin resistance cassette was removed using the digest enzyme *Spe*I. Therefore, the following reagents were mixed together:

Restriction enzyme buffer (10x)	5.0 µL
DNA (µg/mL)	5.0 µL
BSA (10x)	5.0 µL
Restriction enzyme *Spe*I (5 U/µl)	2.5 µL
ad 50µL ddH_2O	

The digest was incubated for 3 h at 37℃ and heat-inactivated for 20 minutes at 65℃.

5.13.4.2 Religation

After the restriction the cluster was religated using the following reagents:

Ligase buffer (10x)	1.0 µL
DNA (µg/mL)	8.0 µL
T4 ligase (5 U/µl)	1.0 µL

The religation was incubated overnight at 4℃ and heat-inactivated at 65℃ for 20 minutes. After successful religation, the cosmid was conjugated in the host organism *S. albus* for expression.

5.14 Reverse transcriptase PCR (RT-PCR)

5.14.1 RNA isolation

RNA was isolated using a Qiagen RNA isolation kit with some modifications. *S. albus* cultures were grown for 3 days at 30℃, 1.5 mL of the culture was harvested at 10,000 rpm for 2 minutes and the supernatant was carefully removed. The pellet was then suspended in 100 µL of lysozyme-containing TE buffer (for Gram-positive bacteria: 6 µl of 50 mg/mL lysozyme stock solution were added per 100 µL TE buffer) by vortexing and incubating at RT for 10 minutes. 350 µL of the RLT buffer in ß-mercaptoethanol (ß-ME) (for the stock solution: 10 µL of ß-ME were added per 1 mL buffer RLT) were then added and mixed by vortexing. 250 µL 100% ethanol were added to the lysate and mixed by inversion. The sample was applied to an RNeasy column that was placed in a 2 mL collection tube and centrifuged for 15 s at 10,000 rpm and the flow-through was discarded. 350 µL RW1 buffer were added into the RNeasy column, centrifuged for 15 s at 10,000 rpm and the flow-through was discarded. The DNase I stock solution was prepared by adding 10 µL DNase I stock solution to 70 µL RDD buffer and mixed gently by inverting the tube. The DNase I incubation mix (80 µL) was added directly onto the RNeasy silica-gel membrane and incubated at RT for 35 minutes.

350 µL RW1 buffer were added into the RNeasy column, centrifuged for 15 s at 10,000 rpm and the flow-through was discarded. The column was then transferred into a new 2 mL collection tube. 500 µL of the RPE buffer were added onto the RNeasy column, centrifuged for 15 s at 10,000 rpm and the flow-through was discarded. Another 500 µL of the RPE buffer were added to the Rneasy column and centrifuged for 2 minutes at 10,000 rpm. The RNeasy column was transferred into a new 2 mL collection tube and centrifuged at 14,000 rpm for 1 minute. For elution, the RNeasy column was transferred into a new 1.5 mL collection tube, 30 µL of the RNase free water was pipetted onto the membrane and the tube was centrifuged at 10,000 rpm for 1 minute. Next, the DNase I stock solution was prepared by adding 10 µL DNase I stock solution to 70 µL RDD buffer. This was added to 30 µL RNA solution and incubated at RT for 45 minutes.

350 µL of the RLT buffer were added and mixed. 250 µL of the 100% ethanol were added to the diluted RNA and mixed by inverting the tube. The sample was applied to an RNeasy column, placed in a 2 mL collection tube and centrifuged for 15 s at 10,000 rpm and the flow-through was discarded. 350 µL of the RW1 buffer were pipetted into the RNeasy column and centrifuged for 15 s at 10,000 rpm. The flow-through was discarded. The DNase I stock solution was prepared by adding 10 µL DNase I stock solution to 70 µL RDD buffer and mixed gently by inverting the tube. The DNase I incubation mix (80 µL) was added directly onto the RNeasy silica-gel membrane and incubated at RT for 35 minutes.

350 µl of the RW1 buffer were pipetted into the RNeasy column and centrifuged for 15 s at 10,000 rpm. The flow-through was discarded. The RNeasy column was transferred into a new 2 mL collection tube. 500 µL of the RPE buffer were added onto the RNeasy column and centrifuged for 15 s at 10,000 rpm. Another 500 µL of the RPE buffer were added to the RNeasy column and centrifuged for 15 s at 10,000 rpm. The RNeasy column was placed into a new 2 mL collection tube and centrifuged at 14,000 rpm for 1 minute. For elution, the RNeasy column was placed into a new 1.5 mL collection tube and 30 µL of the RNase free water were added onto the membrane and was centrifuged at 10,000 rpm for 1 minute.

5.14.2 RT-PCR

In this study, RT-PCR was used to synthesise the cDNA of the minimal PKS from the isolated RNA. For all RT-PCR reactions, the Superscript One Step RT-PCR System (Invitrogen, Karlsruhe, Germany) was used. The following reagents were mixed together:

Reaction mix (2x)	5 µL
RNA (µg/mL)	0.3 µL
Forward primer (10 µM)	0.5 µL
Reverse primer (10 µM)	0.5 µL
OneStep RT-PCR enzyme mix	0.25 µL

RNase-free ddH_2O	3.25 µL

PCR programme:

Lid temperature	105℃		
cDNA synthesis	55℃	30 min	
Initial denaturation	94℃	2 min	
Denaturation	94℃	1 min	40 cycles
Annealing	x ℃	1 min	
Extension (1 kb/min)	68℃	x min	
Final extension	68℃	10 min	
Cooling	4℃		

5.15 Natural product analysis

5.15.1 Extraction

5.15.1.1 Extraction of cells and agar from agar plates

Secondary metabolite production was performed using *S. albus* as a host organism. Initially, a preliminary analysis of the mutants was carried out using agar plates. Therefore, different media such as 2CM, MS and R5 were tested. After appropriate incubation (5-7 days) at 30℃, the cell material was scraped off the plates using a spatula and dissolved in 2 mL of 95:5:1 EtOAc/MeOH/AcOH in a reaction tube. To destroy the cells and to get access to the metabolites, the cell solution was ultra-sonicated (Bandelin Sonopuls HD2070, Berlin, Germany; 80-90% of maximum output; the sonication was carried out five times for 10 seconds each time). The reaction tube was then centrifuged for 5 min at 5,000 rpm and the supernatant taken and dried in a rotary evaporator (Heidolph VV2000, Keilheim, Germany). The dry extract was then dissolved in acetonitrile (ACN) with 0.05% trifluoric acid (TFA) and used directly used for HPLC or

HPLC-MS analysis. Otherwise the extract was further dried under high vacuum and stored at -20℃.

The agar was mixed with 50 mL 95:5:1 EtOAc/MeOH/AcOH and stirred for several hours and then filtered. The solvent was removed using a rotary evaporator. The dry extract was then dissolved in acetonitrile (ACN) with 0.05% trifluoric acid (TFA) and used directly used for HPLC or HPLC-MS analysis.

5.15.1.2 Liquid cultures extraction

5.15.1.2.1 EtOAc/MeOH/AcOH and EtOAc extraction

The extraction of metabolites from the liquid cultures required a separation of the cells from the media. Therefore, the liquid culture was divided into 1 L plastic centrifuge tubes and centrifuged at 3600 rpm for 1 h. The media was poured into flasks and extracted three times with 95:5:1 EtOAc/MeOH/AcOH or with 100% EtOAc. Subsequently, the organic phase was washed three times with ddH_2O (if acidic conditions were used), dried with Na_2SO_4 and rotary-evaporated to dryness.

The cells were freeze-dried prior to extraction using liquid nitrogen and a freeze-dryer (Thermo Heto PowerDry LL3000, Langenselbold, Germany). The next day, the cells were subjected to 100% MeOH and stirred for several hours and then filtered. MeOH was removed using a rotary evaporator and the cells were extracted three times using 100% EtOAc. Subsequently, the extract was rotary-evaporated to dryness. The concentrated crude extract was then subjected to a silica gel column (section 5.13.3.1).

5.15.1.2.2 MeOH/celite extraction

A portion of the freeze-dried cells were extracted using 100% MeOH and celite. Therefore, the cells were subjected to 100% MeOH and stirred for

several hours. Afterwards, the cells were filtered through celite under vacuum. The cells with the celite material were then scraped off the filter, subjected again to fresh 100% MeOH, stirred for several hours and filtered again through celite. This was repeated three times and subsequently MeOH was removed using a rotary evaporator. The concentrated crude extract was then subjected to a LH20 column (section 5.13.3.2)

5.15.2 Thin layer chromatography (TLC)

5.15.2.1 Normal phase (NP)

NP TLC was used as a standard procedure in the analysis of metabolite production. For this, different TLC plates such as amine, cyano and silica plates were used (Macherey-Nagel, Düren, Germany). The mobile phase used here was a mix of petrolether/ethylacetate, whereas different ratios were applied as well as 9:1 $CHCl_3$/MeOH.

5.15.2.2 Reverse phase (RP)

RP TLC was used for the analysis of the metabolites as well. For this, alugram RP-18 W/UV_{254} TLC plates (Macherey-Nagel, Düren, Germany) were used. The mobile phase used was ACN/H_2O with 0.05% TFA in a ratio of 7:3 as well as $CHCl_3$/MeOH which was used in a ratio of 9:1. Detection was carried out using UV light at 254 nm as well as 366 nm.

5.15.3 Column chromatography

5.15.3.1 Silica gel flash chromatography

The concentrated crude extract from the cells and the media was subjected to silica gel flash chromatography. Prior to use, the column material was impregnated with 2 M NaH_2PO_4 by mixing 500 mg column material with 1 L 2 M NaH_2PO_4, strirring for 2 h and eventually dried at 80°C. An isocratic solvent system 9:1 $CHCl_3$/MeOH was used for elution. The fractions were

dried in a rotary evaporator and a preliminary analysis of the fractions was performed using the Jasco HPLC system (section 5.13.4.1).

5.15.3.2 LH20 chromatography (Jasco)

The media extract was subjected to LH20 chromatography. An isocratic solvent system with 100% MeOH was used for elution of the fractions and to purify the column material, DMSO was eluted through the column. The fractions were dried in a rotary evaporator and a preliminary analysis of the fractions was performed using the Jasco HPLC system (section 5.13.4.1).

5.15.3.3 LH20 chromatography (Dionex)

The concentrated cell crude extracts originating from the *ΔgrhU* and *ΔgrhV* mutants were separated on a LH20 column. An isocratic solvent system with 100% MeOH was used for elution at a flow rate of 2 mL/min. The absorbance at 254 nm was monitored throughout the experiment using a UV detector and a chart recorder. Fractions were collected at 5 min intervals starting from the peak observed on the chart recorder until the absorbance stabilised at the baseline. The fractions were dried in a speed vac and analysed using the Dionex HPLC system (section 5.12.4.2).

5.15.4 High pressure liquid chromatography (HPLC)

For all HPLC runs, HPLC-grade ACN and ddH_2O were used. Furthermore, the ddH_2O was acidified with 0.05%TFA.

5.15.4.1 Analytical HPLC (Jasco)

Analytical HPLC was performed using a Jasco HPLC system with a MD-2015 PDA detection system (Groß-Umstadt, Germany). The samples were run on a reverse phase column (PerfectChrom 100 C18, 5µm, 250 mm x 4 mm) with a flow rate of 1.5 mL/min and monitored at 254 nm.

HPLC Method 1:

1 min of 10% ACN/ddH_2O, a linear gradient to 100% ACN for 30 min; isocratic at 100% ACN for 5 min and then returned to 10% ACN/ddH_2O in 2 min and re-equilibriated for 3 min.

HPLC Method 2:

5 min of 10% ACN/ddH_2O, a linear gradient to 95% ACN/H_2O for 20 min; isocratic at 95% ACN/ddH_2O for another 5 min and then returned to 10% ACN/H_2O in 2 min and re-equilibriated for 3 min.

5.15.4.2 Analytical HPLC (Dionex)

Analytical HPLC was performed as well with a Dionex HPLC equipped with a UVD 340U diode array detector (Göttingen, Germany). The LH20 chromatography fractions were run by repetitive analytical RP HPLC (column: Phenomex Prodigy ODS3, 5 µm, 250 mm x 4 mm) at a flow rate of 1 mL/min and monitored at 254 nm.

HPLC Method 3:

1 min of 10% ACN/ddH_2O, a linear gradient to 100% ACN for 30 min; isocratic at 100% ACN for 5 min and then returned to 10% ACN/ddH_2O in 2 min and re-equilibriated for 3 min.

5.15.4.3 Semi-preparative HPLC

Semi-preparative HPLC was performed with a Knauer HPLC equipped with a UV detector S-2800 (Berlin, Germany). Fractions from the preparative HPLC were run by repetitive semi-preparative RP HPLC (column: Macherey Nagel Sphinx RP5 µm, 250 mm x 8 mm) at the flow rate of 3.4 mL/min and monitored at 254 nm.

HPLC method 4:

5 min of 60% ACN/ddH_2O, a linear gradient to 65% ACN for 15 min; isocratic at 100% ACN for 5 min and then returned to 60% ACN/ddH_2O in 5 min and re-equilibriated for 5 min.

5.15.4.4 Preparative HPLC

Preparative HPLC was performed using a Shimadzu HPLC equipped with a UV detector SPD-20A (Duisburg, Germany). The fractions were run by repetitive preparative RP HPLC (column: Kromasil 100 C 18, 5 µ, 250 mm x 20 mm) at flow rates of 6 mL and monitored at 254 nm.

HPLC method 5:

1 min of 10% ACN/H_2O, a linear gradient to 100% ACN for 30 min; isocratic at 100% ACN for 5 min and then returned to 10% ACN/H_2O in 2 min and re-equilibriated for 3 min.

5.15.5 Mass spectrometry (MS)

5.15.5.1 HPLC-High Resolution (HR) Electrospray Ionisation (ESI) MS (Bruker Daltonik)

For all HPLC-HRESIMS runs, HPLC-grade ACN and ddH_2O were used. Furthermore, ddH_2O was acidified with 0.05%TFA.

HPLC-MS analysis were carried out using an Agilent 1200 Series HPLC system with an autosampler, microOTOF-Q flight of time spectrometer and an Apollo-ESI source (Bruker Daltonik, Bremen, Germany). HPLC was performed using analytical RP columns (PerfectChrom 100 C18, 5µm, 250 mm x 4 mm; Macherey Nagel Sphinx RP RP5 µm, 250 mm x 4 mm) at a flow rate of 1 mL/ml and monitored at 254 nm. For the determination of the exact masses an external calibration was carried out with sodium formate. The HPLC method 2 (section 5.15.4.1) was used for the HPLC.

HPLC Method 2:

5 min of 10% ACN/ddH_2O, a linear gradient to 95% ACN/H_2O for 20 min; isocratic at 95% ACN/ddH_2O for another 5 min and then returned to 10% ACN/H_2O in 5 min and re-equilibriated for 5 min.

5.15.5.2 HRESIMS (Thermo Fisher Scientific)

High Resolution ESI-MS and MS/MS spectra were recorded at the University of Naples on a Thermo LTQ Orbitrap mass spectrometer (Thermo Fisher Scientific, Pennsylvania, USA). Spectra were recorded by infusion into the ESI source using MeOH as the solvent.

5.15.6 NMR

5.15.6.1 Capillary NMR

CapNMR data was recorded on a Varian INOVA 500 spectrometer (Palo Alto, USA) at 23℃, operating at 500 MHz. The INOVA was equipped with a variable temperature and a Protasis capillary probe (Marlborough, USA).

5.15.6.2 Cryogenic NMR

^{1}H and ^{13}C NMR was recorded at the University of Naples on a Varian UnityInova spectrometer, operating at 700 and 175 MHz. The UnityInova was equipped with a Varian cryogenic probe. Chemical shifts were referenced to the residual solvent signal (MeOH: δ_H 3.31, δ_C 49.0). For an accurate measurement of the coupling constants, the one-dimensional ^{1}H NMR spectra were transformed at 64K points (digital resolution: 0.09 Hz). Homonuclear ^{1}H connectivities were determined by a COSY experiment. The HSQC spectra were optimized for $^{1}J_{CH}$ = 142 Hz, and the HMBC experiments for $^{2,3}J_{CH}$ = 8.3 Hz.

5.16 Synthesis of diazomethane[148]

For the synthesis of diazomethane, 0.5 mg potassium hydroxide was dissolved in 1 ml water diluted with 95% ethanol in a flask. It was cooled in an ice bath and a solution of 0.5 mg Diazald in 7.5 ml diethyl ether was slowly added with a Pasteur pipette. When all the Diazald was added, the neck of the reaction flask was closed and heated in a warm water bath up to 65℃. The yellow diazomethane-ether mixture was distilled until all the yellow colour had disappeared from the reaction flask. The yellow distillate in the receiver contained diazomethane and it was immediately mixed with the sample to be derivatised.

5.17 Chemicals used in this study

Solvents in p.a. quality (acetone, acetonitrile, chloroform, isopropanol, ethyl acetate, acetic acid and methanol) were purchased from the companies Fluka / Riedel-de-Haën (Seelze, Germany), Merck (Darmstadt, Germany), Fisher Scientific (Schwerte, Germany). HPLC-grade solvents were purchased from the companies Merck and J. T. Baker / Mallinckrodt Baker (Deventer, Netherlands).

Table 16: Chemicals used in this study.

Chemical	Company
Agar	Roth, Karlsruhe
Agarose NEEO quality	Roth, Karlsruhe
L-Arabinose	Fluka / Riedel-de-Haën, Seelze
Ammonium heptamolybdate tetrahydrate	Merck, Darmstadt
Ammonium sulphate	Applichem, Darmstadt, Germany
Ampicillin sodium salt	Roth, Karlsruhe
Apramycin sulphate	Sigma-Aldrich, Seelze, Germany
Bovine serum albumine (BSA-solution 10 mg/mL)	NEB, Frankfurt/Main
5-Bromo-4-chloro-3-indolyl-β-D-galactopyranoside (X-Gal)	AppliChem, Darmstadt, Germany
Bromo phenol blue sodium salt	AppliChem, Darmstadt
Calcium carbonate	Roth, Karlsruhe

Calcium chloride	KMF, Lohmar, Germany
Carbenicillin disodium salt	Roth, Karlsruhe
Casamino acids	Becton Dickinson, Heidelberg, Germany
Chloramphenicol	Fluka / Riedel-de-Haën, Seelze
[D_1] Chloroform ($CDCl_3$)	Euriso-Top, Gif sur Yvette, France
Copper(II) chloride dihydrat	Grüssing, Filsum, Germany
Copper (II) sulphate	AppliChem, Darmstadt
Desoxythiamine-5'-triphosphate (dTTP)	Invitrogen, Karlsruhe
Desoxynucleotide (dNTPs)	Invitrogen, Karlsruhe
Dipotassiumhydrogenphosphate dehydrate	Merck, Darmstadt
N,N-Dimethylformamide (DMF)	Fisher-Scientific, Schwerte, Germany
Dimethylsulfoxide (DMSO)	Roth, Karlsruhe
[D_6] Dimethyl sulfoxide (DMSO-d_6)	Euriso-Top, Gif sur Yvette
Dinatriumhydrogenphosphate dehydrate	Fluka / Riedel-de-Haën, Seelze
1kb DNA ladder	Roth, Karlsruhe
Hydrochloric acid	Fluka / Riedel-de-Haën, Seelze
Iron(II)sulphate heptahydrate	Merck, Darmstadt
Iron(III)chloride hexahydrate	Alfa Aesar, Karlsruhe, Germany
Ethidium bromide	Roth, Karlsruhe
Ethylenediaminetetraacetic acid (EDTA)	KMF, Lohmar
D(+)-Glucose monohydrate	Fluka / Riedel-de-Haën, Seelze
Glycerol	Merck, Darmstadt
Glycine	Fisher-Scientific, Schwerte
Isopropyl β-D-1-thiogalactopyranoside (IPTG)	Roth, Karlsruhe
Potassium acetate	ABCR; Karlsruhe, Germany
Potassium carbonate	AppliChem, Darmstadt
Potassium chloride	Acros Organics, Geel (Belgium)
Potassium dihydrogen phosphate	Merck, Darmstadt
Potassium sulphate	Grüssing, Filsum
Kanamycin sulphate	Roth, Karlsruhe
Potato starch, soluble	Sigma-Aldrich, Seelze
Lysozyme	Roth, Karlsruhe
Magnesium chloride hexahydrate	Fluka / Riedel-de-Haën, Seelze
Magnesium sulphate heptahydrate	Roth, Karlsruhe
Manganese chloride tetrahydrate	Merck, Darmstadt
Mannitol	Roth, Karlsruhe
3-(N-morpholino) propanesulfonic acid (MOPS)	Sigma-Aldrich, Seelze
Nalidixic acid	Roth, Karlsruhe
L-Prolin	Acros Organics, Geel
Ribonuclease A (RNase A)	Roth, Karlsruhe
Silica gel 60 (0,040- 0,063 mm)	Merck, Darmstadt
Sulfuric acid	Fluka / Riedel-de-Haën, Seelze
Sodium acetate	Acros Organics, Geel
Sodium tetraborat decahydrate	Sigma-Aldrich, Seelze

Sodium carbonate	KMF, Lohmar
Sodium chloride	Grüssing, Filsum
Sodium dihydrogen phosphate dehydrate	Roth, Karlsruhe
Sodium dodecyl sulphate (SDS)	Roth, Karlsruhe
Sodium hydroxide	KMF, Lohmar
Tris(hydroxymethyl)aminomethane (Tris)	Roth, Karlsruhe
Tryptic Soy Broth (TSB)	Becton Dickinson, Heidelberg
Tryptone	Becton Dickinson, Heidelberg
Xylene cyanol	Merck, Darmstadt
Yeast extract	Becton Dickinson, Heidelberg
Zinc chloride	Acros Organics, Geel
Zinc sulphate	Merck, Darmstadt

5.18 Equipment used in this study

Single-use reaction- and centrifuge tubes, serological pipettes, pipette tips, Petri dishes and tubes were purchased from the company Sarstedt (Nümbrecht, Germany).

Table 17: Equipment used in this study.

Equipment	Company
Analytical balance CP225D	Sartorius, Göttingen, Germany
Autoclave V65	Systec, Wettenberg, Germany
Balance 440-47N	Kern, Balingen-Frommern, Germany
Balance BP110	Sartorius, Göttingen,
Micro cuvette (1,6 mL)	Sarstedt, Nümbrecht
Incubation shaker Certomat BS-1	Sartorius, Göttingen
Incubator B12	Thermo, Langenselbold, Germany
Membrane vacuum pump	Vacuubrand, Wertheim, Germany
Micro cuvette UltraVette (70-850 µL)	Roth, Karlsruhe
Microwave Lifetec	Medion, Essen, Germany
Micro centrifuge Mikro200	Hettich, Tuttlingen, Germany
Micro centrifuge 5417R	Eppendorf, Hamburg, Germany
Micro centrifuge Mikro200R	Hettich, Tuttlingen
Multipette: Eppendorf Research 100	Eppendorf, Hamburg
Pipetten Pipetman P2 - P10 mL	Gilson, Middleton, USA
HPLC vials with lid and septum for autosampler	Bio-Rad, Munich
Shaker Rotamax 120	Heidolph, Kelheim
Sterile bench Biowizard	Kojair, Vilppula, Finland

Steril filter (0,2 µm, Celluloseacetat, FP 30/0,2)	Whatman / Schleicher & Schuell, Dassel, Germany
Table centrifuge Rotina 35R	Hettich, Tittlingen
Table centrifuge Z513K	Hermle, Wehingen, Germany
UV-Crosslinker CL1000	UVP, Cambridge, United Kingdom
Vortex VTX-3000L	LMS, Tokio, Japan
Water bath	GFL, Burgwedel, Germany

6 List of abbreviations

A	Ampere
AA	Amino acid
ACN	Acetonitrile
AcOH	Acetic acid
ACP	Acyl carrier protein
Act/*act*	Proteins and genes of the actinorhodin gene cluster
Amp^{100}	Ampicillin in final concentration 100 µg/ml
ARO	Aromatase
Apr^{50}	Apramycin in final concentration 50µg/ml
AT	Acyltransferase
Aur/*aur*	Proteins and genes of the aurachin gene cluster
Ben/*ben*	Proteins and genes of the benastation gene cluster
BLAST	Basic Local Alignment Search Tool
BVMO	Baeyer-Villiger monooxygenase
bp	Base pair
BSA	Bovine Serum Albumine
℃	Degree Celsius
CapNMR	Capillary probe NMR
CD_3Cl	Deuterated chloroform
CE	Capillary electrophoresis
CapLC	Capillary HPLC
CLF	"chain length factor" = $Ketosynthase_{ß}$
cDNA	Complementary DNA
Cm^{25}	Chloramphenicol in final concentration 25 µg/ml
Cmm	Proteins and genes of the chromomycin gene cluster
COSY	two-dimensional NMR correlation spectroscopy with ^{1}H-^{1}H correlation

CYC	Cyclase
CYP-450	Cytochrome P450
ddH_2O	Double distilled water
DEBS	6-deoxyerythronolid B synthase
DH	Dehydrogenase
DMAC	Dihydroxymethylanthrachinone
DMF	Dimethylene formamide
DMSO	Dimethylene sulfideoxide
DNA	Deoxyribonucleic acid
dNTP	Deoxynucleotide triphosphate
et al.	*et alii* (and others)
E. coli	*Escherichia coli*
E-tube	Eppendorf tubes (1.5 or 2 ml plastic tubes)
EDTA	Ethylene di-amine tetra-acetic acid
Enc/*enc*	Proteins and genes of the enterocin gene cluster
ER	Enoylreductase
ESI	Electrospray ionisation
EtOAC	Ethyl acetate
FA	Fatty acid
FAD	Flavin adenine dinukleotide
FAS	Fatty acid synthase
Fig.	Figure
Fdm/f*dm*	Proteins and genes of the fredericamycin gene cluster
Frn/*frn*	Proteins and genes of the frenolicin gene cluster
Grh/*grh*	Proteins and genes of the griseorhodin A gene cluster
GT	Glycosyltransferase
h	Hour
Hed/*hed*	Proteins and genes of the hedamycin gene cluster
Hifi	High Fidelity Polymerase

HMBC	Heteronuclear multiple bond coherence (long-range coupling between different nuclear species)
HMQC	Heteronuclear multiple quantum coherence (direct coupling between different nuclear species)
HPLC	High pressure liquid chromatography
HRMS	High resolution mass spectrometry
g	Relative centrifugal force
g	Gram
IPTG	Isopropyl β-D-1-thiogalactopyranoside
Jad/*jad*	Proteins and genes of the jadomycin gene cluster
K	Kelvin
Kb	Kilobase
Kan^{25}	Kanamycin in final concentration 25 µg/ml
KR	Ketoreductase
KS	Ketosynthase
L	Litre
LB	Luria Bertani
LC	Liquid chromatography
LC-MS	Liquid chromatography mass spectrometry
Llp/*llp*	Proteins and genes of the lysolipin gene cluster
Lnd/*lnd*	Proteins and genes of the landomycin gene cluster
m	Milli- (1×10^{-3})
M	Molar
MCAT	Malonyl-CoA:APC transferase
MCS	Multiple cloning site
µ	Micro- (1×10^{-6})
mM	Millimolar
MeOH	Methanol

Minimal PKS	The minimal set of PKS containing ACP and KS_{α}-KS_{β}
min	Minutes
MOPS	3-(N-morpholino)propanesulfonic acid
MS	Mass spectrometry/mass spectrometer
MT	Methyltransferase
Mtm/*mtm*	Proteins and genes of the mithramycin gene cluster
MW	Molecular weight
NAD	Nicotiamide adenine dinucleotide
NaOH	Sodium hydroxide
NMR	Nuclear magnetic spectroscopy
NP	Normal phase
OD	Optical density
ORF	Open reading frame
Oxy/*oxy*	Proteins and genes of the oxytetracycline gene cluster
p	Pico- (1×10^{-12})
P/Chl/I	Phenol/choloroform/isoamylalcohol
PCR	Polymerase chain reaction
PKS	Polyketide synthase
RBS	Ribosomal binding site
RNA	Ribonucleic acid
RNase A	Ribonuclease A
rpm	Rotation per minute
resp.	Respectively
RP	Reverse phase
RT	Room temperature
RT-PCR	Reverse transcriptase PCR
s	Seconds
SAM	S-adenosyl methionine
SDS	Sodium dodecyl sulphate
S. albus	*Streptomyces albus*
s/n	Signal-to-noise ratio

sp.	Species
Str^{50}	Streptomycin in final concentration 50 µg/ml
TAE	Tris-acetate-EDTA buffer
Taq polymerase	DNA Polymerase from *Thermus aquaticus*
TFA	Trifluoric acid
TLC	Thin layer chromatography
Tcm/*tcm*	Proteins and genes of the tetracenomycin gene cluster
TE	Thioesterase
U	Unit (Unit of enzyme activity)
µl	Microlitre
UV	Ultraviolet
w/v	Weight per volume
wt	Wildtype
X-Gal	5-Bromo-4-chloro-3-indolyl-β-D-galactopyranoside

Nucleotide bases

A Purine base Adenine	G Purine base Guanine
C Pyrimidine base Cytosine	T Pyrimidine base Thymine

7 References

1. Reinhardt, K. PhD thesis: Griseorhodin A: Biosynthesestudien und kombinatorische Biosynthese. Rheinisch Friedrich-Wilhelms-University of Bonn, Bonn, 2009.
2. Shen, B., Polyketide biosynthesis beyond the type I, II and III polyketide synthase paradigms. *Curr Opin Chem Biol* **2003,** 7, (2), 285-95.
3. Piel, J.; Butzke, D.; Fusetani, N.; Hui, D.; Platzer, M.; Wen, G.; Matsunaga, S., Exploring the chemistry of uncultivated bacterial symbionts: antitumor polyketides of the pederin family. *J Nat Prod* **2005,** 68, (3), 472-9.
4. Weissman, K. J.; Leadlay, P. F., Combinatorial biosynthesis of reduced polyketides. *Nat Rev Microbiol* **2005,** 3, (12), 925-36.
5. Katz, L.; Ashley, G. W., Translation and protein synthesis: macrolides. *Chem Rev* **2005,** 105, (2), 499-528.
6. Hertweck, C.; Luzhetskyy, A.; Rebets, Y.; Bechthold, A., Type II polyketide synthases: gaining a deeper insight into enzymatic teamwork. *Nat Prod Rep* **2007,** 24, (1), 162-90.
7. Schwecke, T.; Aparicio, J. F.; Molnar, I.; Konig, A.; Khaw, L. E.; Haydock, S. F.; Oliynyk, M.; Caffrey, P.; Cortes, J.; Lester, J. B.; et al., The biosynthetic gene cluster for the polyketide immunosuppressant rapamycin. *Proc Natl Acad Sci U S A* **1995,** 92, (17), 7839-43.
8. Staunton, J.; Weissman, K. J., Polyketide biosynthesis: a millennium review. *Nat Prod Rep* **2001,** 18, (4), 380-416.
9. Cane, D. E., Introduction: Polyketide and Nonribosomal Polypeptide Biosynthesis. From Collie to Coli. *Chem Rev* **1997,** 97, (7), 2463-2464.
10. Birch, A. J., Biosynthesis of polyketides and related compounds. *Science* **1967,** 156, (772), 202-6.
11. Hopwood, D. A., Cracking the polyketide code. *PLoS Biol* **2004,** 2, (2), E35.
12. Reeves, C. D., The enzymology of combinatorial biosynthesis. *Crit Rev Biotechnol* **2003,** 23, (2), 95-147.
13. Smith, S.; Tsai, S. C., The type I fatty acid and polyketide synthases: a tale of two megasynthases. *Nat Prod Rep* **2007,** 24, (5), 1041-72.
14. McDaniel, R.; Welch, M.; Hutchinson, C. R., Genetic approaches to polyketide antibiotics. 1. *Chem Rev* **2005,** 105, (2), 543-58.
15. Cox, R. J., Polyketides, proteins and genes in fungi: programmed nano-machines begin to reveal their secrets. *Org Biomol Chem* **2007,** 5, (13), 2010-26.
16. Weissman, K. J., Introduction to polyketide biosynthesis. *Methods Enzymol* **2009,** 459, 3-16.
17. Gokhale, R. S.; Hunziker, D.; Cane, D. E.; Khosla, C., Mechanism and specificity of the terminal thioesterase domain from the erythromycin polyketide synthase. *Chem Biol* **1999,** 6, (2), 117-25.
18. Katz, L.; Donadio, S., Polyketide synthesis: prospects for hybrid antibiotics. *Annu Rev Microbiol* **1993,** 47, 875-912.

19. Hendrickson, L.; Davis, C. R.; Roach, C.; Nguyen, D. K.; Aldrich, T.; McAda, P. C.; Reeves, C. D., Lovastatin biosynthesis in *Aspergillus terreus*: characterization of blocked mutants, enzyme activities and a multifunctional polyketide synthase gene. *Chem Biol* **1999,** 6, (7), 429-39.
20. Alfonso, Y.; Fraga, J.; Jimenez, N.; Fonseca, C.; Dorta-Contreras, A. J.; Cox, R.; Capo, V.; Bandera, F.; Pomier, O.; Ginorio, D., Detection of *Toxoplasma gondii* in cerebrospinal fluid from AIDS patients by nested PCR and rapid identification of type I allele at B1 gene by RFLP analysis. *Exp Parasitol* **2009,** 122, (3), 203-7.
21. Spencer, J. B.; Jordan, P. M., Purification and properties of 6-methylsalicylic acid synthase from *Penicillium patulum*. *Biochem J* **1992,** 288 (Pt 3), 839-46.
22. Dimroth, P.; Walter, H.; Lynen, F., Biosynthese von 6-Methylsalicylsäure. *Eur J Biochem* **1970,** 13, (1), 98-110.
23. Kennedy, J.; Auclair, K.; Kendrew, S. G.; Park, C.; Vederas, J. C.; Hutchinson, C. R., Modulation of polyketide synthase activity by accessory proteins during lovastatin biosynthesis. *Science* **1999,** 284, (5418), 1368-72.
24. Gaisser, S.; Trefzer, A.; Stockert, S.; Kirschning, A.; Bechthold, A., Cloning of an avilamycin biosynthetic gene cluster from *Streptomyces viridochromogenes* Tu57. *J Bacteriol* **1997,** 179, (20), 6271-8.
25. Li, A.; Piel, J., A gene cluster from a marine *Streptomyces* encoding the biosynthesis of the aromatic spiroketal polyketide griseorhodin A. *Chem Biol* **2002,** 9, (9), 1017-26.
26. Austin, M. B.; Noel, J. P., The chalcone synthase superfamily of type III polyketide synthases. *Nat Prod Rep* **2003,** 20, (1), 79-110.
27. Moore, B. S.; Hopke, J. N., Discovery of a new bacterial polyketide biosynthetic pathway. *Chembiochem* **2001,** 2, (1), 35-8.
28. Hopwood, D. A., Genetic Contributions to Understanding Polyketide Synthases. *Chem Rev* **1997,** 97, (7), 2465-2498.
29. Malpartida, F.; Hopwood, D. A., Molecular cloning of the whole biosynthetic pathway of a *Streptomyces* antibiotic and its expression in a heterologous host. *Nature* **1984,** 309, (5967), 462-4.
30. Shen, B., Biosynthesis of aromatic polyketides. *Top. Curr. Chem* **2000,** 209, (1), 1-51.
31. Zhou, H.; Li, Y.; Tang, Y., Cyclization of aromatic polyketides from bacteria and fungi. *Nat Prod Rep* **2010,** 27, (6), 839-68.
32. Rawlings, B. J., Biosynthesis of polyketides (other than actinomycete macrolides). *Nat Prod Rep* **1999,** 16, (4), 425-84.
33. Hitchman, T. S.; Crosby, J.; Byrom, K. J.; Cox, R. J.; Simpson, T. J., Catalytic self-acylation of type II polyketide synthase acyl carrier proteins. *Chem Biol* **1998,** 5, (1), 35-47.
34. McDaniel, R.; Ebert-Khosla, S.; Hopwood, D. A.; Khosla, C., Engineered biosynthesis of novel polyketides. *Science* **1993,** 262, (5139), 1546-50.
35. Tang, Y.; Tsai, S. C.; Khosla, C., Polyketide chain length control by chain length factor. *J Am Chem Soc* **2003,** 125, (42), 12708-9.

36. Keatinge-Clay, A. T.; Maltby, D. A.; Medzihradszky, K. F.; Khosla, C.; Stroud, R. M., An antibiotic factory caught in action. *Nat Struct Mol Biol* **2004,** 11, (9), 888-93.
37. Xu, Z.; Metsa-Ketela, M.; Hertweck, C., Ketosynthase III as a gateway to engineering the biosynthesis of antitumoral benastatin derivatives. *J Biotechnol* **2009,** 140, (1-2), 107-13.
38. Moore, B. S.; Hertweck, C., Biosynthesis and attachment of novel bacterial polyketide synthase starter units. *Nat Prod Rep* **2002,** 19, (1), 70-99.
39. Rock, C. O.; Jackowski, S., Forty years of bacterial fatty acid synthesis. *Biochem Biophys Res Commun* **2002,** 292, (5), 1155-66.
40. Grimm, A.; Madduri, K.; Ali, A.; Hutchinson, C. R., Characterization of the *Streptomyces peucetius* ATCC 29050 genes encoding doxorubicin polyketide synthase. *Gene* **1994,** 151, (1-2), 1-10.
41. Bibb, M. J.; Sherman, D. H.; Omura, S.; Hopwood, D. A., Cloning, sequencing and deduced functions of a cluster of *Streptomyces* genes probably encoding biosynthesis of the polyketide antibiotic frenolicin. *Gene* **1994,** 142, (1), 31-9.
42. Marti, T.; Hu, Z.; Pohl, N. L.; Shah, A. N.; Khosla, C., Cloning, nucleotide sequence, and heterologous expression of the biosynthetic gene cluster for R1128, a non-steroidal estrogen receptor antagonist. Insights into an unusual priming mechanism. *J Biol Chem* **2000,** 275, (43), 33443-8.
43. Xu, Z.; Schenk, A.; Hertweck, C., Molecular analysis of the benastatin biosynthetic pathway and genetic engineering of altered fatty acid-polyketide hybrids. *J Am Chem Soc* **2007,** 129, (18), 6022-30.
44. Bililign, T.; Hyun, C. G.; Williams, J. S.; Czisny, A. M.; Thorson, J. S., The hedamycin locus implicates a novel aromatic PKS priming mechanism. *Chem Biol* **2004,** 11, (7), 959-69.
45. Yu, T. W.; Shen, Y.; McDaniel, R.; Floss, H. G.; Khosla, C.; Hopwood, D. A.; Moore, B. S., Engineered biosynthesis of novel polyketides from *Streptomyces* spore pigment polyketide synthases. *J Am Chem Soc* **1998,** 120, (31), 7749-7759.
46. McDaniel, R.; Ebert-Khosla, S.; Hopwood, D.; Khosla, C., Engineered biosynthesis of novel polyketides: actVII and actIV genes encode aromatase and cyclase enzymes, respectively. *J Am Chem Soc* **1994,** 116, (24), 10855–10859.
47. Zawada, R. J.; Khosla, C., Domain analysis of the molecular recognition features of aromatic polyketide synthase subunits. *J Biol Chem* **1997,** 272, (26), 16184-8.
48. Shen, B.; Hutchinson, C. R., Tetracenomycin F2 cyclase: intramolecular aldol condensation in the biosynthesis of tetracenomycin C in *Streptomyces glaucescens*. *Biochemistry* **1993,** 32, (41), 11149-54.
49. Shen, B.; Hutchinson, C. R., Deciphering the mechanism for the assembly of aromatic polyketides by a bacterial polyketide synthase. *Proc Natl Acad Sci U S A* **1996,** 93, (13), 6600-4.
50. Ames, B. D.; Korman, T. P.; Zhang, W.; Smith, P.; Vu, T.; Tang, Y.; Tsai, S. C., Crystal structure and functional analysis of

tetracenomycin ARO/CYC: implications for cyclization specificity of aromatic polyketides. *Proc Natl Acad Sci U S A* **2008,** 105, (14), 5349-54.

51. Sultana, A.; Kallio, P.; Jansson, A.; Wang, J. S.; Niemi, J.; Mantsala, P.; Schneider, G., Structure of the polyketide cyclase SnoaL reveals a novel mechanism for enzymatic aldol condensation. *Embo J* **2004,** 23, (9), 1911-21.
52. Fu, H.; Hopwood, D. A.; Khosla, C., Engineered biosynthesis of novel polyketides: evidence for temporal, but not regiospecific, control of cyclization of an aromatic polyketide precursor. *Chem Biol* **1994,** 1, (4), 205-10.
53. Gullon, S.; Olano, C.; Abdelfattah, M. S.; Brana, A. F.; Rohr, J.; Mendez, C.; Salas, J. A., Isolation, characterization, and heterologous expression of the biosynthesis gene cluster for the antitumor anthracycline steffimycin. *Appl Environ Microbiol* **2006,** 72, (6), 4172-83.
54. Lombo, F.; Blanco, G.; Fernandez, E.; Mendez, C.; Salas, J. A., Characterization of *Streptomyces argillaceus* genes encoding a polyketide synthase involved in the biosynthesis of the antitumor mithramycin. *Gene* **1996,** 172, (1), 87-91.
55. Tsai, S. C.; Ames, B. D., Structural enzymology of polyketide synthases. *Methods Enzymol* **2009,** 459, 17-47.
56. McDaniel, R.; Hutchinson, C. R.; Khosla, C., Engineered biosynthesis of novel polyketides: analysis of tcmN function in tetracenomycin biosynthesis. *J Am Chem Soc* **1995,** 117, (26), 6805-6810.
57. Hutchinson, C. R., Biosynthetic studies of daunorubicin and tetracenomycin C. *Chem Rev* **1997,** 97, (7), 2525-2536.
58. Thompson, T. B.; Katayama, K.; Watanabe, K.; Hutchinson, C. R.; Rayment, I., Structural and functional analysis of tetracenomycin F2 cyclase from *Streptomyces glaucescens*. A type II polyketide cyclase. *J Biol Chem* **2004,** 279, (36), 37956-63.
59. Han, L.; Yang, K.; Ramalingam, E.; Mosher, R. H.; Vining, L. C., Cloning and characterization of polyketide synthase genes for jadomycin B biosynthesis in *Streptomyces venezuelae* ISP5230. *Microbiology* **1994,** 140 (Pt 12), 3379-89.
60. Rix, U.; Fischer, C.; Remsing, L. L.; Rohr, J., Modification of post-PKS tailoring steps through combinatorial biosynthesis. *Nat Prod Rep* **2002,** 19, (5), 542-80.
61. Rafanan, E. R.; Hutchinson, C. R.; Shen, B., Triple hydroxylation of tetracenomycin A2 to tetracenomycin C involving two molecules of O_2 and one molecule of H_2O. *Org Lett* **2000,** 2, (20), 3225-3227.
62. Chen, Y.-H.; Wang, C.-C.; Greenwell, L.; Rix, U.; Hoffmeister, D.; Vining, L. C.; Rohr, J.; Yang, Q.-K., Functional analyses of oxygenases in jadomycin biosynthesis and identification of JadH as a bifunctional oxygenase/dehydrase. *J Biol Chem* **2005,** 280, (23), 22508-22514.
63. Zhu, L.; Ostash, B.; Rix, U.; Nur, E. A. M.; Mayers, A.; Luzhetskyy, A.; Mendez, C.; Salas, J. A.; Bechthold, A.; Fedorenko, V.; Rohr, J., Identification of the function of gene lndM2 encoding a bifunctional

oxygenase-reductase involved in the biosynthesis of the antitumor antibiotic landomycin E by *Streptomyces globisporus* 1912 supports the originally assigned structure for landomycinone. *J Org Chem* **2005,** 70, (2), 631-8.

64. Meunier, B.; de Visser, S. P.; Shaik, S., Mechanisms of oxidation reactions catalysed by cytochrome P450 enzymes. *Chem Rev* **2004,** 104, (9), 3947-3980.
65. Voet, D.; Voet, J. G.; Pratt, C. W., *Lehrbuch der Biochemie*. WILEY-VCH: Weinheim, 2002.
66. Piel, J.; Hertweck, C.; Shipley, P. R.; Hunt, D. M.; Newman, M. S.; Moore, B. S., Cloning, sequencing and analysis of the enterocin biosynthesis gene cluster from the marine isolate '*Streptomyces maritimus*': evidence for the derailment of an aromatic polyketide synthase. *Chem Biol* **2000,** 7, (12), 943-55.
67. Lomovskaya, N.; Otten, S. L.; Doi-Katayama, Y.; Fonstein, L.; Liu, X. C.; Takatsu, T.; Inventi-Solari, A.; Filippini, S.; Torti, F.; Colombo, A. L.; Hutchinson, C. R., Doxorubicin overproduction in *Streptomyces peucetius*: cloning and characterization of the dnrU ketoreductase and dnrV genes and the doxA cytochrome P-450 hydroxylase gene. *J Bacteriol* **1999,** 181, (1), 305-18.
68. Xu, Z.; Jakobi, K.; Welzel, K.; Hertweck, C., Biosynthesis of the antitumor agent chartreusin involves the oxidative rearrangement of an anthracyclic polyketide. *Chem Biol* **2005,** 12, (5), 579-88.
69. Munro, A. W.; Taylor, P.; Walkinshaw, M. D., Structures of redox enzymes. *Curr Opin Biotechnol* **2000,** 11, (4), 369-76.
70. Fraaije, M. W.; Mattevi, A., Flavoenzymes: diverse catalysts with recurrent features. *Trends Biochem Sci* **2000,** 25, (3), 126-32.
71. van Berkel, W. J.; Kamerbeek, N. M.; Fraaije, M. W., Flavoprotein monooxygenases, a diverse class of oxidative biocatalysts. *J Biotechnol* **2006,** 124, (4), 670-89.
72. Mihovilovic, M. D.; Müller, B.; Stanetty, P., Monooxygenase-mediated Baeyer-Villiger oxidations. *Eur J Org Chem* **2002,** 2002, (22), 3711-3730.
73. Decker, K. F., Biosynthesis and function of enzymes with covalently bound flavin. *Annu Rev Nutr* **1993,** 13, 17-41.
74. Ostash, B.; Rix, U.; Rix, L. L.; Liu, T.; Lombo, F.; Luzhetskyy, A.; Gromyko, O.; Wang, C.; Brana, A. F.; Mendez, C.; Salas, J. A.; Fedorenko, V.; Rohr, J., Generation of new landomycins by combinatorial biosynthetic manipulation of the LndGT4 gene of the landomycin E cluster in *S. globisporus*. *Chem Biol* **2004,** 11, (4), 547-55.
75. Xiang, L.; Kalaitzis, J. A.; Moore, B. S., EncM, a versatile enterocin biosynthetic enzyme involved in Favorskii oxidative rearrangement, aldol condensation, and heterocycle-forming reactions. *Proc Natl Acad Sci U S A* **2004,** 101, (44), 15609-14.
76. Kamerbeek, N. M.; Janssen, D. B.; van Berkel, W. J.; Fraaije, M. W., Baeyer-Villiger monooxygenases, an emerging family of flavin-dependent biocatalysts. *Adv Synth Catal* **2003,** 345, (6-7), 667-678.
77. Prado, L.; Lombo, F.; Brana, A. F.; Mendez, C.; Rohr, J.; Salas, J. A., Analysis of two chromosomal regions adjacent to genes for a type II

polyketide synthase involved in the biosynthesis of the antitumor polyketide mithramycin in *Streptomyces argillaceus*. *Mol Gen Genet* **1999,** 261, (2), 216-25.

78. Fischer, C.; Lipata, F.; Rohr, J., The complete gene cluster of the antitumor agent gilvocarcin V and its implication for the biosynthesis of the gilvocarcins. *J Am Chem Soc* **2003,** 125, (26), 7818-9.
79. Liu, T.; Fischer, C.; Beninga, C.; Rohr, J., Oxidative rearrangement processes in the biosynthesis of gilvocarcin V. *J Am Chem Soc* **2004,** 126, (39), 12262-3.
80. Rix, U.; Wang, C.; Chen, Y.; Lipata, F. M.; Remsing Rix, L. L.; Greenwell, L. M.; Vining, L. C.; Yang, K.; Rohr, J., The oxidative ring cleavage in jadomycin biosynthesis: a multistep oxygenation cascade in a biosynthetic black box. *Chembiochem* **2005,** 6, (5), 838-45.
81. Hertweck, C.; Xiang, L.; Kalaitzis, J. A.; Cheng, Q.; Palzer, M.; Moore, B. S., Context-dependent behavior of the enterocin iterative polyketide synthase; a new model for ketoreduction. *Chem Biol* **2004,** 11, (4), 461-8.
82. Dickens, M. L.; Ye, J.; Strohl, W. R., Cloning, sequencing, and analysis of aklaviketone reductase from *Streptomyces* sp. strain C5. *J Bacteriol* **1996,** 178, (11), 3384-8.
83. Hutchinson, C. R.; Fujii, I., Polyketide synthase gene manipulation: a structure-function approach in engineering novel antibiotics. *Annu Rev Microbiol* **1995,** 49, 201-38.
84. Trefzer, A.; Salas, J. A.; Bechthold, A., Genes and enzymes involved in deoxysugar biosynthesis in bacteria. *Nat Prod Rep* **1999,** 16, (3), 283-99.
85. Salas, J. A.; Mendez, C., Engineering the glycosylation of natural products in actinomycetes. *Trends Microbiol* **2007,** 15, (5), 219-32.
86. Thibodeaux, C. J.; Melancon, C. E.; Liu, H. W., Unusual sugar biosynthesis and natural product glycodiversification. *Nature* **2007,** 446, (7139), 1008-16.
87. Newman, D. J.; Cragg, G. M., Natural products as sources of new drugs over the last 25 years. *J Nat Prod* **2007,** 70, (3), 461-77.
88. Berdy, J., Bioactive microbial metabolites. *J Antibiot (Tokyo)* **2005,** 58, (1), 1-26.
89. Jensen, P. R.; Williams, P. G.; Oh, D. C.; Zeigler, L.; Fenical, W., Species-specific secondary metabolite production in marine actinomycetes of the genus *Salinispora*. *Appl Environ Microbiol* **2007,** 73, (4), 1146-52.
90. Newman, D. J.; Cragg, G. M., Marine natural products and related compounds in clinical and advanced preclinical trials. *J Nat Prod* **2004,** 67, (8), 1216-38.
91. Olano, C.; Mendez, C.; Salas, J. A., Antitumor compounds from marine actinomycetes. *Mar Drugs* **2009,** 7, (2), 210-48.
92. Olano, C.; Mendez, C.; Salas, J. A., Post-PKS tailoring steps in natural product-producing actinomycetes from the perspective of combinatorial biosynthesis. *Nat Prod Rep* **2010,** 27, (4), 571-616.
93. Demain, A. L.; Sanchez, S., Microbial drug discovery: 80 years of progress. *J Antibiot (Tokyo)* **2009,** 62, (1), 5-16.

94. White, R. E., High-throughput screening in drug metabolism and pharmacokinetic support of drug discovery. *Annu. Rev. Pharmacol. Toxicol.* **2000**
(40), 133-157.
95. Habich, D.; von Nussbaum, F., Platensimycin, a new antibiotic and "superbug challenger" from nature. *ChemMedChem* **2006,** 1, (9), 951-4.
96. Wang, J.; Soisson, S. M.; Young, K.; Shoop, W.; Kodali, S.; Galgoci, A.; Painter, R.; Parthasarathy, G.; Tang, Y. S.; Cummings, R.; Ha, S.; Dorso, K.; Motyl, M.; Jayasuriya, H.; Ondeyka, J.; Herath, K.; Zhang, C.; Hernandez, L.; Allocco, J.; Basilio, A.; Tormo, J. R.; Genilloud, O.; Vicente, F.; Pelaez, F.; Colwell, L.; Lee, S. H.; Michael, B.; Felcetto, T.; Gill, C.; Silver, L. L.; Hermes, J. D.; Bartizal, K.; Barrett, J.; Schmatz, D.; Becker, J. W.; Cully, D.; Singh, S. B., Platensimycin is a selective FabF inhibitor with potent antibiotic properties. *Nature* **2006,** 441, (7091), 358-61.
97. Brakhage, A. A.; Schroekch, V., Fungal secondary metabolites - Strategies to activate silent gene clusters. *Fungal Genet Biology* **2010,** 48, (1), 15-22.
98. Steele, H. L.; Streit, W. R., Metagenomics: advances in ecology and biotechnolgy). *FEMS Microbiol Lett* **2005,** 2, (15), 105-111.
99. Wilkinson, B.; Micklefield, J., Mining and engineering natural-product biosynthetic pathways. *Nat Chem Biol* **2007,** 3, (7), 379-86.
100. Palmu, K.; Ishida, K.; Mantsala, P.; Hertweck, C.; Metsa-Ketela, M., Artificial reconstruction of two cryptic angucycline antibiotic biosynthetic pathways. *Chembiochem* **2007,** 8, (13), 1577-84.
101. Mendez, C.; Weitnauer, G.; Bechthold, A.; Salas, J. A., Structure alteration of polyketides by recombinant DNA technology in producer organisms--prospects for the generation of novel pharmaceutical drugs. *Curr Pharm Biotechnol* **2000,** 1, (4), 355-95.
102. Lombo, F.; Brana, A. F.; Salas, J. A.; Mendez, C., Genetic organization of the biosynthetic gene cluster for the antitumor angucycline oviedomycin in *Streptomyces antibioticus* ATCC 11891. *Chembiochem* **2004,** 5, (9), 1181-7.
103. Mendez, C.; Kunzel, E.; Lipata, F.; Lombo, F.; Cotham, W.; Walla, M.; Bearden, D. W.; Brana, A. F.; Salas, J. A.; Rohr, J., Oviedomycin, an unusual angucyclinone encoded by genes of the oleandomycin-producer *Streptomyces antibioticus* ATCC11891. *J Nat Prod* **2002,** 65, (5), 779-82.
104. Lombo, F.; Abdelfattah, M. S.; Brana, A. F.; Salas, J. A.; Rohr, J.; Mendez, C., Elucidation of oxygenation steps during oviedomycin biosynthesis and generation of derivatives with increased antitumor activity. *Chembiochem* **2009,** 10, (2), 296-303.
105. Khosla, C., Harnessing the Biosynthetic Potential of Modular Polyketide Synthases. *Chem Rev* **1997,** 97, (7), 2577-2590.
106. Cane, D. E.; Walsh, C. T.; Khosla, C., Harnessing the biosynthetic code: combinations, permutations, and mutations. *Science* **1998,** 282, (5386), 63-8.
107. Hutchinson, C. R., Combinatorial biosynthesis for new drug discovery. *Curr Opin Microbiol* **1998,** 1, (3), 319-29.

108. Omura, S.; Ikeda, H.; Malpartida, F.; Kieser, H. M.; Hopwood, D. A., Production of new hybrid antibiotics, mederrhodins A and B, by a genetically engineered strain. *Antimicrob Agents Chemother* **1986,** 29, (1), 13-9.
109. Madduri, K.; Kennedy, J.; Rivola, G.; Inventi-Solari, A.; Filippini, S.; Zanuso, G.; Colombo, A. L.; Gewain, K. M.; Occi, J. L.; MacNeil, D. J.; Hutchinson, C. R., Production of the antitumor drug epirubicin (4'-epidoxorubicin) and its precursor by a genetically engineered strain of *Streptomyces peucetius. Nat Biotechnol* **1998,** 16, (1), 69-74.
110. Metsa-Ketela, M.; Palmu, K.; Kunnari, T.; Ylihonko, K.; Mantsala, P., Engineering anthracycline biosynthesis toward angucyclines. *Antimicrob Agents Chemother* **2003,** 47, (4), 1291-6.
111. Shen, Y.; Yoon, P.; Yu, T. W.; Floss, H. G.; Hopwood, D.; Moore, B. S., Ectopic expression of the minimal whiE polyketide synthase generates a library of aromatic polyketides of diverse sizes and shapes. *Proc Natl Acad Sci U S A* **1999,** 96, (7), 3622-7.
112. Tang, Y.; Lee, T. S.; Khosla, C., Engineered biosynthesis of regioselectively modified aromatic polyketides using bimodular polyketide synthases. *PLoS Biol* **2004,** 2, (2), E31.
113. Baltz, R. H., Molecular engineering approaches to peptide, polyketide and other antibiotics. *Nat Biotechnol* **2006,** 24, (12), 1533-40.
114. Zhang, W.; Tang, Y., Combinatorial biosynthesis of natural products. *J Med Chem* **2008,** 51, (9), 2629-33.
115. Treibs, W.; Eckardt, K., Über Griseorhodin A, ein neues rotes Antibiotikum aus Actinomyceten. *Die Naturwissenschaften* **1961,** 48, (11), 430.
116. Tresselt, D.; Eckardt, K.; Ihn, W., Antibiotika aus Actinomyceten. Zur chemischen konstitution des antibiotikums griseorhodin A. *Tetrahedron* **1978,** 34, (17), 2693-2699.
117. Eckardt, K.; Tresselt, D.; Schönecker, B., Antibiotika aus Actinomyceten. Zur Stereochemie der Griseorhodine. *Tetrahedron* **1979,** 35, (13), 1621-1624.
118. Yunt, Z.; Reinhardt, K.; Li, A.; Engeser, M.; Dahse, H. M.; Gutschow, M.; Bruhn, T.; Bringmann, G.; Piel, J., Cleavage of four carbon-carbon bonds during biosynthesis of the griseorhodin a spiroketal pharmacophore. *J Am Chem Soc* **2009,** 131, (6), 2297-305.
119. Puder, C.; Loya, S.; Hizi, A.; Zeeck, A., Structural and biosynthetic investigations of the rubromycins. *Eur J Biochem* **2000,** 2000, (5), 729–735.
120. Ueno, T.; Takahashi, H.; Oda, M.; Mizunuma, M.; Yokoyama, A.; Goto, Y.; Mizushina, Y.; Sakaguchi, K.; Hayashi, H., Inhibition of human telomerase by rubromycins: implication of spiroketal system of the compounds as an active moiety. *Biochemistry* **2000,** 39, (20), 5995-6002.
121. Goldman, M. E.; Salituro, G. S.; Bowen, J. A.; Williamson, J. M.; Zink, D. L.; Schleif, W. A.; Emini, E. A., Inhibition of human immunodeficiency virus-1 reverse transcriptase activity by rubromycins: competitive interaction at the template.primer site. *Mol Pharmacol* **1990,** 38, (1), 20-5.

122. Bringmann, G.; Kraus, J.; Schmitt, U.; Puder, C.; Zeeck, A., Determination of the absolute configurations of -rubromycin and related spiro compounds by quantum chemical CD calculations. *Eur J Biochem* **2000,** 2000, (15), 2729–2734.
123. Yunt, Z., Unpublished data. In 2005-2009.
124. Suwa, M.; Sugino, H.; Sasaoka, A.; Mori, E.; Fujii, S.; Shinkawa, H.; Nimi, O.; Kinashi, H., Identification of two polyketide synthase gene clusters on the linear plasmid pSLA2-L in *Streptomyces rochei*. *Gene* **2000,** 246, (1-2), 123-31.
125. Trefzer, A.; Pelzer, S.; Schimana, J.; Stockert, S.; Bihlmaier, C.; Fiedler, H. P.; Welzel, K.; Vente, A.; Bechthold, A., Biosynthetic gene cluster of simocyclinone, a natural multihybrid antibiotic. *Antimicrob Agents Chemother* **2002,** 46, (5), 1174-82.
126. Sambrook, J.; Russel, D. W., *Molecular Cloning: a Laboratory Manual*. New York, 2001.
127. Salas, J. A., Personal communication. In 2008.
128. Fritzsche, K.; Ishida, K.; Hertweck, C., Orchestration of discoid polyketide cyclization in the resistomycin pathway. *J Am Chem Soc* **2008,** 130, (26), 8307-16.
129. Bao, W.; Wendt-Pienkowski, E.; Hutchinson, C. R., Reconstitution of the iterative type II polyketide synthase for tetracenomycin F2 biosynthesis. *Biochemistry* **1998,** 37, (22), 8132-8.
130. Zhan, J.; Watanabe, K.; Tang, Y., Synergistic actions of a monooxygenase and cyclases in aromatic polyketide biosynthesis. *Chembiochem* **2008,** 9, (11), 1710-5.
131. Gust, B.; Challis, G. L.; Fowler, K.; Kieser, T.; Chater, K. F., PCR-targeted *Streptomyces* gene replacement identifies a protein domain needed for biosynthesis of the sesquiterpene soil odor geosmin. *Proc Natl Acad Sci U S A* **2003,** 100, (4), 1541-6.
132. Ostash, B.; Rebets, Y.; Yuskevich, V.; Luzhetskyy, A.; Tkachenko, V.; Fedorenko, V., Targeted disruption of *Streptomyces globisporus* lndF and lndL cyclase genes involved in landomycin E biosynthesis. *Folia Microbiol.* **2003,** 48, (4), 484-488.
133. Sandmann, A.; Dickschat, J.; Jenke-Kodama, H.; Kunze, B.; Dittmann, E.; Muller, R., A Type II polyketide synthase from the gram-negative Bacterium *Stigmatella aurantiaca* is involved in Aurachin alkaloid biosynthesis. *Angew Chem Int Ed Engl* **2007,** 46, (15), 2712-6.
134. Lopez, P.; Hornung, A.; Welzel, K.; Unsin, C.; Wohlleben, W.; Weber, T.; Pelzer, S., Isolation of the lysolipin gene cluster of *Streptomyces tendae* Tu 4042. *Gene* **2010,** 461, (1-2), 5-14.
135. Matsuda, Y.; Kase, H., KS-619-1, a new inhibitor of Ca2+ and calmodulin-dependent cyclic nucleotide phosphodiesterase. *J Antibiot (Tokyo)* **1987,** 40, (8), 1104-1110.
136. Chen, Y.; Wendt-Pienkoski, E.; Rajski, S. R.; Shen, B., In vivo investigation of the roles of FdmM and FdmM1 in fredericamycin biosynthesis unveiling a new family of oxygenases. *J Biol Chem* **2009,** 284, (37), 24735-43.
137. Yasuzawa, T.; Yoshida, M.; Shirahata, K.; Sano, H., Structure of a novel Ca2+ and calmodulin-dependent cyclic nucleotide

phosphodiesteratse inhibitor KS-619-1. *J Antibiot (Tokyo)* **1987,** 40, (8), 1111-1114.
138. Kim, B. C.; Lee, J. M.; Ahn, J. S.; Kim, B. S., Cloning, sequencing, and characterization of the pradimicin biosynthetic gene cluster of *Actinomadura hibisca* P157-2. *J Microbiol Biotechnol* **2007,** 17, (5), 830-9.
139. Wendt-Pienkowski, E.; Huang, Y.; Zhang, J.; Li, B.; Jiang, H.; Kwon, H.; Hutchinson, C. R.; Shen, B., Cloning, sequencing, analysis, and heterologous expression of the fredericamycin biosynthetic gene cluster from *Streptomyces griseus*. *J Am Chem Soc* **2005,** 127, (47), 16442-52.
140. Gronquist, M.; Meinwald, J.; Eisner, T.; Schroeder, F. C. J., Exploring uncharted terrain in nature´s structure space suing capillary NMR spectroscopy. *J Am Chem Soc* **2005,** 10, (127), 10810-1.
141. Olson, D. L.; Norcross, J. A.; O'Neil-Johnson, M.; Molitor, P. F.; Detlefsen, D. J.; Wilson, A. G.; Peck, T. L., Microflow NMR: concepts and capabilities. *Anal Chem* **2004,** 76, (10), 2966-74.
142. Munro, M. H. G., Personal communication. In 2010.
143. Bailey, N. J.; Marshall, I. R., Development of ultrahigh-throughput NMR spectroscopic analysis utilizing capillary flow NMR technology. *Anal Chem* **2005,** 77, (13), 3947-53.
144. Wu, N.; Peck, T. L.; Webb, A. G.; Magin, R. L.; Sweedler, J. V., Nanoliter volume sample cells for 1H NMR: Application to Online Detection in Capillary Electrophoresis. *J Am Chem Soc* **1994,** 116, (17), 7929-7930.
145. Wu, N.; Peck, T. L.; Webb, A. G.; Magin, R. L.; Sweedler, J. V., 1H-NMR Spectroscopy on the Nanoliter Scale for Static and Online Measurements. *Anal Chem* **1994,** 66, (22), 3849-3857.
146. Behnke, B.; Schlotterbeck, G.; Tallarek, U.; Strohschein, S.; Tseng, L.-H.; Keller, T.; Albert, K.; Bayer, E., Capillary HPLC-NMR Copuling: High-Resolution 1H NMR Sprectroscopy in the Nanoliter Scale. *Anal Chem* **1996,** 68, (7), 1110-1115.
147. Molinski, T., Personal communication. **2010**.
148. Moore, J. A.; Reed, D. E., Diazomethane. *Org Synth Coll* **1973,** 5,(351).
149. Jacobsen, N. E., *NMR Spectroscopy Explained: Simplified Theory, Applications and Examples for Organic Chemistry and Structural Biology*. John Wiley and Sons, Inc., Publication: New Jersey, 2007.
150. Martin, G. E., *Modern Magnetic Resonance*. Springer Netherlands: Dordrecht, 2006.
151. Schenk, A.; Xu, Z.; Pfeiffer, C.; Steinbeck, C.; Hertweck, C., Geminal bismethylation prevents polyketide oxidation and dimerization in the benastatin pathway. *Angew Chem Int Ed Engl* **2007,** 46, (37), 7035-8.
152. Mai, L. P.; Gueritte, F.; Dumontet, V.; Tri, M. V.; Hill, B.; Thoison, O.; Guenard, D.; Sevenet, T., Cytotoxicity of Rhamnosylanthraquinones and Rhamnosylanthrones from *Rhamnus nepalensis*. *J Nat Prod* **2001,** 64, (9), 1162-8.

153. Cameron, D.; Edmonds, J.; Raverty, W., Oxidation of emodin anthrone and stereochemistry of emodin bianthrone. *Aust. J. Chem* **1976,** 29, (7), 1535-1548.
154. Bais, H. P.; Vepachedu, R.; Lawrence, C. B.; Stermitz, F. R.; Vivanco, J. M., Molecular and biochemical characterization of an enzyme responsible for the formation of hypericin in St. John's wort (*Hypericum perforatum* L.). *J Biol Chem* **2003,** 278, (34), 32413-22.
155. Deltito, J.; Beyer, D., The scientific, quasi-scientific and popular literature on the use of St. John's Wort in the treatment of depression. *J Affect Disord* **1998,** 51, (3), 345-51.
156. Yamaguchi, M.; Hasebe, K.; Uchida, M.; Higashi, H.; Minami, T., An oxidative dimerization of anthrones by oxygen-metal acetate system. *Bull. Chem. Soc. Jpn.* **1989,** 62, (8), 2745-2747.
157. Martinmaa, J.; Vanhala, L.; Mustakallio, K. K., Free radical intermediates produced by autoxidation of 1,8-dihydroxy-9-anthrone (dithranol) in pyridine. *Experientia* **1978,** 34, (7), 872-3.
158. Falk, H.; Schoppel, G., On the synthesis of hypericin by oxidative trimethylemodin anthrone and emodin anthrone dimerization:isohypericin. *Monatsh. Chem.* **1992,** 123, (10), 931-938.
159. Müller, M., Chemical diversity through biotransformations. *Curr Opin Biotechnol* **2004,** 15, (10), 591-598.
160. Zhao, B.; Guengerich, F. P.; Bellamine, A.; Lamb, D. C.; Izumikawa, M.; Lei, L.; Podust, L. M.; Sundaramoorthy, M.; Kalaitzis, J. A.; Reddy, L. M.; Kelly, S. L.; Moore, B. S.; Stec, D.; Voehler, M.; Falck, J. R.; Shimada, T.; Waterman, M. R., Binding of two flaviolin substrate molecules, oxidative coupling, and crystal structure of *Streptomyces coelicolor* A3(2) cytochrome P450 158A2. *J Biol Chem* **2005,** 280, (12), 11599-607.
161. Chen, Y.; Wendt-Pienkowski, E.; Ju, J.; Lin, S.; Rajski, S. R.; Shen, B., Characterization of FdmV as an amide synthetase for fredericamycin A biosynthesis in *Streptomyces griseus* ATCC 43944. *J Biol Chem* **2010,** 285, (50), 38853-60.
162. Datsenko, K. A.; Wanner, B. L., One-step inactivation of chromosomal genes in *Escherichia coli* K-12 using PCR products. *Proc Natl Acad Sci U S A* **2000,** 97, (12), 6640-5.
163. MacNeil, D. J.; Gewain, K. M.; Ruby, C. L.; Dezeny, G.; Gibbons, P. H.; MacNeil, T., Analysis of *Streptomyces avermitilis* genes required for avermectin biosynthesis utilizing a novel integration vector. *Gene* **1992,** 111, (1), 61-8.
164. Paget, M. S.; Chamberlin, L.; Atrih, A.; Foster, S. J.; Buttner, M. J., Evidence that the extracytoplasmic function sigma factor sigmaE is required for normal cell wall structure in *Streptomyces coelicolor* A3(2). *J Bacteriol* **1999,** 181, (1), 204-11.
165. Fernandez, E.; Lombo, F.; Mendez, C.; Salas, J. A., An ABC transporter is essential for resistance to the antitumor agent mithramycin in the producer *Streptomyces argillaceus*. *Mol Gen Genet* **1996,** 251, (6), 692-8.
166. Hanahan, D., Studies on transformation of *Escherichia coli* with plasmids. *J Mol Biol* **1983,** 166, (4), 557-80.

167. He, J. PhD thesis Molecular Analysis of the Aureothin Biosynthesis Gene Cluster from *Streptomyces thioluteus* HKI-227; New Insights into Polyketide Assembly. Friedrich-Schiller-University Jena, Jena, 2004.
168. Kieser, T.; Bibb, M. J.; Buttner, M. J.; Chater, K. F.; Hopwood, D. A., *Practical Streptomyces Genetics*. The John Innes Foundation: Norwich, 2000.
169. Hobbs, G.; Frazer, C. M.; Gardner, D. C. J.; Cullum, J. A.; Oliver, S., Dispersed growth of *Streptomyces* in liquid culture. *Appl Environ Microbiol* **1989,** 31, (3), 272-277.
170. Thompson, C. J.; Ward, J. M.; Hopwood, D. A., DNA cloning in *Streptomyces*: resistance genes from antibiotic-producing species. *Nature* **1980,** 286, (5772), 525-7.
171. Flett, F.; Mersinias, V.; Smith, C. P., High efficiency intergeneric conjugal transfer of plasmid DNA from *Escherichia coli* to methyl DNA-restricting *Streptomycetes*. *FEMS Microbiol Lett* **1997,** 155, (2), 223-9.

8 Appendix

8.1 Vector maps

The following cosmid and vectors were used in the present study.

8.1.1 pMP31

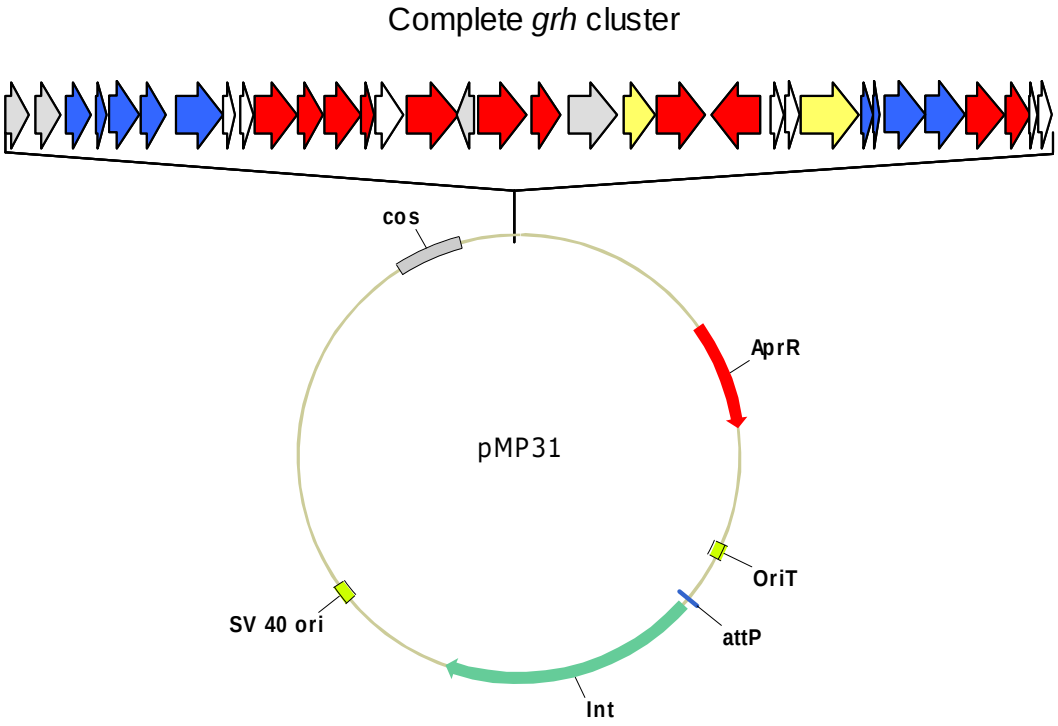

Fig. 62: Vector map of the cosmid pMP31.

The expression cosmid pMP31 containing the complete *grh* biosynthetic gene cluster (46.7kb). The cosmid enables the conjugation of the *grh* cluster into the expression host *S. albus* by intergrating into its genome.

8.1.2 pIJ790

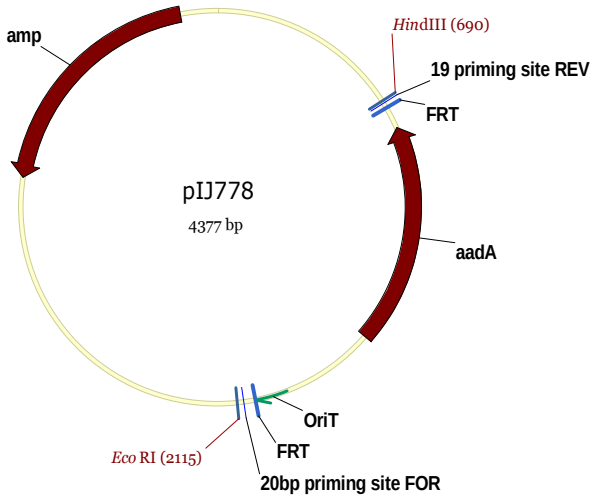

Fig. 63: Vector map of pIJ778.

The plasmid pIJ778 containing a streptomycin resistance cassette *aadA*. This plasmid was used as DNA template for the amplification of the resistance cassette.

8.1.3 pKJ55

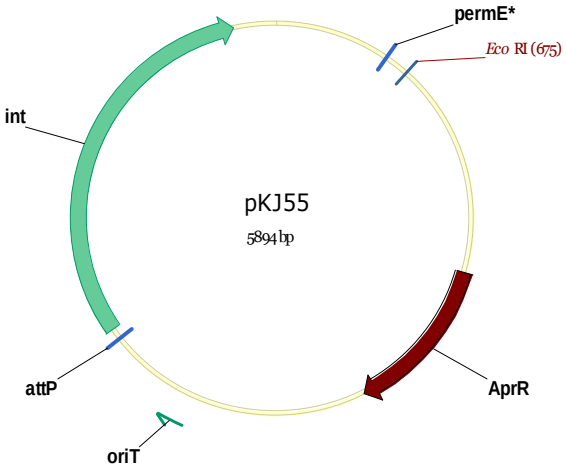

Fig. 64: Vector map of pKJ55.

The plasmid pKJ55 is an *E. coli – Streptomyces* shuttle vector. This vector enables conjugation into the expression host *S. albus* by integrating into its genome.

8.2 NMR spectra

8.2.1 13,13´-fused bis-tridecaketide dimer **78**

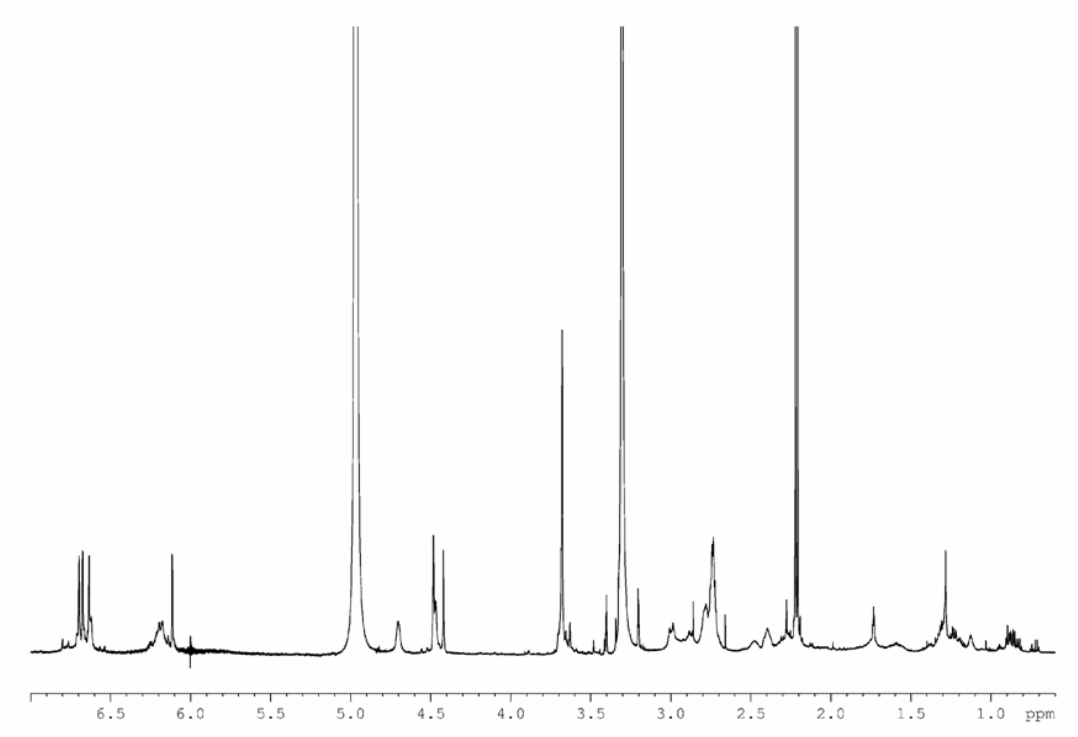

Fig. 65: ^{1}H NMR spectra of 13,13´-fused bis-tridecaketide dimer 78.

The acquisition was performed in CD_3OD at 700 MHz.

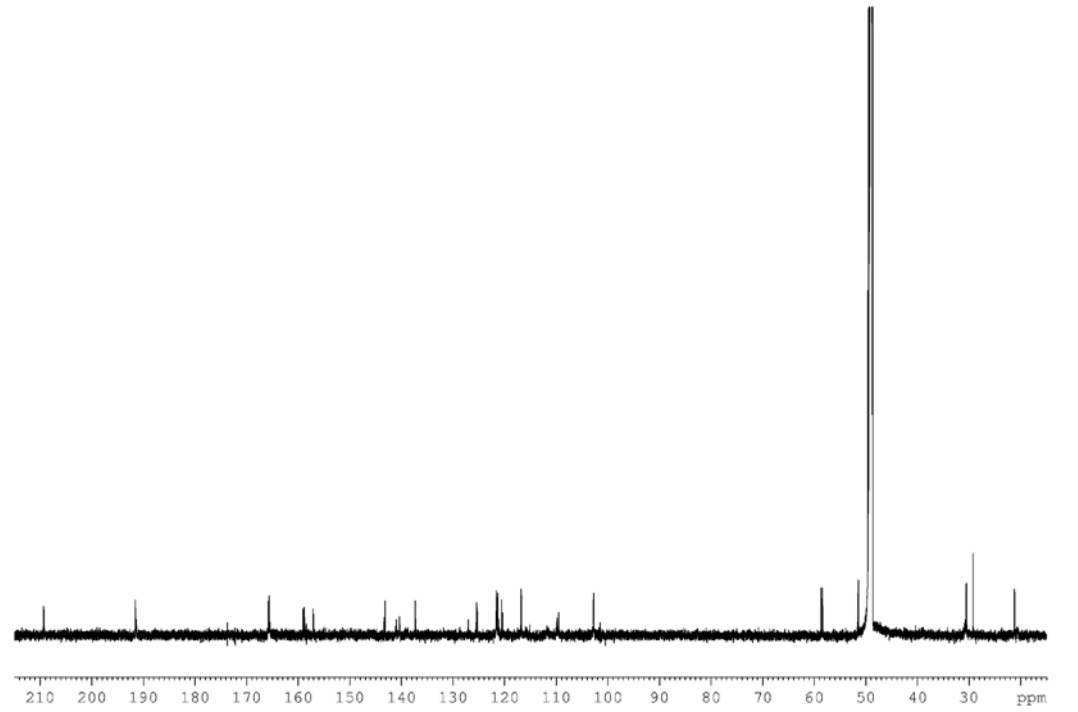

Fig. 66: ^{13}C-NMR spectra of 13,13´-fused bis-tridecaketide dimer 78.

The acquisition was performed in CD_3OD at 700 MHz.

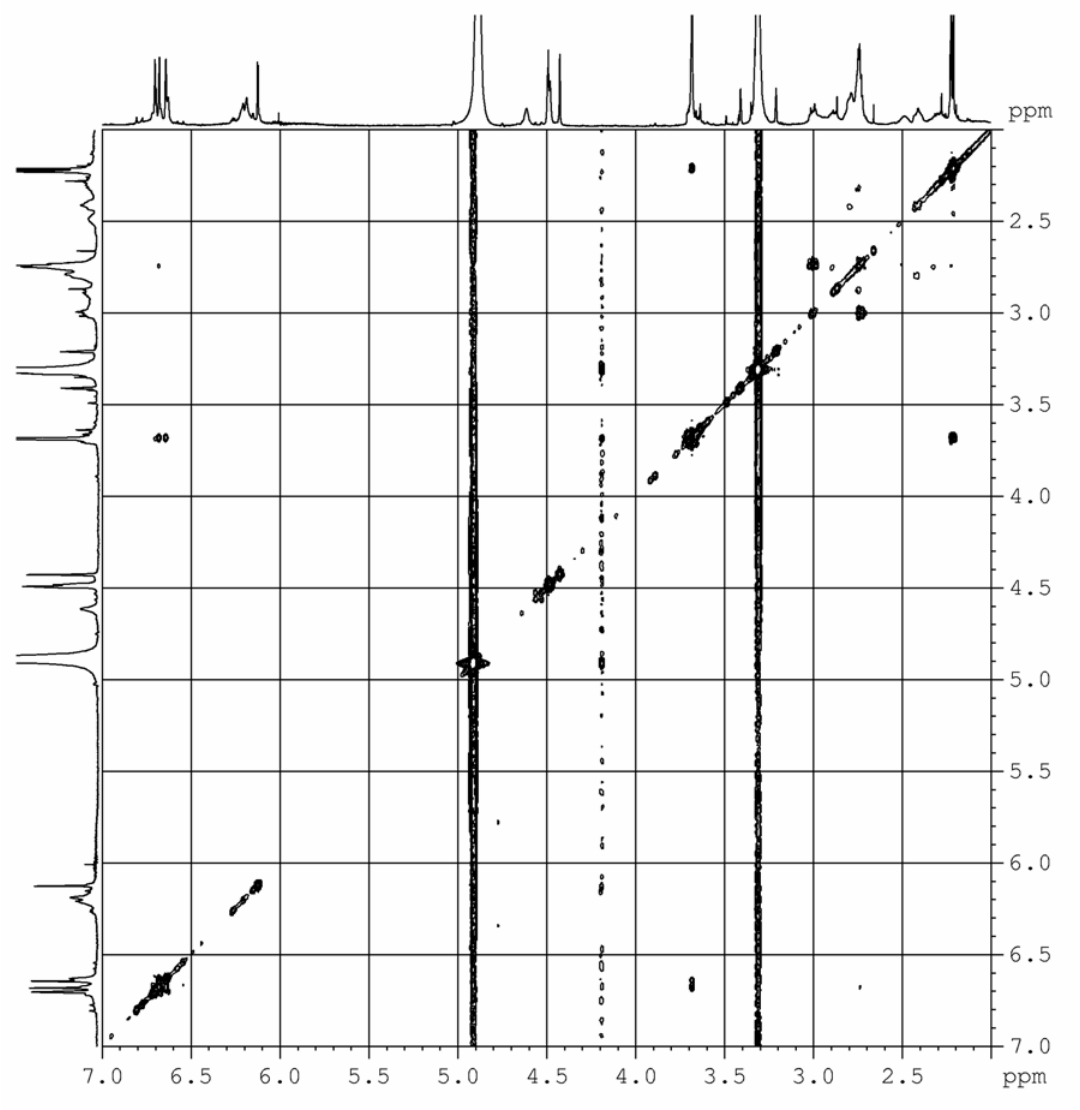

Fig. 67: ^{1}H-^{1}H-COSY NMR spectra of 13,13´-fused bis-tridecaketide 78.

The acquisition was performed in CD_3OD at 700 MHz.

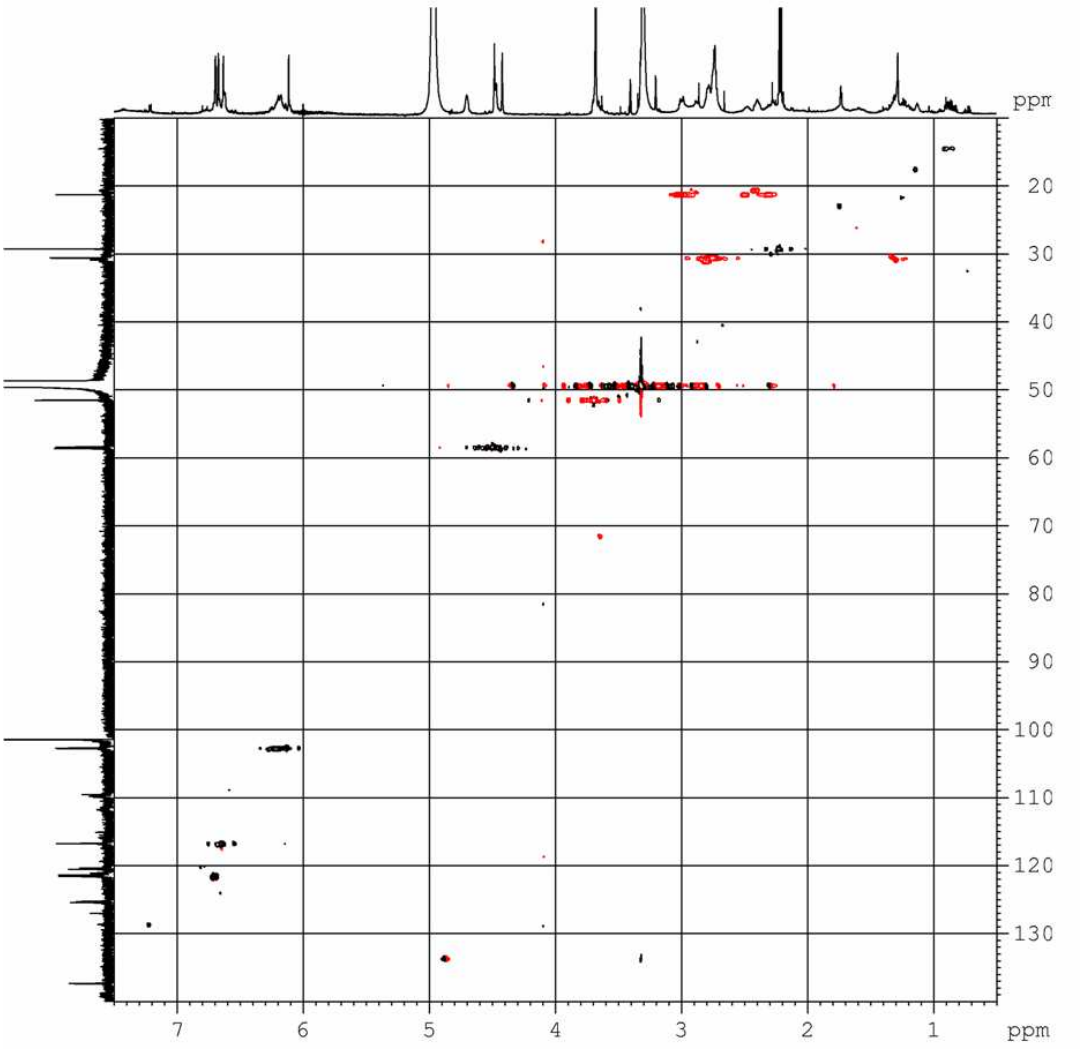

Fig. 68: HSQC-NMR spectra of 13,13´-fused bis-tridecaketide 78.

The acquisition was performed in CD_3OD at 700 MHz.

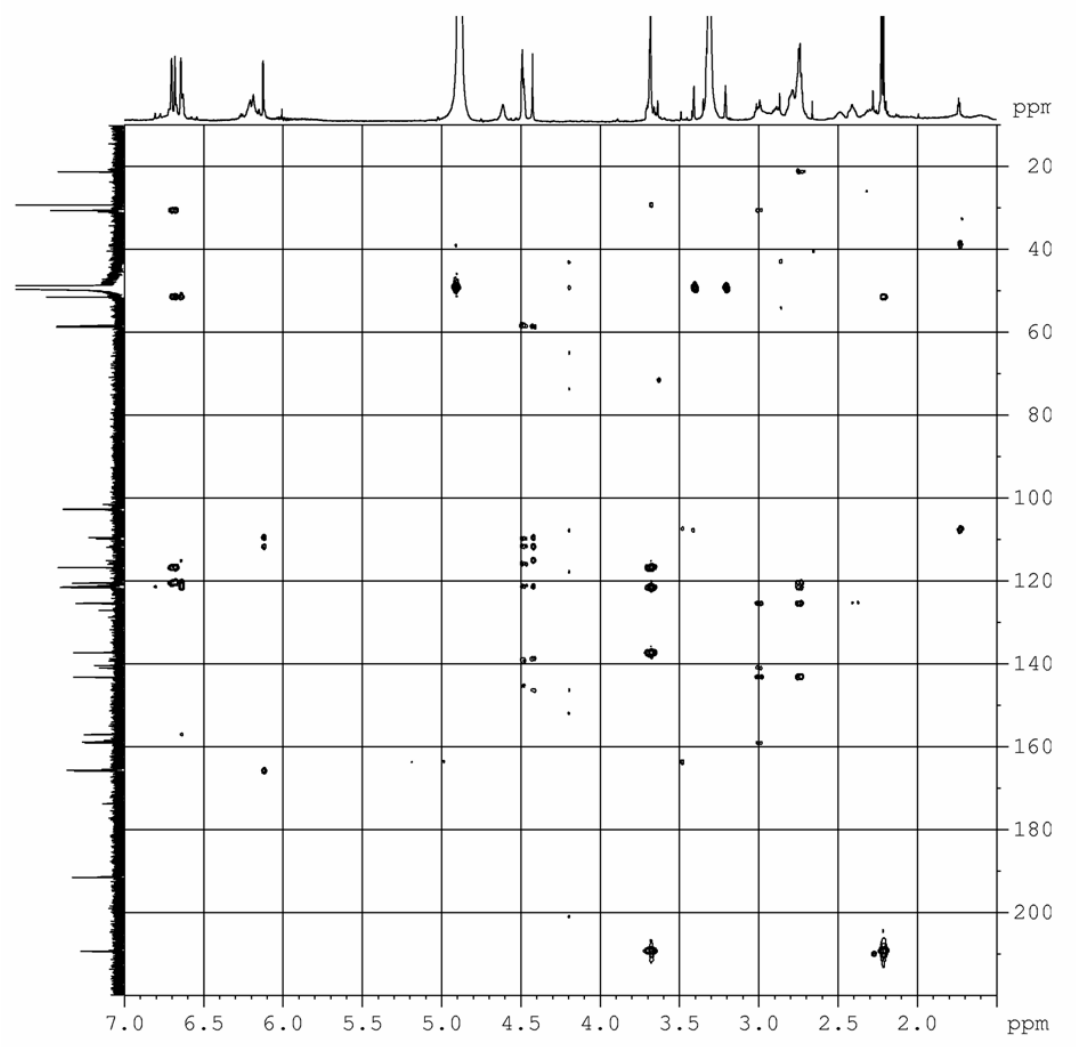

Fig. 69: HMBC-NMR spectra of 13,13´-fused bis-tridecaketide dimer 78.

The acquisition was performed in CD_3OD at 700 MHz.

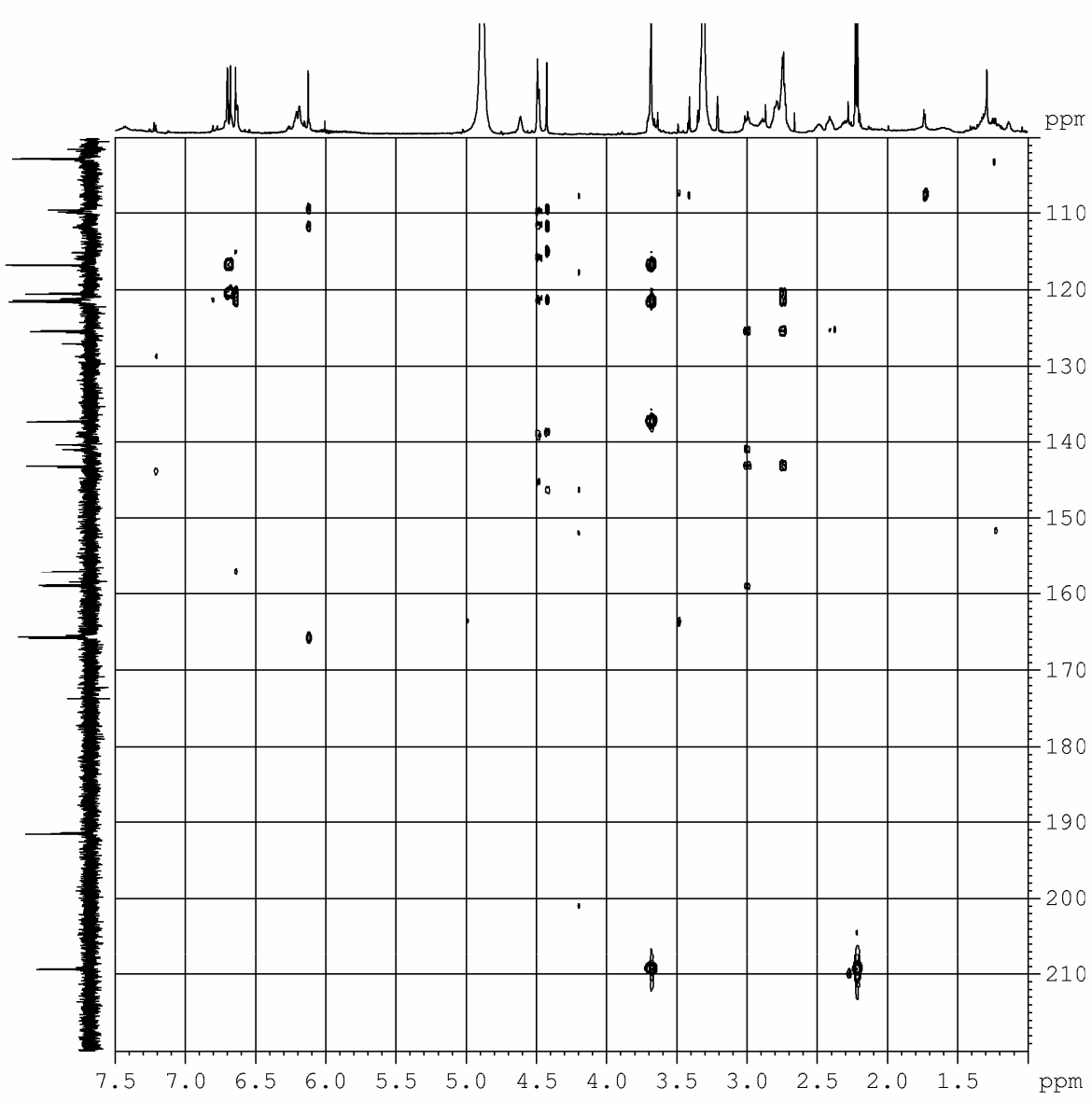

Fig. 70: HMBC-NMR spectra of 13,13´-fused bis-tridecaketide dimer 78.

The acquisition was performed in CD_3OD at 700 MHz.

8.2.2 HP1

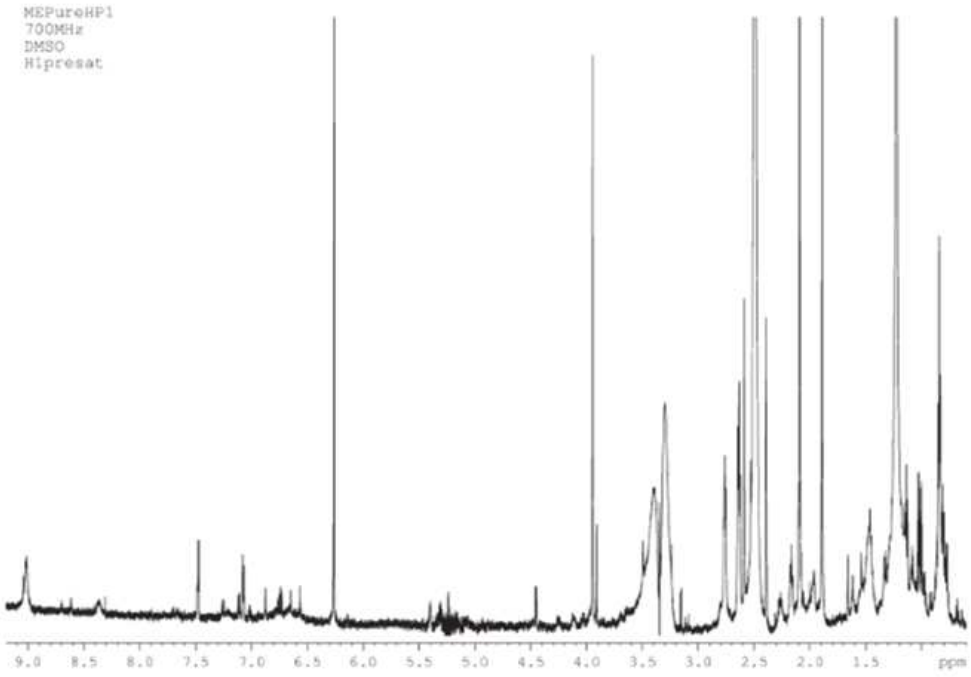

Fig. 71: 1H NMR spectra of HP1.

The acquisition was performed in DMSO-*d6* at 700 MHz.

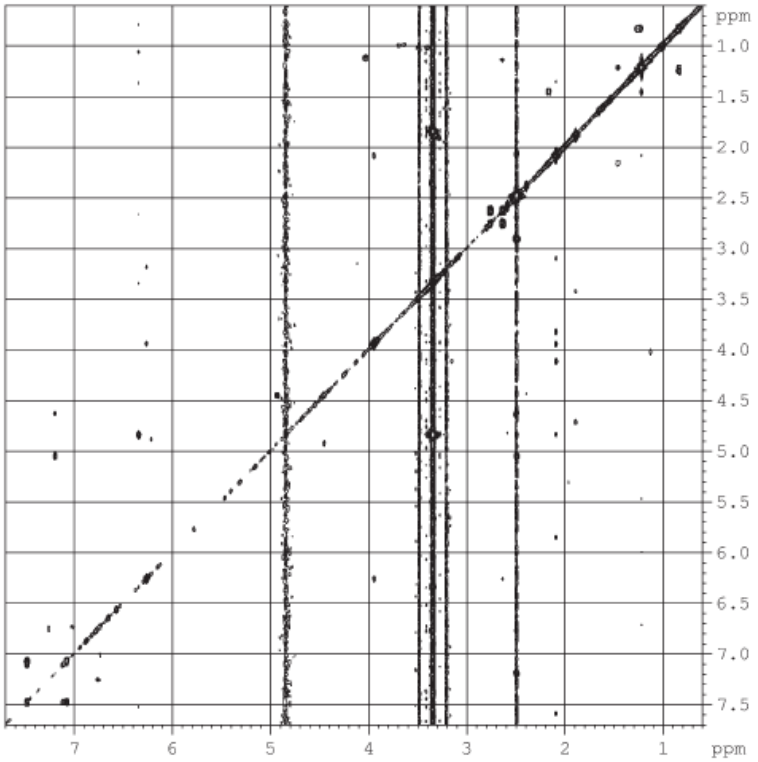

Fig. 72: 1H-1H COSY spectra of HP1.

The acquisition was performed in DMSO-*d6* at 700 MHz.

8.3 UV spectra

8.3.1 *ΔgrhV* mutant

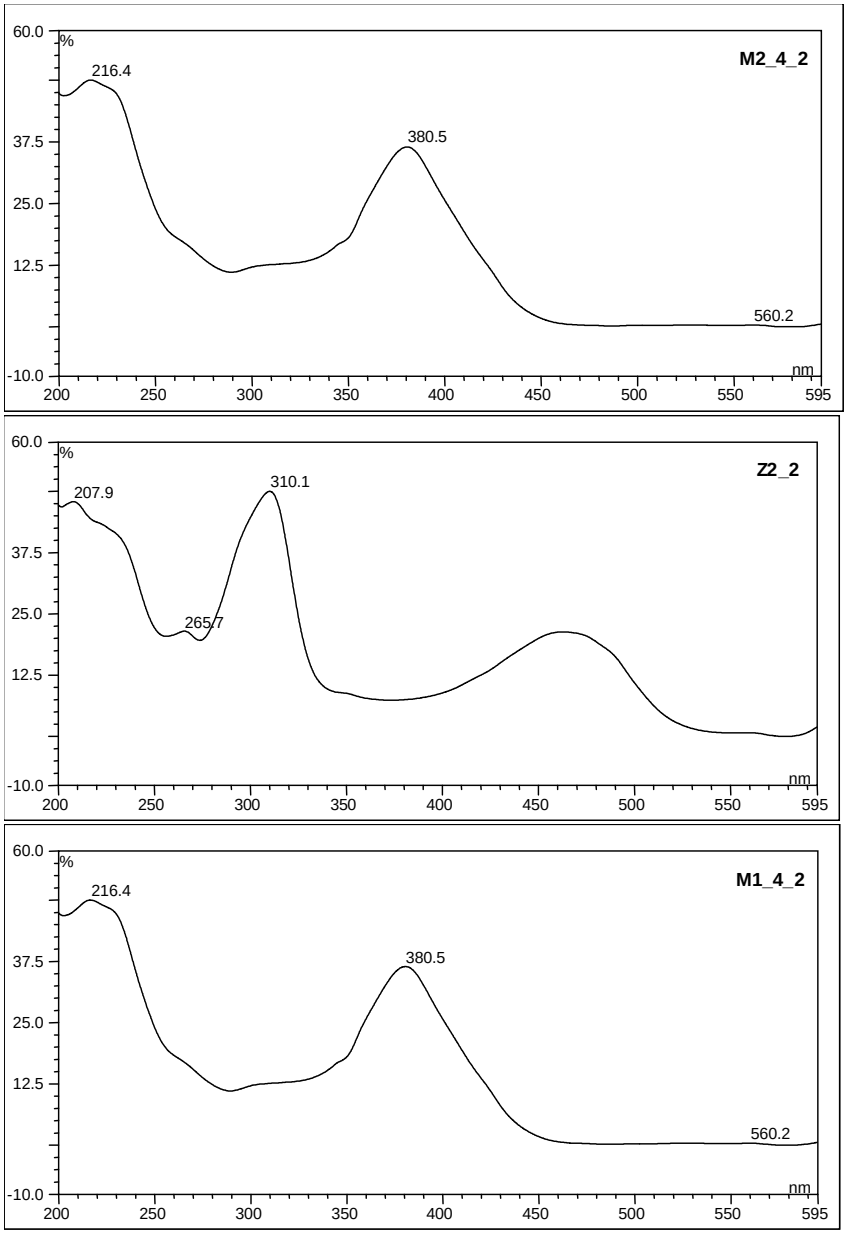

Fig. 73: UV spectra of the compounds from the *ΔgrhV* mutant.

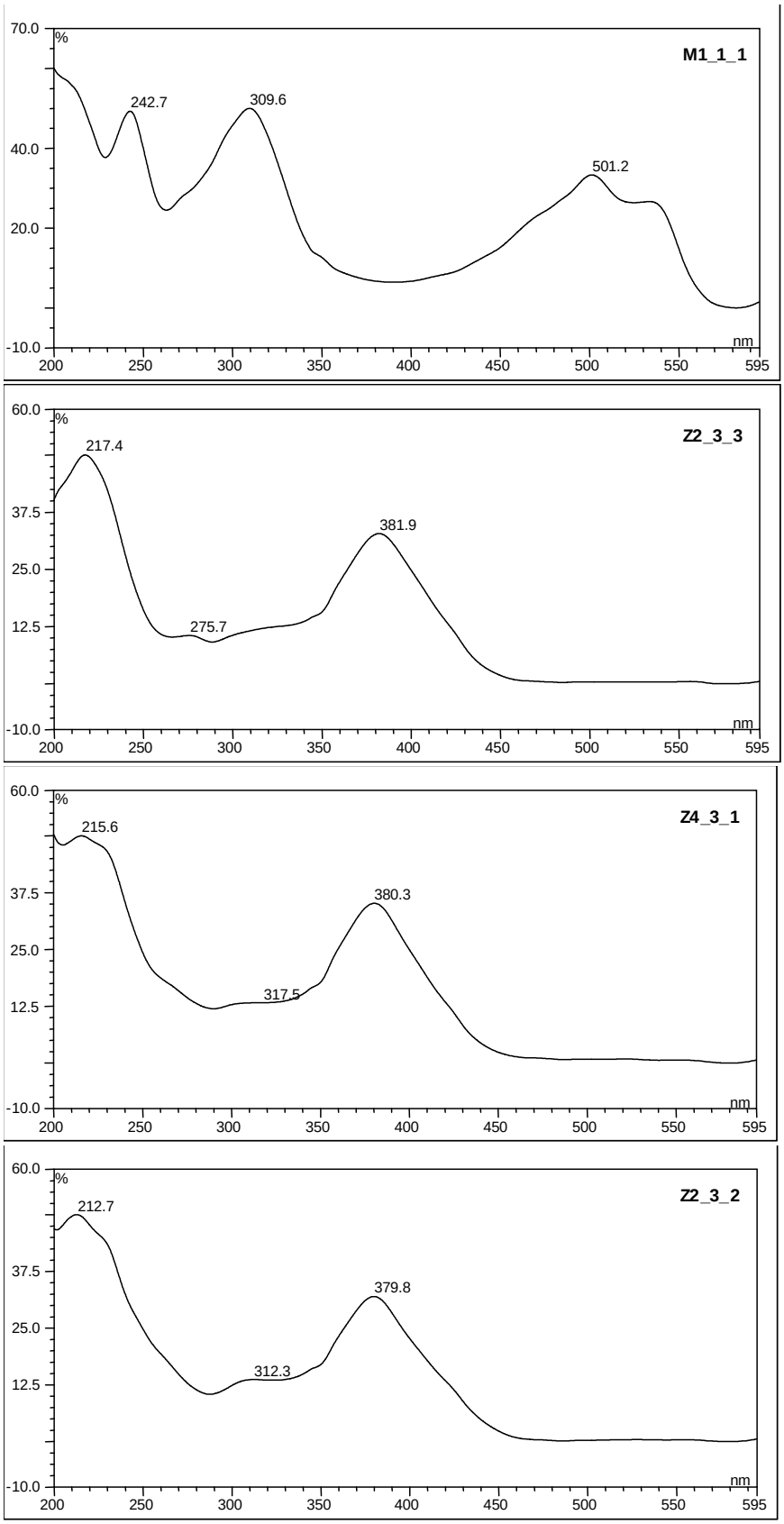

Fig 73 continued: UV spectra of the compounds from the *ΔgrhV* mutant.

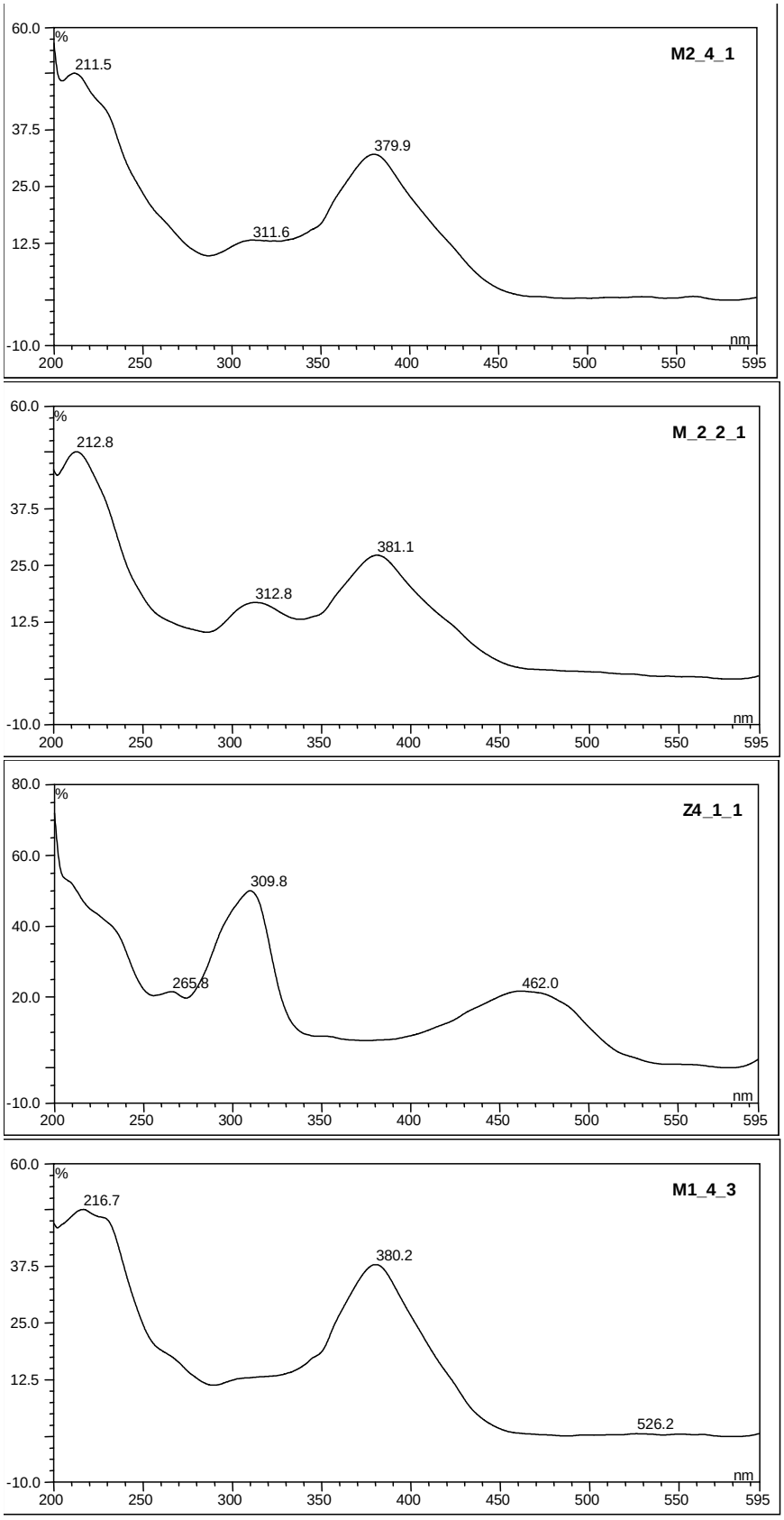

Fig 73 continued: UV spectra of the compounds from the *ΔgrhV* mutant.

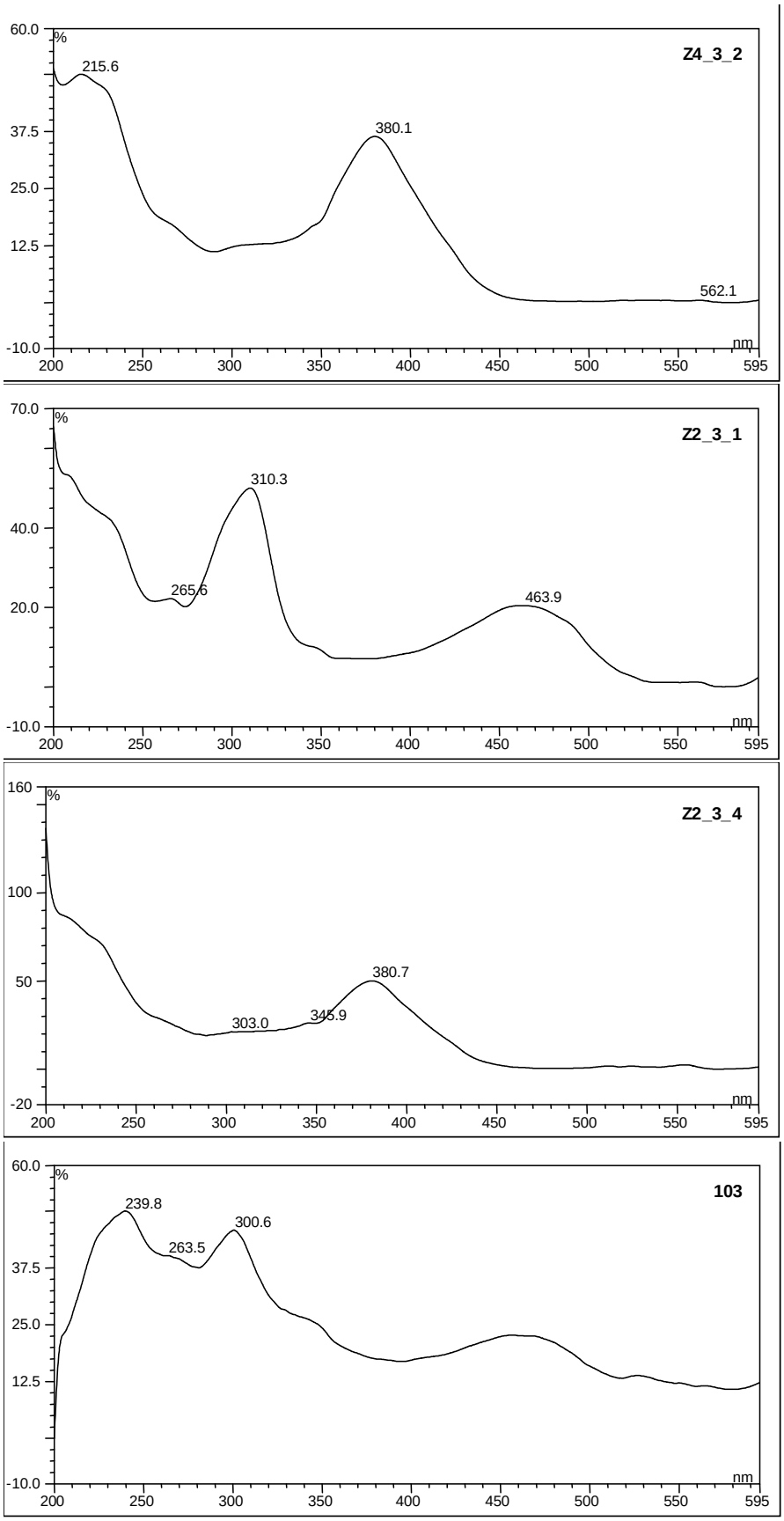

Fig 73 continued: UV spectra of the compounds from the *ΔgrhV* mutant.

8.3.2 *ΔgrhU* mutant

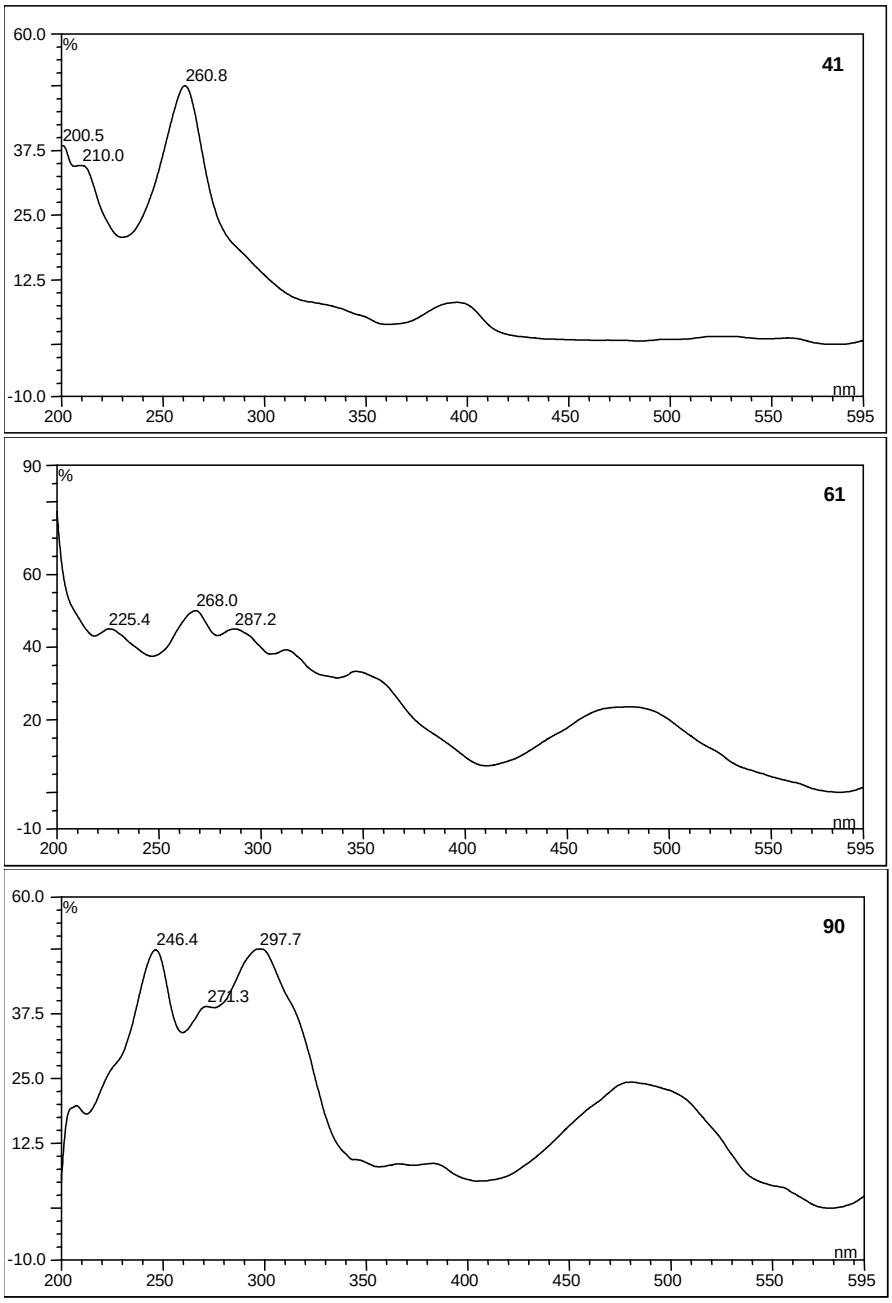

Fig. 74: UV spectra of the compounds from the *ΔgrhU* mutant.

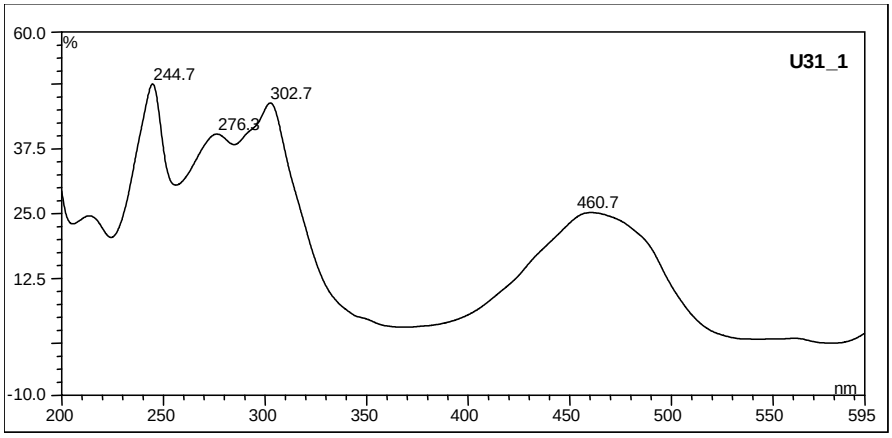

Fig 74 continued: UV spectra of the compounds from the *ΔgrhU* mutant.

8.3.3 *ΔgrhH-P* mutant

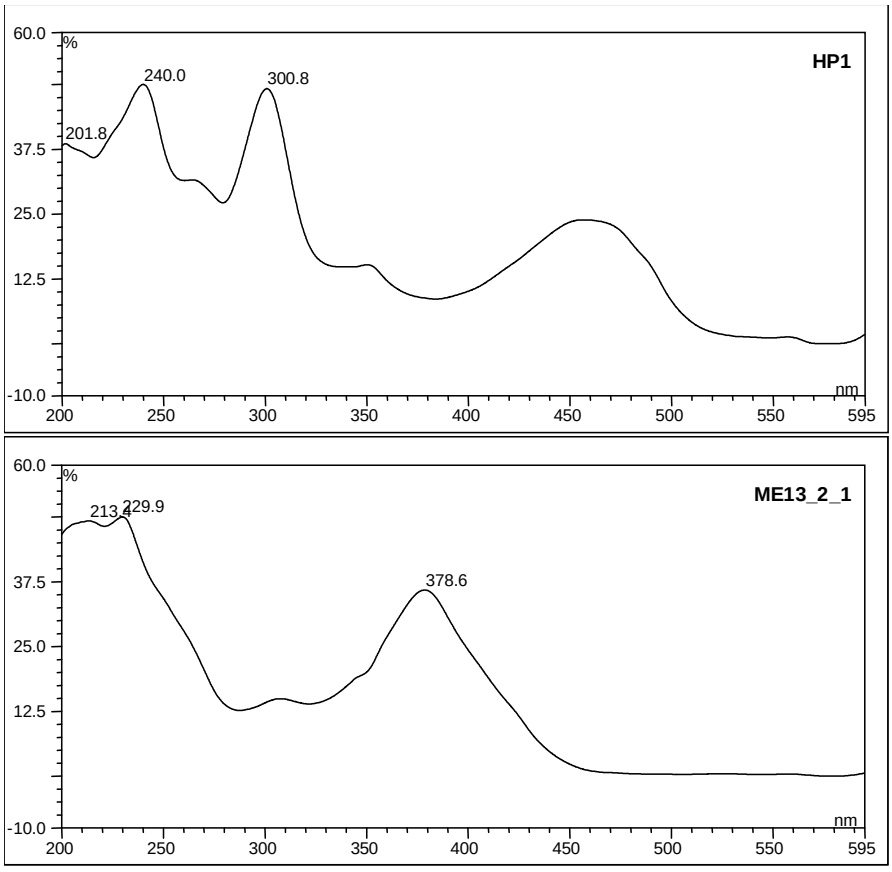

Fig. 75: UV spectra of the compounds from the *ΔgrhH-P* mutant.

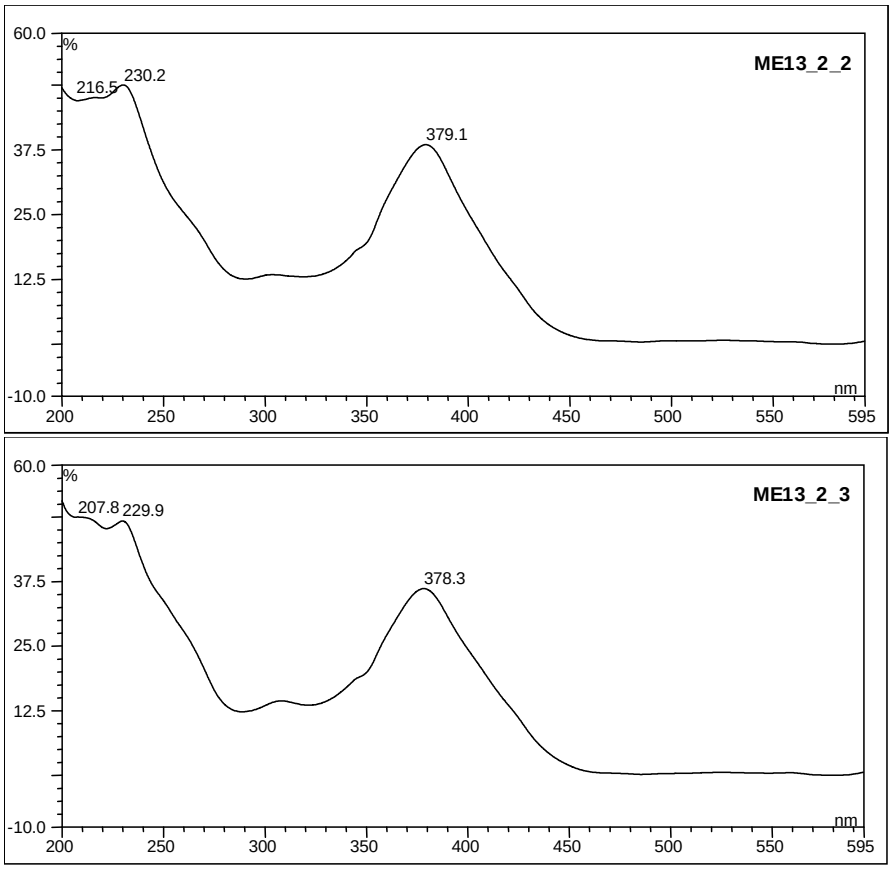

Fig 75 continued: UV spectra of the compounds from the *ΔgrhH-P* mutant.

8.4 Mass spectra

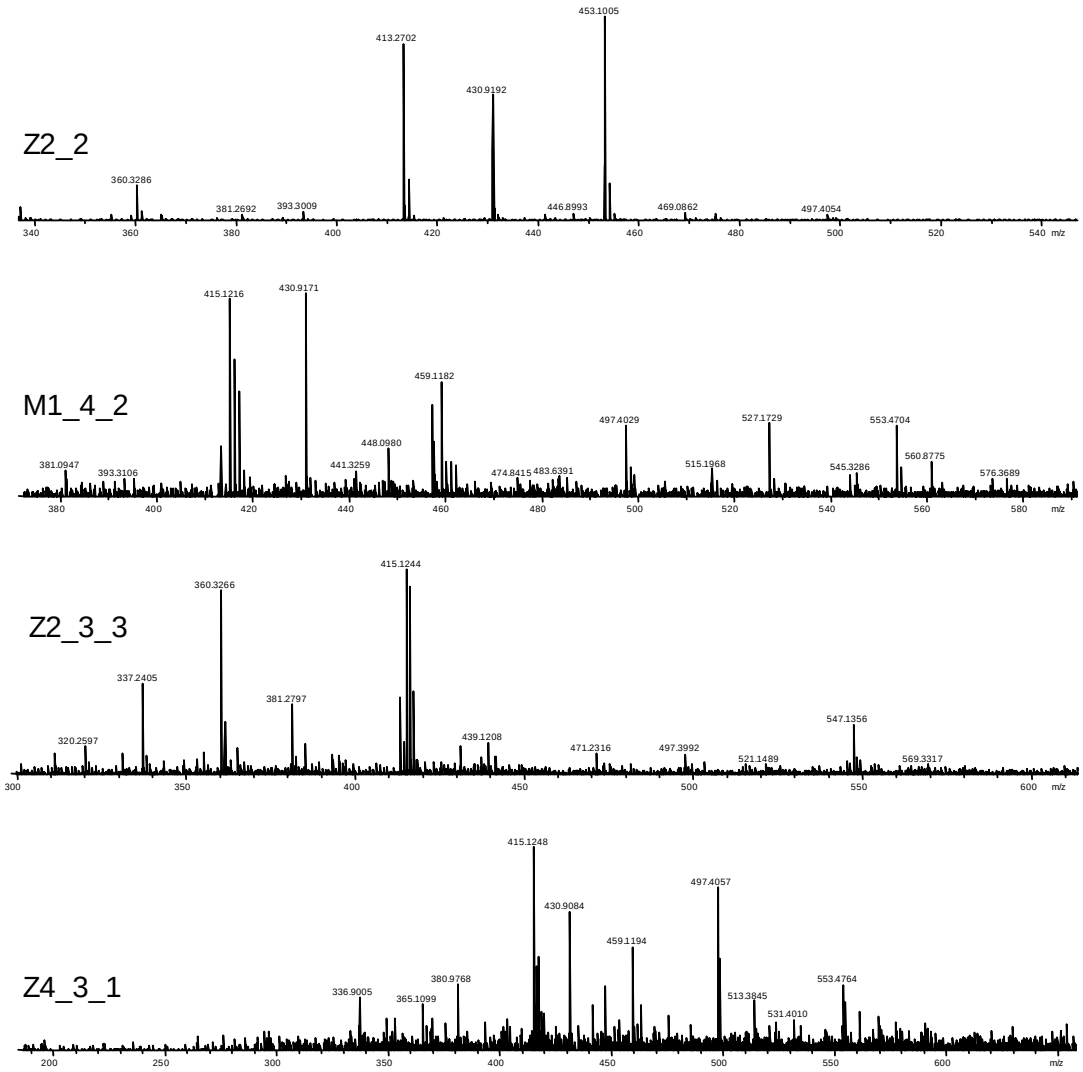

Fig. 76: HRESIMS of the compounds from the Δ*grhV* mutant.

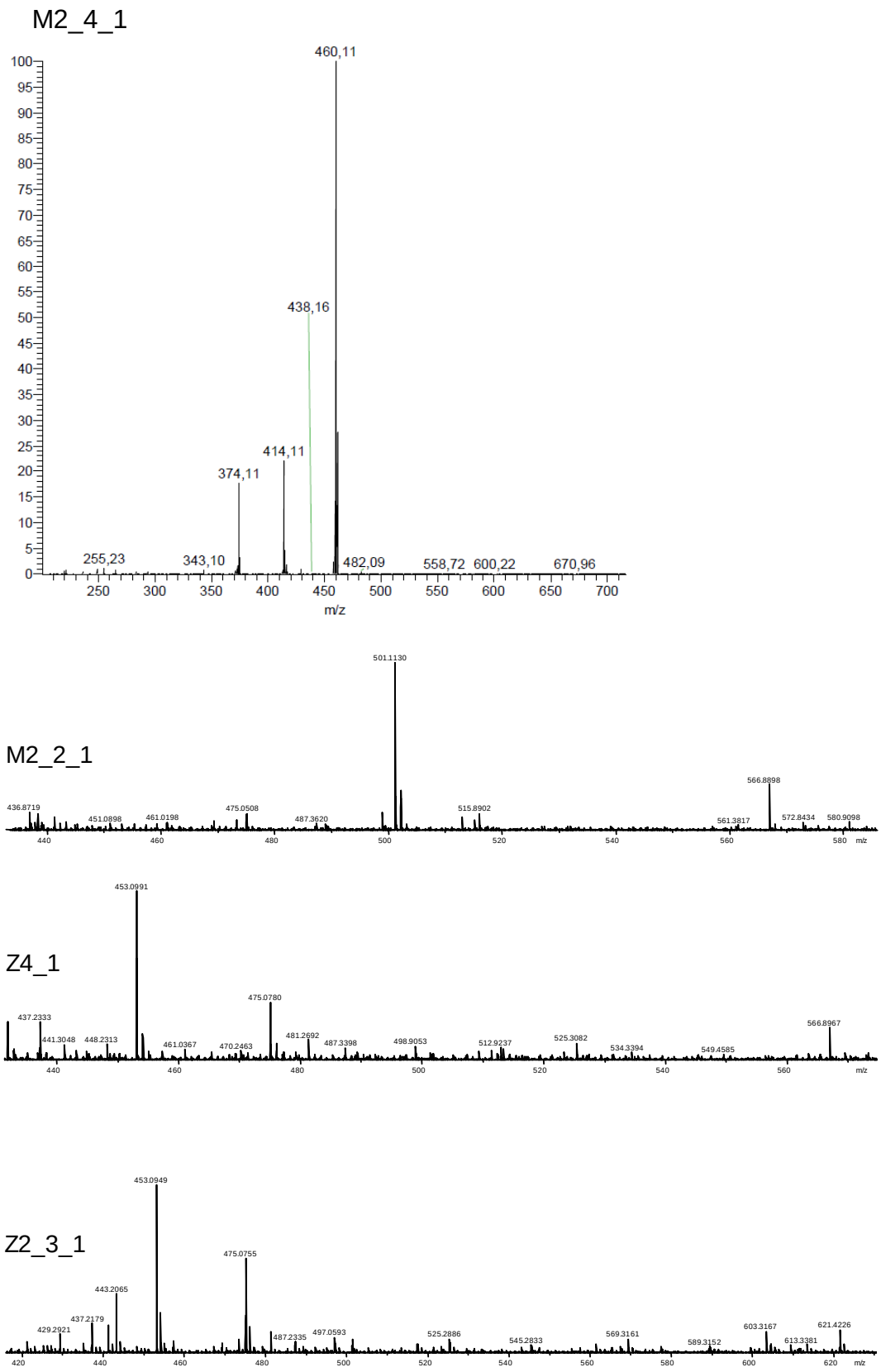

Fig. 76 continued: HRESIMS of the compounds from the Δ*grhV* mutant.

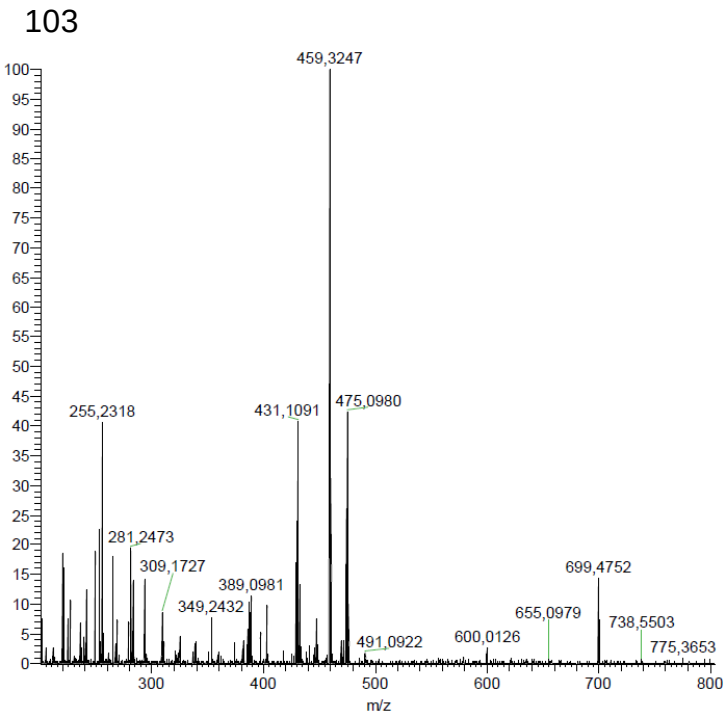

Fig. 76 continued: HRESIMS of the compounds from Δ*grhV* mutant.

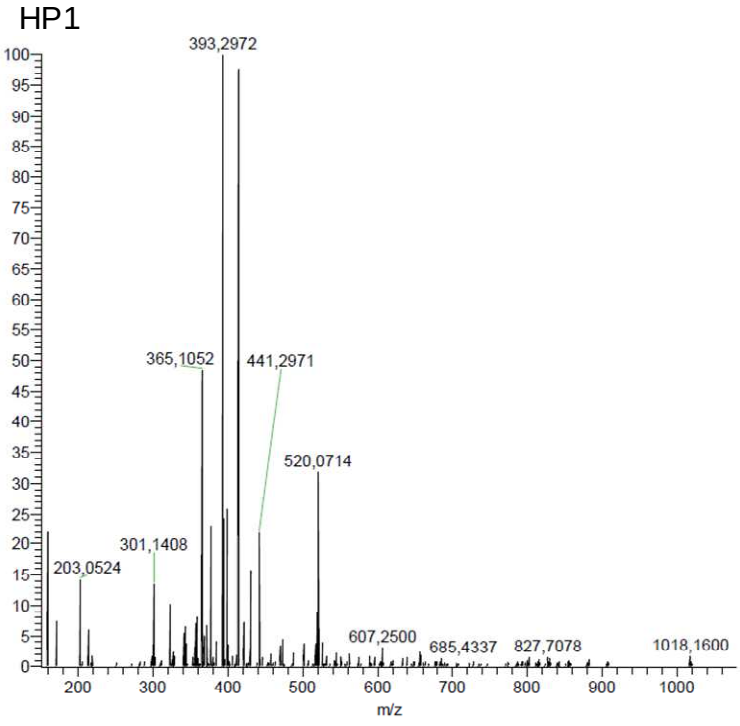

Fig. 77: HRESIMS of the compounds from the Δ*grhH-P* mutant.

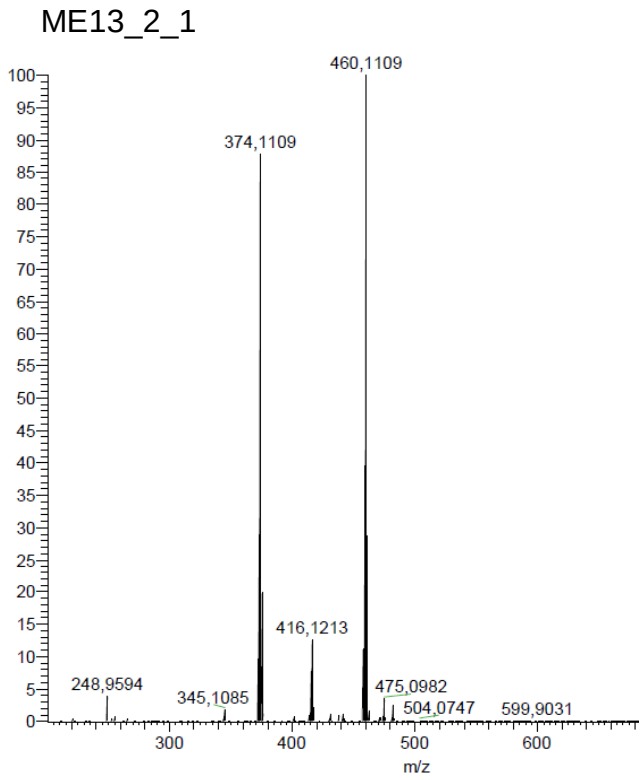

Fig 77 continued: HRESIMS of the compounds from the Δ*grhH-P* mutant.

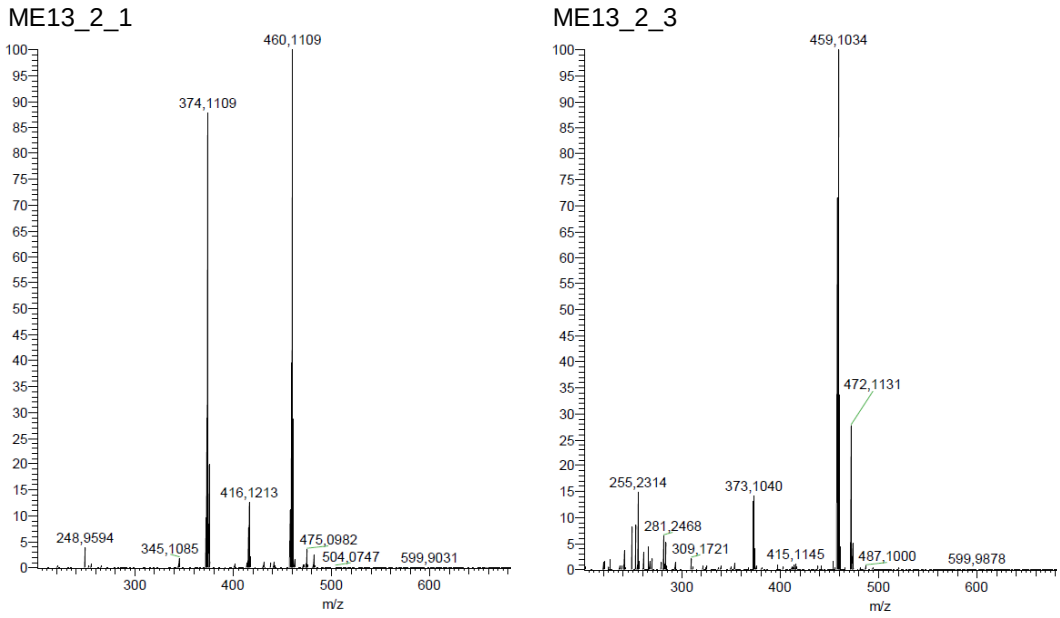

Fig 77 continued: HRESIMS of the compounds from the Δ*grH-P*mutant.

8.4.1 *ΔgrhE* mutant

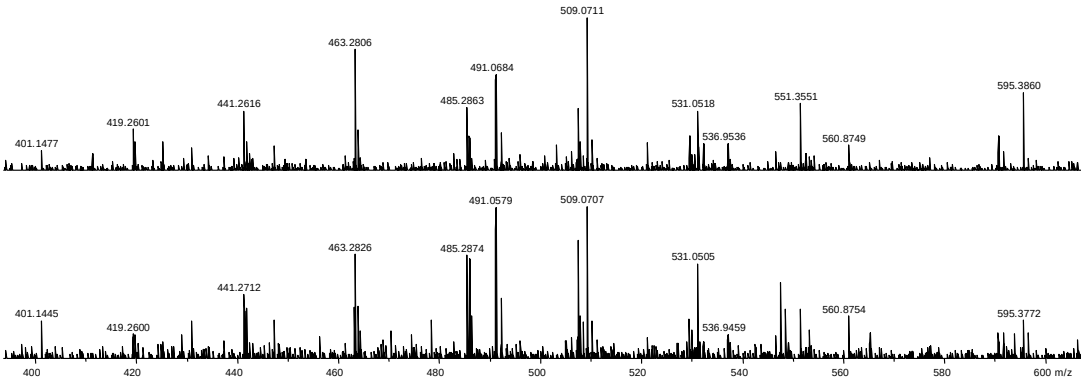

Fig. 78: HRESIMS of the compound from the *ΔgrhE* mutant.

9 Publications

Poster presentations

VAAM International Workshop:

4-6 October 2007, Nonnweiler, Germany

Yunt, Z. S.; Reinhardt, K.; Eklund, M.; Xu, Z.; Hertweck, C.; Bruhn, T.; Bringmann, G.; Piel, J.

Titel: Unusual oxidoreductases involved in pharmacophore generation of the aromatic polyketide griseorhodin A

21. Irseer Naturstofftage:

25-27 February 2009, Irsee, Germany

Yunt, Z. S.; Reinhardt, K.; Eklund, M.; Xu, Z.; Hertweck, C.; Bruhn, T.; Bringmann, G.; Piel, J.

Titel: Insights into the biosynthesis of the unusual aromatic polyketide griseorhodin A

6th European Conference on Marine Natural Products:

19-23 July 2009, Porto, Portugal

Reinhardt, K.; Yunt, Z. S.; Eklund, M.; Xu, Z.; Hertweck, C.; Bruhn, T.; Bringmann, G.; Piel, J.

Titel: Griseorhodin A: Biosynthetic Studies and Combinatorial Biosynthesis

Publication in preparation

Eklund, M.L.; Reinhardt, K.; Yunt, Z.S.; Xu, Z.; Hertweck, C.; Müller, C.E.; Teta, R.; Alfonso, M.; Piel, J. (2011) Griseorhodin A: investigations of the early biosynthetic steps and combinatorial biosynthesis.

11 Declaration

Hiermit erkläre ich, die eingereichte Arbeit selbstständig verfasst und keine anderen Hilfsmittel und Quellen als die angegebenen benutzt zu haben.

Diese Arbeit ist weder identisch noch teilidentisch mit einer Arbeit, die an der Rheinischen Friedrich-Wilhelms-Universität Bonn oder einer anderen Hochschule zur Erlangung eines akademischen Grades oder als Prüfungsleistung vorgelegt worden ist.

Die Promotionsordnung der Mathematisch-Naturwissenschaftlichen Fakultät der Rheinischen Friedrich-Wilhelms-Universität Bonn ist mir bekannt.

Minna Leena Eklund